

DISSERTATION

Geological evolution and stratabound Cu-Pb-Ba mineralization of the
Jillawarra Belt in the Proterozoic Bangemall Basin, Western Australia

ausgeführt zur Erlangung des akademischen Grades eines Doktors
der montanistischen Wissenschaften

eingereicht am Institut für Geowissenschaften, Mineralogie und
Petrologie, Montan-Universität Leoben, Österreich

von

Jörn Hubertus Vogt

Leoben, 16. November 1984

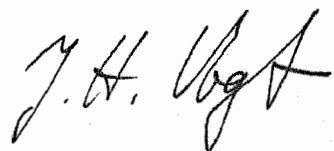


15.2.14

Promotion am 14.12.1984

Ich erkläre an Eides statt, die vorliegende Arbeit selbst verfaßt
und die verwendeten Hilfsmittel vollständig angegeben zu haben.

Leoben, 16. November 1984

A handwritten signature in black ink, appearing to read 'J. H. Vogt'. The signature is stylized with a large, sweeping 'V' and a distinct 'A' at the end.

Jörn Hubertus Vogt

Abstract

Geological evolution and stratabound Cu-Pb-Ba mineralization of the Jilawarra Belt in the Proterozoic Bangemall Basin, Western Australia

A stratabound, sediment-hosted Cu-Pb-Ba mineralization named Abra has recently been discovered in the Bangemall Basin, the youngest intracratonic sedimentary basin in Western Australia. Rb-Sr dating of a rhyolite in the lower part of the Bangemall Group yielded 1100 m.y. This is the first occurrence of a significant Proterozoic base metal mineralization in Western Australia, distinguished from major Proterozoic base metal deposits by the following features:

- The occurrence in low-grade metamorphic (lower greenschist facies) sedimentary rocks
- the abundance of Pb and Ba within 1100 m.y. "copper age" strata
- widespread veining not only in the footwall stringer zone but in the stratiform part of the mineralization
- the absence of an euxinic facies, i.e. the hematitic host sediments in the upper part indicate fully oxidizing depositional conditions.

The mineralization is covered by 250-450 m barren clastites; drilling of eight exploration holes during 1981-1983 established an orebody of 130 mt grading 1.15% lead, 0.25% copper and 2.5% barium. Due to the vertical distribution of the three ore minerals - galena, chalcopyrite and barite - the 130 mt low-grade mineralization can be separated into a lower copper body (60 mt at 0.5% Cu), overlain by a lead body (50 mt at 3.0% Pb), and an upper barium zone (25 mt at 20.0% Ba).

The Bangemall Basin is an intracratonic basin into which over 10,000 metres of shallow water sediments were deposited in a number of transgressional-regressional cycles. It is one of the largest intrusive continental tholeiite provinces of the world. Intrusion of dolerite into the sediments commenced during deposition of the middle Bangemall Group, and was related to a tensional crustal regime in the sialic basement.

The tectonic and sedimentary history of the Bangemall Basin can be viewed

in context with the development of an intracratonic rift. The distribution of different volumes of dolerite in relation to major lineaments implies the presence of a triple junction in the area of the Abra mineralization, adjacent to a granitic basement dome.

The host rock sequence of the Abra mineralization, in the lower Bangemall Group, comprises over 500 m inter- to subtidal medium-grained clastites, overlain by some 40 m subaqueous evaporitic iron formation deposited in a fault-bounded restricted basin. These ferruginous laminites ("black zone") grade upwards into hematitic sabkha sediments (40 to 100 m thickness) with local interbeds of coarse clastites ("red zone"). This regressional development in a fault-bounded basin (doming) is followed by a period of pronounced transgression depositing some 300 m of shallow water turbidites. (rifting, subsidence).

Major ore minerals are chalcopyrite, galena, barite, subordinate fahlore and minor sphalerite. Most remarkably is the general paucity of zinc and the dominance of stratiform barite (over 40 core m of more than 20% barium) in the top zone of the mineralization. Relative metal abundances show a vertical zonation pattern of Cu-(Zn)-Pb-Ba where Cu is restricted to the discordant feederzone, Pb has an intermediate position and some Ba is of concordant nature within the sabkha sediments. Sulphur isotope analyses yielded $\delta^{34}\text{S}$ values of +21 ‰ for sulphides and of +40 ‰ for barite.

Comparison with the lower Bangemall Group elsewhere in the basin suggests that the host rock sequence is underlain by a thick arkose unit (1600 m). The arkose was deposited subaerially from a granitic basement source and developed red-bed copper features. Anomalous heat flow lead to rapid decomposition of feldspars releasing Pb and Ba, and to mobilization of Cu from the red beds. Thermodynamic constraints on the coexistence of barite with the hematite-magnetite-pyrite triple point allowed assessment of a mineralizing temperature of about 250°C; higher temperatures in the source rocks are likely. These hot metal-bearing fluids accumulated up-dip in a structural trap provided by the doming of the strata. With the onset of rifting deep-seated faults were generated providing a conduit into which the metal-

bearing fluids were channelled, and ascended to host rock level where they percolated the shallow water and sabkha sediments. Precipitation of metals occurred in a vertical Cu-Pb-Ba zoning sequence within veins and as replacement of pre-existing syndiagenetic pyrite layers in the evaporitic sediments. Further galena (chalcopyrite) mineralization took place where the metal ions encountered H_2S from bacterial sulphate reduction trapped in the sediments. Besides some vein mineralization, the bulk of barite formed at the top of the mineralization within the sabkha sediments through quantitative replacement of Ca in sedimentary sulphates by Ba, facilitated by very low solubilities of barite and the abundance of formation waters in the early diagenetic sediments.

Doming and concomitant development of fault-bounded basins in the periphery of the dome (accommodation of strain), and subsequent generation of a triple junction and rifting are attributed to a thermal mantle plume (hot spot). The hot spot also accounted for high heat flow resulting in mobilization of metals, accumulation of hot metal-bearing fluids in a structural trap, and provided thermal energy required to drive the hydrothermal system.

A model of the genesis of sediment-hosted base metal deposits, including Late Proterozoic copper deposits, is presented where a hot spot determines the thermal regime and structural setting of such deposits (first-order controls). Other parameters like discordant or concordant mineralization, exhalative or syndiagenetic replacement processes of ore formation, and relative metal abundance of the individual deposits, merely depend on the physical and chemical conditions at the site of ore deposition, and on the composition and metamorphic grade of the source rocks (second-order controls).

Geologische Entwicklung und schichtgebundene Cu-Pb-Ba Vererzung des Jilawarra Belt im proterozoischen Bangemall Basin, West-Australien

Zusammenfassung

Eine schichtgebundene Cu-Pb-Ba Vererzung in Sedimenten("Abra") ist vor etwa 3 Jahren im Bangemall Basin, dem jüngsten proterozoischen, intracratonischen Sedimentbecken West-Australiens, entdeckt worden. Das ungefähre Alter der Sedimente im unteren Teil der Bangemall Group ist durch eine Rb-Sr Datierung von etwa 1100 ma umrissen.

Abra ist die erste proterozoische Buntmetallvererzung in West-Australien und unterscheidet sich von den großen proterozoischen Buntmetallagerstätten Australiens hinsichtlich der folgenden Charakteristika:

- Aufsitzen in niedrig-gradigen(untere Grünschieferfazies) Metasedimenten
- Gehalt an Pb und Ba in Schichten des 1100 ma "Kupferalter"
- weitverbreitete Gangvererzung nicht nur in der liegenden stringer zone, sondern auch im stratiformen Teil der Vererzung
- Fehlen einer euxinischen Fazies; die hematitischen Wirtsgesteine im oberen Teil der Vererzung zeigen voll oxidierende Sedimentationsbedingungen an

Die Vererzung liegt unter 250-450 m erzfreien Klastiten; durch 8 Explorationsbohrungen zwischen 1981 und 1983 konnte ein Körper von geschätzten 130 mt mit 1.15% Pb, 0.5% Cu und 2.5% Ba nachgewiesen werden.

Das Bangemall Basin ist ein intracratonisches Becken mit mehr als 10.000 m Flachwassersedimenten, die von der mittleren Bangemall Group aufwärts von Doleriten intrudiert werden. Die tektonische und sedimentäre Entwicklung des Bangemall Basin gleicht der eines intracratonischen Rifts; die Geometrie der Dolerit-Verteilung und der regionalen Lineamente impliziert das Vorhandensein einer triple junction im Bereich der Abra-Vererzung.

Die Abfolge der Wirtsgesteine der Abra-Vererzung(untere Bangemall Group) umfasst mehr als 500 m intertidale Klastite, überlagert von 40 m subaquatisch-evaporitischer Eisenformation, die in einem störungsbegrenzten, eingeschnürten Becken abgelagert wurden. Die eisenführenden, feingeschichteten Sedimente("black zone") gehen zum Hangenden in hematitische Sabkha-Ablagerungen("red zone") mit 40-100 m Mächtigkeit, über. Auf diese regressive Entwicklung(doming) folgt eine Transgression mit ungefähr 300 m Flachwasserturbiditen(rifting, Absenkung).

Die hauptsächlichen Erzminerale sind Kupferkies, Bleiglanz und Barit; bemerkenswert ist das Fehlen von Zinkblende. Die Metallverteilung ist durch eine vertikale Cu-(Zn)-Pb-Ba Zonierung gekennzeichnet, wobei Cu auf die liegende Gangvererzung beschränkt ist, Pb eine intermediäre Position einnimmt und einiges der oberen Ba-Vererzung schichtkonform in den laminierten Sabkha-

Sedimenten auftritt.

Als Muttergestein der Vererzung wird eine ca. 2000 m mächtige Arkoseeinheit in der basalen Bangemall Group angenommen. Terrestrische Sedimentationsbedingungen führten zur Ausbildung von red-bed copper. Durch hohen Hitze fluß im Bereich der Vererzung wurden Cu und Pb, Ba (aus den Feldspäten der Arkose) mobilisiert. Mit Beginn des Rifting entstanden tiefgreifende Störungen, von denen eine als Förderkanal für hydrothermale Lösungen diente. Die aufsteigenden Lösungen durchdrangen die Wirtsgesteine, wobei es zur Ausfällung von Pb- und Cu-Sulfiden und wenig Barit in feinen Gängen kam. Der größte Teil des Bariums blieb jedoch in Lösung bis die gipsführenden Sabkha-Sedimente der red zone erreicht waren, wo Barium sämtliches Ca aus den Gipsen verdrängte und mächtige Baritlager bildete.

Die Heraushebung eines Domes sowie das anschließende Rifting an einer triple junction stehen im Zusammenhang mit einem hot spot im unterliegenden, oberen Mantel, wodurch auch der hohe Hitze fluß im Bereich der Vererzung zu erklären ist. Der Zusammenhang hot spot - intracratonisches Rifting - Buntmetallvererzung wird anhand bekannter Buntmetallagerstätten diskutiert, und in einem Modell für die Genese solcher Lagerstätten formuliert.

C O N T E N T S

=====

	page
Introduction	1
 <u>Section I Regional geology of the Bangemall Basin</u>	
1.1. The Western Australian Shield	4
1.1.1. Archean	5
1.1.2. Proterozoic	6
1.1.3. Proterozoic tectonics	9
1.2. The Bangemall Basin (First-Order-Basin)	10
1.2.1. Physiography	11
1.2.2. Recognition of the Bangemall Group	12
1.2.3. Evidence of age	13
1.2.4. Structure and tectonics of the Bangemall Basin	
1.2.4.1. Tectonic controls of the Bangemall Basin	15
1.2.4.2. Deformation and faulting	15
1.2.4.3. Conclusions	18
1.2.5. Stratigraphy of the Bangemall Group	
1.2.5.1. Facies provinces	19
1.2.5.2. Stratigraphy of the western facies	21
1.2.5.3. Development of the western facies	27
1.2.6. Igneous rocks in the Bangemall Basin	
1.2.6.1. Mafic igneous rocks	28
1.2.6.2. Implications of mafic magmatism	34
1.2.6.3. Felsic volcanogenic rocks	36
1.2.6.4. Summary	37
1.2.7. Mineralization in the Bangemall Basin	
1.2.7.1. Description of low-grade mineralizations outside the Jillawarra Basin	38
1.2.7.2. Summary	44

<u>Section 2</u> <u>The Jillawarra Belt</u>	page
2.1. Introduction	45
2.2. The basement	47
2.3. Stratigraphy, lithology and facies of the Bangemall Group in the Jillawarra Belt	48
2.3.1. The Gap Well Formation	
2.3.1.1. GW ₁	51
2.3.1.2. GW ₂	55
2.3.1.3. GW ₃	61
2.3.1.4. Woodlands Arenite Member (GW _{W4})	67
2.3.1.5. GW ₅	74
2.3.1.6. GW ₆	88
2.3.2. The West Creek Formation	
2.3.2.1. WC ₁	105
2.3.2.2. WC ₂	110
2.3.2.3. WC ₃	121
2.3.2.4. WC ₄	126
2.3.3. The Jillawarra Formation	
2.3.3.1. Mjd	129
2.3.3.2. Mjs	130
2.4. Structure of the Jillawarra Belt	
2.4.1. Folds	132
2.4.1.1. Slump folds	133
2.4.1.2. Drape folds	133
2.4.1.3. Tight folds	134
2.4.1.4. Variation in fold style	139
2.4.2. Cleavage and lineation	142
2.4.3. Faults	
2.4.3.1. Normal faults	144
2.4.3.2. Reverse faults and thrust faults	147
2.4.4. Summary	149
2.5. Igneous rocks of the Jillawarra Belt	
2.5.1. Mafic intrusives	150

	page
2.5.2. Felsic volcanic activity of the Coobarra Dome	
2.5.2.1. Rhyolite	151
2.5.2.2. Lapilli tuff	155
2.5.2.3. Other volcanoclastic rocks	158
2.5.2.4. Felsic pipes	160
2.5.2.5. Summary	161
2.6. Development of the Jillawarra Basin (Second-Order-Basin)	
2.6.1. Transgression	162
2.6.2. Regression (Doming)	164
2.6.3. Transgression (Rifting)	165
2.6.4. Further basin development	166
2.6.5. Summary	166
<u>Section 3</u> <u>The Abra sub-basin</u>	
3.1. Introduction	169
3.2. Stratigraphy of the Abra succession	
3.2.1. The Gap Well Formation	171
3.2.1.1. Stringer zone	173
3.2.1.2. Black zone	183
3.2.1.3. Red zone	196
3.2.1.4. The sulphate problem	213
3.2.1.5. Correlation with the Gap Well Formation of the Jillawarra Belt	217
3.2.2. The West Creek Formation	
3.2.2.1. WC ₁	218
3.2.2.2. WC ₂	219
3.2.2.3. WC ₃	220
3.3. Deformation of the Abra sub-basin	220
3.3.1. Faults	221
3.3.2. Cleavage	223
3.3.3. Pseudo-tectonic features	223
3.4. Development of the Abra sub-basin (Third-Order-Basin)	224

<u>Section 4 The Abra mineralization</u>	page
4.1. Mineralogy of the Abra mineralization	
4.1.1. Sulphides	
4.1.1.1. Pyrite	232
4.1.1.2. Galena	236
4.1.1.3. Chalcopyrite	241
4.1.1.4. Sphalerite	243
4.1.1.5. Sulphosalts	246
4.1.2. Sulphates	249
4.1.3. Oxides	
4.1.3.1. Fe-oxides	251
4.1.3.2. Scheelite	252
4.1.4. Carbonates	254
4.1.5. Silicates	
4.1.5.1. Chlorite	257
4.1.5.2. Feldspar	259
4.1.5.3. Quartz	261
4.1.6. Summary	262
4.2. Metal zonation in the Abra mineralization	264
4.4. Physical and chemical controls on ore formation in the Abra mineralization	
4.4.1. Vein mineralization	269
4.4.2. Conformable mineralization in the black and red zones	277
4.5. Sulphur isotopes of the Abra mineralization	279
4.6. Alteration and metamorphism in the Abra mineralization and in the Jillawarra Belt	
4.6.1. Alteration	287
4.6.2. Metamorphism in the Jillawarra Belt	293
4.7. Source of metals in the Abra mineralization	294
4.8. Mineralizations in the Jillawarra Belt (except Abra)	304

Section 5 Genesis of the Abra mineralization and some implications for the development of sediment-hosted base metal deposits

- 5.1. A model for the genesis of the Abra mineralization
 - 5.1.1. Geotectonic setting
 - 5.1.2. Source rocks
 - 5.1.3. Accumulation of metal-bearing fluids
 - 5.1.4. Ascent of the hydrothermal fluids
 - 5.1.5. Emplacement of the Abra mineralization
 - 5.1.6. Summary
- 5.2. Comparison with sediment-hosted base metal deposits
 - 5.2.1. Late Proterozoic copper deposits
 - 5.2.2. Sediment-hosted massive sulphide lead-zinc deposits
 - 5.2.3. Discussion and conclusions
- 5.3. A model for hot spot induced base metal deposits

Acknowledgements

References

APPENDIX

- map 1 Geological map of the Jillawarra Belt
- map 2 Bedrock map of the Jillawarra Belt
- map 3 Location map

Introduction

Some of the world's major base metal deposits (Mt. Isa, McArthur River, Broken Hill) occur on the Australian continent. They are hosted by Proterozoic sediments of 1500 - 1800 m.y. age. Western Australia has a wealth of mineral deposits, and an advanced mining industry; however, no major Proterozoic base metal mineralization has been found prior to the discovery of the Abra sediment-hosted Pb-Cu-Ba mineralization by Geopeko in 1981/82.

This is a body of an estimated 130 million tons (mt) of ore grading 1.15 % lead, 0.25 % copper and 2.5 % barium. Due to the vertical distribution of the three ore minerals - galena, chalcopyrite and barite - the 130 mt low-grade mineralization can be separated into a lower copper body (60 mt at 0.5 % Cu), overlain by a lead body (50 mt at 3.0 % Pb), and an upper barium zone (25 mt at 20.0 % Ba).

The mineralization is covered by 250 to 450 metres barren clastites; drilling of eight exploration holes during 1981 - 1983 revealed that there are a number of features distinguishing Abra from the major Australian deposits.

- The occurrence in low grade metamorphic (lower greenschist facies) sedimentary rocks
- Widespread veining not only in the footwall stringer zone but in the stratiform part of the mineralization
- The hematitic host sediments in the upper part indicate fully oxidizing depositional conditions, i.e. the absence of an euxinic facies
- The sulphide minerals comprise pyrite, galena and chalcopyrite only; remarkably, no sphalerite occurs
- The abundance of barite in the upper zone of the mineralization

These peculiar features, and the metal abundance ratio, suggest an unique and new type of base metal deposit.

The mineralization is located in an east-west elongated area of about 100 x 20 kilometres - the Jillawarra Belt - within the central Bangemall Basin. This is a Proterozoic intracratonic sedimentary basin dated at 1100 m.y. by Rb-Sr methods. There are a number of geological features, however, which distinguish the rocks of the Jillawarra Belt from those of the Bangemall Basin, raising uncertainties with respect to the stratigraphic relationship. In addition, four model-lead ages (from about 1500 - 1600 m.y.) place constraints on the age of the Jillawarra Belt and the Abra mineralization, and suggest a basement high of older Proterozoic rocks within the Bangemall Basin.

The discrepancy between the apparent age of the Jillawarra Belt and that of the Bangemall Basin, and the unique features of the mineralization described above, provided the incentive for launching a joint programme of the Mining University at Leoben, the Geological Survey of Western Australia, and Geopeko and Amoco Australia in order to throw some light on the age of the Jillawarra Belt and the age and genesis of the mineralization.

The aims of the study initiated include:

- Identification of the stratigraphic and structural setting of the mineralization with respect to the Jillawarra Belt
- Detailed investigation of the mineralization
- Evaluation of the stratigraphy and structure of the Jillawarra Belt
- Examination of the relationship between the stratigraphy of the Jillawarra Belt and the Bangemall Basin in order to establish the age of the Jillawarra Belt, and thereby, the age of the Abra mineralization
- Understanding of the ore forming processes and their relation to the geotectonic setting, and development of a genetic model of the Abra mineralization, which may assist in the search for further mineralizations of this type in Proterozoic sediments.

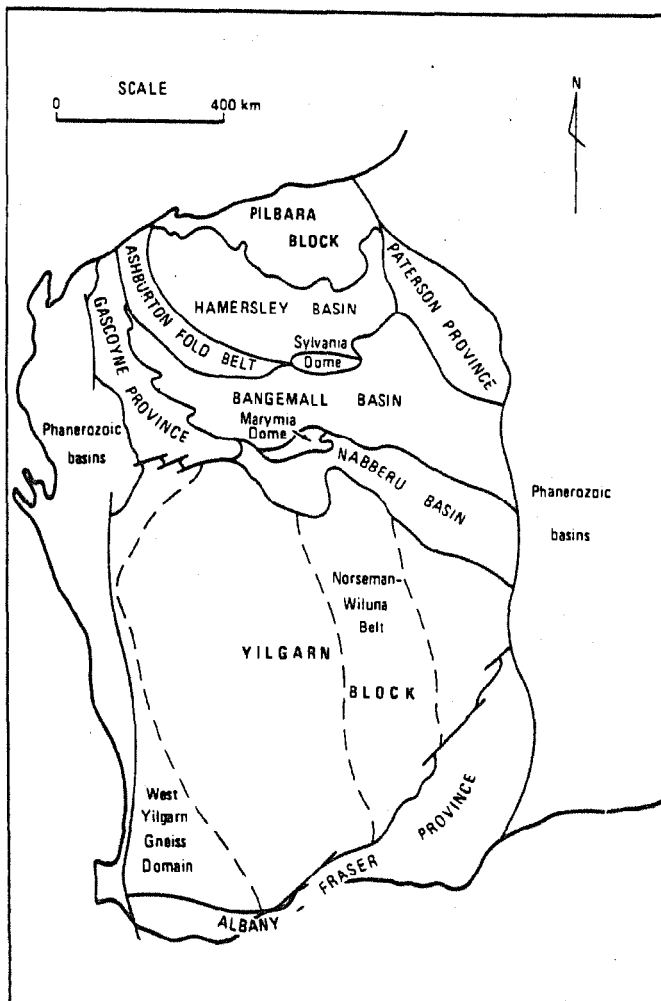
The methodological approach taken is twofold; first, a detailed investigation of stratigraphy, sedimentary facies and structure, both on a regional scale and on the scale of the mineralized area and, second, assessment of the chemistry and mineralogy of the mineralization. The results are combined to erect a model of the genesis of the Abra mineralization and comparison is made with major base metal deposits worldwide.

The size of 130 mt of ore would place the Abra mineralization into the class of major base metal deposits. However, low grade, sub-surface occurrence and remoteness of the area make this mineralization sub-economic, at current base metal prices. This, no doubt, is one of the reasons why exploration work was discontinued in June, 1984.

1.1. The Western Australian Shield

The Western Australian Shield is a roughly rectangular area consisting of two large Archean cratons that are partly covered by remnant Proterozoic sedimentary basins and partly surrounded by Proterozoic mobile belts.

Fig. 1.01 shows the major tectonic units of the Western Australian Shield.



Major tectonic units of the Western Australian Shield.
Fig. 1.01, from Gee (1979)

1.1.1. Archean

The crustal evolution of the Archean cratons - the Pilbara Block in the north and the Yilgarn Block in the south - has been studied in detail by Hickman (1981) and Gee et al. (1981), respectively, Archean terrains are either granitoid-greenstone, or high grade gneiss (i.e. the Western Gneis Terrain), the regional distribution of which influences the style of Proterozoic tectonism (Gee, 1979).

Granitoid-greenstone terrains consist of thick volcanogenic sequences, now occurring as dismembered synclinal keels within voluminous granitoid. Available evidence suggests that greenstone deposition and granite emplacement in the Yilgarn Block took place over a narrow time span between 2800 and 2600 m.y. ago (Gee et al., 1981). In the Pilbara Block comparable events of crustal evolution are older and seem to cover a wider range of time (3350 - 2600 m.y., Hickman, 1981).

The gneiss terrains comprise repeatedly deformed and metamorphosed sediments, infolded sheets of orthogneiss and intrusions of mafic and ultramafic rocks. The gneissic rocks date back at least to 3300 m.y. and are interpreted as basement upon which the greenstone sequences were deposited (Gee et al., 1981).

The most extensive area of gneiss lies in an arc around the western part of the Yilgarn Block. Recent ion microprobe identification of 4100 - 4200 m.y. old detrital zircons from the Mt. Narryer region within the northwestern part of this gneiss terrain (Froude et al., 1983) suggests the presence of pre-3800 m.y. silica-saturated crustal rocks in this region.

Most recent workers on the Western Australian Shield (e.g. Glickson and Lambert, 1973; Horwitz and Smith, 1978; Gee, 1979) consider

it possible that the granitoid - greenstones of the Pilbara and Yilgarn Block formed on a continuous crustal substratum. Different views, however, are expressed by the above authors about the nature of this primary crust, and the mode and timing of greenstone emplacement.

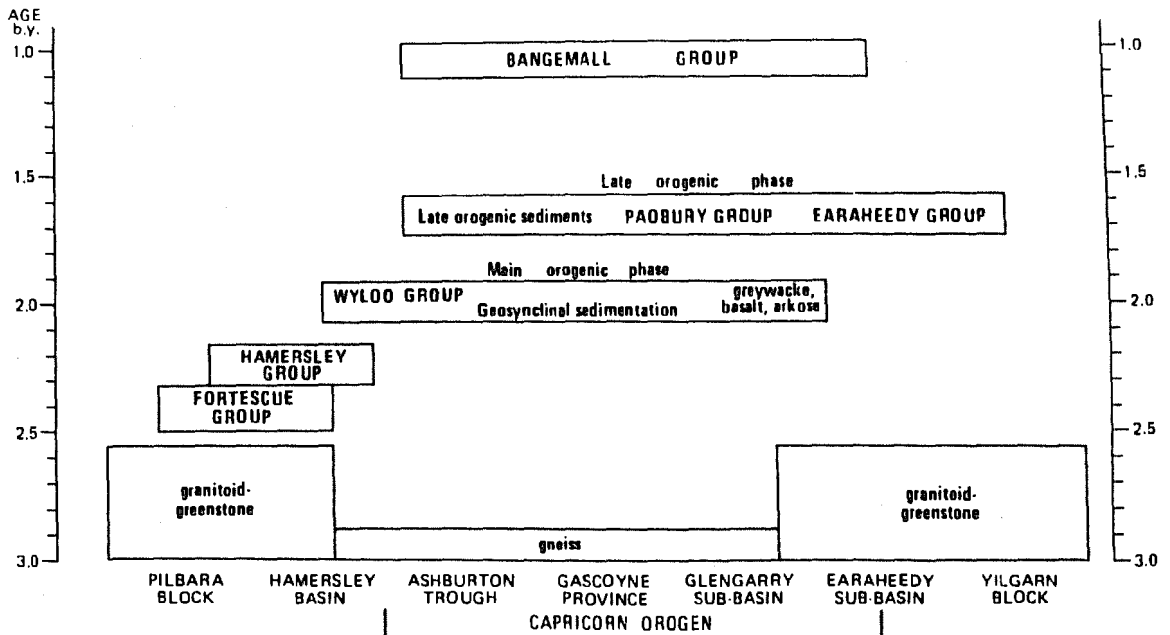
Relevant for this study is the general consensus that the Proterozoic "mobile belt" between the Pilbara and Yilgarn Blocks developed as an ensialic orogen. Where basement can be recognized in structural highs it appears to be of Archean gneiss (Muhling et al., 1976; Elias and Williams, 1977).

1.1.2. Proterozoic

Between the two Archean blocks are a number of Proterozoic sedimentary sequences of various ages. Where these directly overly the stable Archean cratons they are shielded from significant deformation; however, where they transgress inferred boundaries of the cratons onto a median zone (orogen), they are deformed, metamorphosed and intruded by granitoids, and the basement is reworked. The granite-greenstone areas had largely stabilized by about 2500 m.y. (Gee, 1979).

The median, highly deformed and metamorphosed zone (orogen) is recognized by many workers but termed "Ophthalmian Mobile Belt" by Glickson and Lambert (1973), "Median Belt" by Horwitz and Smith (1978) or "Capricorn Orogen" by Gee (1979).

Fig. 1.02 gives the stratigraphic framework for the region between the Pilbara and Yilgarn Blocks and further shows the spatial relation of the stratigraphic units to the Capricorn Orogen.

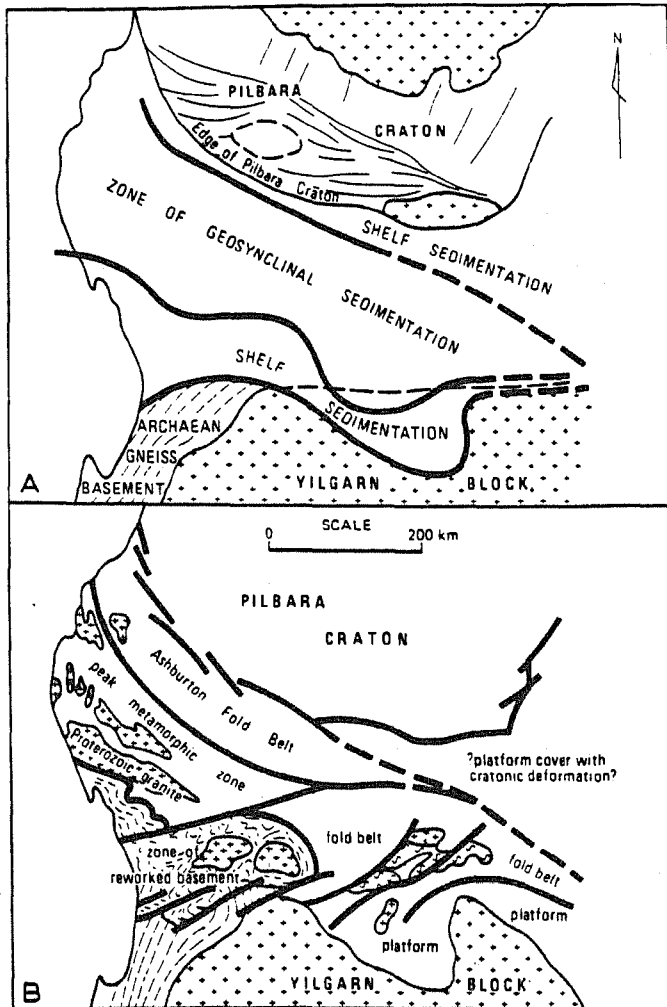


Stratigraphic framework for the region between the Pilbara and Yilgarn Blocks.
 Fig. 1.02, from Gee (1979)

The Capricorn Orogen is defined by Gee (1979) as a major orogenic zone involving geosynclinal sedimentation, metamorphism, basement reworking and granitoid emplacement in the region between the Yilgarn and Pilbara Block. It takes its name from the Tropic of Capricorn, at which latitude it is approximately located.

The Bangemall Basin, which marks a much later major sedimentary cycle unrelated to this orogenic zone, blankets much of the orogen.

As a basis for reconstructing the major basin of deposition beneath the Bangemall Basin, Gee (1979) proposed that the thick greywacke-type sediments of the Glengarry Sub-Basin are equivalent in tectonic setting to those in the Ashburton Trough. This reconstruction points to an elongate belt of thick greywacke and volcanic fill, occupying almost the entire area between the Pilbara and Yilgarn Blocks (Fig. 1.03).



Two main stages of the Capricorn Orogen. A. Sedimentation stage, about 2000 m.y. ago, showing zone of geosynclinal sedimentation. B. After climax of orogenic activity, about 1600 m.y. ago.
Fig. 1.03, from Gee (1979)

Furthermore, the distribution of lithofacies is symmetrical across the geosyncline. Thus, the stratigraphically lower part of the Wyloo Group consisting of sandstone, conglomerate and dolomite could be regarded as a shelf facies on the northern margin of the geosyncline. Similarly a shelf facies is present along the southern edge in the Glengarry Sub-Basin.

The Capricorn Orogen evolved over a period of about 400 m.y. (2000-1600 m.y., see Fig. 1.03). After the climax of orogenic activity with basement reworking and granitoid emplacement about 1600 m.y. ago, the region between the Pilbara and Yilgarn Blocks probably underwent a phase of tectonic quiescence (except minor block faulting) and was subject to erosion for a considerable

time (200-400 m.y.?) until the Bangemall Group was deposited unconformably as an intercratonic basin filling.

1.1.3. Proterozoic tectonics

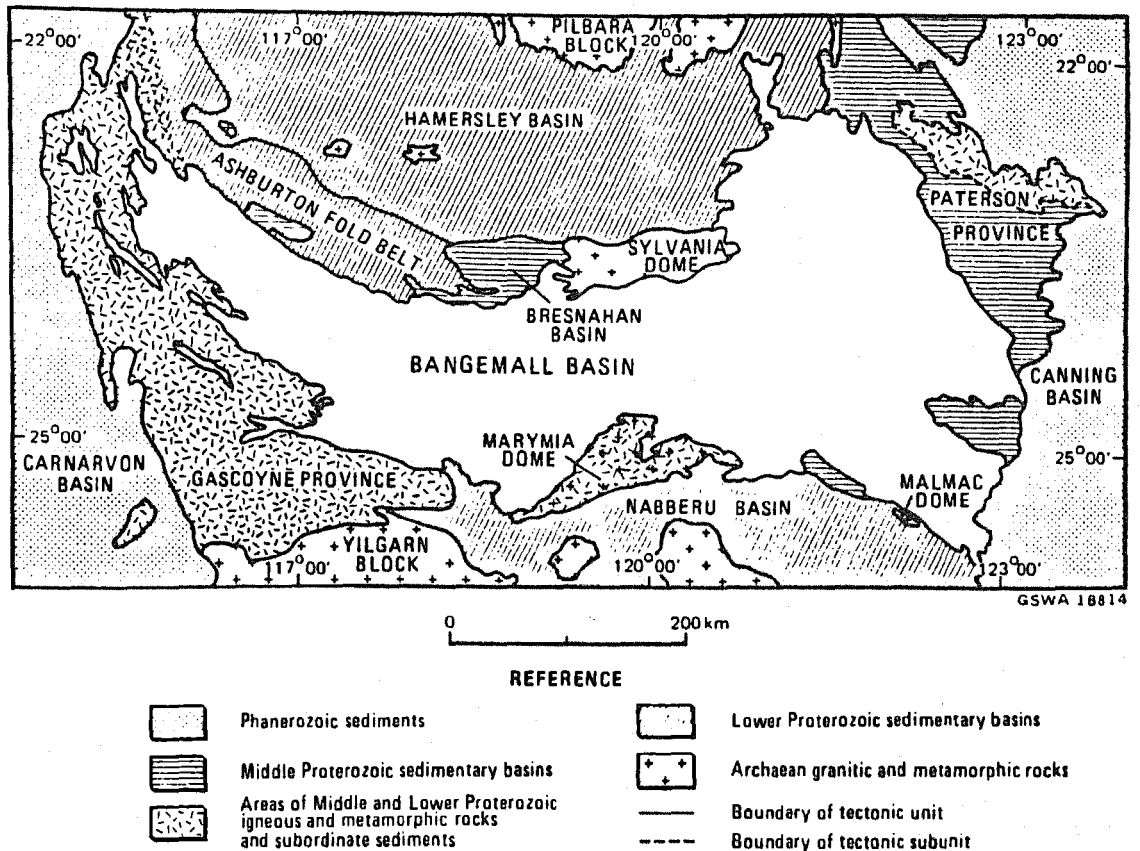
Gee (1979) concluded that, primarily because of its ensialic nature, no evidence for Phanerozoic-type plate tectonics in the Capricorn Orogen can be recognized. However, the basement control of the Capricorn Orogen may illustrate a style of plate tectonics typically of the early Proterozoic, whereby cratonic blocks, which geometrically can be described as plates move relative to each other while the strain is accommodated in linear belts (Sutton and Watson, 1974). Horizontal translations or rotations of rigid plates of the order of one hundred kilometres could exist, and would be well within the statistical error of the palaeomagnetic constraints placed by data of McElhinney and Embleton (1976).

Some areas of higher degree of deformation and thrusting in the overlying Bangemall Group may be related to discrete zones of strain in the basement along which plate movement could have occurred.

1.2. The Bangemall Basin

The Bangemall Basin is a late Proterozoic (ca. 1100 m.y.) intra-cratonic sedimentary basin, which occupies about 145,000 km². It unconformably overlies older Precambrian sedimentary basins and metamorphic complexes of the Western Australian Shield in the northwest of Western Australia (Fig. 1.04).

Fig 1.04: Tectonic setting of the Bangemall Basin



1.2.1. Physiography

There are no towns within the Bangemall Basin and the Great Northern Highway, passing through the central part of the basin, is the only sealed road while all further access is by gravel roads.

Most of the Bangemall Basin lies more than 500 metres above sealevel. While an internal drainage region east of longitude 120° has produced a low relief with gentle topography the external drainage region west of longitude 120° is dissected into a more rugged landscape with occasional rocky ranges between wide alluvial and colluvial plains.

The climate is semi-arid to arid, and is characterized by low and unreliable rainfall, high evaporation rates, mild temperatures during winter, and hot summers. The rainfall ranges from 200 to 250 mm per year, and the eastern desert areas receive slightly less.

Vegetation in the western part of the basin comprises shrubs (dominantly Acacia species) and hummocky grassland with occasional tall (30 m) gum trees along the major water courses. In the eastern parts of the basin, there is extensive sandplain with spinifex and related grasses being the dominant vegetation.

The area of the Bangemall Basin has been mapped during the 1 : 250.000 regional mapping programme of the Geological Survey of Western Australia by several geologists; Fig. 1.05 shows the position and names of the 1 : 250.000 sheets available at the Survey.

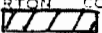
YANREY	WYLOO	MT BRUCE	ROY HILL	BALFOUR DOWNS	RUDALL	TABLETOP
WINNING POOL	EDMUND	TUREE CREEK	NEWMAN	ROBERTSON	GUNANYA	RUNTON
KENNEDY RANGE	MT PHILLIPS	MT EGERTON 	COLLIER	BULLEN	TRAINOR	MADLEY
WOODAMEL	GLENBURGH	ROBINSON RANGE	PEAK HILL	NABBERU	STANLEY	HERBERT

Fig. 1.05: Index to 1 : 250.000 sheets covering the Bangemall Basin. Area of the Jillawarra Belt is cross-hatched.

1.2.2. Recognition of the Bangemall Group

The first recognition of the Bangemall sequence as a comparatively young and separate Precambrian entity was in 1890 by the Government Geologist H.P. Woodward, and his discoveries are summarized on the State geological map, which was published in 1894.

The name, Bangemall Group, was first applied by Halligan and Daniels (1964). Further stratigraphic subdivision was undertaken by Daniels (1969) in the western half of the basin, and by Brakel and Muhling (1976) and Williams et al. (1976) in the eastern half.

Regional appraisals of structure and stratigraphy of the Bangemall Basin have been produced by Daniels (1966, 1975) and Brakel and Muhling (1976), who all recognized the basement control of folding in the western part of the Bangemall Basin, and by Gee (1975).

A comprehensive and detailed work covering all aspects of the Bangemall Basin is currently being prepared by the Geological Survey of Western Australia and will be published as the "Bangemall Bulletin" in the Geological Survey Memoir Series.

1.2.3. Evidence of age

A poor Rb-Sr isochron of about 1080 m.y. was obtained by Compston and Arriens (1968) from felsic rocks at Mount Palgave (in the western part of the Bangemall Basin), believed to be a dyke and related flow, and the same workers obtained the same age from black shale in the Curran Formation, which lies about 600 metres above the sub-Bangemall unconformity.

Gee et al. (1976) report an isochron of 1098 ± 42 m.y. from rhyolite in the lower West Creek Formation (WC₂), 60 metres above the basal unconformity, some 20 km east of the Abra mineralization (see chapter 2.4.). But the rock has an unusually high K₂O content, indicating alteration after eruption, so that the ratios date either early devitrification of the volcanic glass or early metamorphism. Although the reliability of each of these dates can be questioned, each is independent of the others, and when taken together they are remarkably consistent. The age of the Bangemall Group can thus be stated to be about 1100 m.y.

Walter (1972) notes that a stromatolite which occurs in the Irregularly Formation (equivalent to the Gap Well Formation in this study) at the base of the Bangemall Group has an age range of 1350 ± 50 to 950 ± 50 m.y.

1.2.4. Structure and tectonics

1.2.4.1. Tectonic controls on the Bangemall Basin

The Bangemall Basin (about 1100 m.y.) was the last phase of activity in the orogenic belt which separates the Yilgarn and Pilbara cratons. It formed initially over two basement components, namely the Gascoyne Province and the Ashburton Fold Belt, and then spread to the east. The Gascoyne Province was formerly (2000 - 1600 m.y. ago) the locus of sedimentation, deformation, plutonic and metamorphic activity, during which the Wyloo Group was subjected to medium to high-grade metamorphism. By contrast, in the Ashburton Fold Belt (formerly a major sedimentary trough), the Wyloo Group was folded but metamorphosed to only a low grade. The difference in tectonic style and activity between these two components of the orogenic belt influenced subsequent sedimentation and deformation events in this orogenic zone and was a major cause of contrasting sedimentary and structural styles of the three main structural zones of the Bangemall Basin - the Pingandy Shelf, Edmund Fold Belt and Bullen Platform.

Fig. 1.06 shows the occurrence of the three major structural provinces, their relation to lineaments, to the nature of the basement and to the major sedimentary facies provinces within the Bangemall Group.

1.2.4.2. Deformation and faulting

A detailed description and interpretation of the structure of the Bangemall Basin will be published in the "Bangemall Bulletin" in the Geological Survey Memoir Series. Here, only a summary of the tectonic style in the Bangemall Basin is presented.

The nature of the three main basement segments did not only control the regional facies distribution but governed the intensity of

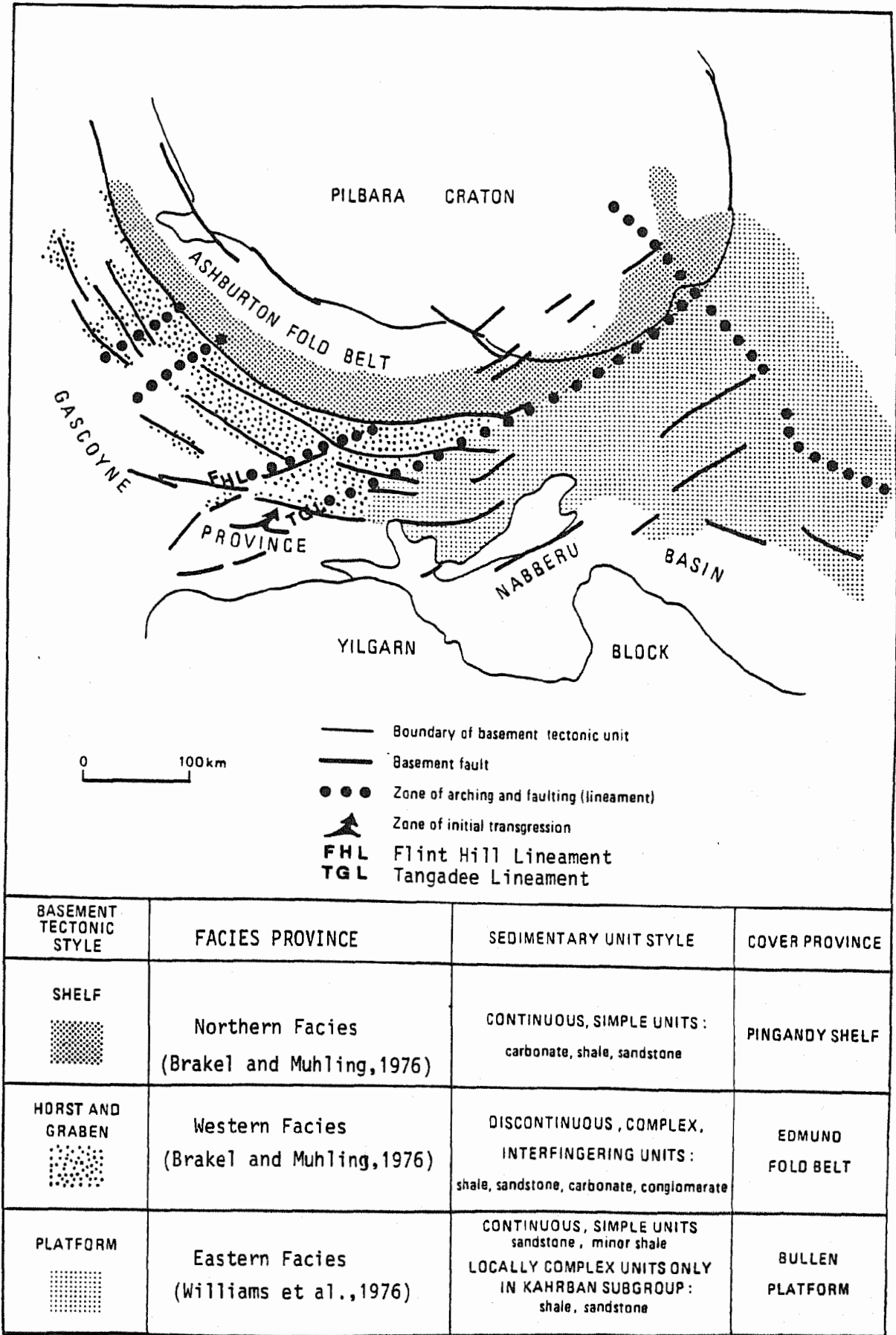


Fig. 1.06: Structural provinces in relation to facies provinces and lineaments

deformation and tectonic style. The tectonic activity displayed by the basement units during sedimentation increased during deformation of the basin.

The Pingandy Shelf overlies a tectonically inert basement, and did not participate in the deformation affecting the Edmund Fold Belt which overlies the Gascoyne Province. The sedimentary pile dips gently south and west of the Ashburton Fold Belt.

The stable marine shelf forming the eastern part of the basin became the Bullen Platform. Here, broad open folds (many of which were domes and basins) formed by draping of sediments over basement blocks controlled by northeast and northwest-trending faults. The northeasterly trend usually is dominant.

The horst-and-graben terrain which developed on active basement became the Edmund Fold Belt. North of the Flint Hill lineament, south-easterly shear zones were dominant in the basement and interacted with a more widely spaced, subordinate northeasterly set. East of the lineament, northeast and easterly trending shear zones controlled the deformation. In the Edmund Fold Belt, the horst and graben blocks had continued to move on normal faults, stretching the overlying sediments to form drape folds (the block faulting may have occurred in both tensional or compressional tectonic regimes, see chapter 2.3.).

The crustal shortening in the basement, possibly a function of relative movements of the Gascoyne Province and Pilbara Craton towards each other (NNE directed forces), caused lateral shortening of the cover and squeezed some fold structures tight. Notably most regional tight folds occur in a graben setting.

Strain was concentrated in ductile zones of metasediments in the basement and along faults forming basement block boundaries. The

metasediments usually were incompetent in comparison with the intervening blocks of crystalline rocks and so become folded together with the cover. Crystalline rocks underwent no shortening, as commonly did their sedimentary cover. In chapter 2.3. however, a mechanism is discussed how significant shortening in the cover also can occur over crystalline basement (granite).

Normal faults forming the boundaries of some basement blocks were reactivated and become the sites of reverse faults. With continuous shortening, the basement was either thrust (if crystalline) or squeezed between rigid blocks (if metasediments or other ductile zones) producing reverse faults and thrust faults, locally, in the cover.

Total shortening across the western part of the basin was in the range of 10 km.

1.2.4.3. Conclusions

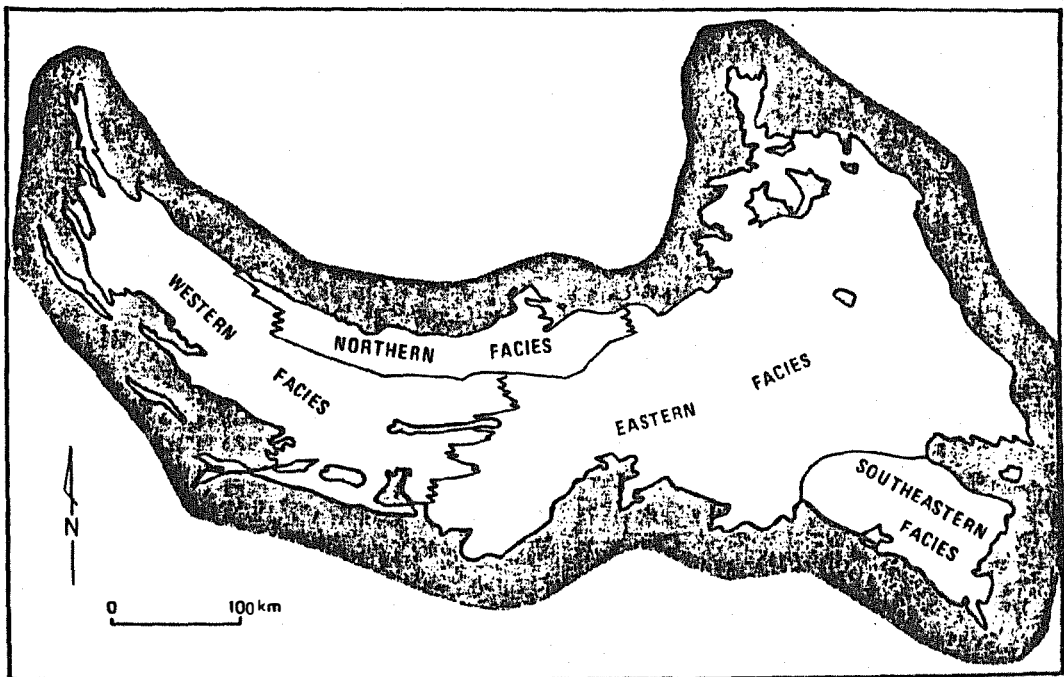
In summary, the tectonic style in the Bangemall Group is controlled by the nature and the tectonic forces applied to the basement and the deformational features observed are compatible with a tectonic regime in the basement which has been tensional first, and subsequently has changed to compressional.

1.2.5. Stratigraphy

1.2.5.1. Facies provinces

Three major facies, each with distinctive litho-stratigraphic assemblages, are recognized in the Bangemall Basin; the western, northern and eastern facies (Brakel and Muhling, 1976). The southeastern region could constitute a fourth facies. Their distribution are shown in Fig. 1.07 and by comparison with Fig. 1.06 the control of the basement tectonic style on the facies distribution becomes evident.

Fig. 1.07: Facies Provinces in the Bangemall Basin

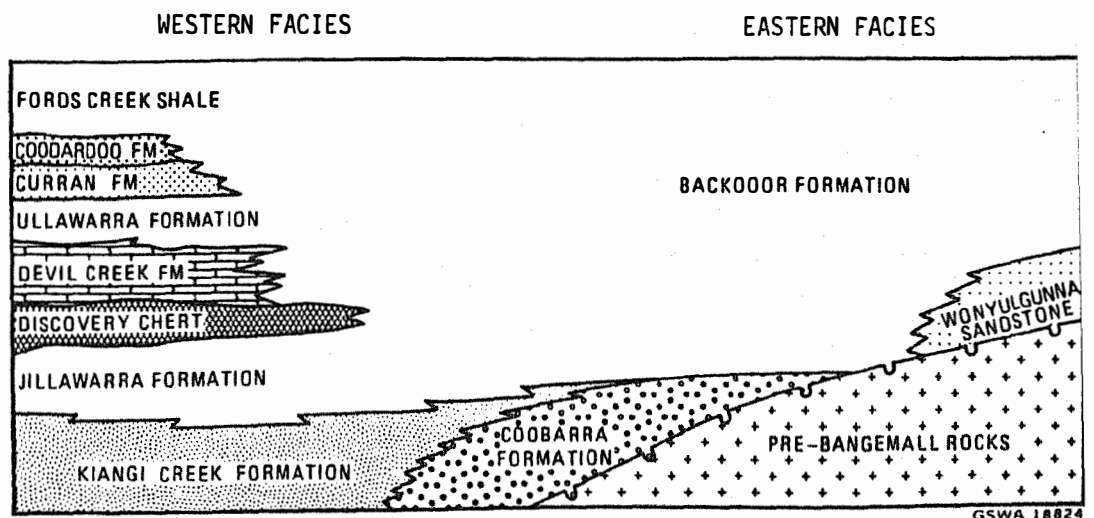


The Jillawarra Belt (outlined by the elongated, grey zone in the central Bangemall Basin in Fig. 1.07) is situated within the western facies province. Therefore, in the following (chapter 1.2.5.2.) a description is given of the western facies only, based mainly on Brakel and Muhling (1976), Muhling et al. (1978) and the Bangemall Bulletin (in press).

The comparatively simple cross-lithologies of the northern and eastern facies are shown in Fig. 1.06; facies changes between the facies provinces are usually due to lensing out of some units and changes in lithology along strike of others.

The change between the western and eastern facies in the eastern-most part of the Jillawarra Belt (central Bangemall Basin) is shown diagrammatically in Fig. 1.08 (after Brakel and Muhling, 1976). In this study the Kiangi Creek and Coobarra Formations are combined to the West Creek Formation; the Coobarra lithology is regarded as a local facies variety of this formation.

Fig. 1.08: Facies change, after Brakel and Muhling (1976)



Recent mapping of the Geological Survey of W.A. in the north-eastern part of the Bangemall Basin (Balfour Downs area) revealed some inconsistency in the stratigraphic relation between the eastern and western facies. It now appears possible that the whole of what Brakel and Muhling (1976) considered as the eastern facies is significantly younger. The existence of a major unconformity between the eastern facies and western facies has thus to be re-examined (Gee, 1984; written comm.).

1.2.5.2. Stratigraphy of the western facies

The chief lithologies are shale, siltstone, sandstone, dolomite, chert, and conglomerate. The stratigraphic sequence according to Muhling et al. (1978) is shown in Tab. 1.01.

Table 1.01: Stratigraphy of the western facies after Muhling et al. (1978)

	Age Group	Map Symbol	Formation	Lithology	Thickness (m)	Remarks	
PROTEROZOIC	Middle Proterozoic	Bangemall	<i>Emq</i>	Kurabuka Formation	Shale, siltstone, minor dolomite	1500	
			<i>Emn</i>	Mount Vernon Sandstone	Sandstone	240	
			<i>Ems</i>	Fords Creek Shale	Shale, minor sandstone and siltstone	1300-1900	
			<i>Emsj</i>	Jeeaila Sandstone Member	Sandstone, with subordinate shale	60-80	
			<i>Emc</i>	Coodardoo Formation	Sandstone, minor siltstone and shale	0-60	
			<i>Emu</i>	Curran Formation	Shale	250	
			<i>Eml</i>	Ullawarra Formation	Shale, siltstone, and minor dolomite	650	Extensively intruded by dolerite
			<i>Emv</i>	Devil Creek Formation	Dolomite and shale	0 to 800 +	
			<i>Emd</i>	Discovery Chert	Chert, subordinate shale	50-125	Laminated rocks, wavy bedding common
			<i>Emj</i>	Jillawarra Formation	Shale, siltstone, minor chert and dolomite	0-1 300	
			<i>Emk</i>	Kiangi Creek Formation	Sandstone, shale, subordinate dolomite and minor conglomerate.	0-1 800	Stromatolites in one dolomite member
			<i>Emkg</i>	Glen Ross Shale Member	Shale	125-525 +	
			<i>Emi</i>	Irregularly Formation	Dolomite, dolomitic shale, shale and minor sandstone	0-2 000	Stromatolites present
			<i>Eme</i>	Tringadee Formation	Sandstone with conglomerate lenses	0-1 650	Lenticular basal formation of Bangemall Group

All units except the basal Tringadee Formation are marine. The sequence from the Jillawarra Formation upwards has a simple, laterally persistent stratigraphy. In the lower half of the sequence, lensing and interfingering of units is common, although the Discovery Chert is continuous, and is the best marker horizon in the sequence. Facies changes in the lower half of the sequence are thought to be the result of an interplay between the lateral migration of contrasting adjacent environments, and varying clastic input (Brakel and Muhling, 1976).

Tringadee Formation

The Tringadee Formation is discontinuous on the basal unconformity. Thicknesses vary greatly and range up to an estimated 1650 metres. The Mount Augustus Sandstone (over 600 metres thickness), also unconformably resting on pre-Bangemall rocks (granite), is believed to be equivalent to (although not continuous with) the Tringadee Formation.

The Tringadee Formation and the Mount Augustus Sandstone both consist of coarse, often pebbly sandstone and lenses of pebble, cobble, and boulder conglomerate. The clasts are vein quartz, schist, gneiss and granite, and are mainly derived from the underlying basement rocks. Fine-grained arenite and siltstone interbeds are rare near the base, but increase in frequency towards the top of the formation where lenses of dolarenite and fine-grained dolomite appear. The unit seems to pass conformably upward into the dolomitic Irregularly Formation.

Most of the Tringadee Formation and Mount Augustus Sandstone is considered to have been deposited subaerially by braided streams. The isolated developments on the unconformity suggest that they were discrete alluvial fans. Dolomites in the upper part of the Tringadee Formation indicate periods of marine incursion which heralded the marine conditions prevailing for the rest of the Bangemall Group sedimentation.

Irregully Formation

This formation is largely equivalent to the Gap Well Formation in the Jillawarra Belt which is hosting the Abra mineralization.

Except where it overlies the Tringadee Formation or the Mount Augustus Sandstone, the Irregully Formation is the lowest formation of the Bangemall Group.

It consists mainly of dolomite, shale and mudstone, with minor chert, sandstone, conglomerate and breccia. The dolomite is finely laminated or massively bedded and stromatolites and algal layers have been found in places. Hematite and goethite cubes, presumably after pyrite, are locally abundant. Some desiccation cracks are present. In the Edmund and Wyloo Sheet areas (cf Fig. 1.05) Daniels (1965) records irregular sheets of sedimentary breccia, thought to be the result of intraformational erosion.

There are abundant indications that the formation was deposited in shallow lagoonal and tidal flat conditions.

Kiangi Creek Formation

This formation is equivalent to the West Creek Formation in the Jillawarra Belt.

The Kiangi Creek Formation, generally overlying the Irregully Formation, consists of interbedded quartz arenite, siltstone and shale, but minor dolomite members are widespread. Typical arenites are medium-grained, well sorted with a small feldspar component, which in rare cases exceeds 20 %. The dolomite members of the Kiangi Creek Formation are similar to those of the Irregully Formation; cumulate-type stromatolite columns have been reported from one locality.

The Kiangi Creek Formation appears to have been deposited in a near-shore marine environment, chiefly as shoals and barrier islands.

Jillawarra Formation

The Jillawarra Formation, with an estimated thickness of 1300 metres near Jillawarra Bore (within the Jillawarra Belt), lies between the Kiangi Creek Formation and the Discovery Chert, and interfingers with the arenites of the former. The depocentre (area of maximum thickness) is assumed to be in the vicinity of the Jillawarra Bore, i.e. the southern part of the Jillawarra Belt (Bangemall Bulletin).

It consists of vari-coloured and black shale, mudstone, chert and minor dolomite and sandstone. The shale and mudstone are usually silty and contain abundant detrital muscovite. In less dissected areas, the rock resembles chert, probably because of surface silification. Cubic crystal moulds, usually less than 10 mm on edge, are plentiful in some beds. Many contain powdery iron oxides, and are presumably after pyrite, however some may be after halite. Smaller, elongate crystal moulds filled with clay or pyrite (see chapter 1.2.6.) are locally abundant, and may be after gypsum.

The sediments are interpreted as shelf muds laid down on the seaward side of the Kiangi Creek Formation sands, and the water was at times euxinic (black shale) and hypersaline.

Brakish to marine depositional conditions of part of the Jillawarra Formation have been shown by Davy (1980) using boron-gallium-rubidium (B-Ga-Rb) diagrams, which were designed by Degens et al. (1958).

Discovery Chert

This is a distinct, remarkably persistent chert unit which forms the best marker horizon in the Bangemall Group. Its lithology is black, massive chert, which can be homogenous in appearance or characterized by diffuse, light coloured laminations that are planar, wavy or contorted.

Cubic crystal moulds, presumably after pyrite, are widespread. Possible gypsum moulds occur in several localities. Marshall (1968) has reported acritarch microfossils from the formation. Micro-textures show the chert was deposited as a silica gel, which has undergone at least 80 % compaction.

The depositional environment seems to have been that of shallow, stagnant, and at times hypersaline water in which silica was precipitated chemically in anaerobic conditions.

The Discovery Chert is the first unit in the Bangemall Basin which does not show major facies variations.

Devils Creek Formation

This is predominantly a dolomite and silty shale sequence, with occasional siltstone and fine-grained sandstone. Cross-bedding is uncommon, but low angle, small to medium scale troughs and planar foresets, as well as climbing ripples, are locally abundant. Erosional scours up to 10 cm deep, and a breccia consisting of slabs of dolomite (up to 30 cm long) in coarse-grained dolarenite are present. A few oolite bands and one stromatolite occurrence have been found.

Some 10 km south of the Irregully Gorge (on Edmund Sheet) the author was shown an outcrop of Devils Creek Formation (Fig. 1.09), 20 metres stratigraphically above the Discovery Chert, consisting of chert fragments and slabs of dolomitic siltstone in dolomite. This rock is interpreted by G.Chuck (1983, pers.comm.) as a debris flow.



Fig. 1.09: Possible debris flow in the Devils Creek Formation.

The shale, siltstone and fine-grained sandstone beds of the Devils Creek Formation are vari-coloured, and often have small load casts on the bedding surfaces; the proportion of shale to dolomite in the formation is laterally and vertically variable.

The environment of deposition is interpreted as lagoonal (carbonate deposition) and shallow water shoals (coarser grained dolomite, siltstone). Shallow water mass-gravity flows however, may have occurred locally.

Overlying formations

Younger formations of the Bangemall Group than the Devils Creek Formation do not occur in the vicinity of the Jillawarra Belt, and will only be summarized briefly, here. Description of these units is given in Brakel and Muhling (1976) and Muhling et al. (1979).

The Ullawarra and Curran Formations are overlying the Devils Creek Formation and are composed of shale, mudstone and chert, with sand-

stone and minor dolomite (in the Ullawarra Formation). Both formations have been deposited in deeper water open marine setting.

The overlying Coodardoo Formation and Fords Creek Shale are characterized by well bedded greywacke, and interbedded shale/siltstone with minor amount of quartz arenite and greywacke. These sediments were introduced into the basin by turbidite flows and traction currents.

From the Fords Creek Shale upwards the Mount Vernon Sandstone and Kurabuka Formation are characterized by decreasing water depth of deposition; a near-shore barrier bar system is inferred for the Mount Vernon Sandstone, and lagoonal deposition for the shale and mudstone of the Kurabuka Formation. The latter is the youngest unit in the western facies of the Bangemall Basin.

1.2.5.3. Development of the western facies

Sedimentation began in the western part of the basin which overlies the core of the Capricorn Orogen - the Gascoyne Province. Subsidence created horsts and grabens with steeply dipping faults.

Alluvial fan deposits, on the flanks of horst blocks, are overlain by a transgressive marine sequence of stromatolitic dolomite, sandstone and pyritic (black) shale, which was deposited in lagoon, barrier bar and shelf (at times euxinic) environments. The basement granitic and metamorphic rocks were the source of the terrigenous clastic sediments.

The transgressive sequence ended with deposition of the Discovery Chert, which covers an area of 38.000 km² and shows no major facies variations. Gypsum crystal moulds and traces of barite indicate the chert was deposited in hypersaline water.

A shallow marine platform sequence overlies the Discovery Chert and represents shoals of carbonate interfingering with terrigenous shale and sandstone. Local debris flows indicate seismic activity. An ensuing phase of widespread subsidence is marked by turbidite sheets overlain by marine shelf shale.

The end of sedimentation in the basin is characterized by a regression development from the Fords Creek Shale upwards. This is seen as a progradational sequence which could portray the last stage of the infilling of the basin before the end of marine deposition.

1.2.6. Igneous rocks in the Bangemall Basin

The igneous rocks in the Bangemall Basin consist of basic intrusive and felsic volcanogenic rocks. The intrusives represent enormous volumes of basaltic magma and were injected chiefly as sills, but also as dykes. Rhyolite and basalt occur rarely. The following description is mainly based on the yet unpublished Bangemall Bulletin (in press).

1.2.6.1. Mafic igneous rocks

a) Dolerite sills

Dolerite sills crop out over an area of about 143.000 km² in the Bangemall Basin, thus making one of the largest intrusive tholeiite provinces of the world.

Sills can exceed 100 metres in thickness, and may be simple tabular bodies, or irregular bodies that vary in thickness quite markedly. The most extensive single sheet has a length of over 60 km. Sheets are generally concordant with the bedding of the country rock but may locally crosscut it in zones that vary from less than a metre to hundreds of metres.

The sills occur preferentially in shale, siltstone and chert, but are uncommon in sandstone. The Discovery Chert and the Curran Formation, both relatively thin units, are commonly split in two by a sill. Dolerite is especially abundant in the Ullawarra Formation.

Sills are absent from the Tringadee and Coodardoo Formation, and the Mount Augustus Sandstone. In the Irregularly Formation they are present only on Edmund Sheet, in the northwestern part of the basin; and they are rare in the Kiangi Creek Formation.

There are apparently two controls on the stratigraphic sites of dolerite emplacement:

- I) The relation between intrusives and host lithology can be attributed to the relative ease of injection of magma into the more fissile rocks at a specific stratigraphic level.
- II) The absence of significant sills in the three lower formations (Tringadee, Irregularly, Kiangi Creek Formation) suggests a time-dependence of dolerite intrusion; i.e. the geotectonic situation developed to a tensional crustal regime before injection of dolerite took place.

It is evident that the sills were intruded before folding of the Bangemall Group because they are folded and in fold cores are converted to chlorite schist.

Petrology

The primary mineralogy of a typical specimen is plagioclase, augite, pigeonite or orthopyroxene, magnetite, subordinate quartz and orthoclase in interstitial granophyric intergrowth, pyrite, and rare olivine. This mineral assemblage is typical of tholeiitic rocks.

The texture is sub-ophitic, and plagioclase laths are wholly or partially enclosed in larger pyroxenes. The grain size is usually less than 3 mm. Apart from fine-grained chilled margins and gabbroic phases in few thick sills, there is little variation in the medium-grained texture.

The petrology of the intrusive rock is uniform over the region, indicating an unvarying origin and rapid emplacement without assimilation of country rock. Xenoliths of wall rock are rare, but examples occur where flow banding is visible in the dolerite around the xenoliths, which themselves have been rounded and plastically deformed.

Chemistry

Thirteen dolerite samples have been analysed for the Geological Survey of Western Australia. The variation in chemistry of the Bangemall dolerites is small (Tab. 1.02), and is consistent with their uniform appearance and the lack of evidence of differentiation. Comparison of the chemical composition and C.I.P.W. norms of typical tholeiitic and alkaline basalt elsewhere in the world (Carmichael et al., 1974; Table 2-1) with those of the Bangemall dolerites confirms the latter are tholeiitic.

A discrimination diagram (Fig. 1.10), using Ti, Zr and Y, shows that the Bangemall dolerites plot in the field of "within plate" basalts (modern oceanic island and continental basalts) rather than in the field of "plate margin" basalts (volcanic arc and oceanfloor basalts), after Pearce and Cann (1973).

CHEMICAL COMPOSITIONS OF BASIC INTRUSIONS, BANGEMALL BASIN

	37458	37459	37460	37461	37462	37463	37464	39409	39435	41604	50721
20	50.80	50.80	53.00	56.60	49.80	51.10	51.40	49.80	51.20	48.90	48.00
61	1.58	1.59	2.66	1.56	2.47	1.77	2.26	2.02	1.42	2.97	1.94
40	13.80	14.00	11.30	14.20	12.70	13.60	14.50	13.00	13.60	12.40	13.30
70	3.20	2.00	6.50	2.70	7.10	3.30	5.60	4.00	1.60	7.10	2.90
18	8.90	10.10	10.50	8.40	8.76	8.76	7.94	9.40	8.83	9.33	11.90
19	0.18	0.18	0.25	0.16	0.21	0.17	0.16	0.21	0.18	0.20	0.23
46	6.80	5.04	2.07	2.39	4.91	5.17	3.65	5.50	5.37	4.11	5.97
64	9.18	9.24	4.89	5.74	8.92	8.34	7.82	10.50	6.12	7.01	8.56
29	2.36	2.53	5.19	3.72	2.37	2.40	2.56	1.67	1.64	3.02	2.86
59	1.27	1.26	0.79	1.66	0.93	1.78	1.90	0.42	1.31	1.43	0.57
15	0.20	0.18	0.50	0.28	0.26	0.21	0.19	0.20	0.17	0.26	0.14
57	1.30	1.33	2.08	2.06	1.29	2.67	2.03	3.07	4.77	2.40	3.30
33	0.33	0.36	0.52	0.35	0.61	0.63	0.42	0.35	0.32	0.43	0.25
03	0.05	0.05	0.05	0.03	0.11	0.05	0.06	0.03	3.74	0.04	0.02
50	100.00	98.70	100.30	99.80	100.40	99.90	100.50	100.20	100.30	99.60	99.90
30	0.60	0.56	0.17	0.50	0.44	0.83	0.83	0.28	0.90	0.53	0.21
00	300.00	263.00	330.00	145.00	308.00	269.00	197.00	233.00	218.00	264.00	470.00
12	0.14	0.19	0.27	0.50	0.13	0.23	0.27	0.08	0.42	0.17	0.04
50	450	500	220	600	300	1000	450	240	350	400	180
<1	<1	<1	<1	<1	<1	<1	<1	<1	<1	<1	<1
60	40	40	80	60	60	40	80	20	20	80	40
50	50	45	35	30	50	40	50	40	30	60	50
20	160	850	70	50	200	170	95	70	90	210	150
18	18	18	15	21	21	18	18	15	12	18	15
20	<20	40	40	40	<20	<20	60	<20	<20	40	<20
20	10	30	20	10	80	20	10	10	20	10	10
1	1	1	1	1	1	1	1	1	<1	<1	1
70	140	80	5	15	60	80	30	50	60	55	60
<5	<5	5	20	10	5	<5	<5	<5	<5	5	<5
25	35	30	10	94	14	55	80	15	50	45	10
35	35	35	45	35	40	35	30	50	50	40	45
<5	<5	<5	<5	<5	<5	<5	<5	<5	<5	<5	<5
210	260	210	75	190	200	240	300	200	120	260	240
<10	<10	<10	<10	10	<10	<10	10	10	<10	<10	<10
8	6	70	2	2	80	6	4	6	4	4	16
<20	<20	<20	<20	<20	<20	<20	<20	<20	<20	<20	<20
<1	<1	<1	<1	<1	2	<1	<1	<1	<1	<1	<1
320	280	340	180	280	420	300	460	420	360	550	440
25	25	30	50	35	35	30	30	30	25	30	25
110	200	115	98	110	140	115	82	110	94	125	130
150	165	180	240	240	420	180	210	150	120	225	135

Sample numbers. Analysis by Western Australian Government Chemical Laboratories.

LONGITUDE	LITHOLOGY	SAMPLE	LATITUDE	LONGITUDE	LITHOLOGY
118°40'15"E	Dolerite	37463	24°55'15"S	120°05'30"E	Dolerite
118°45'30"	Dolerite	37464	25°11'40"	121°53'40"	Dolerite
117°05'50"	Dolerite	38409	24°09'30"	116°26'45"	Dolerite
119°28'45"	Dolerite	39435	24°25'15"	117°18'30"	Dolerite
118°10'45"	Gabbro	41604	24°16'45"	118°36'00"	Dolerite
117°19'20"	Leuco-Dolerite	50721	23°41'15"	115°36'30"	Dolerite
118°14'15"	Fine grained dolerite.				

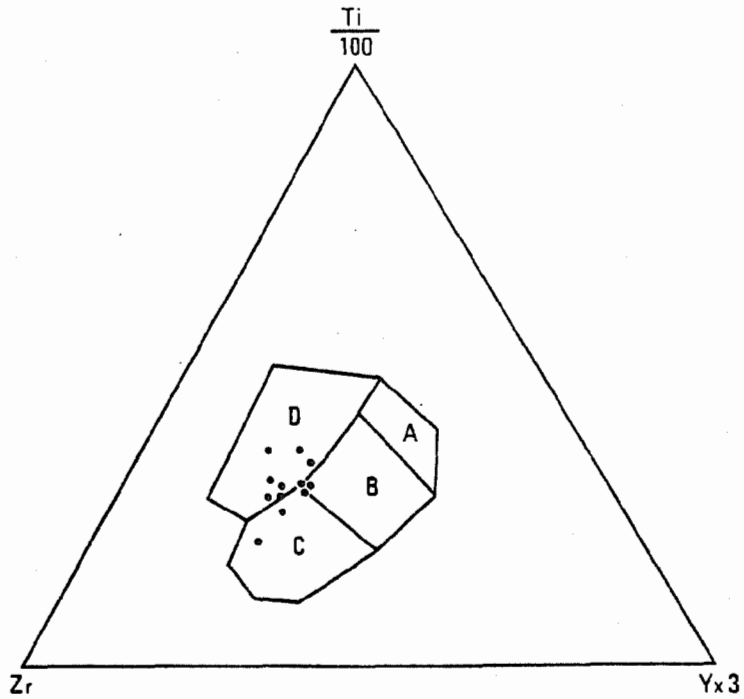


Fig. 1.10: Discrimination diagram using Ti,Zr and Y. Fields of tectonic setting of basalts are after Pearce and Cann(1973).

- D - "Within plate"basalts i.e. ocean island or continental basalts
- C and B - Calc-alkali basalts
- B - Ocean floor basalts
- A and B - Low-potassium-tholeiites

The other chemical features of the Bangemall dolerites (Tab.1.03) are similar to continental tholeiites in that they have high K_2O , a high $Fe_2O_3:FeO$ ratio, and high Ba, Rb, Pb, Th and U compared with oceanic tholeiites. In summary, the chemistry of the Bangemall dolerites could be regarded as that of high- TiO_2 continental tholeiite.

b) Dolerite dykes

The mineralogy of the dykes is similar to that of the dolerite sills. Most are 1 to 2 metres wide, but the largest is 50 metres wide and 15 km long.

Table 1.03 Geochemical ranges for oceanic and continental tholeiites compared with Bangemall dolerite

		Oceanic tholeiite	Continental tholeiite		
			Karoo	Oenpelli	Bangemall
K ₂ O	%	0.08-0.57	0.60-0.95	0.38-1.06	0.42-1.93
TiO ₂		1.26-2.03	0.45-1.29	0.95-2.66	1.17-2.97
P ₂ O ₄		0.12-0.23	0.03-0.17	0.08-0.37	0.14-0.50
Fe ₂ O ₃ /FeO		0.25-0.36	0.02-0.88	0.09-0.33	0.18-0.81
K/Rb		230-1020	130-170	224-378	145-470
Ba	ppm	5-16	16-360	149-305	180-1000
Rb		1.14-22	20-38	9-32	10-95
Sr		90-320	140-400	216-338	75-300
Pb		1.29-0.56	< 10	2-8	10-80
Th		0.15-0.13	80-160	2-40	<10-10
U		0.09-0.16	8	<2-2	< 1-2
Zr		45-160	85-90	46-170	105-420

Source of data:

Oceanic tholeiite - from Table 8-1, columns 1-3 and 5-8, Carmichael et al. (1974)

Karoo - from Table 9-2, columns 2-6, Carmichael et al. (1974)

Oenpelli - from Table 2, Stuart-Smith and Ferguson (1978)

Note: complete analyses of Bangemall dolerites are given in Table 1.02

Two generations of dykes exist. The earlier dykes are seen to be feeders to the sills, while later dykes transect the sills and folds in the sedimentary formations and postdate the main period of tectonism.

Many dykes of the later generation trend between north and east-northeast. There are also dykes in some of the north-northeasterly lineaments of the eastern part of the basin, and most of these lineaments are probably unexposed dykes.

c) Basic volcanics

Some altered basalt occurs in the northwest of Bullen Sheet (lat. $24^{\circ}12'20''$ S, long. $120^{\circ}04'30''$ E). The flow is approximately 4 metres thick, has a sharp basal contact on pebbly quartz arenite, and is overlain by coarse-grained quartz arenite.

Unequivocal evidence of basaltic flows elsewhere in the basin is lacking.

1.2.6.2. Implications of mafic magmatism

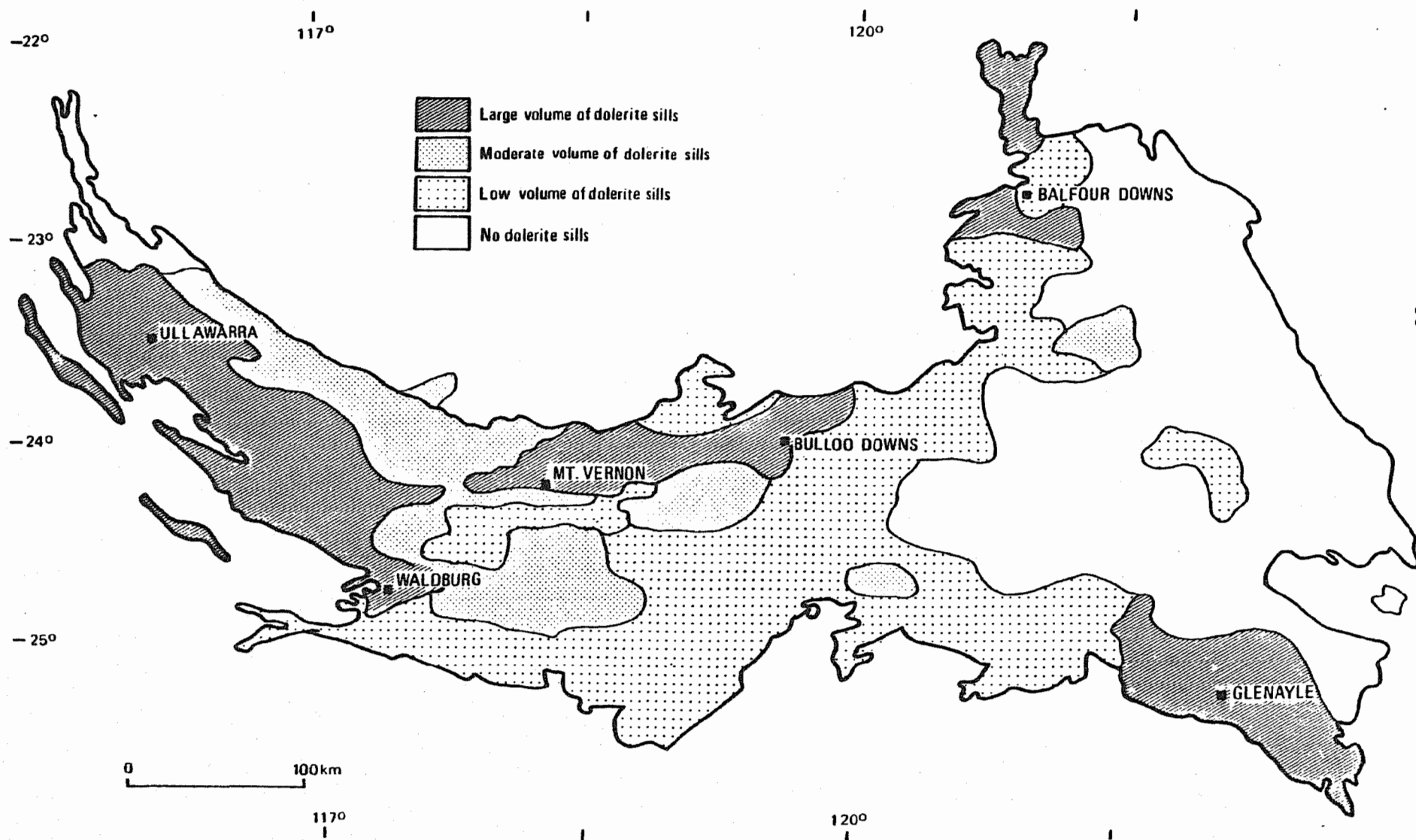
The isolated small basalt flow described above (paragraph c) demonstrates that tholeiitic igneous activity had started while sedimentation was still going on.

A passive intrusion at shallow depth is inferred, in which dense, mafic magma flowed gravitationally under less dense sediments.

The presence of a major tholeiite province where mantle-derived magma was passively emplaced at shallow depths in a subsiding, infilling basin must indicate a tensional regime in the crust during sedimentation.

The distribution of sills (Fig. 1.11) shows that the greatest concentrations occur in the western part of the basin, and along the

Fig. 1.11: Abundance of dolerite sills within the Bangemall Basin



southern and northwestern margins of the wide eastern part of the basin. The pattern suggests (Bangemall Bulletin, in press) "an embryonic rift valley which bifurcates into two smaller arms east of a triple junction at the 120° E meridian".

1.2.6.3. Felsic volcanogenic rocks

Only two definite occurrences of rhyolite and two probable tuffs were found during regional mapping of the GSWA, and it is concluded in the Bangemall Bulletin (in press) that felsic volcanics played a very minor role in the evolution of the Bangemall Basin.

Rhyolite and felsic lavas

The most significant rhyolite occurs in the eastern part of the Jillawarra Belt within the lowermost West Creek Formation. It has been studied and dated (1098 ± 42 m.y.) by Gee et al. (1976) and is described in chapter 2.4.

Compston and Arriens (1968) dated an acid lava by the Rb-Sr method at approximately 1080 m.y.; the location and petrology of the rock is not documented, but it is believed to form a dyke and related flow in the Jillawarra Formation near Mount Palgrave, in the westernmost part of the Bangemall Basin.

11 km southeast of Abra ($24^{\circ}43'43''$ S / $118^{\circ}39'05''$ E) a further volcanogenic rock has been found within ferruginous shale of the Backdoor Formation (eastern facies). It is a greyish, massive, siliceous rock with angular clasts of altered ferruginous shale, and without any lamination or bedding. The area of outcrop is about 80 x 80 metres and rapid pinching out into all directions can be observed. It consists of a very fine-grained quartz-chlorite groundmass in which occasional angular and/or embayed quartz grains float. The shale clasts are composed almost entirely of chlorite and other very fine-grained phyllosilicates.

The rock has been interpreted as a waterlain tuff by Geopiko petrologists. However, it is plug-shaped and cuts across the stratigraphy, it continues along strike for less than 80 metres, and it carries angular clasts of country rock; all this rather suggests a felsic volcanic vent.

Possible volcanogenic rocks (tuffs)

Fine-grained highly potassic rocks were found at two localities; one again in the Backdoor Formation 12 km northwest of Tangadee (in the eastern facies), and the other in the Ullawarra Formation, about 7 km southeast of Jillawarra Bore.

The possible derivation of high K-content of sedimentary rocks from a tuffaceous component has been reviewed by Davy (1975) and it is suggested in the Bangemall Bulletin (in press) that the high-potash rocks in the Bangemall Basin represent devitrified glassy tuffs.

1.2.6.4. Summary

The igneous rocks of the Bangemall Basin comprise large volumes of mantle derived continental tholeiite and very few occurrences of felsites, which probably are products of localized crustal melting (Gee et al., 1976).

Thus, the components of bimodal volcanism are present in the Bangemall Basin; however, comparing the volume of mafic and felsic igneous rocks the latter can be neglected.

1.2.7. Mineralization in the Bangemall Basin

According to the Bangemall Bulletin (in press) mineralization in the Bangemall Basin can be divided into the following groups:

1. Lead-copper-barite in the Gap Well Formation of the Jillawarra Belt (this Formation correlates with the Irregularly Formation elsewhere in the Bangemall Basin)
2. Copper and lead in carbonates of the Irregularly Formation
3. Stratabound zinc with minor copper
4. Fault/fissure deposits of copper at the contact between shale and dolerite
5. Gold at the Bangemall Mining Centre
6. Surface enrichment of manganese
7. Stratabound phosphate

1.2.7.1. Description of low-grade mineralizations outside the Jillawarra Basin

The lead-copper-barite mineralization in the Gap Well Formation (Group 1) is one of the main subjects of this study (see section 4). Here, only groups 2 and 3 are described; the remaining groups seem unrelated to the mineralizing processes operative in the Jillawarra Belt and reference is made to the Bangemall Bulletin (in press) for groups 5 to 7, and to Marston (1980) for group 4.

2. Copper and lead in carbonates of the Irregularly Formation: Minor showings of copper and lead (\pm zinc) are scattered throughout carbonates of the Irregularly Formation in the western Bangemall Group. The mineralization is either disseminated or associated with quartz veins, some of which occupy shear zones in dolomite. The mineralization may also form irregular lodes within brecciated,

silicified algal dolomite (Blockley, 1971). Primary minerals commonly are galena and chalcopyrite. Blockley (op.cit.) has classified one deposit as Mississippi Valley type. He also gives details of the form and grade of all these occurrences. However, the Cu-Pb association is uncommon in Mississippi Valley deposits (e.g. Sangster, 1976).

Alcoa of Australia Ltd. (unpublished report) has recently drilled three diamond holes into the Irregularly Formation between the Isabella and Candolle Synclines (app. 24°25' S / 116°58' E). Low-grade Zn-Cu mineralization in carbonaceous mudstone, and minor Pb-Zn mineralization in brecciated dololomite were encountered in two holes. This mineralization is analogous to the Abra mineralization with respect to the following features:

- a) hosted by the Irregularly Formation (correlating with the Gap Well Formation in Abra);
- b) adjacent to a basement structural high of granite, the Mount Augustus "Block" (Alcoa Report), like the Coobarra Dome east of Abra;
- c) adjacent to a major NE-trending, synsedimentary photo-lineament, marking the eastern margin of the Mount Augustus "Block", like the Abra Fault System.

An important difference to Abra however, is the dominance of zinc and the lack of barium.

3. Stratabound zinc with minor copper:

Stratabound zinc-copper occurrences are present in black shales and carbonaceous siltstone of the Jillawarra Formation (three occurrences) and the Glen Ross Shale Member of the Kiangi Creek Formation (one occurrence).

The mineralogy and geochemical features of the mineralization are studied by Smith and Davy (1978), Davy (1980) and Marston (1980).

Main primary sulphides are pyrite, sphalerite and covellite, and Davy (1980) concluded that the greater part of the mineralization has formed syngenetically in unconsolidated sediments, in a strongly reducing environment. The mineralizations are very low grade and are sub-economic.

The Quartzite Well mineralization is of particular interest among these occurrences of stratabound zinc with minor copper. It is located in overthrust siltstone and calcareous siltstone of the Jillawarra Formation, on the northern side of the Quartzite Well Fault, in the central Jillawarra Belt (see map 1 for location of Quartzite Well, and section C-D on map 1 for structure of the Jillawarra Formation).

The main sulphide mineral is pyrite (up to 60 % of whole rock) in several morphological types ranging from fine-grained disseminated over massive to authigenic euhedra. Locally pyrite is pseudomorphous probably after gypsum (Fig. 1.12) indicating hypersaline conditions of sedimentation. Interestingly, Inco Australia interpreted the facies of the Jillawarra Formation in their Glen Ross Spring prospect (some 30 km WNW of Quartzite Well) as hypersaline or sabkha, too (P.Harrison, 1983, pers.comm.).

Pyrite also occurs in the form of atoll structures (Fig. 1.13) which are described by Love and Zimmermann (1961) from the Mount Isa Shale. However, no replacement of the core or the rim by other sulphides has been observed. In Tab. 1.04 microprobe analysis of various morphological types of pyrite are presented.



3 cm

Fig. 1.12: Lath-shaped moulds filled by pyrite, possibly after gypsum, in black siliceous shale.

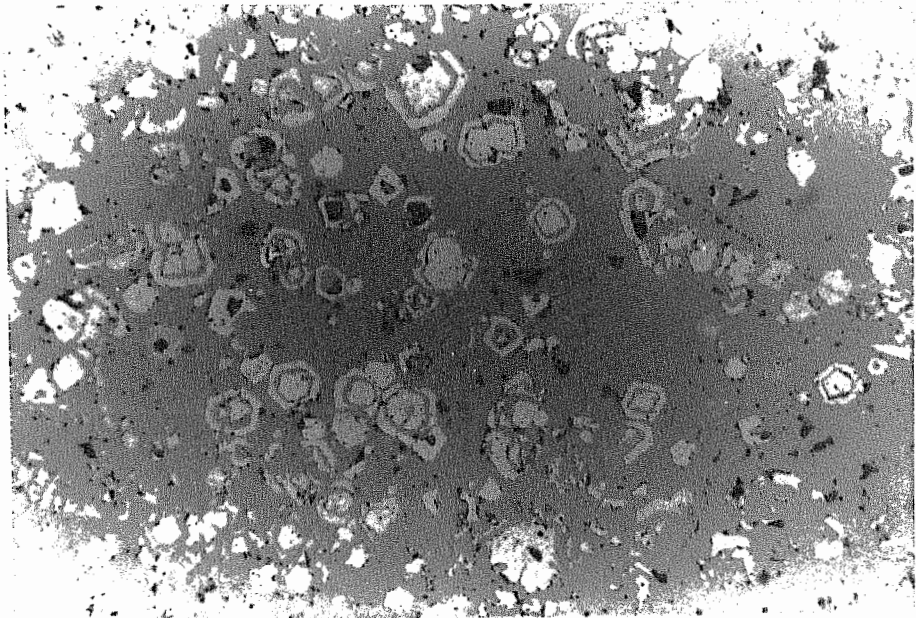


Fig. 1.13: Atoll pyrite in black siliceous shale of the Jilla-warra Formation. White - pyrite; grey - shale; black - holes. Base of picture = 0.58 mm, reflected light (-).

Table 1.04

Microprobe analyses of pyrite from carbonaceous shale (up to 60% pyrite) with zinc-mineralization, Jilawarra Formation

	76-14-250m anhedral, massive	76-14-250m subhedral, aggregates	15916 euhedral	15916 atoll-core	15916 atoll-rim
Fe	46.142	46.023	45.689	45.588	45.328
S	52.601	53.699	52.409	47.603	51.152
As	0.348	0.058	2.274	1.005	1.556
Co	0.000	0.000	0.000	0.000	0.000
Ni	0.000	0.051	0.001	0.031	0.075
Total	99.091 %	99.831 %	100.373 %	94.227 %	98.110 %
Fe	47.044	46.077	46.026	44.996	45.675
S	54.359	54.042	50.919	48.157	50.165
As	0.217	0.097	0.329	1.566	1.219
Co	0.000	0.000	0.000	0.000	0.000
Ni	0.000	0.000	0.015	0.030	0.115
Total	101.619 %	100.198 %	97.289 %	94.750 %	97.174 %
Fe	47.253		44.707	45.434	45.594
S	53.981		50.709	51.082	51.815
As	0.117		2.857	1.991	1.224
Co	0.000		0.000	0.000	0.000
Ni	0.004		0.000	0.000	0.039
Total	101.356 %		98.247 %	98.507 %	98.673 %

Sphalerite is the main ore mineral, and occurs in veins, disseminated or as irregular masses within aggregates of pyrite. Microprobe analyses (Tab. 1.05) are in accordance with the Fe-content reported by Davy (1980) for sphalerite from the other stratabound zinc with minor copper occurrences in the Bangemall Basin.

Tab. 1.05: Electron microprobe analyses of sphalerite

Quartzite Well 76-12 195.2 m, "ore chert"				
Fe	0.687	2.378	2.246	1.280
Cu	4.004	1.170	0.294	1.407
S	30.819	32.647	33.795	33.167
Zn	64.581	66.376	62.045	61.664
Cd	0.123	0.180	0.258	0.278
Mn	0.003	0.000	0.000	0.000
In	0.000	0.000	0.000	0.137
Total	100.217	102.751	98.737	97.933

The above description of the Quartzite Well mineralization is intended to highlight some features which may have connotation for the ore forming processes of the Abra-type mineralization. A more detailed and comprehensive study of the Quartzite Well mineralization is given by Davy (1980).

Most striking is the predominance of zinc in the Quartzite Well mineralization as opposed to the copper-lead dominance and paucity of zinc in the Abra-type mineralization. In view of the different metal abundances the conclusions of Davy (1980) seem inappropriate. He suggests that the source of metals is either connate or paleo-river (spring) water for zinc, and mechanical erosion of older strata for (detrital?) copper. But connate or other ground waters should transmit the geochemical characteristics of the underlying strata, i.e. should be Cu, Pb dominated and not carry zinc. For the copper sulphide, a detrital origin from e.g. the adjacent "basement high"

(the rocks of the Manganese Range Anticline, see map 2) is unlikely, because this area was covered by younger sediments at that time, and has been upfaulted and eroded after the deposition of the Bangemall Group (see chapter 2.3.).

In this study it is concluded that the metals were derived from hydrothermal solution which ascended along the Quartzite Well Fault. The vicinity of most of the stratabound zinc with minor copper occurrences to major fault zones or lineaments is recognized in the Bangemall Bulletin (in press) and it is tentatively suggested that they principally have the same mode of origin.

The barium content of the Quartzite Well mineralization (about one order to magnitude higher than the other mineralization) may indicate a link to the Abra-type hydrothermal system; this possible relation is discussed in chapter 4.7.

1.2.7.2. Summary

The mineralizations in the Jillawarra Belt have features in common with the Zambian Copperbelt (Fleischer et al., 1976) and McArthur River (Lambert, 1976) for group 3, and carbonate hosted lead-zinc deposits (Sangster, 1976) or sediment-hosted massive sulphide deposits (Sangster and Scott, 1976) for group 2. However, the metal abundances within these groups of mineralizations are unique, and render comparison with the above deposits difficult.

All mineralizations in the Bangemall Basin are sub-economic with the exception of the Abra mineralization, Section 4. Currently, no mining activities occur. Mining in the past included treatment of approximately 6000 tons of Cu-ore and concentrate yielding 1403 tons of copper (Marston, 1980), from the group 4 type of mineralization. And 4.735 kg gold recovered from 179.18 tons of ore in the Carnarvon Gem, the main mine of the Bangemall Mining Centre (group 5).

Section 2 The Jillawarra Belt

2.1. Introduction

In the course of the GSWA 1 : 250 000 mapping program of Western Australia the area of the Jillawarra Belt (on Mt Egerton 1 : 250 000 sheet) was mapped by P.C.Muhling, A.T.Brakel and W.A.Davidson in 1973-4. In their map and the respective explanatory notes (Muhling et al., 1978) they attributed the rocks of the Jillawarra Belt to the Irregully and Kiangi Creek Formation.

In the explanatory notes of the adjacent sheet to the east (Collier 1 : 250 000 sheet, Brakel et al., 1978), however, the authors state a "more complex deformational history in the phyllitic varieties" of the same rocks and therefore postulate an older age. They conclude that the rocks are related to the western part of the Nabberu Basin and that they may be equivalent to either the Padbury Group of Robinson Range (Elias and Williams, 1977) or the axial sequence of the Glengarry Sub-basin (Bunting et al., 1977).

Similar uncertainties with respect to the stratigraphic position of the rocks of the Jillawarra Belt are evident from company reports: while Geopeko (1980) attributes them to the Bangemall Group, Amoco (1977) inferred an upthrust block of older Proterozoic rocks.

There are indeed a number of distinct features of the Jillawarra Belt which have not been reported from the Bangemall Basin:

- a) An apparent high metamorphic grade expressed by some chlorite-biotite-quartz-magnetite schists of the Manganese Range and a widespread chloritization of sedimentary rocks in the Jillawarra Belt.
- b) The variability in lithology of the chloritic carbonate rocks compared to the dolomitic siltstones and dolomites of the Irregully Formation in the Bangemall Basin.

- c) The occurrence of tight anticlines and open synclines, both with subsidiary folding on the limbs while in the Bangemall Basin usually the synclines are tight.
- d) The apparent lack of mafic igneous rocks so abundant in the Bangemall Group (i.e. the dolerites).

Four model lead datings performed by J.R.Richards since 1980/81 put further constraints on the age of the Jillawarra Belt. For the fault mineralization of the Quartzite Well Fault the model ages yield 1490 m.y. while for samples from the TP Prospect and 46-40 Prospect (see map 3 for locations) the calculated age is in the order of 1510 ± 10 my. (Richards, written communication, 1982). Leads from the Abra mineralization give an apparent age around 1600 m.y. However, isotopic inhomogeneities (i.e. mixing) of the lead masses analysed cannot be excluded (Richards, written communication, 1984).

To clarify the uncertainties caused by the peculiar geological features and the problems of the lead-lead modelling a study of the sedimentary and tectonic history of the rocks of the Jillawarra Belt was undertaken. In the following chapters the results are presented which attribute the Jillawarra Belt to the Bangemall Group and thereby erect a stratigraphic and tectonic framework for the genesis of Abra Pb-Cu-Ba mineralization.

2.2. The basement

Granitic basement is occupying large areas in the Coobarra Dome at the eastern margin of the Jillawarra Belt. The granite is a biotite-muscovite adamellite which is deeply weathered leaving a loosely aggregated rock with gritty appearance. Probably due to weathering the only abundant minerals recognized in hand-specimen are even and medium-grained muscovite and quartz arranged in typical granitic textures; foliation is poorly developed; locally some quartz-tourmaline veins and pegmatitic phases are present and veins of colourless fluorite have been noted occasionally (Brakel et al., 1978). No thin section could be prepared from this rock.

In 1981 a very small granitic outcrop has been found in the bottom of a creek bed in the western part of the Jillawarra Belt. It is stratigraphically important as it is forming the core of the Woodlands Dome which now is the only locality where the entire stratigraphy of the Jillawarra Belt can be seen. Of the Bangemall Group overlying the eastern granite some 1000 metres of the Gap Well Formation are missing.

Whereas the eastern granite is overlain unconformably by the Bangemall Group, in the area of the western granite poor outcrop renders the same statement difficult; it is assumed in this study, though, that the granites form a common basement to the younger rocks of the Jillawarra Belt.

2.3. Stratigraphy, lithology and facies of the Bangemall Group in the Jillawarra Belt

In view of the distinct nature of the rocks outcropping and encountered in drill holes in the Jillawarra Belt, and their apparent peculiarity, new stratigraphic terms have been designed.

The lowermost part of the sedimentary succession rests unconformably on granitic basement; it is now termed Gap Well Formation, which is overlain by the West Creek Formation. From the West Creek Formation upwards the similarity of the rocks of the Jillawarra Belt with Bangemall formations elsewhere allows the use of established formation names of the Bangemall Group. Table 2.01 shows the stratigraphy of the Jillawarra Belt and the possible correlation with the Bangemall Group.

Field mapping of the Gap Well Formation, in which the mineralization occurs, suggests a subdivision into six units. Total thickness can exceed 1000 metres. The hanging wall West Creek Formation - lacking significant mineralization - consists of four units and its thickness is in the range of 1000 metres, too.

In the Jillawarra Formation a lower dolomitic and/or arenaceous unit can be distinguished from the well known upper shaly portion.

It should be noted that these subdivisions have been established on the basis of field appearance; in drill core the respective lithological boundaries are sometimes difficult to recognize. In this chapter the stratigraphic units of the Jillawarra Belt are described with respect to their field characteristics, their representatives in drill cores and their petrology. For each unit the assumed depositional environment is discussed at the end.

The classification of the clastic rocks was performed according to Pettijohn (1975), that of the carbonate rocks according to Dunham (1962).

Table 2.01: Stratigraphy of the Jillawarra Belt and possible correlation with the Bangemall Group stratigraphy of Muhling et al.(1978)

Thickness	Map Symbol	Formation	Lithology	Map Symbol	Formation	Lithology	Thickness	Remarks
50-100	MV	DEVILS CREEK FORMATION:	turbiditic dolomitic siltstone and shale; locally large volumes of dolerite sills					
	MD	DISCOVERY CHERT:	massive to laminated chert; locally large volumes of dolerite sills					
100-600	MJ _a	JILLAWARRA FORMATION:	varicoloured silica-rich and iron-rich laminated shale; subordinate dolerite sills common siltstone; shale; sandstone; dolomitic siltstone; dolomite					
0-300	MJ _d							
0-230	WC ₄	WEST CREEK FORMATION:	coarse grained sandstone; quartz-pebble conglomerate intercalations; limited lateral strike extent					
0-750	WC ₃		siltstone; dolomitic siltstone; minor immature sandstone					
170-500	WC ₂		turbiditic sandstone, siltstone and shale; grades eastward into feldspathic sandstone and conglomerate					
0-200	WC ₁		rhyolite and minor related lapilli tuff; emplaced in basal portion of WC ₂					
	WC ₁		interbedded siltstone, coarse grained immature sandstone and polytacl conglomerate; discontinuous laterally					
350	GW ₆	GAP WELL FORMATION:	laminated siltstone; dolomitic shale; barrier reef stromatolitic dolomite					
250-350	GW ₅		siltstone with coarse grained sandstone intercalations; minor stromatolitic dolomite					
0-250	GW ₄	WOODLANDS ARENITE MEMBER:	coarse grained sandstone; discontinuous laterally					
20-150	GW ₃		siltstone with ripple marks; interbedded sandstone, 2-300 cm thick					
100	GW ₂		dolomite; dolomitic shale; minor coarse grained sandstone					
80	GW ₁		laminated siltstone; sandstone; minor dolomitic siltstone					
				Emv	Devil Creek Formation	Dolomitic and shale	0 to 800 +	
				Emd	Discovery Chert	Chert, subordinate shale	10-125	Laminated rocks, wavy bedding common
				Emj	Jillawarra Formation	Shale, siltstone, minor chert and dolomite	0-1300	
				Emk	Kiangi Creek Formation	Sandstone, shale, subordinate dolomite and minor conglomerate.	0-1800	Stromatolites in one dolomite member
				Emkg	Glen Ross Shale Member	Shale	125-325 +	
				Emi	Irregully Formation	Dolomite, dolomitic shale, shale and minor sandstone	0-2000	Stromatolites present
				Eme	Tringadce Formation	Sandstone with conglomerate lenses	0-1650	Lenticular basal formation of Bangemall Group
				Emt	Top Camp Dolomite equivalent	Shale, dolomite and Sandstone	2300	Stromatolites present. Equivalent to all units below Ford's Creek Shale

The term calcareous implies a carbonate component in general which comprises calcite, dolomite and some Fe-Mn carbonates.

For evaluation of the petrology thin sections from about 160 field samples and about 100 core samples were examined. In figure captions to the photographs of thin sections, (+) indicates crossed nicols and (-) parallel nicols.

2.3.1. The Gap Well Formation

is subdivided into 6 units which are numbered GW₁ to GW₆ comprising the basal 1000 metres of the Bangemall Group. This formation is characterized by dominant carbonates, and the name Gap Well is derived from the Gap Well and Bore, 24^o 38'5, 118^o 14 E, where topographic dolomite ridges are abundant.

2.3.1.1. GW₁

This unit is outcropping only in the central part of the Woodlands Dome, dipping radially away from the granite core. Its thickness exceeds 100 metres with a variable lithology. Abundant quartz veins (up to 20 cm wide) form an irregular cross pattern of "reefs" in the breakaway valley plains.

The base of this unit consists of a basal grit which formed on the granitic surface. The field appearance is that of a quartz-muscovite rock with poor schistosity. In thin section it is confirmed that the rock is composed only of quartz and muscovite. Quartz is characterized by large angular grains, a few moderately rounded grains and aggregates of cherty quartz. Metamorphic muscovite flakes are abundant, occurring in a honeycomb texture within quartz. Some textures resemble sericitized feldspars; however, the zones of relict-feldspar are made up of quartz (Fig. 2.01).

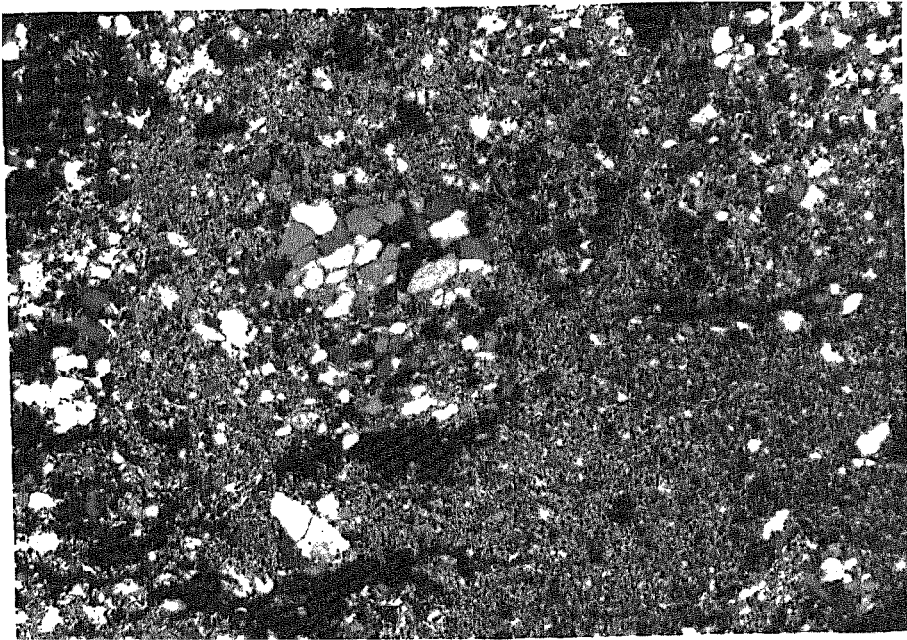


Fig. 2.01: Angular quartz aggregate resembling feldspar; in a quartz-muscovite matrix. Base of picture = 3.6 mm (+).

An irregular banding, expressed by the arrangement of quartz and muscovite may be interpreted as either incipient schistosity or relict bedding.

A rock chip from a percussion drill hole at Coobarra Hill (i.e. from the area of the eastern granite) exhibits a similar texture; however, the composition is dominated by microcline (plus some sanidine) and quartz with subordinate newly grown muscovite, minor plagioclase, weathered biotite and rare chlorite and zircon.

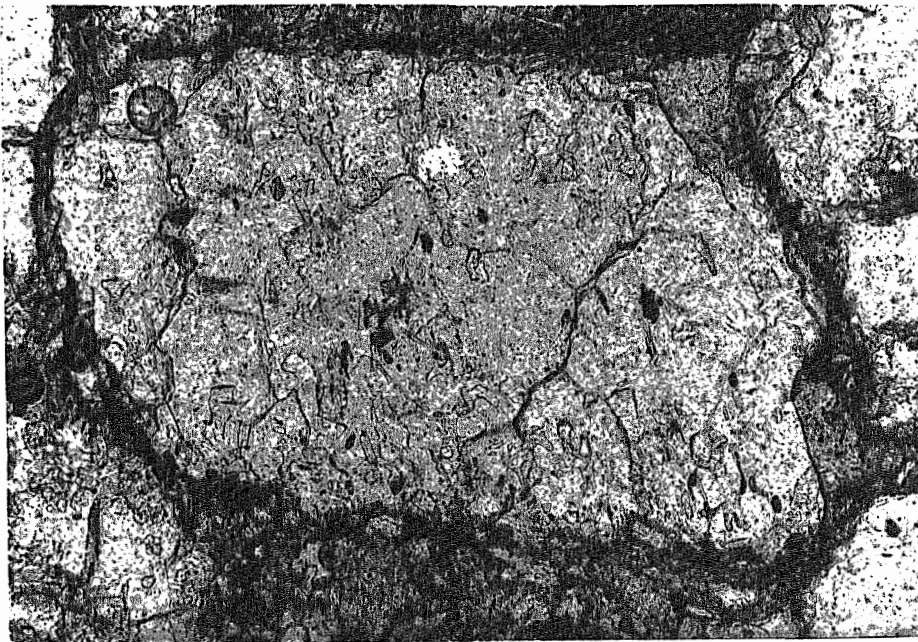
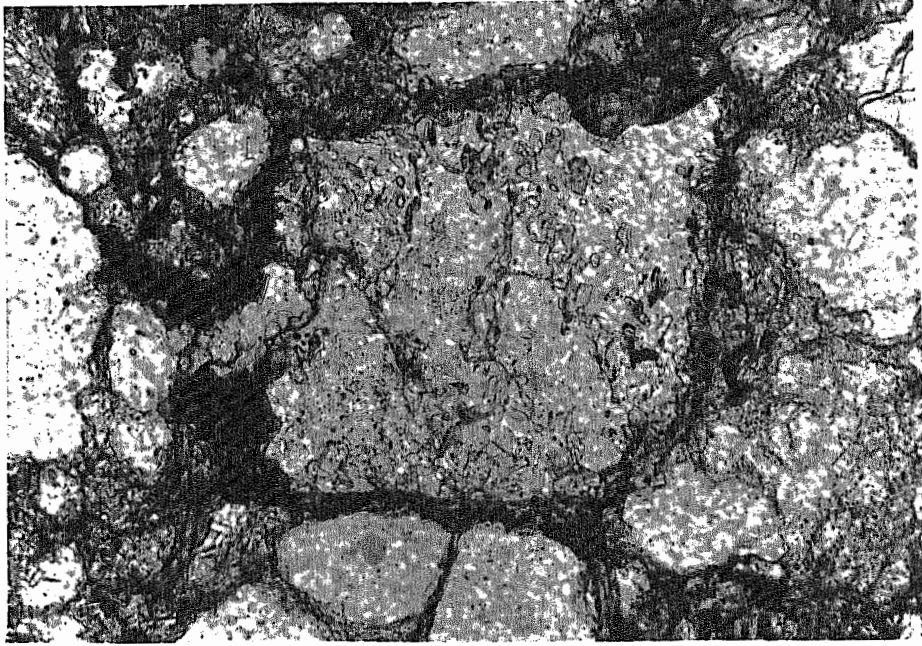
From the fact that potash feldspar was not significantly altered and muscovite is the only newly formed mineral a very low metamorphic grade can be inferred.

The basal grit above both the western and eastern granite probably was deposited as a talus slope breccia during times of subaerial exposure of the granite.

The dominant rock type of the GW₁ unit however, is a laminated shale and siltstone which often has a silicified appearance (possibly due to surficial processes). Locally the siltstones are very rich in irregularly distributed cubic moulds, probably representing former pyrite cubes.

In thin section sericitic shale is intercalated with well defined thin layers (50-700 μ) of poorly sorted and poorly rounded siltstone. The siltstone layers consist of angular to subrounded quartz, detrital (?) muscovite and few tourmaline grains whereas the shale bands are dominated by microcrystalline phyllosilicates with brownish tint (surficial ?), some muscovite flakes (400 μ) - elongated parallel to bedding - and rare scattered quartz grains. No feldspars have been observed. Some diffuse opaque aggregates (ca. 200 μ in diameter) in the shale possibly are organic remains.

Arenite beds are more abundant in the basal portion of GW₁. They consist of poorly sorted, moderately rounded medium to coarse-grained quartz sandstone with minor tourmaline and rare zircon. The matrix of very fine-grained phyllosilicates has a brownish tint. It is remarkable that no feldspars could be found although a relatively close, probably granitic source for the clastics can be assumed. However, approximately 5 % angular quartz-sericite aggregates may represent sericitized feldspars which have been silicified later (Figs. 2.02 and 2.03).



Figs. 2.02 and 2.03: Angular quartz-sericite aggregates resembling sericitized feldspars; in medium to coarse grained quartz sandstone. Base of pictures = 0.9 mm (-).

Another significant rock type is a massive, micritic dolomite with abundant magnetite throughout, and frequent quartz-carbonate-barite-magnetite veins. This rock has only been encountered in the bottom 100 m of a diamond drill hole (TP-81-8) of the TP-prospect ca. 2,5 km east of Woodlands Dome, where its position in relation to the overlying units GW₂ to GW₆ places it in GW₁. If this massive dolomite is accepted as time-equivalent of the clastic rocks, the GW₁-unit can be seen as a time of rapidly varying sedimentary environments, laterally and probably with time.

A near-shore, perhaps deltaic environment with carbonate deposition in a more seaward position - indicating that seaward was due east with respect to the Woodland Dome - might account for the features described.

2.3.1.2. GW₂

The distribution of the GW₂-units is shown in Fig. 2.04. This unit forms prominent topographic highs of dolomite on both sides of the Woodlands Dome and is encountered in 2 diamond drill holes in this western area (TP-81-8, TP-Prospect and WD-81-5, Woodland Prospect, Fig. 2.05). In the Manganese Range Anticline the oldest rocks exposed are also attributed to the GW₂-unit, consisting of chloritic siltstone and coarse arenite. Thus this unit, with a thickness of about 100 metres, can be subdivided into a western carbonate and an eastern clastic facies.

The carbonate facies comprises silicified, often manganese capped dolomite (Fig. 2.06) which are distinctly laminated and locally stromatolitic. The stromatolites are extensively altered, at least partially through surficial processes, therefore no determination was possible.

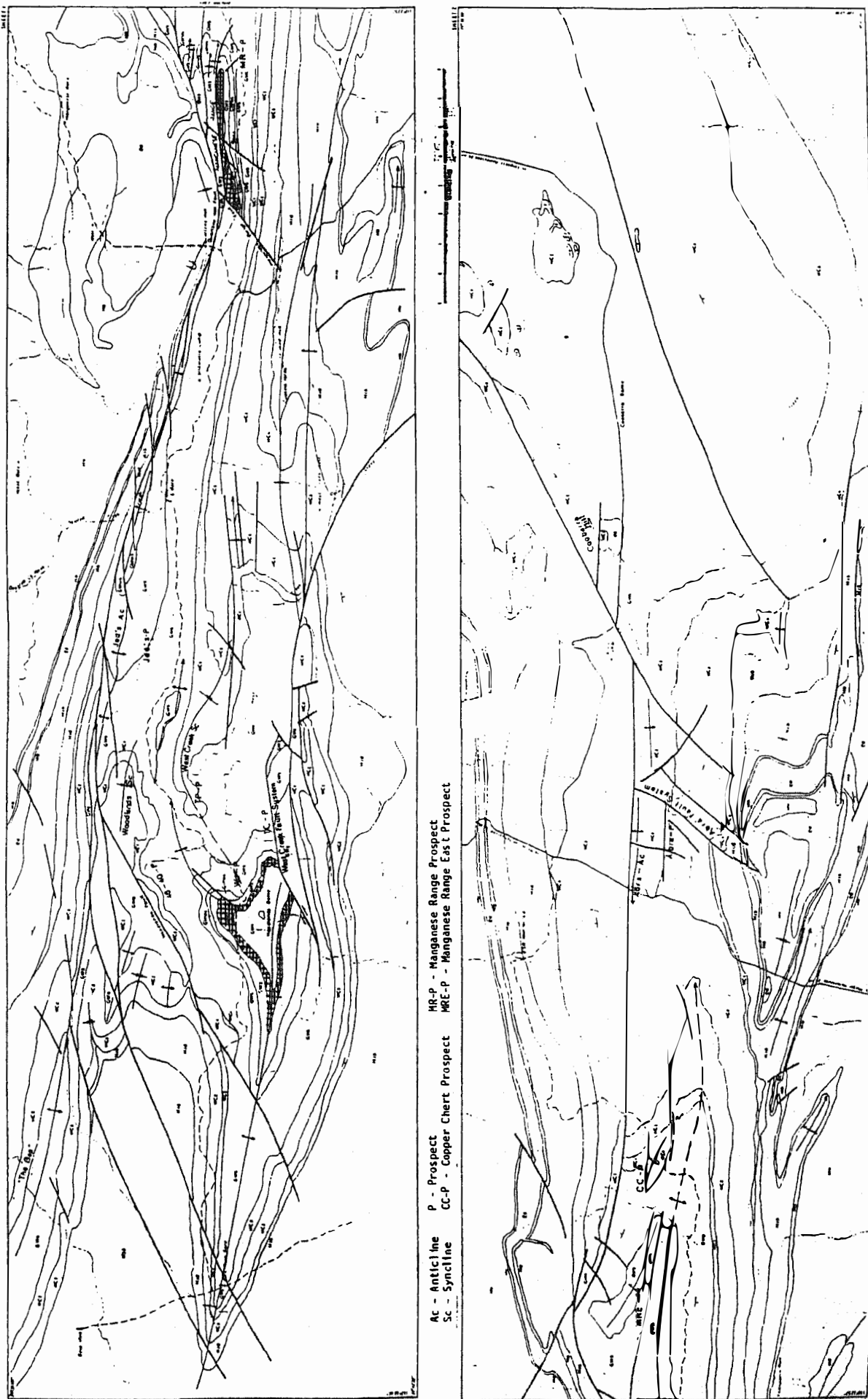
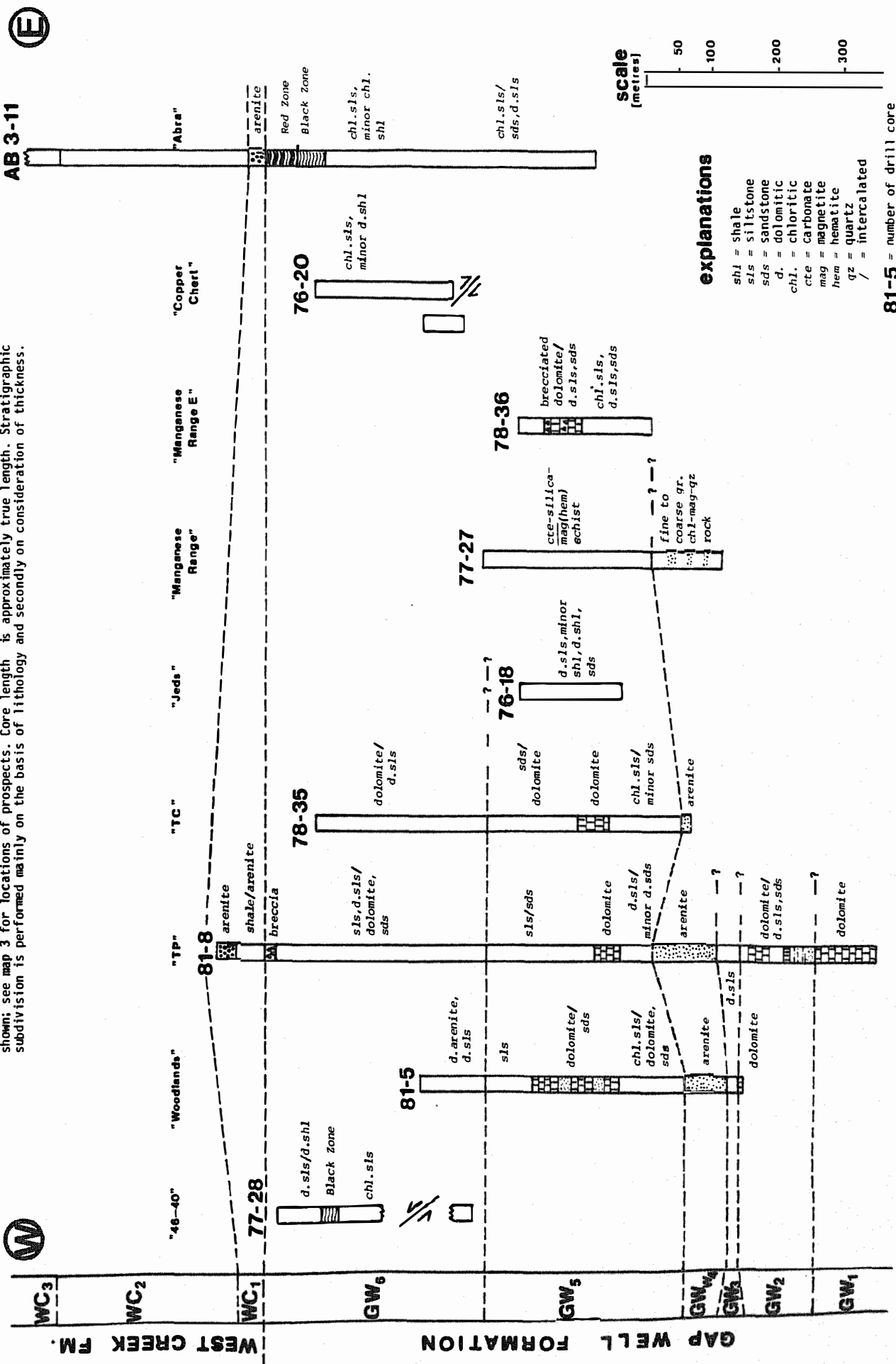


Fig. 2.04: Showing outcrop of the GW₂-unit (cross-hatched) and locations referred to in the text. For detailed geology and locations see map 1 and 3.

Fig. 2.05: Diagrammatic drill core correlation projected onto a W - E section, over 51 km through the Jilawarra Belt (not to scale). Datum is the GW6/MC1 boundary. Names of prospects and numbers of drill holes are shown; see map 3 for locations of prospects. Core length is approximately true length. Stratigraphic subdivision is performed mainly on the basis of lithology and secondarily on consideration of thickness.



explanations

shl = shale
 sls = siltstone
 sds = sandstone
 d. = dolomitic
 chl. = chloritic
 cte = carbonate
 mag = magnetite
 hem = hematite
 qz = quartz
 / = intercalated

81-5 = number of drill core



Fig. 2.06: Silicified, laminated dolomite of the GW₂-unit

On both sides of Woodlands Dome the dolomite forms ridges with approximately 1 km strike length. The southern body is almost surrounded by coarse-grained arenites - possibly former limesands - while the clastites in the vicinity of the northern body are finer grained.

The dolomite is micritic with some lenses and streaks of neomorphic sparite. Layering is defined by variable amounts of dispersed organic material. The amount of clastic quartz grains is probably less than 5 %; some of the quartz now visible in thin section seems to be introduced by early silification processes as witnessed by small, wispy and discontinuous quartz veinlets bordered by sparitic carbonate.

In some of the lenses of neomorphic sparite newly grown euhedral carbonate crystals have incorporated organic material during growth (Fig. 2.07).

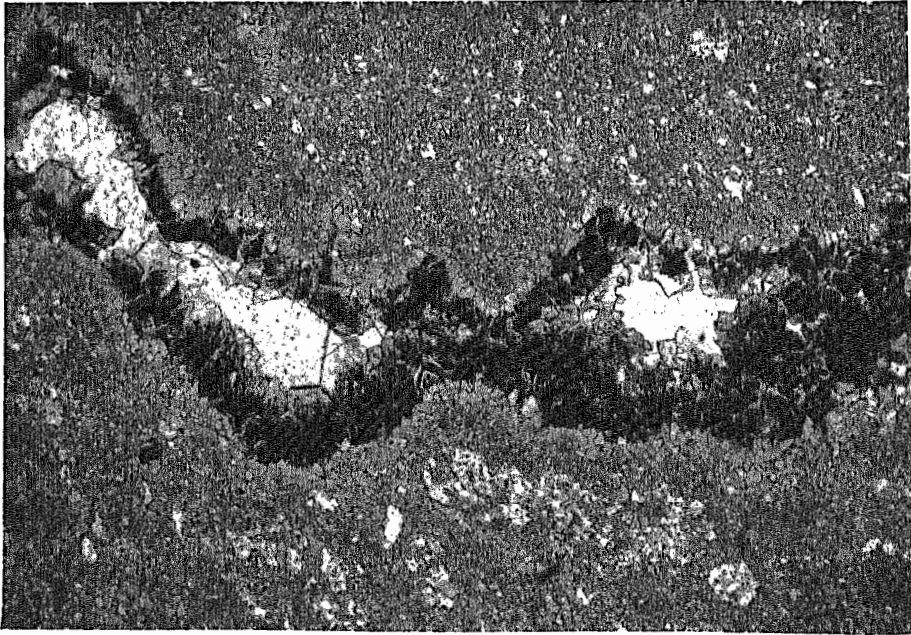


Fig. 2.07: Part of a disrupted algal layer in micritic carbonate. During decay of the organic material sparitic carbonate has grown into the layer. Central parts of the layer consist of quartz. Base of picture = 3.6 mm (-).

Crystal growth has been intermittent as indicated by repeated layers of organic material charting the trigonal edges of several growth stages. These sparitic carbonates commonly form the margin of the lenses while the centre is filled with quartz. On the scale of a thin section it becomes evident that the lenses are a disrupted thin layer (ca. 1mm) of an microbial mat.

If one assumes that the decay of the microbial mats mainly occurs diagenetically it follows that sparitization into open space created by the organic decay was also diagenetic. The central quartz filling could not have been much later, as voids in a soft sediment would be destroyed by incremental compaction.

The presence of quartz in the centre of the lenses further indicates that the chemistry of the diagenetic formation waters in a carbonate sediment pile once reached silica saturation.

The clastic facies occurs in the Manganese Range Anticline. In the eastern part highly chloritic shale and siltstone, locally with strong schistosity obliterating the bedding, are forming the southern limbs of the anticline. Due west towards the probably synsedimentary Manganese Range Fault, a prominent cross-bedded arenite ridge is over- and underlain by dolomitic siltstone and shale.

The arenite can be classified as a well rounded, moderately sorted, medium to coarse-grained quartz sandstone. On fractures in the quartz grains carbonate rhombs can be found. The interstices are filled either with silica cement, or with some opaque cubes (pyrite) and some dark brown to black clusters of needle-like minerals (20 μ long) of rutile or pseudobrookite. The presence of stromatolites indicate a shallow-water environment. Limited strike extent and surrounding clastics suggests that the dolomites of the Woodlands Dome are patch reefs. Although a main feature of patch reefs is their isolated occurrence (James, 1979) the GW₂-reefs are found almost symmetrically on both sides of the Woodlands Dome. A possible explanation would be that the dome had been already emergent in GW₂-times, whereby the central dome was a lagoon or tidal flat bordered seawards by some patch reefs (in the sense of isolated components of a barrier reef).

The high degree of rounding of the arenite at the Manganese Range Anticline suggests a similar environment where the barrier is built of beach sand; however, the arenite itself bears no clear evidence of such a facies as it is generally difficult to recognize the specific facies of high energy deposits and identification only is possible through evaluation of the environmental context.

The dolomitic siltstones and shales including the chloritic schists in the Manganese Range Anticline (probably chloritized former dolomitic lutites, cf. chapter 4.6.) possibly represent the corresponding intertidal facies.

2.3.1.3. GW₃

The distribution of the GW₃-unit is shown in Fig. 2.08. The GW₃-unit, which outcrops in large areas of the Manganese Range Anticline, has a thickness of 100-150 metres. On the limbs of Woodlands Dome and in diamond drill holes in this western part of the Jillawarra Belt (TP-81-8-8, WD 81-5, see Fig. 2.05) thickness is variable and significantly less than in the Manganese Range Anticline.

In the west, outcrop is poor and discontinuous. The dominant rock type is a dolomitic fine-grained siltstone with some interbeds of ferruginous arenite; in drill core dolomitic siltstone is seen to have interbeds of carbonate-cemented arenite suggesting that the ferruginous arenites in outcrop have formerly been dolomitic.

A similar rock type in the southern limb of the Manganese Range Anticline however, lacks carbonates. Here the sericitic, chloritized siltstone has numerous interbeds of arenites from 5-300 cm in thickness. These commonly show ripple marks of the irregular, symmetrical type and are not current ripples. On the northern limb, particularly in proximity to the Quartzite Well Fault and its subsidiaries, deformation is strong and a strong schistosity obliterates the bedding. Significant amounts of iron and manganese seem to have been added to the original sediment here, thus the field appearance is that of a black magnetite-chlorite-quartz schist.

The petrology of rocks from the Manganese Range Anticline is remarkably simple. Quartz, magnetite and chlorite in various proportions

are the dominant constituents with common muscovite and/or sericite plus rare tourmaline and zircon. No feldspars have been found, and the occurrence of carbonate seems restricted to marginal, less deformed or altered rocks away from the major fault system.

In thin section the common siltstone is fine grained, sericitic and contains ubiquitous dispersed opaques. Some very coarse grained detrital quartz grains are scattered irregularly through the rock. Chlorite is abundant and enriched in certain layers. Areas of complete quartz recrystallization are often free of chlorite. Chlorite frequently has grown in pressure shadows of magnetite grains (Fig. 2.09) which can be taken as evidence that a) chlorite generation postdates that of magnetite and b) the formation of this chlorite is related to tecto-metamorphism.

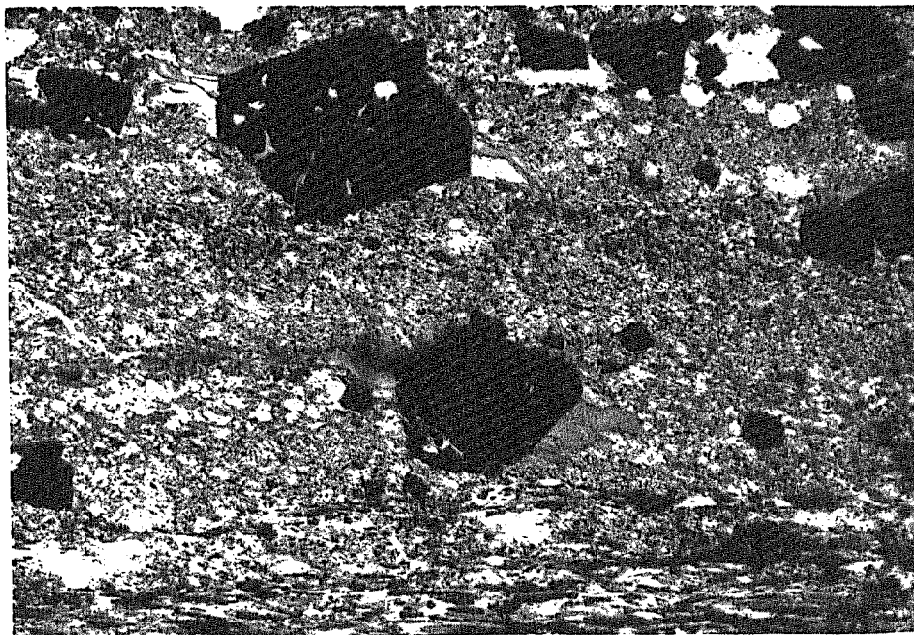


Fig. 2.09: Growth of chlorite in the pressure of shadow of magnetite grains. Base of picture = 3.6 mm (+).

Muscovite behaves similar to chlorite: it clearly has formed later than the magnetite grain it is surrounding (Fig. 2.10), and it is also tailing the edges of euhedral magnetite grains (i.e. has grown in the pressure shadow).

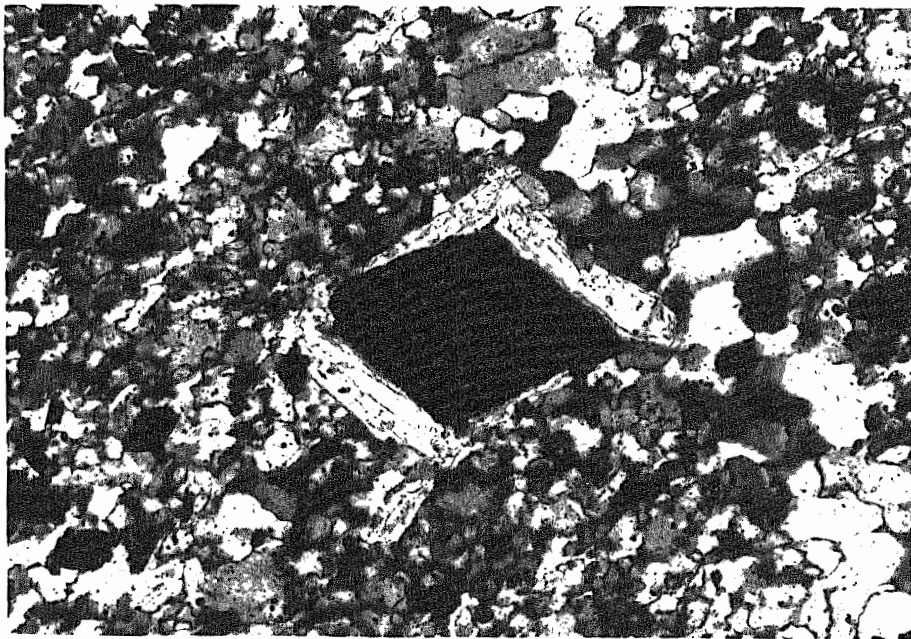


Fig. 2.10: Muscovite surrounding euhedral magnetite.
Base of picture = 0.9 mm (+).

Both chlorite and muscovite have probably been generated through the same process at the same time and it is assumed that compositional variations in the original sediment had some control on the type of phyllosilicates eventually formed.

The arenites often interbedded with the above siltstones are poorly sorted and poorly rounded, medium to coarse-grained quartz sandstones with minor tourmaline. The matrix consists of fine grained chlorite and few scattered muscovite flakes; embedded in the matrix are

10-15 % subhedral, sometimes fractured magnetite grains.

In both arenites and siltstones opaque material of the following forms is abundant:

- a) disseminated subhedral or euhedral magnetite grains (0.1 - 1 mm) which have grown prior to deformation. The grain size seems to decrease with the grain size of the surrounding silicates.
- b) thin (0.05 - 0.5 mm) wispy layers - up to 5 mm long - of an amorphous dark brown material (arranged parallel to the incipient schistosity). They are possibly a late diagenetic product of formerly more dispersed iron oxides and had existed prior to the final compaction. They "wrap" around some detrital quartz grain (Fig. 2.11).

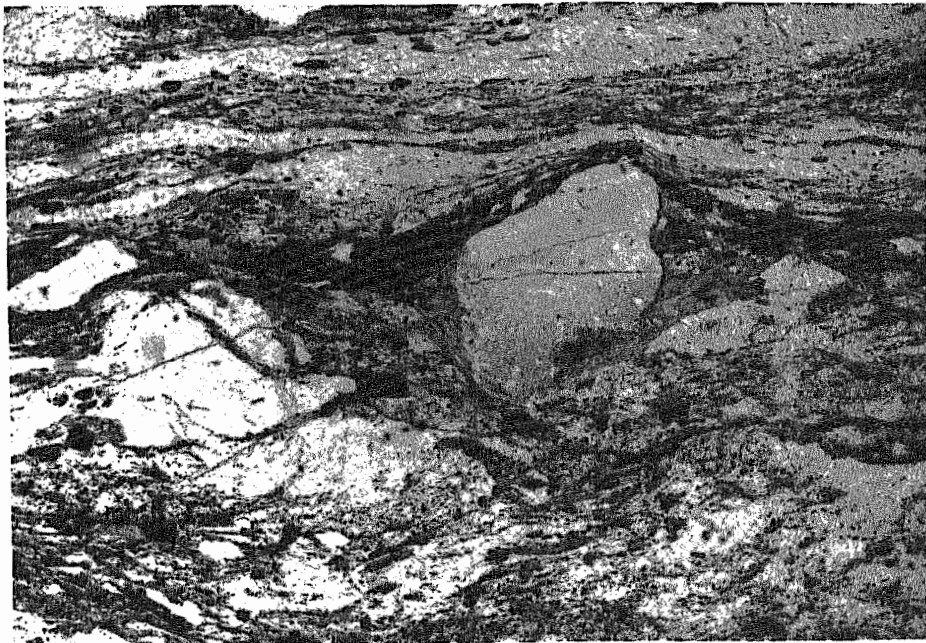


Fig. 2.11: Amorphous iron (hydr-) oxide layer (dark) wrapped around clastic quartz grains. Base of picture = 3.6 mm (-).

- c) fine crystals (15-50 μ), dispersed in phyllosilicate-rich portions and recrystallized quartz layers. The crystals are either anhedral or subhedral and elongated parallel to the bedding. From this elongated crystal shape, in places resembling distorted rhombs (Fig. 2.12), it is inferred that they are hematite.

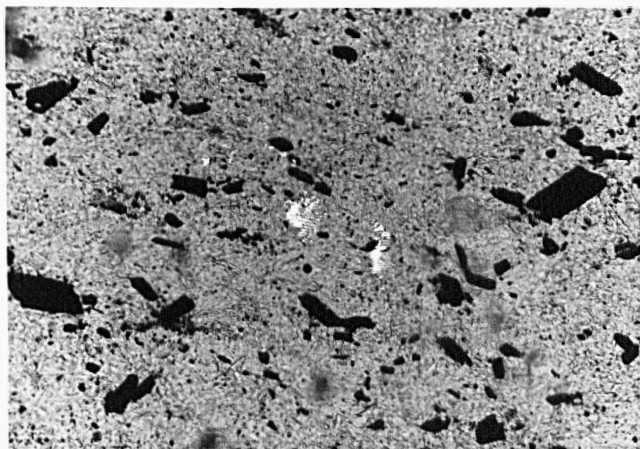


Fig. 2.12: Rhomb-shaped crystals of iron oxides in recrystallized quartz. Base of picture = 0.9 mm (-).

The absence of significant magnetite/hematite bearing veins, the schistose and dispersed nature of the finer iron-oxide phases and the age of larger magnetite grains relative to chlorite/muscovite suggest that most of the iron oxides have existed prior to faulting and thrusting along the Quartzite Well Fault and that the tectono-metamorphism accompanying the thrusting merely led to redistribution of the iron.

Poor outcrop in the west (Woodlands Dome) and high grade of deformation in the east (Manganese Range) complicate the facies analysis. In order to evaluate the nature of the original sediment the lack of carbonate in the GW₃-unit of the Manganese Range requires consideration: In the west as well as in the Manganese Range the sediment is a siltstone with several arenite interbeds, and it is assumed that in both areas the sediment originally was carbonate bearing. In the Manganese Range a later hydrothermal system resulted in extensive silification and introduction of iron, manganese (and base metals), and expulsion of carbonate. The nature and significance of these processes will be discussed elsewhere (see Chapter 4.6.).

Thus, for the facies interpretation it is assumed that the GW₃-sediments are fine grained, laminated, carbonate-bearing siltstones with symmetrical ripple marks, irregularly intercalated with a number of medium- to coarse-grained, poorly sorted and poorly rounded, carbonate cemented arenites. Such sediments are commonly encountered in an intertidal environment where deposition of fine clastics and carbonate occurs. Action of tidal currents produces symmetrical ripple marks, and the poor roundness and sorting of the interbedded arenites suggest deposition as storm deposits (Dimroth, 1979).

2.3.1.4. Woodlands Arenite Member (GW₄)

The name of this sub-unit is derived from the Woodlands Dome around which it forms a prominent ridge of about 2 km strike length. It is convenient to give this unit a special member name because it is consistently mineralized with barite and chalcopyrite (Fig. 2.13).

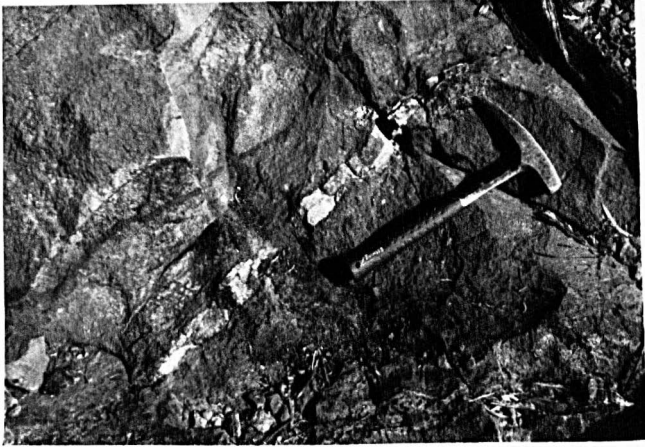


Fig. 2.13: Barite vein in coarse-grained Woodlands Arenite

This unit also outcrops in the Jeds Anticline and in the Manganese Range Anticline (Fig. 2.14). On the southern side of the Woodlands Dome the unit is absent, in the Manganese Range Anticline massive arenite is restricted to the northern limb and the eastern closure. On the southern limb abundant intercalated siltstone render distinction from the GW_3 -unit difficult and it could be argued whether the unit is absent here.

In the Woodlands Dome area the arenite usually is manganiferous and massive with indistinct bedding. Only the western part of the outcrop has some medium scale (1 m) planar cross bedding. Planar cross bedding and ripple marks are common in Jeds Anticline. In the Manganese Range Anticline the arenite is manganiferous and massive, and planar (occasionally of trough type) cross bedding is visible.

Locally, in Jeds Anticline and Manganese Range Anticline, intercalated conglomerates occur, consisting mainly of well rounded quartz pebbles (about 0,5 cm in diameter).

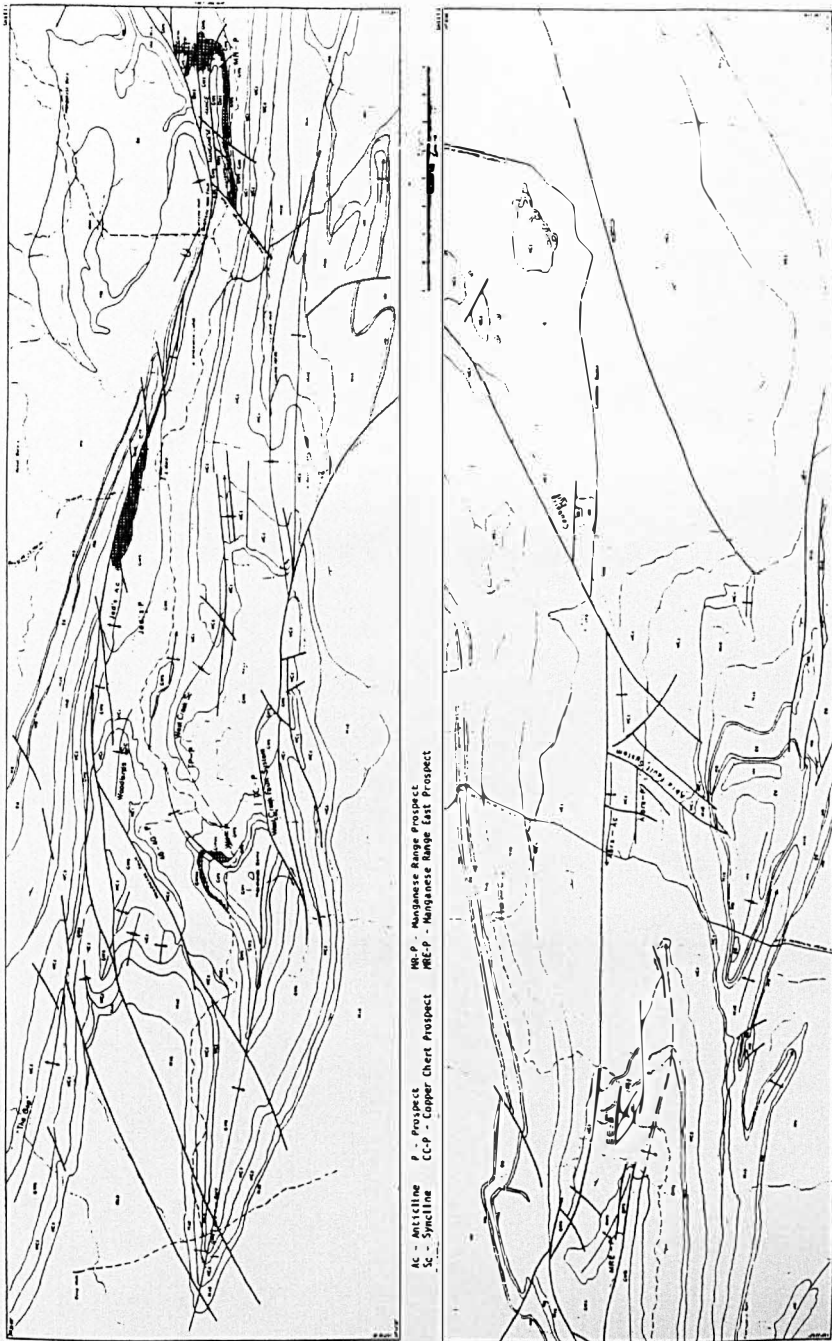
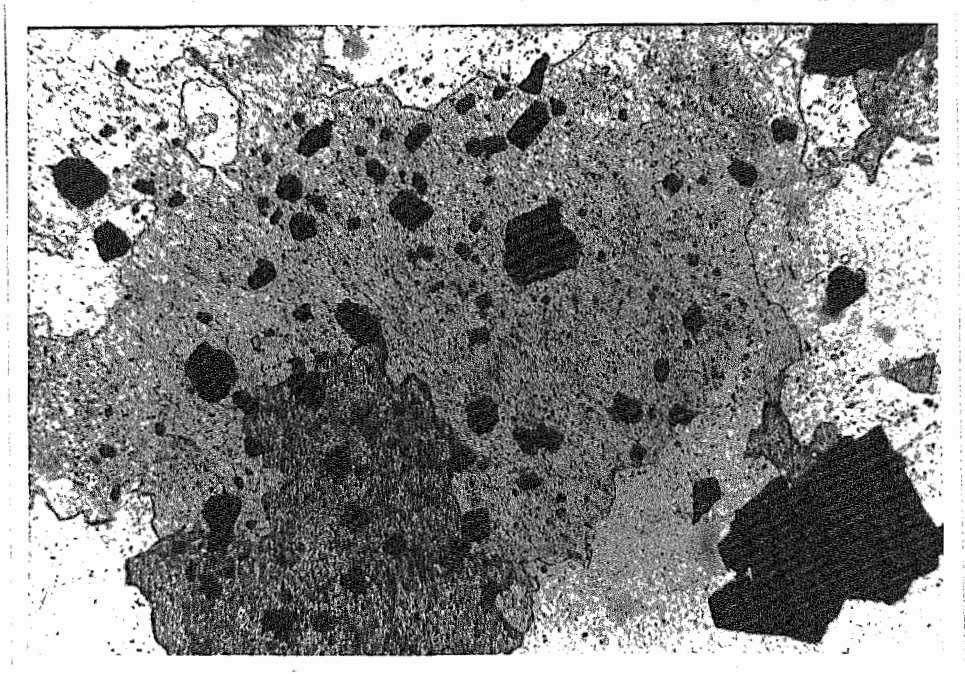


Fig. 2.14: Showing outcrop of the Woodlands Arenite (OWA, cross-hatched) and locations referred to in the text. For detailed geology and locations see map 1 and 3.

The Woodlands Arenite Member is a coarse-grained, rounded, moderately sorted quartz sandstone, the quartz grains having wide seams of secondary quartz. The interstices are occupied by ferroan carbonate (ferroan dolomite; about 10 % Fe as determined by electron microprobe). Abundant anhedral to subhedral opaques (mainly magnetite) usually are dispersed in the carbonate (Fig. 2.15).



· Fig. 2.15: Magnetite grains dispersed in ferroan carbonate.
Base of picture = 0.9 mm (-).

Anhedral irregular masses of barite intermittently are present in places, and various amounts of chlorite and biotite are abundant. Only chlorite however, has been found along the cleavage of feldspars (Fig.2.16).

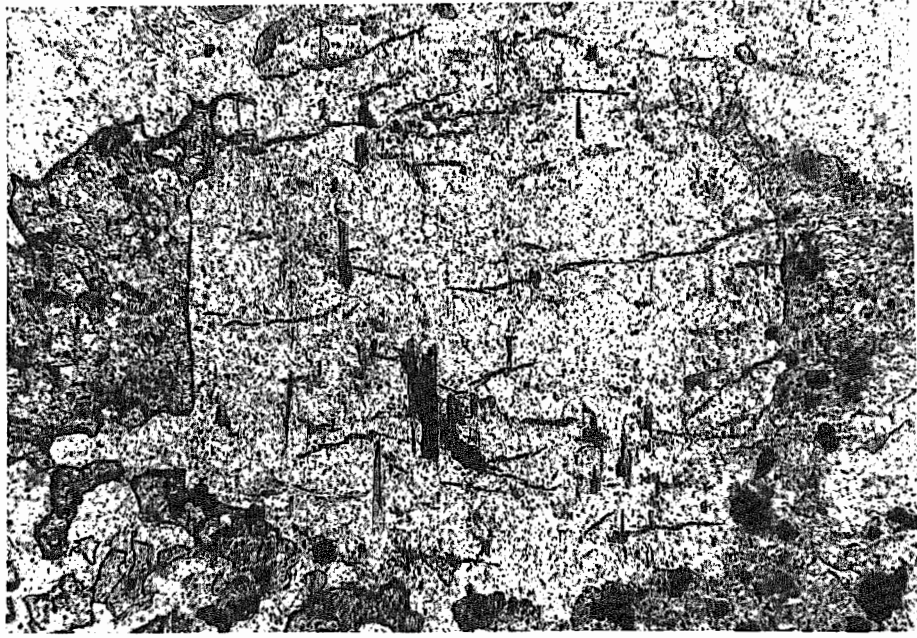


Fig. 2.16: Chlorite on the cleavage of a feldspar grain; associated ferroan carbonate and quartz. Base of picture = 0.9 mm (-).

All feldspars seem to be authigenic, the existence of chlorite along the cleavage of plagioclase suggests that they formed early, probably during diagenesis (Tröger, 1969). Some feldspars associated with magnetite are distinctly zoned, microprobe analysis revealed that they are barium bearing hyalophane (Fig.2.17).

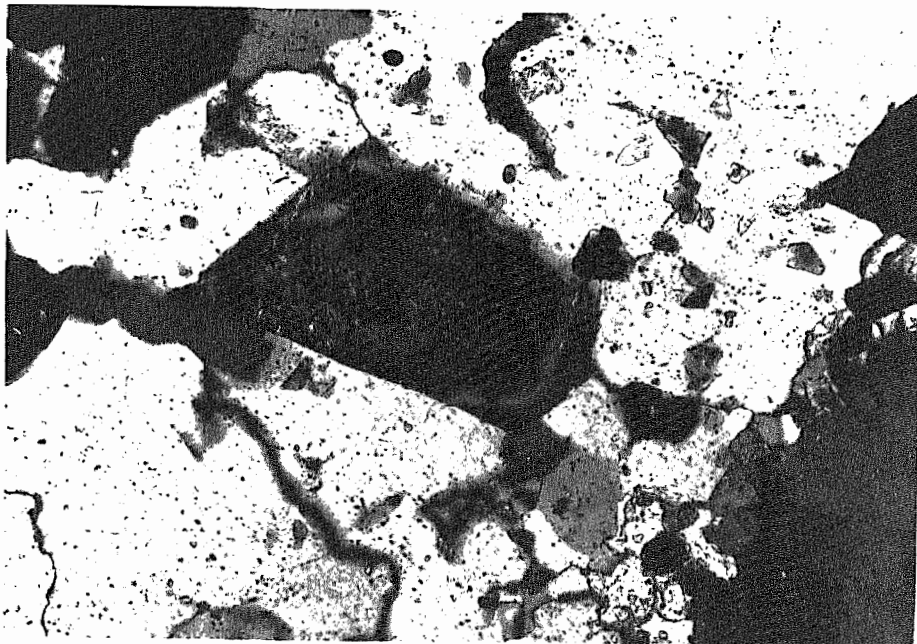


Fig. 2.17: Zoned subhedral hyalophane in recrystallized quartz. Base of picture = 0.9 mm (+).

All components are cemented by abundant secondary quartz the amount of which could hardly be produced by recrystallization of the detrital grains. Most likely additional quartz, together with barite, carbonate and magnetite was introduced into the coarse grained arenite, possibly during diagenesis. Some interstices are filled by a secondary quartz-euhedral carbonate-dispersed opaque phase. Fig. 2.18 illustrates the mobility of these components.



Fig. 2.18: Quartz phase interstitial to carbonate containing inclusions of sub-euhedral carbonate, opaques (mainly magnetite) and barite. Base of picture = 0.36 mm (-).

In the Jeds Anticline the limits of the GW_{W4} outcrop are defined through subsidiary faults of the Quartzite Well Fault. In proximity to one of these faults the arenite is veined by silica-magnetite with an adjacent hematite zone of several millimetres width (Fig. 2.19).



Fig. 2.19: Magnetite veins with hematite halo in silicified arenite. Base of picture approximately 1 m.

This veining has caused some recrystallization of quartz in the immediate vicinity to the vein (1 mm). However, the whole outcrop (100 x 30 metres) is characterized by silification and abundant disseminated magnetite.

The veining probably is contemporaneous with faulting of the Quartzite Well Fault; the straight and sharp nature of the veins resembles veining in lithified rocks and the hematite alteration would be more diffuse in a still water-rich diagenetic sediment. However, it is uncertain whether all iron and silica enrichment of the rock can be attributed to the veining.

Whereas in core samples Fe-carbonate in the interstices is ubiquitous it is lacking in field samples, where the interstices are occupied by diffuse quartz- iron-⁺chlorite phases which may represent the weathered Fe-carbonate (c.f. chapter 4.6.).

A barrier beach complex would serve as a genetic model for the depositional features observed. The arenites are well rounded, coarse-grained, possibly with some penecontemporaneous carbonate as a cementing component. Planar cross-bedding is dominant over trough cross-bedding. Strike length is restricted, the occurrence

of the unit is widespread however. According to the facies model of barrier island systems (Reinson, 1979), these features are compatible with the tidal delta/barrier island parts of the system.

With the above facies interpretation, the Woodlands Arenite Member would be time-equivalent to the GW₃-unit. Thus, the Woodlands Arenite would represent the barrier island system to the GW₃ inter-tidal flats. This view is supported by differences in thickness of GW₃ on the Woodlands Dome: In the North where the Woodlands Arenite has a thickness of more than 100 metres GW₃-outcrop is small; however, on the southern side Woodlands Arenite is absent but GW₃-thickness is significantly larger than in the North.

2.3.1.5. GW₅

The distribution of the GW₅-unit is shown in Fig. 2.20. This unit has variable lithology and thickness. It was encountered in several diamond drill holes (see Fig. 2.05) with a thickness ranging from 250 to 330 metres. Defining the upper and lower limits - particularly when the GW_{W4}-unit is absent - sometimes is difficult due to generally similar lithology of GW₃, GW₅ and GW₆.

Laminated siltstone with interbedded arenite are the prevailing rock types. The siltstone frequently is calcareous, ripple marks are common. At one locality in Jeds Anticline the method of Tanner (1971) for water-depth calculation was applied to some short, irregular, symmetrical ripple marks in fine-grained sandstone. With an assumed grain size of 120 μ the calculation yielded a water depth of 10's of centimetres, a wave height of about 10 centimetres and a fetch (distance from shore line) of 10's of kilometres. If the value of the fetch (which is commonly less with such a water depth) is real, an unusually wide shallow water area was present at that time.

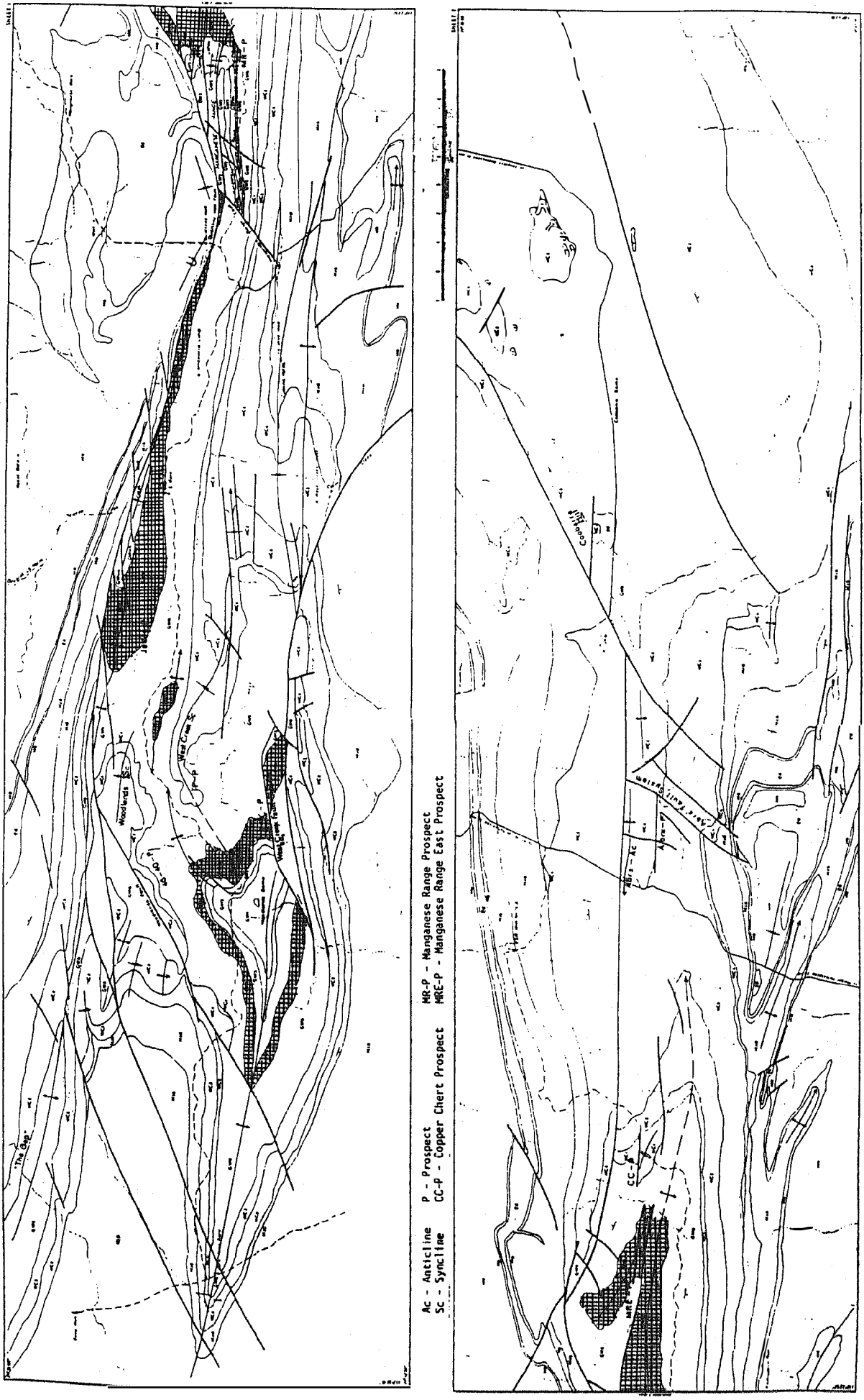


Fig. 2.20: Showing outcrop of the GM5-unit (cross-hatched) and locations referred to in the text. For detailed geology and locations see map 1 and 3.

Arenite intercalations are abundant forming either massive bodies of less than 50 metres strike length or thin sheets (10 - 30 cm thick) with greater strike length. Particularly in the sheet like arenites, cross bedding varies from high to low angle with respect to the bedding planes, the type of cross bedding being dominantly planar.

Towards the top of this unit, regular intercalation of fine-grained dolomitic siltstone and calcareous wacke is common, giving the rock a rhythmically bedded appearance (Fig. 2.21).



Fig. 2.21: Rhythmically interbedded dolomitic siltstone and calcareous wacke in Jeds Anticline.

Occasionally the unit is represented by isolated dolomite bodies, locally with some hitherto unknown stromatolites (Fig. 2.22) forming the top of a well laminated (microbial mats?) fine-grained dolomitic wacke sequence.



Fig. 2.22: Unknown stromatolites in dolomite of the upper GW₅-unit.

South of Woodlands Dome a prominent ridge consists of chloritic fine-grained arenite with intercalations of coarse-grained arenite plus thin (about 20 cm) quartz-pebble conglomerate. Locally very coarse grained, poorly sorted conglomerate with flat, rounded silicified shale clasts of up to 10 cm length occurs.

It becomes evident that the GW₅-unit comprises a number of different lithologies which are subject to rapid changes both vertically and along strike. Their microscopical features will be described in the following:

- a) The laminated siltstone varies from fine to coarse grained and usually has considerable carbonate component. The epiclastic content can become minor, producing a micritic carbonate. The carbonate frequently is ferruginous, usually micritic with patches of neomorphic sparite. Locally bedding is defined by thin (0.4 mm) organic layers into which euhedral carbonate has grown.

The siltstones are sericitic and in places contain large muscovite flakes. When carbonate-rich, biotite and subordinate chlorite are abundant. The biotite is a brownish, weakly pleochroitic variety, but of "usual" biotite composition as confirmed by electron microprobe. Chlorite is pale green and has a characteristic grey birefringence colour. Authigenic albite is widespread.

Chlorite seemingly has grown in the carbonate sediment and later was transformed to biotite as witnessed by patches of biotite in the chlorite (Fig. 2.23). There is textural evidence that

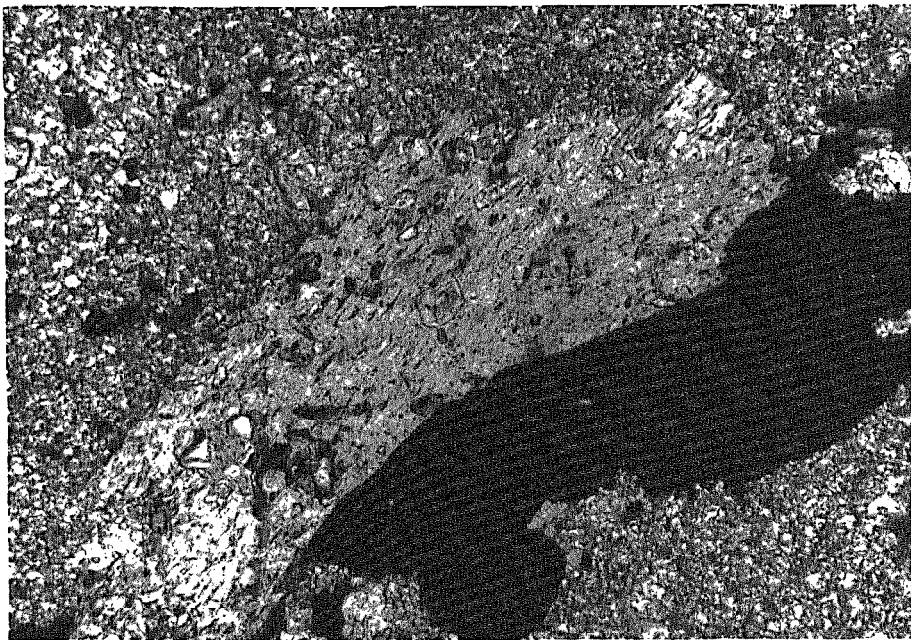


Fig. 2.23: Patches of biotite in almost colourless chlorite adjacent to pyrrhotite. Groundmass is micritic carbonate. Base of picture = 0.9 mm (+).

biotite is one of the latest minerals formed; I) It is replacing authigenic albite (Fig. 2.24) which has grown diagenetically, II) it has formed at the rims of a quartz-galena vein in micritic carbonate and III) its formation apparently is related to tectonic processes as shown in Fig. 2.25 where biotite occurs in the pressure

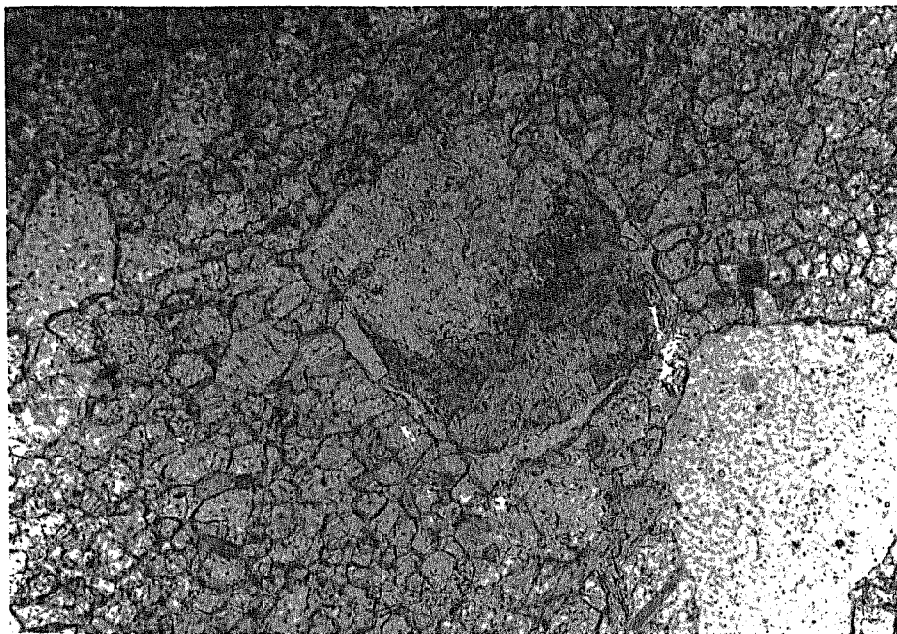


Fig. 2.24: Biotite replacing (?) authigenic albite.
Base of picture = 0.9 mm (-).

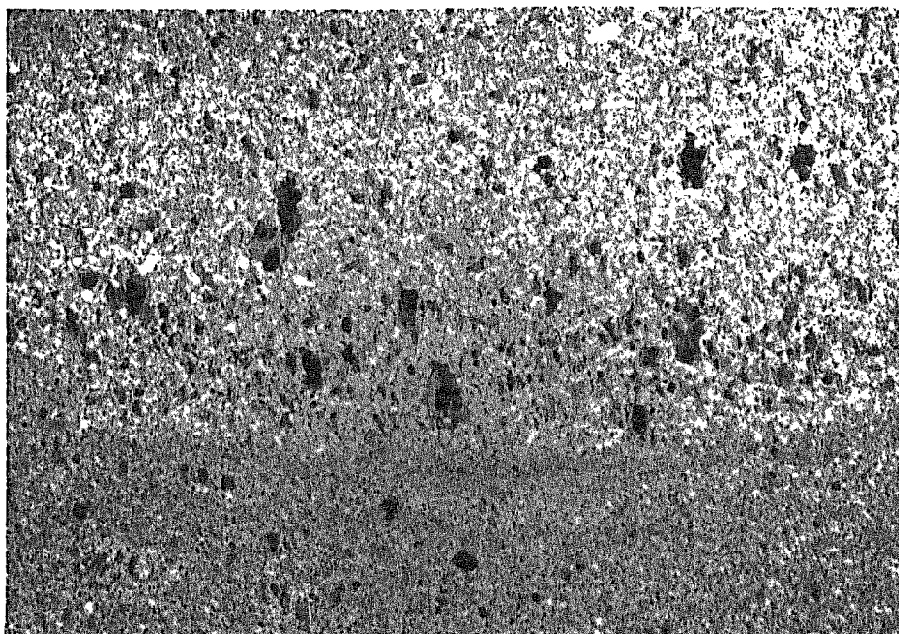


Fig. 2.25: Biotite growth in pressure shadow of magnetite
oblique to bedding. Base of picture = 3.6 mm (-).

shadow of magnetite oblique to bedding. Thus, it probably can be termed (teco-)metamorphic biotite.

However, the composition of the original sediment also has had some control on biotite formation. Some detrital clasts and pellets of micritic (minor sparitic) carbonate in a micritic carbonate matrix have abundant biotite while the surrounding carbonate is almost devoid of it (like Fig. 2.47). The pellets probably were enriched in ferroan dolomite of which the iron and magnesium was utilized for biotite formation during alteration (see chapter 4.1. for chemistry of biotite and carbonate). Regardless of the mechanism of biotite generation it is obvious that it formed later than I) opaque phases, II) the authigenic plagioclase.

Strong alteration can be seen in a drill core interval of MRE (Manganese Range East Prospect) 78-36. A calcareous wacke (described below) is intercalated with some shale bands of about 10 - 30 cm thickness. The shale consists of dominantly pale-green phyllosilicate aggregates intergrown with biotite. In coarser parts authigenic plagioclase is very abundant, along with quartz. Minor relict carbonate is preserved within the shale portion and rare titanite has been found. The alteration processes here removed carbonate and, most important, led to formation of sudoite, which has determined by X-ray diffraction. Sudoite - $K_{<1}(Al, Mg)_2(SiAl)_4O_{10}(OH)_2 \cdot nH_2O$ - belonging to the group of Al-mica clay minerals, has been described by Sudo et al. (1981) as a minor component of the alteration zone (stockwork level) of Kuroko deposits. However, occurrences of sudoite in marls and sandstones with diagenetic overprint are also known (Tröger, 1969).

- b) Calcareous wacke is another abundant rock type of the GW_5 -unit. According to the classification of Dunham (1963) it is a "wackestone". Various portions of clastics (20-50 %) "float" in a micritic carbonate matrix which contains biotite as described

above for the laminated siltstone. Where clastics are absent the rock commonly is recrystallized to sparite.

The clasts comprise mainly angular but some well rounded coarse grained quartz, microcline, ferruginous carbonate pellets and minor shale clasts. Myrmecitic quartz grains indicate some granite in the source region of the epiclastics (Fig. 2.26). Authigenic albite plus secondary muscovite leaves are common, and some of the shale clasts have been entirely biotitized.

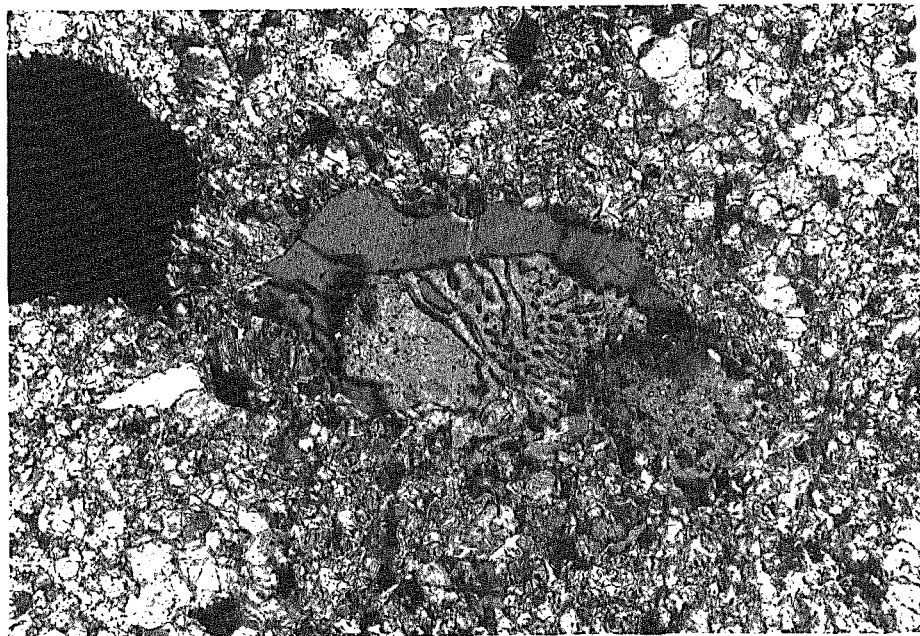


Fig.2.26: Myrmecitic quartz grain with secondary quartz seam in calcareous wackestone. Base of picture = 0.9 mm (+).

When the clast content increases relative to the carbonate matrix, euhedral magnetite and pyrite grains in the interstices are common, i.e. the opaques are more abundant in coarser, porous portions.

In some silty dolomite layers of fine-grained pyrite, in places recrystallized to larger aggregates, are aligned parallel to bedding and most likely represent syndiagenetic pyrite, or pyrrhotite which alternatively occurs .

While most of the plagioclase obviously is authigenic albite, much of the potash feldspar is detrital and in coarser portions probably was subject to significant alteration; some elongated but rounded grains now consisting of a diffuse, fine crystalline intergrowth of sericite and quartz are interpreted as detrital potash feldspars which have been subject to the widespread silification (Fig. 2.27).

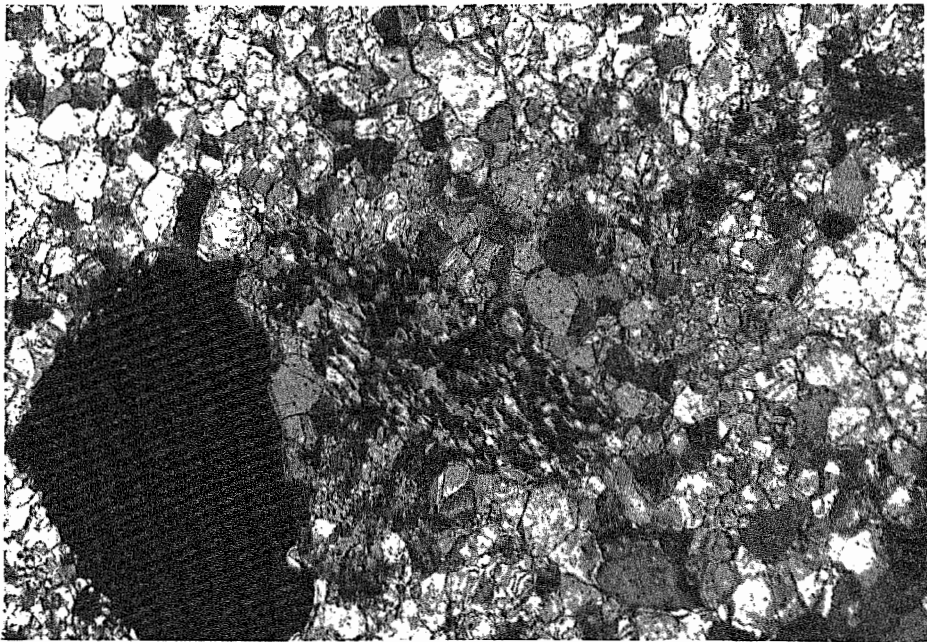


Fig. 2.27: Fine crystalline intergrowth of quartz and sericite possibly representing silicified potash feldspar. Base of picture = 0.9 mm (+).

On the contrary, some microcline in a sandy dolomite at Manganese Range East shows seams (Fig. 2.28) which apparently have grown in situ. According to Tröger (1969) the alkalinity

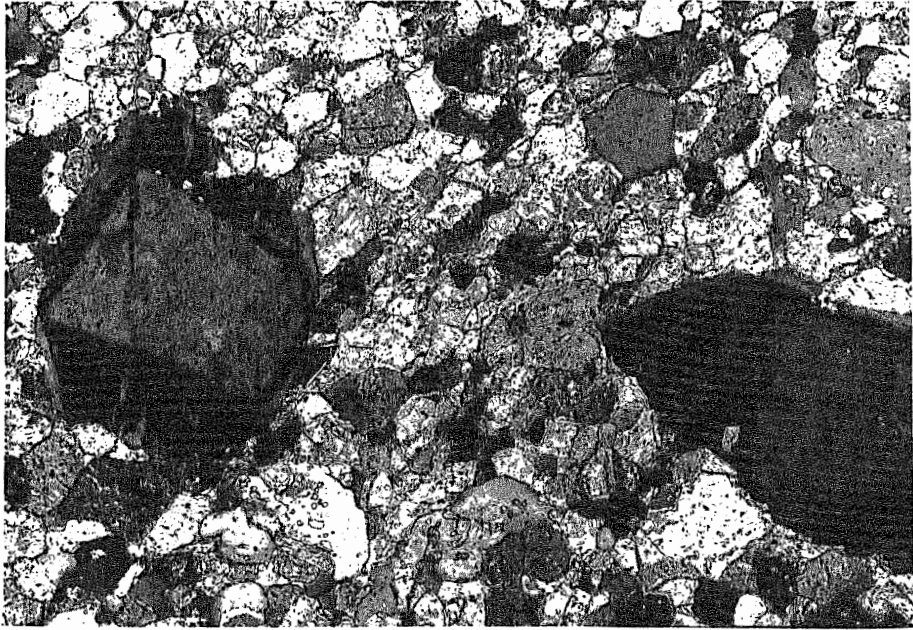


Fig. 2.28: Authigenic seams on detrital microcline in sandy dolomite. Base of picture = 0.9 mm (+).

of a CO₂-free carbonate solution is sufficient for low temperature generation of authigenic potash feldspar. Hypersaline conditions favour this process! Thus it is possible that within the GW₅-unit the salinity of diagenetic waters varied laterally along the Jilla-warra Belt, with increasing salinity towards the east.

- c) Arenaceous rocks of about 170 metres thickness - forming a prominent ridge on the southern limb of the Woodlands Dome - represent a local facies of the GW₅-unit. A distinctive feature of all rocks from this ridge is pervasive chloritization.

The basal portion consists of very coarse-grained, moderately sorted, rounded quartz sandstone (minor quartz-pebble conglomerate) which is considerably recrystallized. No feldspars have been observed. The matrix is dominated by barite, finely crystalline chlorite, minor "cherty" quartz and white micas (Fig. 2.29).

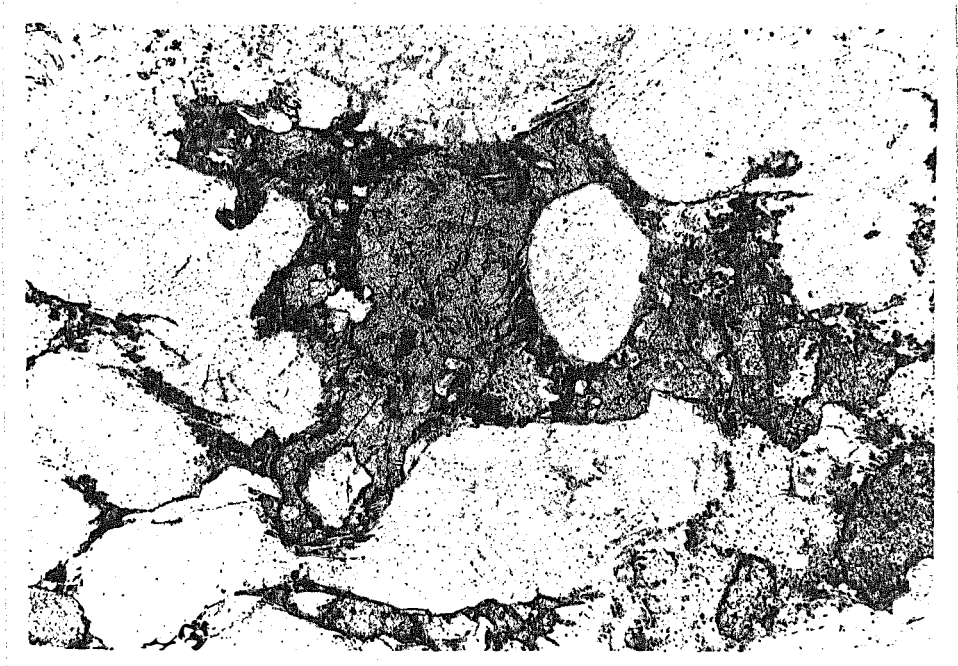


Fig.2.29: Barite (grey) and chlorite (dark grey) matrix of a coarse-grained quartz sandstone. Base of picture = 3.6 mm (-).

The overlying beds comprise a thick sequence of fine to very fine grained, subangular, moderately sorted lithic quartz sandstone with clasts of shale, chloritized shale and a network of "cherty" quartz with sericite. The matrix is of fine-grained, pale green chlorite with interstitial anhedral iron-oxyhydrates.

Eastwards along strike the arenites grade into medium- to coarse-grained [±] calcareous wackestones with shale clasts. The carbonate

matrix is dominantly sparite with angular, anhedral grains. Occasional euhedral rhombs in quartz indicate that recrystallization has taken place.

It is noteworthy that with increasing carbonate content the brown biotite, which is common in all calcareous rocks of the GW₅-unit, becomes the dominant phyllosilicate while chlorite is rare and possibly in chemical disequilibrium with biotite (Fig. 2.30).

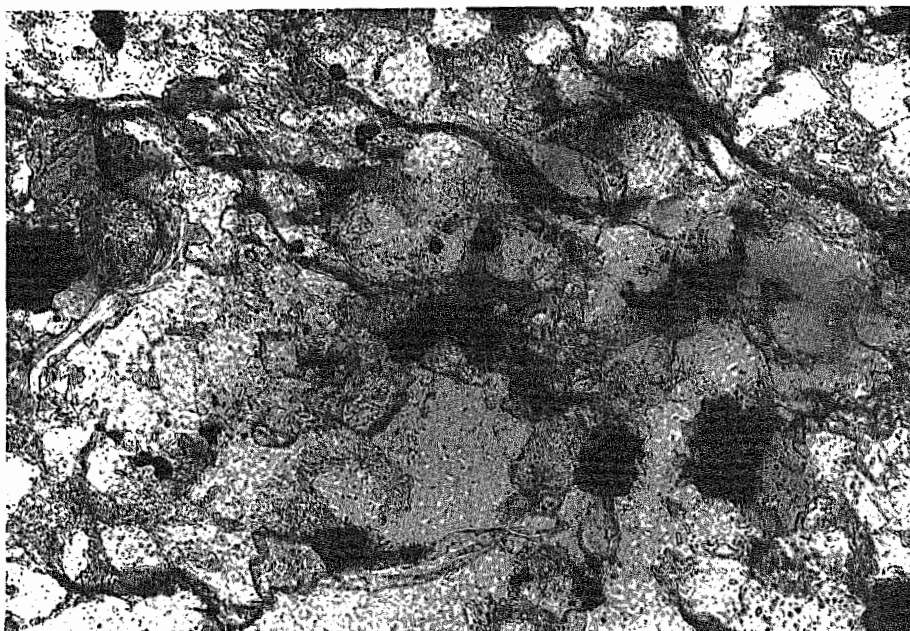


Fig. 2.30: Biotite (dark grey) in chemical disequilibrium with chlorite (medium grey). Both are intergrown with, or possibly have grown on the expense of, carbonate (light grey, high relief); in a calcareous wackestone. Base of picture = 0.9 mm (-).

For the following facies interpretation it will be assumed that the original sediment was a calcareous fine to coarse grained wackestone with clasts of quartz, potash feldspars and shale.

Facies of the GW₅-unit:

The sedimentary environment deduced from the facies variations

is a shallowing upward carbonate sequence in the sense of James (1979). The common laminated calcareous siltstones are intertidal "muddy" deposits with intermittent growth of microbial mats (see Fig. 2.31).

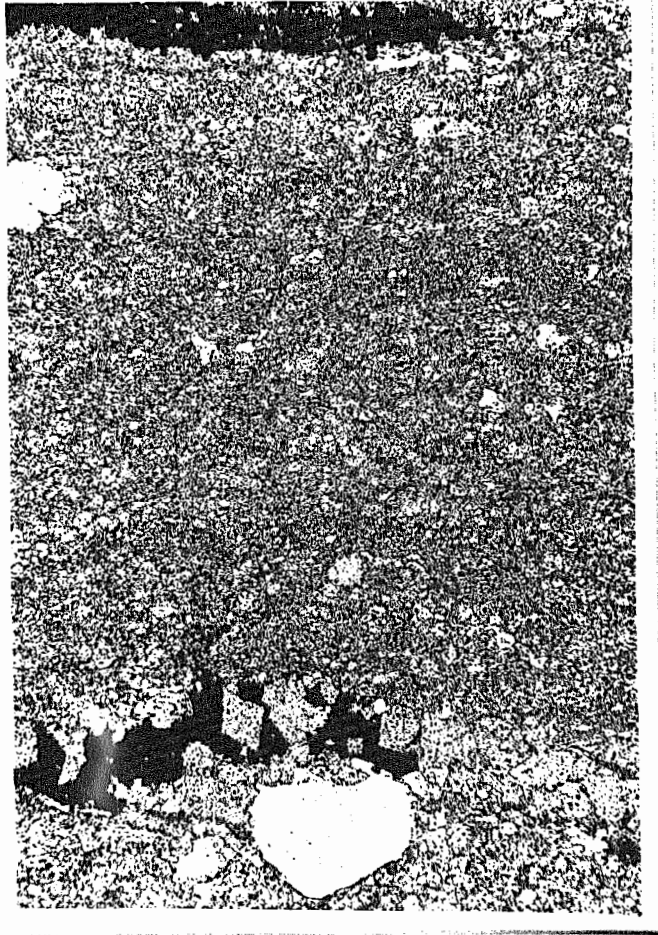


Fig. 2.31: Disrupted microbial mats with sparitization of the micritic carbonate enhanced in these layers. Base of picture = 3.6 mm (-).

Occasional quartz or feldspar grains were provided by tidal currents, shale clasts by reworked intertidal pond deposits. The interbedded carbonate wackestones may represent storm

deposits with quartz and feldspar clasts derived from offshore, subtidal regions; the roundness of most larger clastic grains indicates prolonged reworking in barrier/beach regions.

Towards the top of the GW₅-unit (Fig. 2.21) quite (upper) intertidal carbonate sedimentation with occasional but common addition of more clastic material (resulting in calcareous wackestones) occurred. A characteristic feature of such sediments are pellets, ooides and related structures (Dimroth, 1979). No ooides have been found but Fig. 2.32 shows some ferruginous pellets in a thin section prepared from the outcrop of Fig. 2.21. Possibly at the

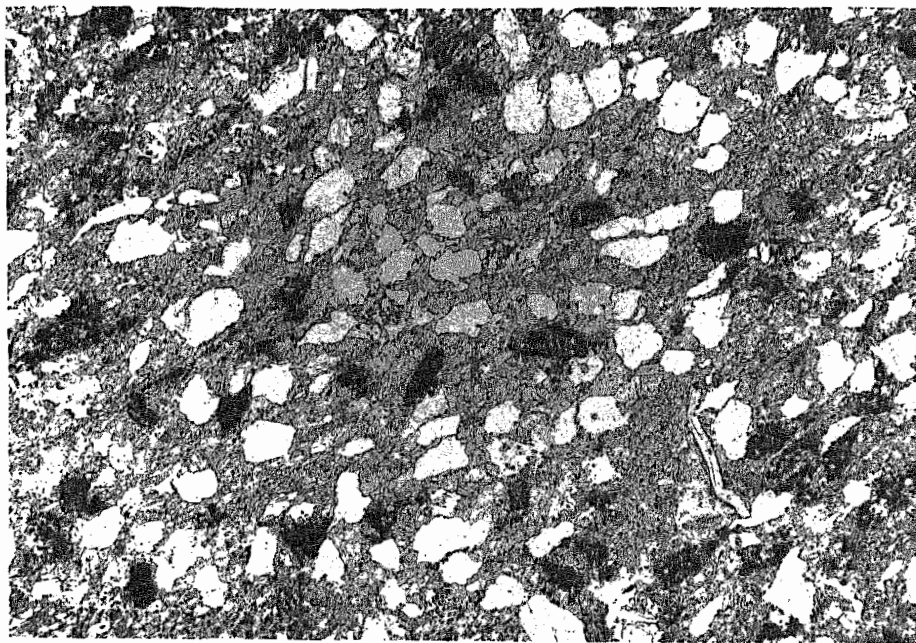


Fig. 2.32: Ferruginous pellets (altered and stretched) in a calcareous wackestone. Base of picture = 3.6 mm (-).

same stratigraphic level - near the top of the GW₅-unit - but further eastwards (i.e. NNE of the Jillawarra Camp) a similar, more fine-grained laminated dolomitic siltstone crops out which grades upwards into stromatolitic dolomite, Fig. 2.22. This can be taken as evidence for a shallowing upward carbonate sequence and regressional development towards the top of the GW₅-unit.

In his facies model James (1979) describes the features of the shallowing upward carbonate sequence in the inter- to subtidal unit when associated with lime sand shoals as: well sorted, oolitic or pelletoidal lime sand with planar bedding and herringbone cross-lamination, large at the base becoming smaller upwards, and individual bedding phases commonly covered with small-scale ripples.

All features apply to the arenaceous, lower and middle parts of the GW₅-unit at Jeds Anticline, except that the cross-bedding is not commonly herringbone type and that it is changing frequently from low to high angle. The water depth calculation using the method of Tanner (1971) was performed on ripple marks from this rock sequence and the resulting water depth of tens of centimetres supports the sedimentological facies interpretation of these arenaceous portions as having been lime sand shoals in an intertidal flat.

Thus, both the dolomitic and arenaceous portions are compatible with a shallowing upward carbonate sequence in the GW₅-unit.

2.3.1.6. GW₆

The distribution of this unit is shown in Fig. 2.33.

The GW₆-unit - most closely resembling the "Irregularly Formation" of the Bangemall Group - is occupying large areas of outcrop in the Jillawarra Belt. It was encountered in several diamond drill holes (see Fig. 2.05) and is extending westwards beyond the Jillawarra Belt for more than 30 kilometres.

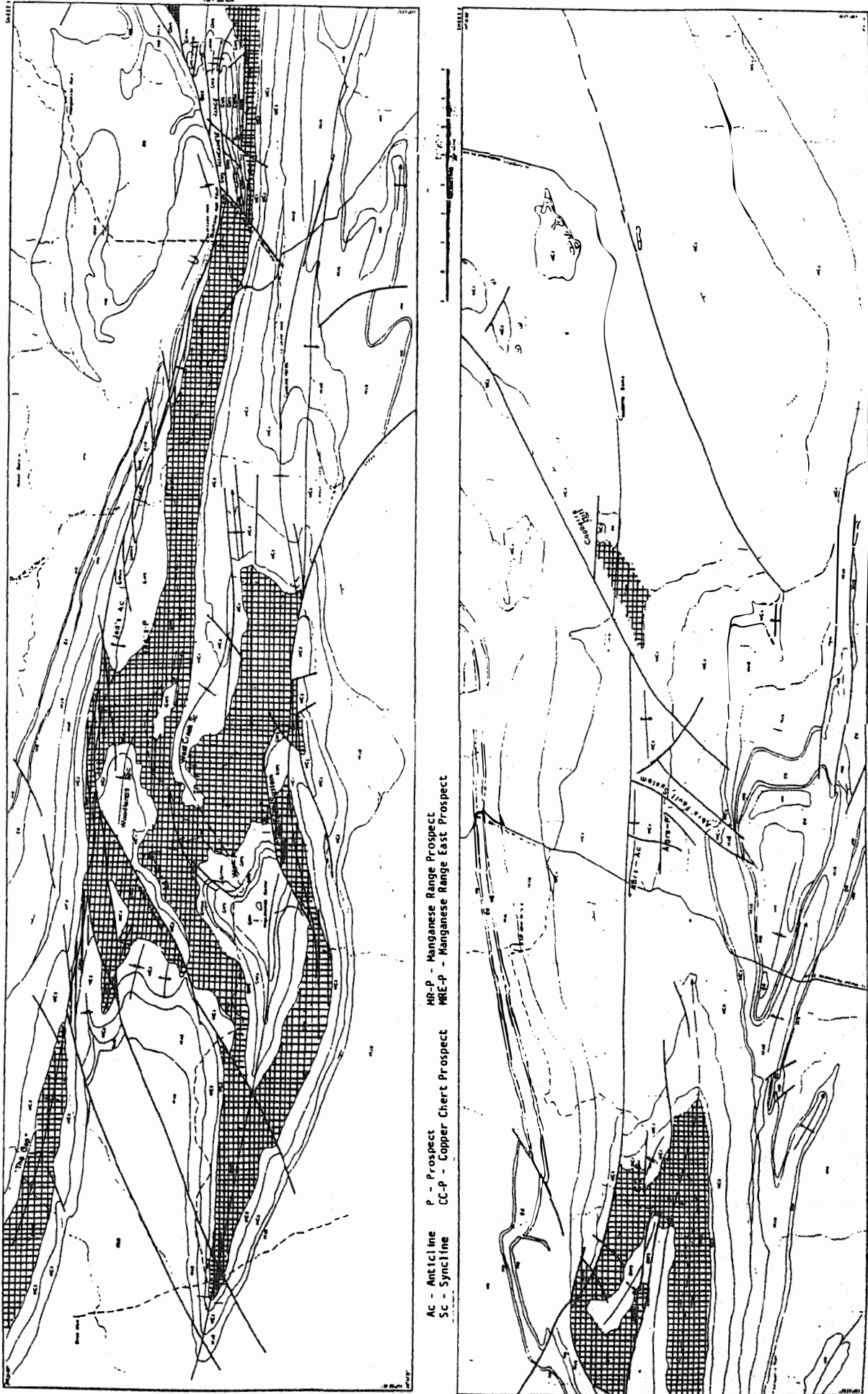


Fig. 2.33: Showing outcrop of the GW6-unit (cross-hatched) and locations referred to in the text. For detailed geology and locations see map 1 and 3.

The thickness generally is in the range of 350 metres but may be more locally. The lower boundary is gradational and taken as the last significant arenite and wacke interbeds of the GW₅-unit, and where laminated dolomitic siltstones and shales predominate. The top is in most cases a very coarse-grained conglomerate defining the onset of the overlying WC₁-unit (Fig. 2.51), but locally the uppermost 20 centimetres are characterized by intense silification and manganese enrichment (Fig. 2.34).

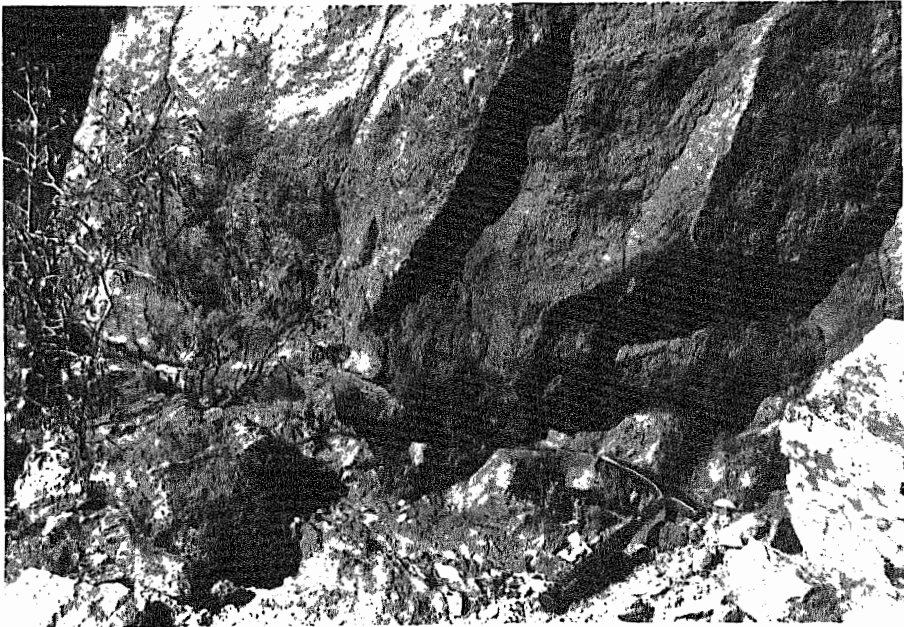


Fig. 2.34: Silification and manganese enrichment at the contact between dolomitic shales (GW₆) and coarse grained arenites (WC₁) in the area of the TP-prospect.

Where the conglomerate is absent, dolomitic siltstones of the GW₆-unit grade, with minor coarse clastic intercalations, into ferruginous dolomitic shale of the overlying WC₁-unit. The WC₁-unit itself locally shows thin conglomerate bands (5-30 centimetres) of the same type as the basal conglomerate. In some diamond drill holes of the Abra Prospect the WC₁-unit is entirely missing

and GW_6 is overlain by WC_2 with a sharp contact (see chapter 3.2.1.3.). Dominant rock types of the GW_6 -unit are sericitic mudstones and laminated dolomitic siltstones/shales which often show undulatory folding.

East of the Manganese Range Fault the overall grain size increases, so that the dominant rock type here is a coarse dolomitic siltstone with thin (in the range of centimetres) calcareous sandstone intercalation.

The usual colour is whitish, but many outcrops are black through significant manganese staining or yellow from iron hydroxides. The colouring can be zonal and discordant to the bedding as shown in Fig. 2.35.



Fig. 2.35: Zone of manganese enrichment oblique to bedding (from left to right in this photograph) in dolomitic siltstone.

Locally veins and layers (Fig. 2.36) of hematite and jaspilite, respectively, occur, indicating a link to sabkha processes of the

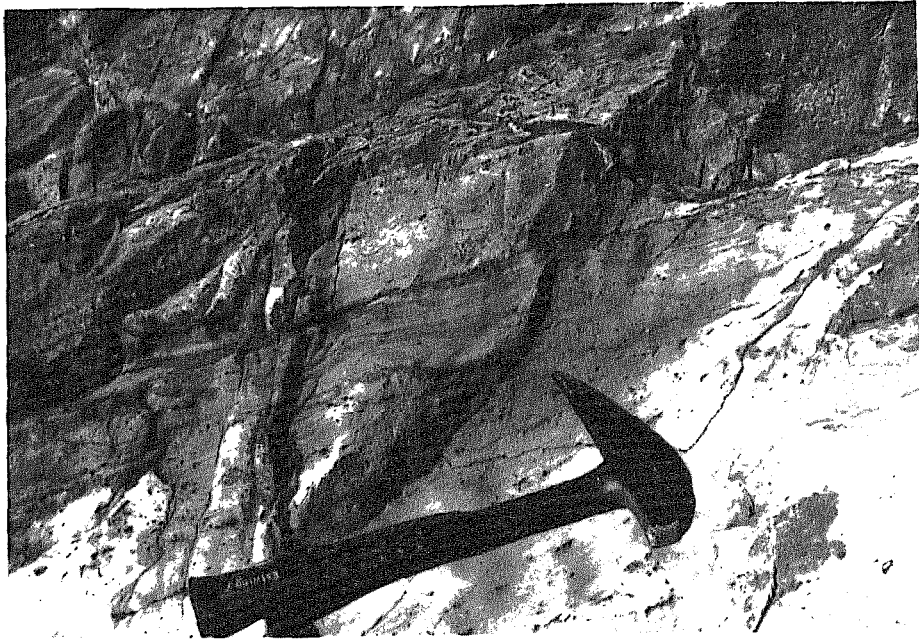


Fig. 2.36: Red zone-type laminae of hematite (or liesegang structures??) in dolomitic siltstone near the TP-Prospect. Note elongated casts - possibly after gypsum - in the bottom half of the photograph.

red zone in Abra as discussed in chapter 3.2.1.3. Some outcrops are intensely silicified and there possibly is a regional control on the degree of silification; rocks in the area of the TP-Prospect, southern Jeds Anticline and, in the area of the Copper Chert prospect are more intensely and sometimes fully silicified. At Copper Chert silification is accompanied by manganese staining which entirely obliterates the original features of the rocks.

Another important feature of some coarse-grained, laminated dolomitic siltstones at Copper Chert are blade-like, sometimes twinned casts (app. 1 cm long) which are irregularly distributed

throughout the bedding and are interpreted as former, diagenetic gypsum crystals.

Particularly in GW₆-outcrops west of the Jillawarra Belt, low or flat ripple marks with variable spacings occur. Some layers of the dolomitic siltstone are rich in pyrite cubes some of which may be more than 3 centimetres on edge.

In the area between Woodlands Fault and Manganese Range Fault (map I), elongated dolomite biostromes are abundant. Remarkably, the largest bodies all occur in the same stratigraphic interval and form an intermittent strike ridge of more than 11 kilometres length, the individual bodies ranging between 0.3 to 2.3 kilometres. The dolomite is either massive or laminated, commonly with grey to yellowish colours. Locally it was subject to silification which seems strongest in the same areas of silification of the dolomitic siltstones described above. In other outcrops especially at Jeds Anticline the dolomite is hematized, silicified and has porous layers where some constituents have been leached during weathering. Hematitic carbonate suggests a sedimentary environment similar to the red zone of Abra (chapter 3.2.1.3.), whereas silification is related to the mineralizing processes in the Jillawarra Belt (chapter 4.8). The petrology of the dominant rock types are summarized in the following:

Some 20 km west of the Jillawarra Belt the GW₆-unit is represented by a monotonous sequence of micritic carbonates with layers of silt-sized clastic quartz. The amount of clastics is in the range of 20 %.

Abundant muscovite (130 μ length in average) and authigenic albite with carbonate inclusions are present irregularly (Fig. 2.37).

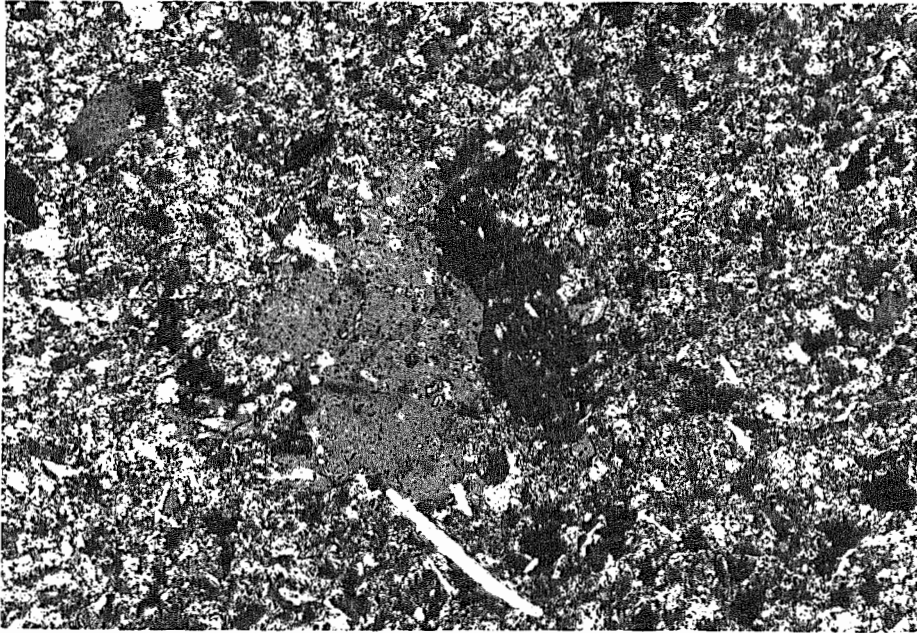


Fig. 2.37: Authigenic albite with carbonate inclusions in silty micritic carbonate. Base of picture = 0.9 mm (+).

The carbonate locally shows incipient sparitization.

Within the Jillawarra Belt the lithology becomes more variable; micaceous "mudstone" is a fine- to medium-grained sericitic siltstone characterized by detrital quartz grains in a matrix consisting of finely intergrown quartz and sericite, locally the matrix is calcareous. In some coarser portions authigenic potash feldspar can be seen. Finer layers of the rock are rich in organic material and iron-hydroxides, and minor leucoxene has been observed. Fine-grained brown biotite is common, and may contain intergrown chlorite in places.

Fig. 2.38 shows intraformational soft sediment deformation overlain by the laminated mudstone.

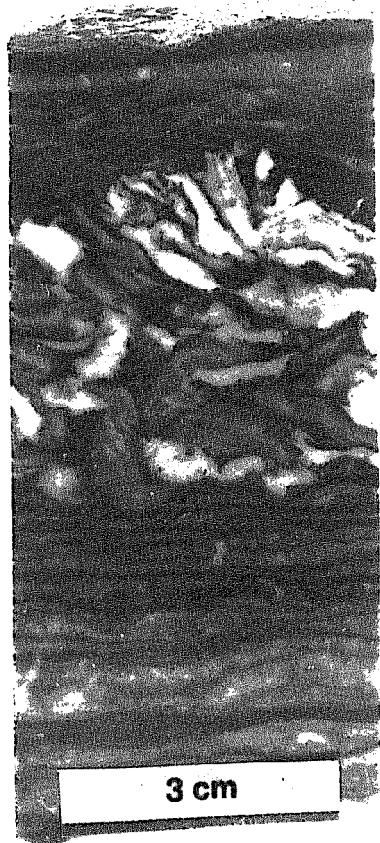


Fig. 2.38: Soft sediment deformation in a calcareous mudstone.

Many of the micaceous siltstones have syndiagenetic pyrrhotite and minor pyrite occurring in single laminae 1-2 millimetres thick or in groups of several layers (Fig. 2.39).

This pyrrhotite is intimately intergrown with large, pale Fe, Mg-chlorites (Fig. 2.40). Most likely the iron sulphide layers formed contemporaneously with the chlorite. As such layers of iron-sulphide usually are generated during early diagenesis, provided that sulphate reducing bacteria are present (Renfro, 1974; Trudinger et al., 1972), it may be inferred that the chlorite also is diagenetic.

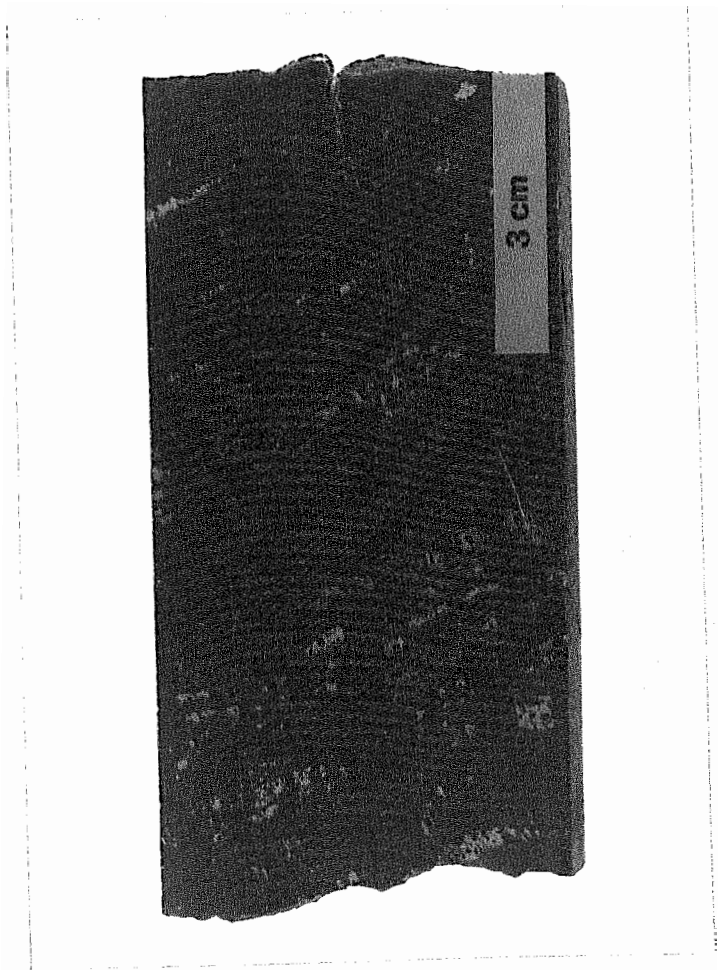


Fig. 2.39: Syndiagenetic pyrrhotite layers in micritic dolomite.

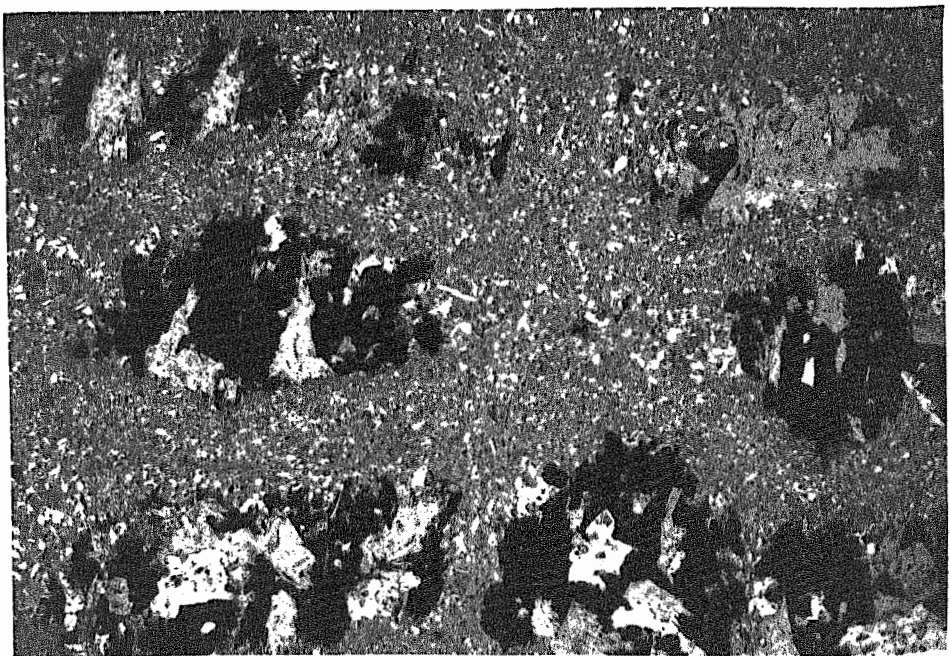


Fig. 2.40: Pyrrhotite intergrown with chlorite in dolomite.
Base of picture = 3.6 mm (+).

In a drill hole of the TP-Prospect (see map III, TP78-37, 309.1 m) a fine grained sericitic and biotite bearing siltstone is veined by pyrrhotite-quartz-carbonate.

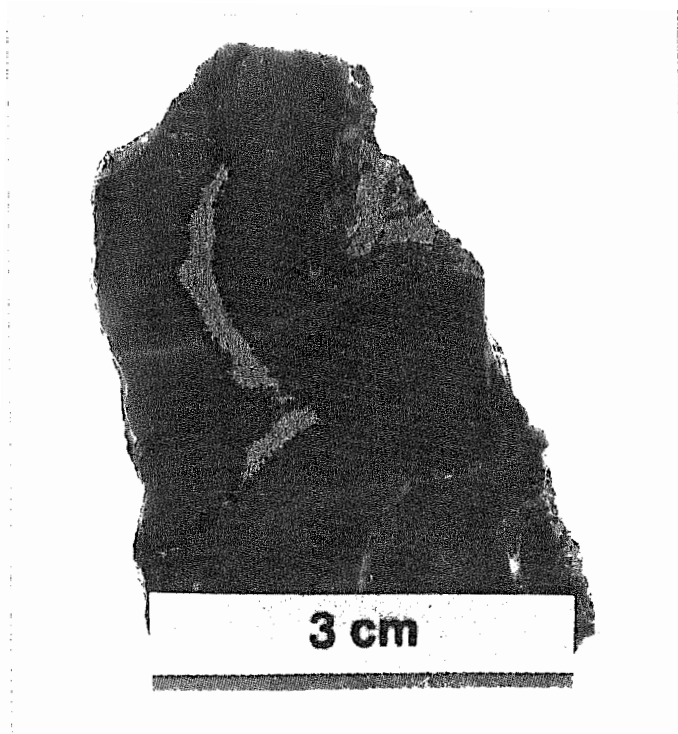


Fig. 2.41: Pyrrhotite-quartz-carbonate vein in fine grained siltstone. Note marginal biotite (black).

The vein margins now consist of biotite prisms (Fig. 2.42) elongated at a high angle to the vein; chlorite occupies the centre of the vein where pyrrhotite and quartz are missing. The biotite apparently formed by wall rock reaction with the fluid, whereas the chlorite may rather resemble the chemistry of the hydrothermal fluid.

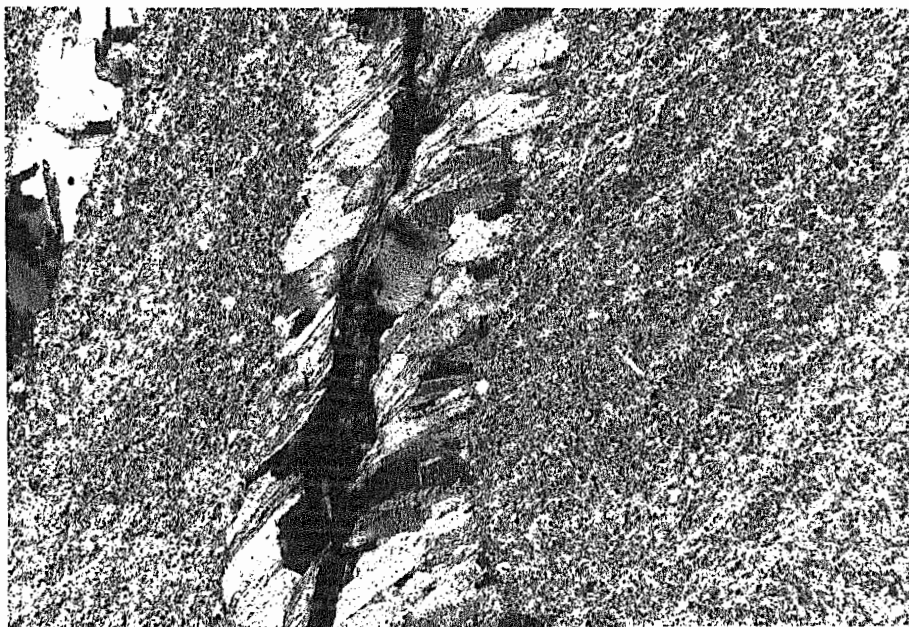


Fig. 2.42: Vein in micaceous fine grained siltstone with central chlorite and marginal prismatic biotite. Base of picture = 3.6 mm (+).

The most abundant rock type of the GW_6 -unit is laminated dolomitic siltstone and shale consisting of micritic dolomite which often shows neomorphic sparite. In some sections the sparite is restricted to poorly defined layers. Within the dolomite secondary muscovite and brown biotite are common while chlorite is a minor constituent. Authigenic plagioclase is found throughout. The carbonate often is intergrown with a diffuse, cryptocrystalline quartz "matrix" which probably does not stem from detrital quartz but was introduced after deposition, i.e. the rock is silicified. The silification ranges from a few quartz specks to almost complete replacement of the carbonate. Abundant coloured inclusions (app. 10μ) however, containing no fluid phase, and probably composed of carbonate, are scattered through the secondary quartz. They witness the former calcareous nature of the rock (Fig. 2.43).

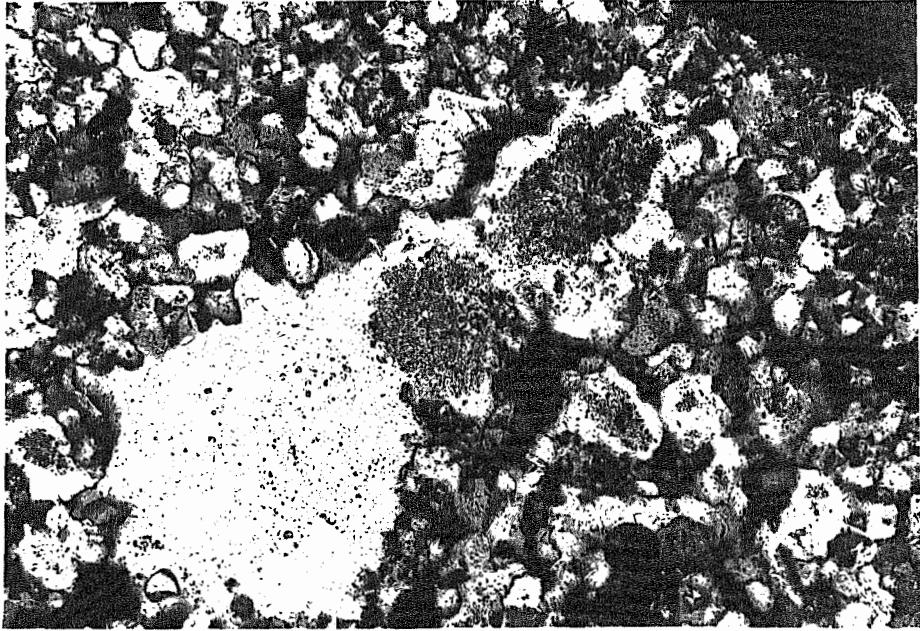


Fig. 2.43: Quartz with abundant inclusions of carbonate. Note that many quartz "grains" have accumulations of these inclusions in the centre. Base of picture = 0.9 mm (+).

Because of this silification it is difficult to recognize the amount of epiclastic quartz, potash feldspar and tourmaline. The content of clastics in dolomitic siltstones in the Jilla-warra Belt varies between 10 % and 40 %, which renders GW₆ the unit poorest in epiclastic content within the Gap Well Formation.

The layering in the dolomitic siltstone and shale usually is defined by thin bands (0.1 - 0.5 millimetres) of organic material most likely being the remains of microbial mats. However, this can be established only when the organic material occurs in carbonate, where it is incorporated in sparite (Figs.2.44 and 2.45).

In pelitic rocks the organic material is intergrown with phyllosilicates; therefore it might rather be called a "black shale".

Another common feature of the dolomitic siltstone-shale sequence is abundant micritic pellets of various sizes (0.5 - 5 millimetres), in a sparite matrix (Fig. 2.46). The pellets mostly consist of ferruginous carbonate. However, in one occurrence of less calcareous siltstone, consisting of fine-grained quartz, poorly oriented

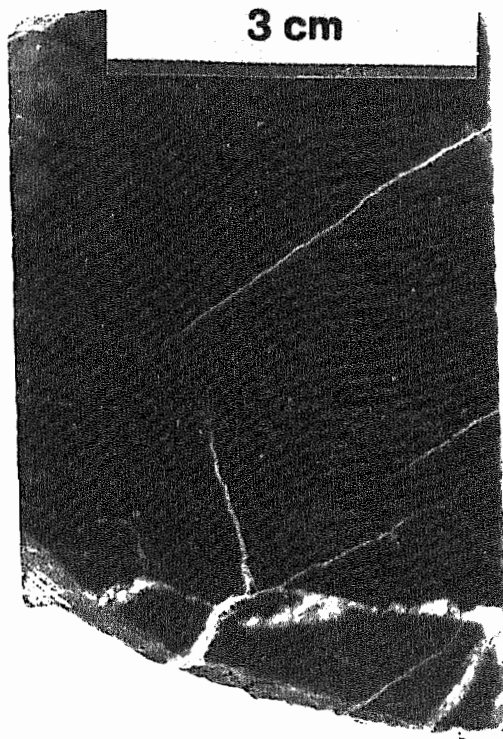


Fig. 2.44: Core slab with organogenic layers in sparitic carbonate containing scattered pyrite. Layers probably represent former algal mats.

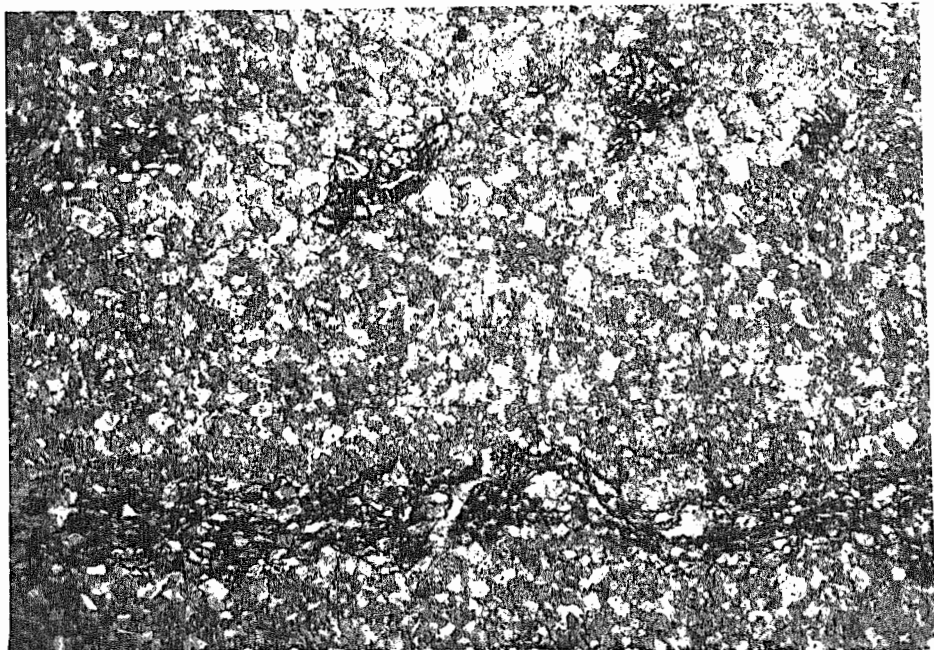


Fig. 2.45: Thin section from the above specimen. Contorted and disrupted organogenic layers in sparitic carbonate. Base of picture = 2.4 mm (-).

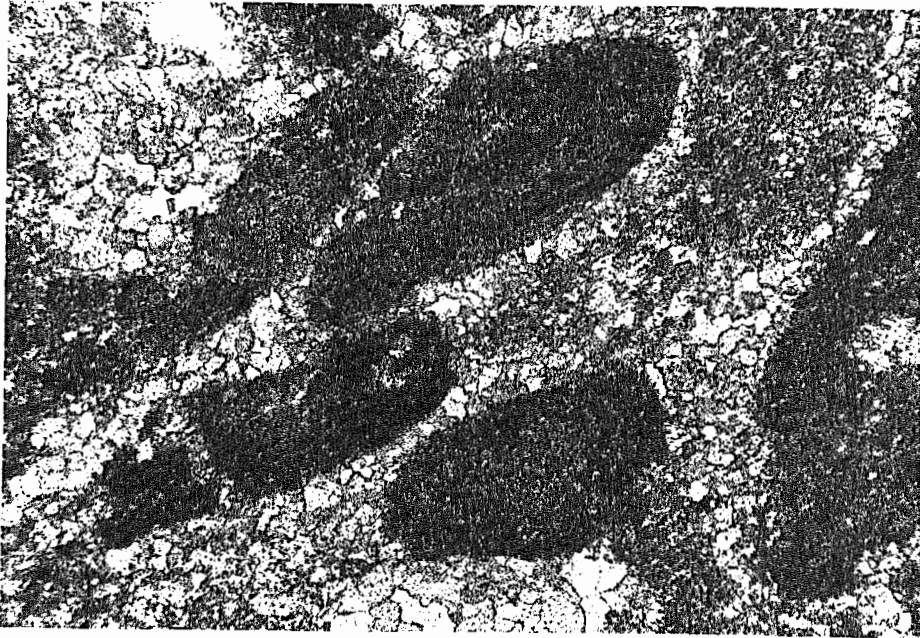


Fig. 2.46: Ferruginous micritic carbonate pellets in a sparitic carbonate. Base of picture = 3.6 mm (-).

muscovite, brown biotite, chlorite and minor carbonate the pellets are significantly enriched in biotite, chlorite (Fig. 2.47), galena and pyrite with concomitant silification. As brown biotite usually is abundant in calcareous rocks it can be assumed that the pellets

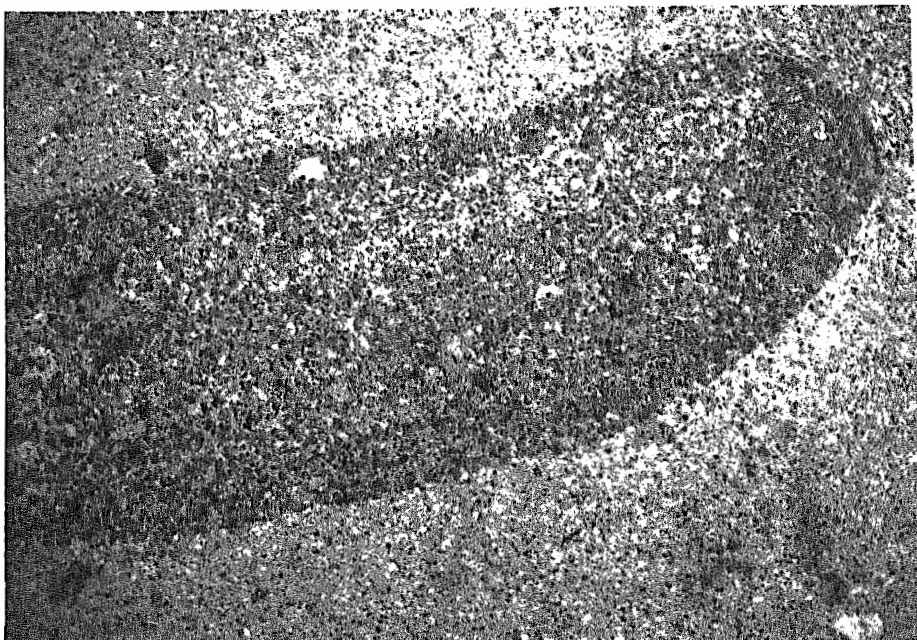


Fig. 2.47: Large pellet (4 mm) in quartz-mica rock is enriched in biotite-chlorite-pyrite-galena. Base of picture = 3.6 mm (-).

originally were more calcareous than the matrix, and that biotite formation was enhanced in the pellets during alteration and mineralization of the whole rock.

The massive dolomite forming the prominent ridges, mainly consists of micritic, often ferruginous, carbonate. Oval patches or nodules of neomorphic sparite, some with secondary quartz in the centre, are common. Rare clastic quartz grains have been observed in the micrite.

Stromatolites and cryptalgal laminations are present in several localities and in the top of the GW₆-unit in drill hole Abra 7. These stromatolites are of an underterminate form.

Facies of the GW₆-unit:

Dominant carbonate sedimentation with subordinate epiclastic input is the main sedimentary feature. Abundant stromatolites, cryptalgal laminations and shallow irregular ripple marks are evidence for a shallow-water, low-energy environment. An upper intertidal zone is inferred; within the sediments reducing conditions prevailed resulting in the formation of occasional diagenetic iron sulphide layers.

Some features indicate that the upper intertidal environment was, at least locally, shifted to supratidal. In Fig. 2.48 "tee pee" structures in dolomitic cryptalgal laminates are shown which are characteristic for a supratidal environment (James, 1979). Gypsum indicates hypersaline conditions close to a sabkha milieu. Authigenic plagioclase and potash feldspar are more abundant in fine-grained calcareous rocks than in non-carbonates; this may be explained in that the former represent hypersaline, low energy conditions favourable for the growth particularly of authigenic potash feldspar (Fig. 2.49).

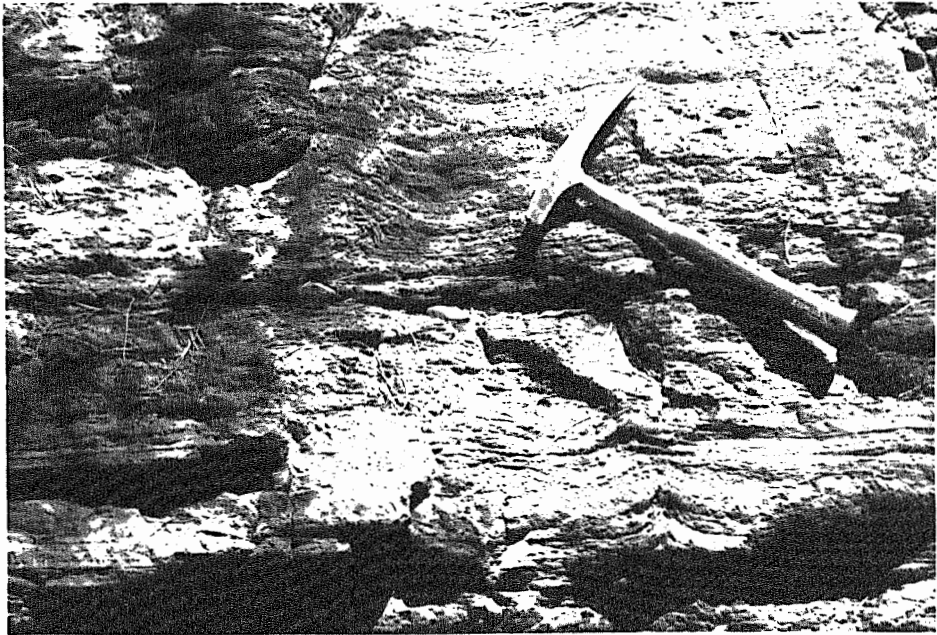


Fig. 2.48: "Tee-pee" structures (lower left) in dolomitic crystalgal laminites.

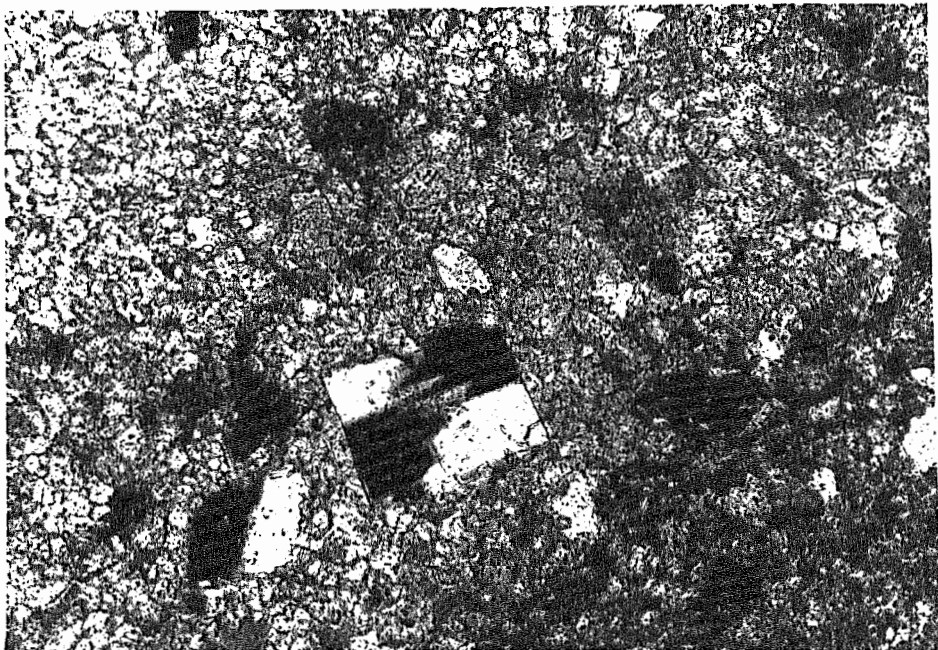


Fig. 2.49: Authigenic potash feldspar in micro-sparite.
Base of picture = 0.9 mm (+)

It is significant that the GW₆-unit has the lowest content of epiclastic material (10 - 40 %) of the units of the Gap Well Formation, indicating relative emergence (i.e. emergence that can be induced by both active uplift of the Jillawarra area or downfaulting of surrounding areas) in the area of the Jillawarra Belt in GW₆-time.

Relative emergence was more pronounced in the eastern parts as the supratidal (hypersaline) features like "tee pee" structures, gypsum casts, abundant cryptalgal lamination, are more common here. In contrast, west of the Manganese Range Fault, which acted as a facies divide, biostromal dolomite and pelletal carbonates prevail and point to an intertidal environment as the growth of biostromes requires predominantly water cover. Hypersaline, shallow water condition were also established in this western part though; Fig. 2.36 shows an interval with wispy laminae of red Fe-hydroxides and some casts of bladed crystals, probably after gypsum.

2.3.2. The West Creek Formation

This formation is subdivided into 4 units (named WC₁ to WC₄) and has an average thickness of about 900 metres, its thickness is variable as both the basal WC₂-unit and the top WC₄-unit may be missing locally. In most case it conformably overlies the Gap Well Formation, but minor disconformity may be present in places. The name is derived from West Creek, north of which the formation is best developed.

2.3.2.1. WC₁

The characteristic lithology of this unit is a massive coarse-grained arenite and conglomerate at the base with a maximum thickness of about 40 metres. This is variably overlain by dolomitic shale and siltstone and one massive dolomite occurrence at Copper Chert, accounting for a variable thickness of the entire WC₁-unit, in places exceeding 200 metres.

Where the basal arenite is missing, WC₁ is similar to, and difficult to distinguish from, the laminated dolomitic siltstone and shale of the underlying Gap Well Formation. The lower contact of the WC₁-unit can only be defined when the basal arenites are present.

The top contact of the WC₁-unit is well defined by the ridge-forming, massive arenites that mark the onset of the WC₂-unit and which contrast with the soft and weathered dolomitic shale and siltstone of the upper WC₁-unit.

In Abra drill cores, the basal arenite of the WC₁-unit is either absent (Abra 6, 7, 11) or present as a massive conglomeratic arenite (up to 40 m thickness, Fig. 2.51), with no overlying dolomitic shale and siltstone. At Abra the top contact is defined by a



Fig. 2.51: Carbonate-and barite-cemented conglomerate in Ab 5.

pyrite layer (Abra 9) containing complex, Cu, Pb, Sb-sulfosalts (Abra 4).

The coarse clastic rocks of the WC₁-unit are discontinuous along strike; for example they are absent west of the Woodlands Fault, whereas between Copper Chert Prospect and Jillawarra Camp this facies is present as small lenses of a few metres thickness (Fig. 2.52).

In contrast, at Abra (see Fig. 2.51), Copper Chert and in the areas around TP-Prospect and, Woodlands Prospect, the coarse clastic rocks are massive and up to 40 metres in thickness (see map 3 for localities).

The petrography of the clastites can be summarized as a rounded to moderately rounded, moderately sorted, coarse-grained arenite with abundant large (up to 1 cm) rounded clasts of vein quartz, potash feldspar (5 - 10 % microcline), micaceous and ferruginous shales, siltstone, chert and minor tourmaline.

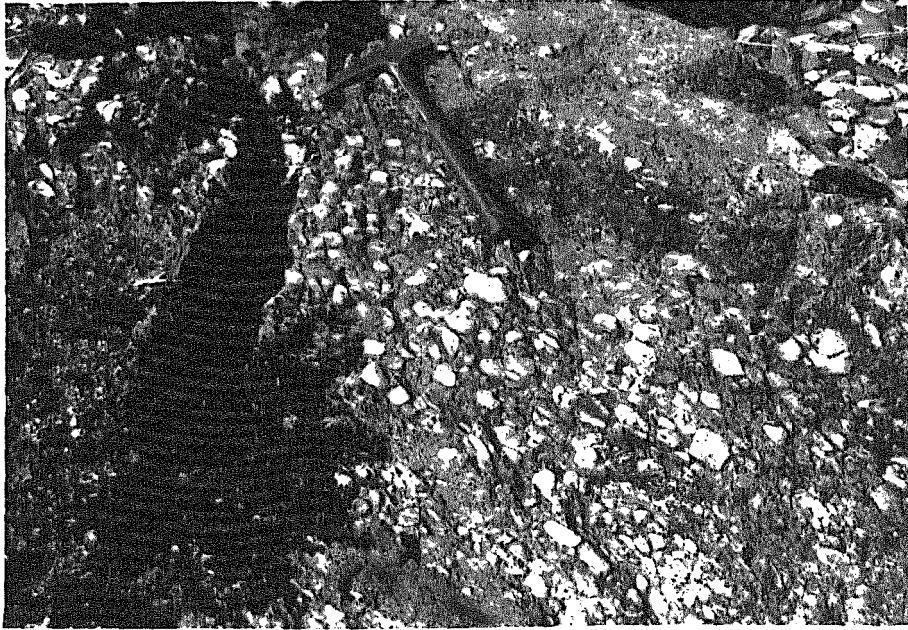


Fig. 2.52: Basal WC₁ conglomerate (about 5 metres thick) discontinuous along strike in the vicinity of the Manganese Range Fault.

No potash feldspar has been found at Abra however, because of the strong alteration, its original presence cannot be ruled out.

The matrix of this arenite in the Abra area is of sparitic carbonate and minor barite (0.5 to 6.4 % Ba, whole rock analyses). Some arenites contain no matrix and the rock is completely cemented by quartz. Detrital Fe-Ti-oxides, which commonly outline cross bedding, have altered to titanite, possibly indicating silification (Ramdohr, 1975).

At Copper Chert the carbonate matrix has been replaced by cryptocrystalline quartz, leaving minute carbonate around the original quartz grain (Fig. 2.53).

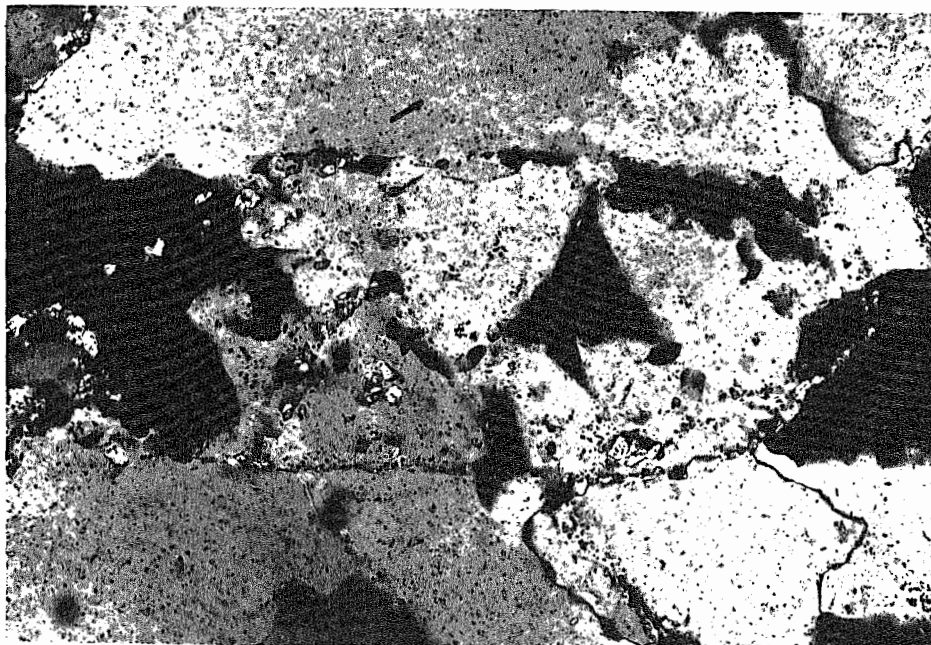


Fig. 2.53: Carbonate inclusions outlining the rim of a detrital grain within recrystallized quartz. Base of picture = 0.9 mm (+).

For a facies interpretation the following observations are considered important:

- I) Despite the presence of considerable thicknesses of clastites, the prevailing sedimentary environment is represented by dolomitic shale and siltstone plus minor dolomite.
- II) Due west of the Manganese Range Fault the basal WC_1 conglomerate is thickest and coarsest (cf Fig. 2.52) with decreasing thickness and grain size westwards away from the fault, indicating control of syndimentary faults on the sites of deposition of coarse clastites.

The Manganese Range Fault also had control on the facies of the GW_6 -unit as no massive biostromal dolomites occur east of it.

- III) Regionally, the thick (30 - 40 metres) clastic facies seems to define subbasins of pronounced clastic deposition; these sub-basins - around TP-Prospect, Copper Chert Prospect and Abra-Prospect - are the explorational target areas which remained prospective after more than 8 years of exploration in the entire Jillawarra Belt.

The sedimentary environment deduced for the WC₁-unit is similar to the GW₆-environment of an upper intertidal to supratidal zone with low clastic input and quiet carbonate deposition. However, in certain areas syndimentary faults initiated sub-basin which were filled with coarse clastic rocks, although carbonate deposition continued away from these sub-basins.

A significant portion of the coarse clasts in the conglomerate derives from granitic and/or metamorphic terrain; as evidenced by quartz grains with undulous extinction, potash feldspars, muscovite, tourmaline. In contrast, jaspilite and chert clasts plus some pellets were derived from a near-by source, probably from the uppermost levels of the GW₆-unit. The fact that material of the GW₆-unit has reached a lithified state at this time is not taken as evidence for a considerable time gap between the Gap Well Formation and West Creek Formation; sediments of the supratidal zone, particularly sabkhas, may lithify rapidly by evaporation (Kendall, 1979).

The coarse clastites, which have a carbonate matrix, and seem to have developed in tidal flat, indicate deposition in subsiding depressions within the intertidal zone. Most of the clastics were derived from a granitic landmass and deposited in the mode of an alluvial mid-fan. But some clasts were contributed from the adjacent tidal flats and local sabkhas.

In summary, the WC₁-unit marks the onset of clastic deposition after a prolonged period of waning clastic input to the Gap Well Formation. The development of depressions where coarse clastic infill occurs is due to rapid subsidence of faults bounded sub-basins. As discussed in chapter 5.2 the movement along the faults with concomitant subsidence of the sub-basin provided conditions favourable for ascending metal-bearing hydrothermal fluids. The presence

of a thick conglomerate facies at this stratigraphic level could, therefore, be used as a guide to Abra-type mineralization.

2.3.2.2. WC₂

The characteristic and strongly outcropping lithology of arenites with siltstone interbeds, renders this a useful unit in the Jillawarra Belt. A thickness of 320 metres can be determined quite accurately from drill cores at the Abra-Prospect. In other areas however, it can only be estimated from field data. Apparently there is an increase in thickness of up to ca. 500 m at the longitude of the Copper Chert Prospect. This value gradually decreases westwards with minimum thickness of about 170 metres at the Manganese Range Fault. Further west the thickness is of 300 metres.

In outcrop, the bottom contact is sharp, and is taken as the appearance of the first major arenite bed overlying the softly weathering dolomitic shale of the WC₁-unit. In Abra drill cores, the bottom contact is marked either by a thin pyrite layer within the arenites, or a shale band; the WC₂-unit differs from WC₁ merely in smaller grain size and better sorting.

The top contact on the other hand is gradational and in Abra drill cores difficult to define. In outcrop in the Jillawarra Belt, it is marked as a decrease in arenites and increase in dolomitic siltstone and shale; for mapping purpose it is taken as the zone from where dolomitic siltstone and shale dominate over arenites.

The arenites are fine- to medium-grained quartz sandstones (Fig. 2.54), commonly with a gritty, coarse-grained and ferruginous arkose. Common cross bedding and rare ripple marks are present.



Fig. 2.54: Flat lying medium-grained massive arenite in a creek bed some 12km WSW of the Abra-Prospect.

Where the arenites have a massive (silicified) appearance moulds of weathered shale clasts are visible (Fig. 2.55).



Fig. 2.55: Moulds of shale clasts in silicified arenite.

East of Coobarra Creek, outcrop of the WC₂-unit is discontinuous and consists of coarse-grained, often chloritic feldspathic arenite and arkose. These sediments directly overlie granitic basement of the Coobarra Dome and are obviously derived from granite. It should be emphasized that the Gap Well Formation is entirely absent here, thus indicating retardment of marine sedimentation in this area corresponding to deposition of about 1000 metres of shallow water sediments elsewhere.

Despite their massive appearance the arenites in the Jillawarra Belt are carbonate cemented and manganese/iron stained. Medium scale cross-bedding (app. 1 m) in coarse-grained calcareous arenites is common.

Most important is the abundance of graded beds, showing micro-Bouma cycles (Fig. 2.56), in Abra drill cores; in addition to further sedimentary features like flaser bedding, scour and fill structures and abundant ripp-off clasts.

Occasionally complete Bouma cycles are encountered (divisions after Walker, 1979):

- E and (D) - pelitic interval of shale, sometimes black shale
- C - cross laminated interval, fine-grained arenite and siltstone, rarely developed
- B - parallel laminated interval, fine- to medium-grained arenite
- A - graded interval, coarse arenite with shale and lithic clasts of more than 2 cm length

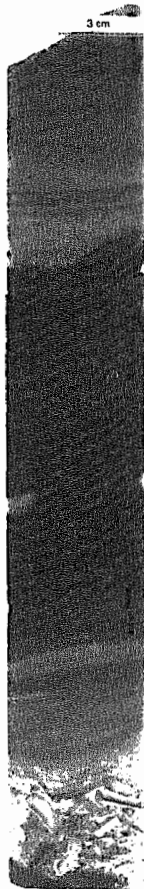


Fig. 2.56: Complete Bouma cycle (A to E) from Ab 4 drill hole.

Unfortunately, no drill cores from the WC₂-unit in the Jilla-warra Belt are available; in outcrop weathering and silification renders recognition of turbiditic cycles difficult. Therefore, it cannot be concluded unequivocally that turbidites are present elsewhere than at Abra however, the common occurrence of shale clasts (cf Fig. 2.55) and frequent interbedding of sandstone/siltstone with minor shale may indicate the presence of some turbidites.

The examination of about 30 thin sections throws some light on the nature of the WC₂-unit: The petrology ranges from organic shale and ferruginous shale to very coarse-grained wacke with various clasts, some as much as 2 centimetres long. Most rocks with a

grain size exceeding silt-size can be termed wacke. They contain clasts of quartz, potash feldspar, siltstone, shale, ferruginous and black shale and minor ferruginous carbonate pellets. The matrix consists of fine-grained micaceous material, sometimes cherty quartz or, of carbonate (dominantly sparitic).

There are two groups of clasts; one, comprising undulose quartz grains, potash feldspars and tourmaline, is derived from pre-Bangemall granitic basement. A second group consists of lithic clasts of micaceous siltstone, shale (locally chloritized), ferruginous carbonate pellets (locally chloritized) and some chert. This group of clasts is characterized by elongated rounded shapes; and the mineralogy of the clasts - mica, quartz, tourmaline, micritic carbonate and no metamorphic minerals - indicates that they were derived from contemporaneous or slightly older sediments.

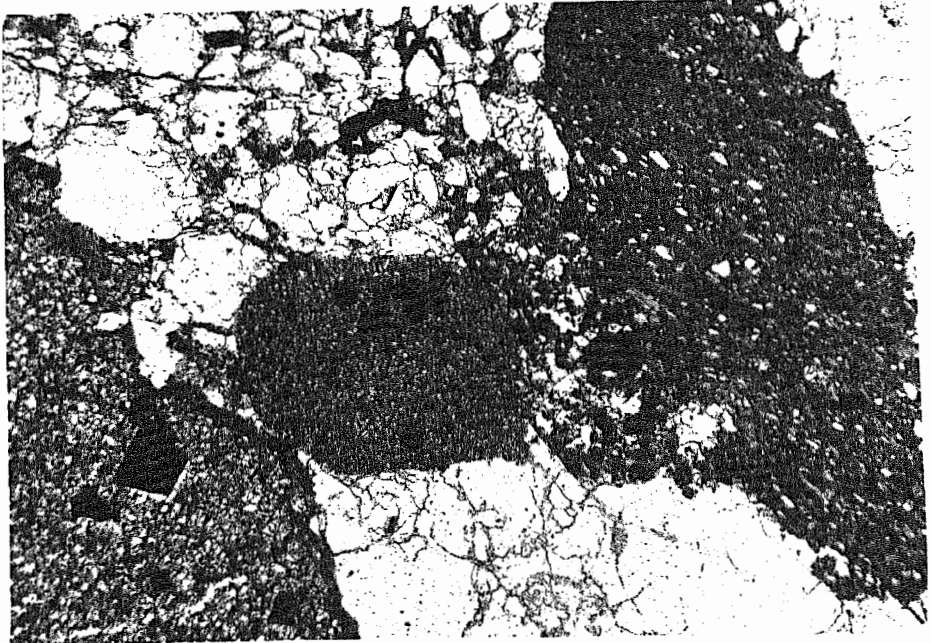


Fig. 2.57: Ferruginous shale clasts containing pyrite-cubes.
Base of picture = 3.6 mm (-).

Although the provenance of micaceous siltstone or shale clasts cannot unequivocally be inferred, some ferruginous shale clasts which contain euhedral iron-hydroxide cubes (after pyrite) probably were derived from tidal sediments (Fig. 2.57).

As mentioned before the dominant rock type of the WC₂-unit from field observations is an arenite, which in places turned out to be a wacke. According to composition of clasts and matrix and the texture three classes of clastites can be distinguished:

- I) A medium- to coarse-grained, moderately to poorly rounded feldspathic arenite with about 15 - 30 % potash feldspar and minor ferruginous shale clasts. Due to the feldspar content it could alternatively be termed arkose. While quartz grains are usually moderately rounded the feldspars however, are sub-angular to angular (Fig. 2.58).

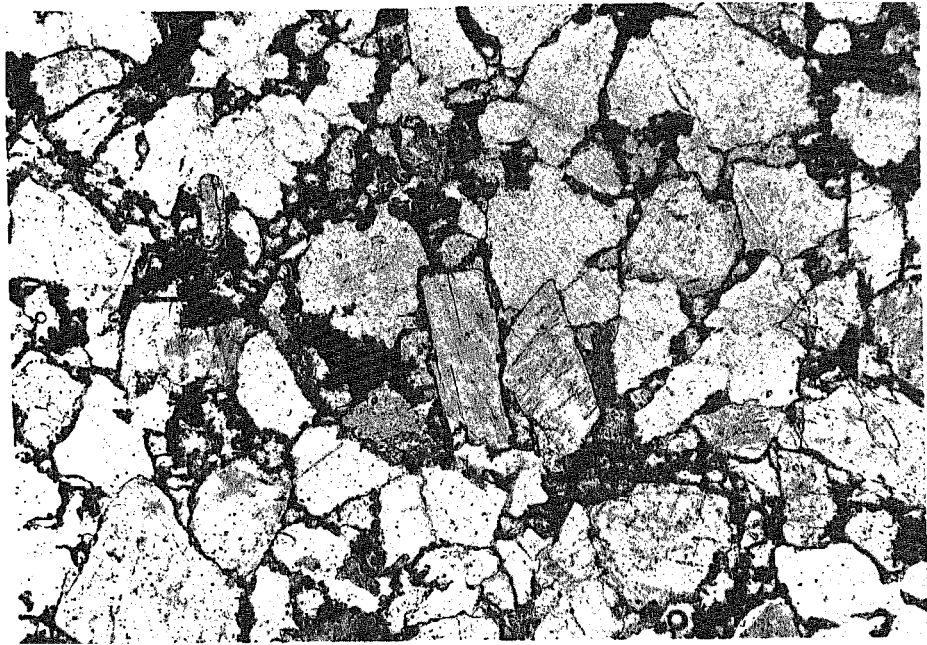


Fig. 2.58: Arkose with angular potash feldspar. Base of picture = 3.6 mm (-).

The amount of matrix with respect to clasts is generally small and it consists of a fine-grained, ferruginous quartz phyllosilicate material; it is unknown whether a carbonate component was present originally.

The angularity and abundance of potash feldspars clearly points to this being first-cycle detritus from a nearby source area. Deposition from a turbulent water regime would explain the small amount of matrix as well as the relatively good sorting.

These features all are encountered in alluvial fan deposits close to source areas, where the micaceous clasts may be derived from mud banks within a braided delta.

- II) This class commonly is represented by medium to very coarse-grained, moderately to well rounded lithic wackestones. The population of clasts differs from the above group in that feldspars (microcline) are subordinate (0 - 5 %) while shale, micaceous siltstone and possibly some formerly ferruginous carbonate pellets (now chloritized) prevail. The lithic clasts are often very large (more than 2 centimetres); some consists of fine-grained wacke themselves indicating reworking of contemporaneous WC₂-sediments. Pyrite pseudomorph containing shale and siltstone fragments as shown in Fig. 2.57 are abundant. Some very large clasts of fine-grained wackestone (up to 1 centimetre across) themselves contain ferruginous pellets.

The matrix is composed of very fine-grained sericite, chlorite and quartz, with some chlorite pellets (Fig. 2.59), and texturally is similar to a micritic dolomite. In addition, some clasts and pellets are of chlorite while others are not; this suggests that the original carbonate content of the matrix and the clasts (including pellets) governed chloritization.

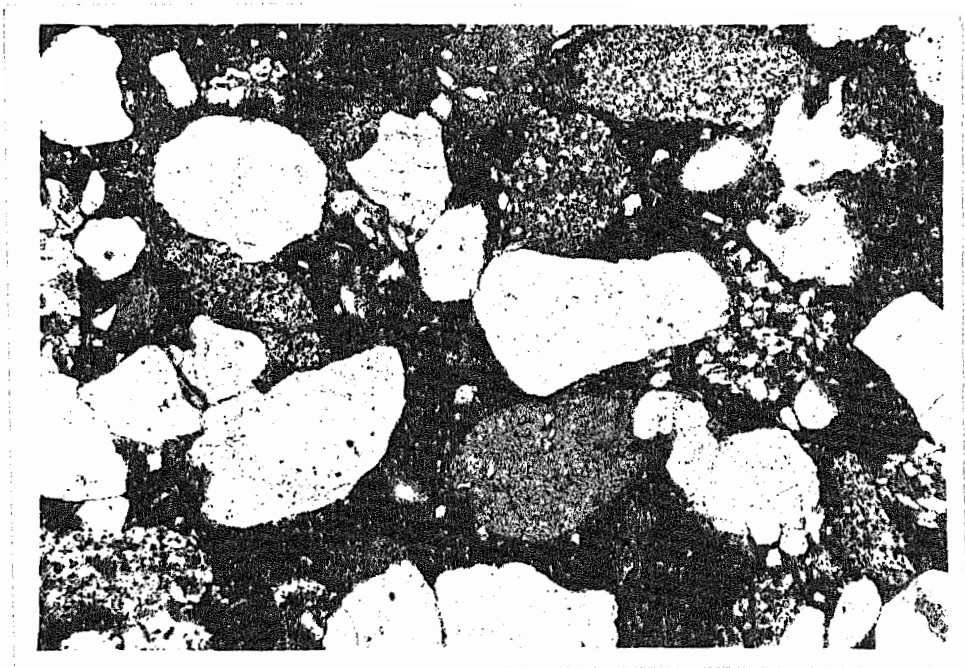


Fig. 2.59: Chloritic matrix with chlorite pellet (lower middle) in a coarse-grained wacke. Base of picture = 3.6 mm (-).

From whole rock analysis of one field sample of a chloritic wacke, yielding an Fe/Mg oxide ratio close to 2 (4.51 % Fe/ 2.22 % Mg), it is inferred that the chlorite belongs to the group of Fe^{2+} -chlorites. Thus it is possible that the original matrix was a ferruginous dolomite which was chloritized during the period of widespread silica-alteration in the Jillawarra Belt (cf chapter 4.6.). Some pellets probably consisted of dolomite less ferruginous than the matrix, resulting in the formation of light-green, hardly pleochroitic chlorite, which has higher Mg content than the matrix chlorite.

A relationship between carbonate-iron-chlorite becomes evident from Fig. 2.60 where part of the matrix material consists of iron-bearing carbonate while the other part is chlorite.

The processes of chloritization is discussed in more detail in chapter 4.6. However, for the following facies analysis it is assumed that the wacke type considered in this paragraph has a carbonate matrix.

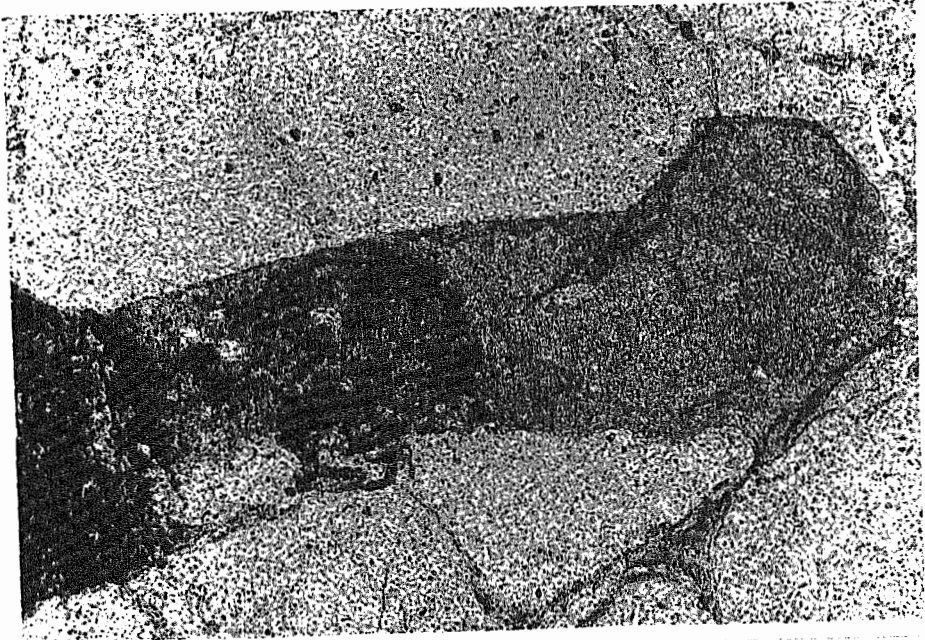


Fig. 2.60: Ferruginous carbonate grading into chlorite (from left to right), interstitially to quartz. Base of picture = 0.9 mm (-).

Constraints on the facies interpretation are a relatively low content of potash feldspar, abundant lithic clasts of pene-contemporaneous sediments of which at least some are derived from tidal sediments (abundant pyrite in micaceous, probably calcareous shale and clasts of pelletal rock), and a good state of roundness of the clasts.

A beach or barrier beach environment is inferred where carbonate deposition is possible and frequent reworking of the clastics occurs. Here, the clastic grains, of granitic provenance are certainly a "poly-cycle deposit", and the proportion of feldspars is considerably reduced. The lithic clasts, derived from adjacent tidal sediments, were transported and deposited by storm waters or in flood tidal deltas.

III) The third class was recognized unequivocally only in drill cores of the Abra prospect, but probably also occurs in outcrops east of the Woodlands Fault and south of the Jillawarra Camp. It comprises fine to very coarse-grained, poorly rounded calcareous wacke, micaceous and calcareous siltstone and some organic shale. The wackes have a moderate amount of clasts (others than quartz), mainly of

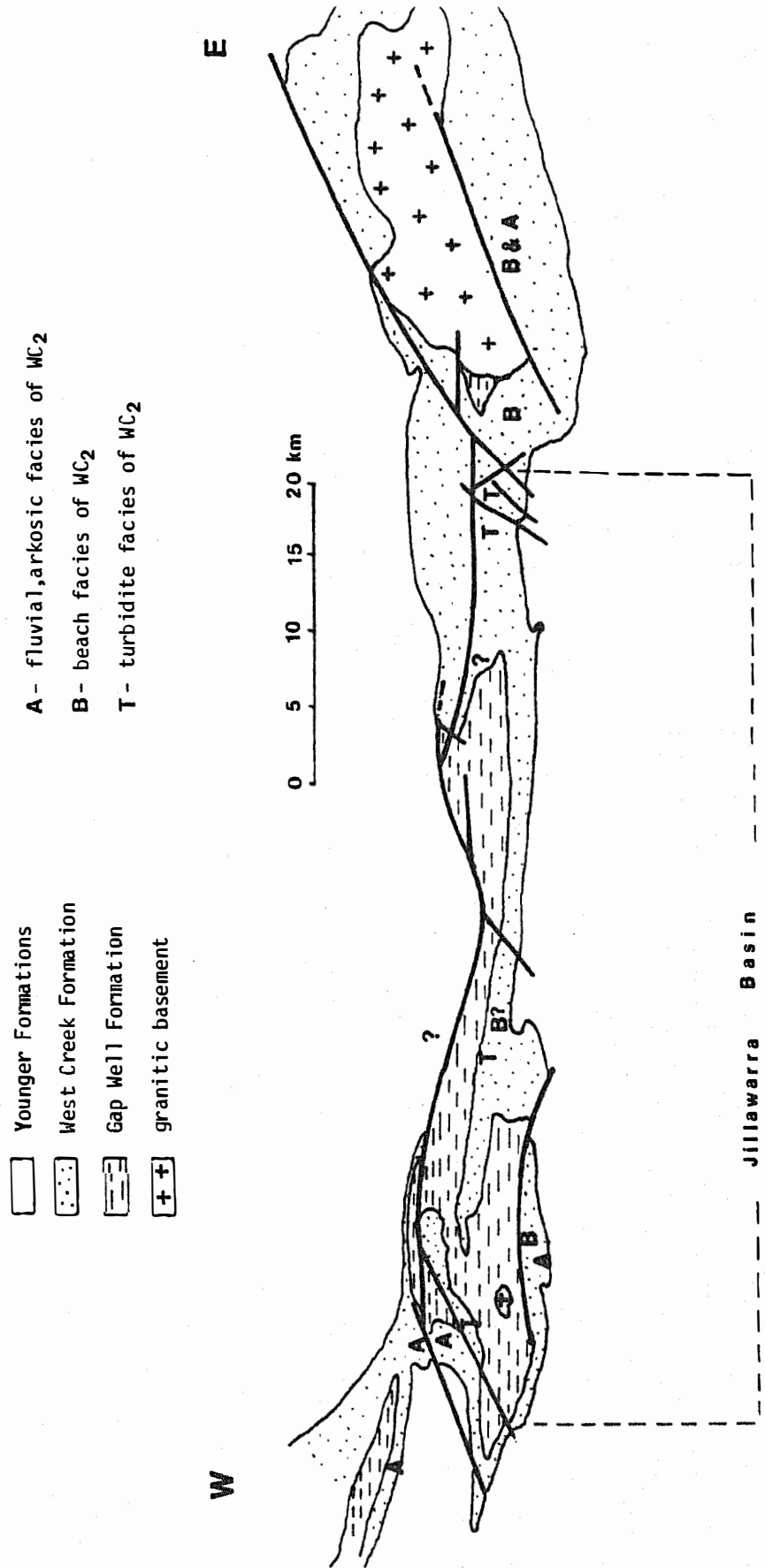
micaceous siltstone, black shale, potash feldspar and some pellets of Fe-carbonate. Graded bedding and scouring of shales is common.

Some rocks are fine-grained quartz arenites with occasional coarse quartz grains and shale clasts and are rich in detrital tourmaline. They represent comparatively mature sediments in which subhedral, minor euhedral, opaque cubes after pyrite indicate reducing conditions during diagenesis.

The most important feature of this class is the presence of turbidites (cf Fig. 2.56), occasional complete Bouma cycles and abundant rip-off clasts. As turbidites may form in a number of environments (e.g. Pettijohn, 1975; Walker, 1979) further characteristics have to be considered to evaluate the actual facies. The omnipresence of carbonate matrix, the occurrence of large subangular potash feldspar, and the frequency of carbonate pellets clearly points to near-shore deposits. On the other hand preservation of fine-grained mature wackes with one-directional low angle cross bedding foresets indicates conditions below wave base. In a model section the above features would be attributed to the foreshore zone, just below wave base but still in the range of carbonate deposition.

However, the occurrence of the beach type wackes (class II) on three sides of the Jillawarra Belt suggests that the turbidites formed in a basin into which clastics were transported from the surrounding terrestrial or beach areas. It is likely that the basin was subsiding due to synsedimentary fault activity and that the turbidites are "earthquake induced turbidites" (the earthquakes correspond to fault movement) as described by Robbins (1983) for intracratonic rifted basins. In this case the depositional environment may be compared with an extensive delta where the erosional gradient is maintained through repeated subsidence of the depository.

Fig. 2.61: Showing the limits of the Jillawarra Basin in relation to the Jillawarra Belt, and facies changes of the lower West Creek Formation (WC₂) in the vicinity of basin margin faults.



In summary, 3 facies division in the WC₂-unit are recognized; near shore alluvial deposits, beach or barrier beach deposits and shallow water, more basinwards turbidites. A regional facies distribution for the WC₂-unit is presented in Fig. 2.61, which shows the Jillawarra Belt surrounded by the alluvial and the beach facies. Palaeocurrent analysis of cross-bedding in coarse arenites of the Abra Prospect showed that transport direction was towards WSW (T.Ballinger pers.comm.) i.e. basinwards and supports the proposed facies zones. The map further shows a change from beach to turbidite facies in the vicinity of inferred synsedimentary fault zones; one the Woodlands Fault in the west, and the other the fault system east of Abra.

As the occurrence of the WC₁-unit is broadly within the limits of the inferred WC₂-turbidite facies, it is likely that it was one basin that commenced submergence at the onset of WC₁-times and continued through the WC₂-interval; it is called "Jillawarra Basin" and will be referred to as such in the following.

2.3.2.3. WC₃

The WC₃-unit dominantly consists of whitish, porous siltstone and shale which often is manganese stained or vari-coloured; subordinate arenite intercalations are common. West of the Jeds Prospect a chert horizon (0 - 5 metres thick) occurs in the lower part of the unit and is persistent westwards along strike for several kilometres extending outside the mapped area. Siltstones prevail adjacent to (and overlying) the chert.

In the vicinity of the Abra Prospect dolomitic rocks are common; SW of Abra there is a massive dolomite of some 400 metres strike length, and to the east and southeast of Abra, at a comparable stratigraphic level, dolomitic siltstone is abundant with a few lenses (less than 1 km along strike) of coarse-grained dolomitic wackestones (Fig. 2.62).



Fig. 2.62: Coarse-grained dolomitic wackestone with occasional lithic clasts (silicified).

Near the top of the WC₃-unit some mangiferous gossans containing 3000 ppm lead occur in the area of Abra; one is located close to the Abra Fault System.

The thickness of the WC₃-unit could only be estimated from field mapping, ranging from 0 to 750 metres. It attains the maximum value south of the Jillawarra Camp, and is possibly absent north of the point near the intersection of the Woodlands Fault and the Quartzite Well Fault.

The lower boundary is gradational and taken as the disappearance of significant arenite intercalations. The upper contact generally is sharp and marked by coarse arenites of the overlying WC₄-unit; however, where they are missing it is difficult to distinguish dolomitic siltstone and shale of WC₃ from the lower parts of the Jillawarra Formation which in general comprises similar rock types.

In thin section the fine-grained clastites are evenly laminated shale and micaceous siltstone, often ferruginous, with 2 - 10 % detrital potash feldspar and a moderate amount of rounded shale

clasts. As all sections are prepared from field samples the carbonate content of some has been dissolved. Chemical analysis of a ferruginous micaceous siltstone yields 2.85 % CaO plus 2.75 % MgO, indicating greater than 5 % dolomite. The barium content of 304 ppm is comparable with the average arenite of Pettijohn et al. (1973) of 440 ppm barium.

The arenite of Fig. 2.62 is a poorly rounded, coarse carbonate wackestone with abundant shale intraclasts and subangular potash feldspar. The ferruginous carbonate matrix may comprise up to 50 % of the rock volume.

One outcrop of the WC₃-unit consists entirely of micritic dolomite (27.30 % CaO/15.97 % MgO) veined by wispy quartz stringers (23.71 % SiO₂). Besides 1.52 % Al₂O₃ and 1.55 % Fe₂O₃ no significant major or trace element values have been detected. In this dolomite there is minimal epiclastic material which distinguishes it from dolomites of the Gap Well Formation.

The quartz veining provides a good illustration of the generation of the carbonate inclusions so common in rocks of this and older units. Fig. 2.63 shows that micritic dolomite of the vein margins grades into carbonate inclusions towards the centre with concomitant increase in quartz content.

Probably a silicified dolomite is represented by the chert horizons common in this unit. The rocks now consist of a fine-grained cherty quartz material with sometimes layered, diffuse iron-hydroxides. Small carbonate inclusions indicate the former carbonate nature of the chert. In one section textures of ferruginous and pyritiferous ooids and ferruginous pellets within the cherty quartz are abundant (Fig. 2.64).

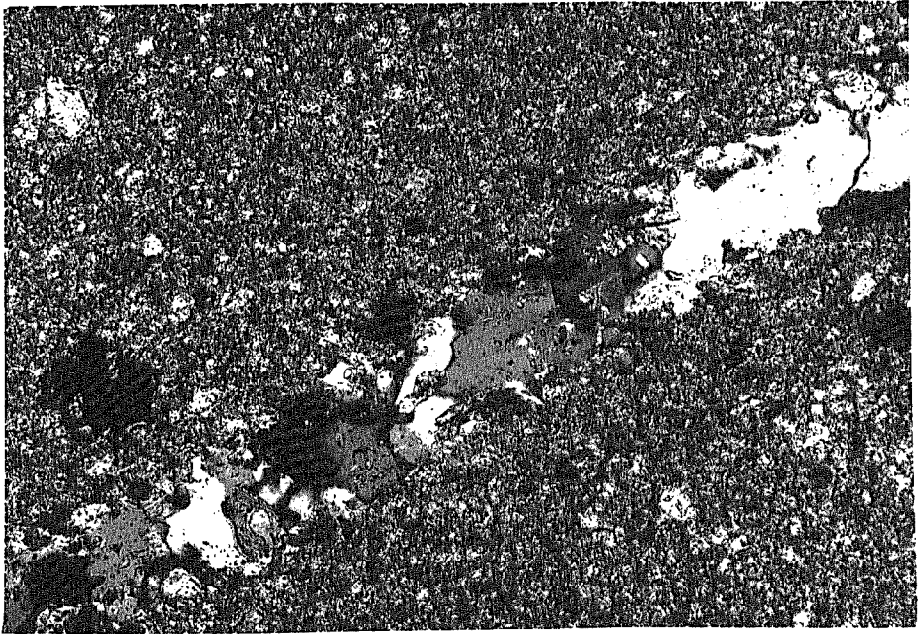


Fig. 2.63: Quartz vein in micritic carbonate with increasing number of carbonate inclusions towards the wall rock. Base of picture = 0.9 mm (+).

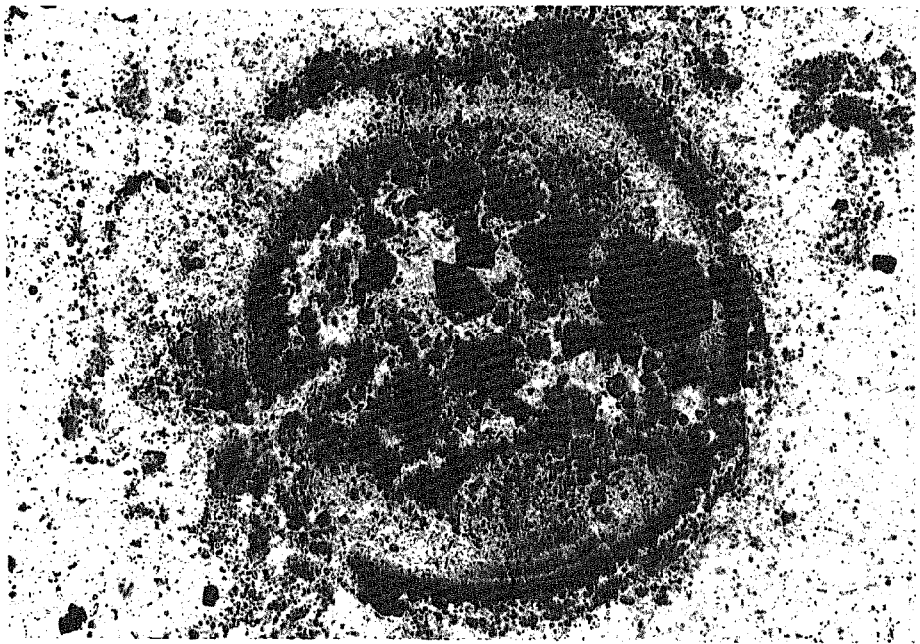


Fig. 2.64: Ferruginous and pyritiferous ooids in chert. Base of picture = 0.9 mm (-).

For the facies interpretation the rock types in WC₃ may be summarized as dolomitic siltstone and shale with minor interspersed dolomite lenses and oolitic, pelletal dolomite horizons. Locally dolomite-cemented coarse-grained, poorly rounded wackestones are embedded in the dolomitic siltstone.

Hence, it is likely that quiet shallow-water, tidal-flat conditions were re-established (as in the Gap Well Formation) after a period of high energy clastic deposition (i.e. the WC₁ and WC₂-units). The dolomitic siltstone and shale are the common intertidal sediments which received some terrigenous clastic input as indicated by subangular potash feldspars. Possibly some mounds or swells did exist where micritic carbonate was deposited without any clastic contribution. The occurrence of ooides suggests reworking of some material at the sediment/water interface by alternating tidal currents or wave action.

Through these tidal flats some tidal channels meandered depositing coarse-grained clastics within their beds; now recognized as the isolated carbonate wackestone bodies. The abundance of lithic clasts and the angularity of potash feldspar supports the interpretation as channel deposits with a nearby source of clastics. Fig. 2.65 shows a small coarse-grained and cross-bedded channel filling within dolomitic siltstone

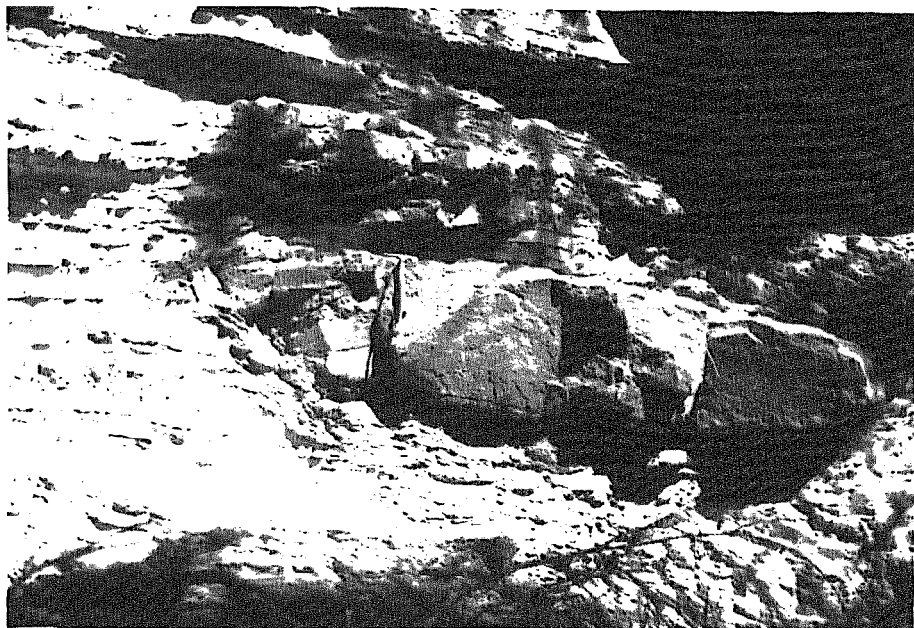


Fig. 2.65: Coarse-grained arenaceous channel filling within dolomitic siltstone.

2.3.2.4. WC₄

This unit consists of coarse-grained, often cross-bedded ferruginous arenite with locally abundant quartz-pebble conglomerate interbeds of 10's of centimetres thickness. Maximum strike length of continuous outcrops is about 8 kilometres at two localities (south of the Abra Prospect and at the West Creek type locality), in other places there are only limited arenite bodies.

The unit has a maximum thickness of 230 metres and in places is absent, the maximum value being estimated from outcrop at the West Creek type locality. The basal contact against softly weathering dolomitic siltstone of the WC₃-unit is well defined (although not sharp) while in the uppermost portion the lithology gradually changes through micaceous and chloritic siltstone, towards the dolomitic siltstone of the lower Jillawarra Formation.

In the vicinity of the Abra Prospect the arenites are intensely silicified causing a bluish colouring and massive quartzite appearance of the rock (Fig. 2.66).

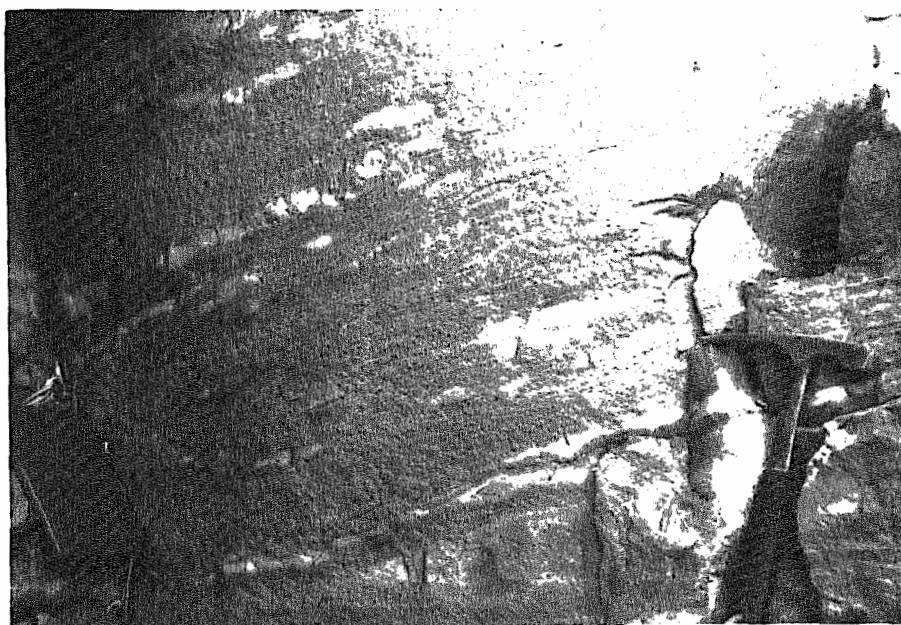


Fig. 2.66: Quartzitic appearance of silicified arenite
3 km south of Abra.

In thin section the arenites proved to be moderately to well rounded, well sorted, coarse-grained quartz sandstones with 0 - 8 % subangular potash feldspar (microcline). The sandstone is completely recrystallized to massive quartzite (120° angles of 3-grain-boundaries). Some interstices are filled with cherty quartz. The abundance of small carbonate inclusions suggests a former carbonate matrix.

For a facies interpretation the following facts have to be considered:

- a) high maturity of the arenite with comparatively low content of potash feldspar
- b) absence of lithic clasts and pellets.
- c) limited strike extent
- d) in the Abra area the WC₄-unit seems to surround the granitic Coobarra Dome
- e) at the West Creek type locality the strike length of the WC₄-unit approximately is limited by the Manganese Range and West Creek Faults.

A beach or barrier beach facies is inferred where frequent reworking of the clastics leads to increased maturity and sorting of the deposits. Shale clasts and calcareous pellets would rapidly be destroyed in such an environment resulting in "clean"-sands. A barrier beach is interpreted to have developed around the Coobarra Dome which probably was a basement high at this time again. Due west, the WC₄-unit is absent. However, in the vicinity of the Manganese Range Fault this unit reappears, where it might tentatively be interpreted as a barrier beach on the eastern side of the Woodlands Dome. In this case the two faults (West Creek and Manganese Range Faults) limiting the extension of the WC₄-unit may define the boundaries of the doming.

Despite the apparent control of faults on the outcrop pattern of the WC₄-unit, particularly at the West Creek type locality it is unlikely that these arenites represent deposits in subsiding basins as invoked for the coarse-grained wackestones of the WC₁-unit. The maturity of the WC₄-sandstones and the absence of lithic clasts rather indicates beach deposits. Reinson (1979) presents three hypotheses concerning the origin of barrier island systems of which one - the submergence of coastal beaches - can be excluded for the Jillawarra Belt as stratigraphically below the WC₄-unit no coastal beach deposits occur. In both the remaining hypotheses barrier beaches develop through growth of submarine sand and siltstone bodies (bars, spits). Thus no tectonism is required and the two limiting faults - which had been active in the lower parts of the West Creek Formation - merely facilitate a pre-WC₄, sea-bottom topography favourable for the development of a barrier beach.

2.3.3. The Jillawarra Formation

The Jillawarra Formation and higher stratigraphic units are characteristic of the overall Bangemall Basin and have been dealt with in the general description of the Bangemall Group (chapter 1.2.5.2.). In the Bangemall stratigraphy established by Daniels (1966) and Brakel & Muhling (1976) the Jillawarra Formation is regarded as one lithological unit. Mapping of the Jillawarra Belt established a subdivision into a lower calcareous unit (Mjd), and an upper unit consisting of vari-coloured shale and minor chert (Mjs) comparable to the Jillawarra Formation of the wider Bangemall Basin. Therefore, attention is focussed on the lower unit (Mjd) as it may be peculiar Jillawarra Belt facies.

2.3.3.1. Mjd

Dominant lithology of this unit is dolomitic shale and subordinate massive pelletal dolomite beds. West of the Woodlands Fault fine-grained quartz arenite prevails while in the area between "The Gap" and Gap Well & Bore (north of the Quartzite Well Fault) ferruginous arenites and calcareous shale are equally abundant.

South of the West Creek Fault a thick lens of greyish ([±] chloritic) laminated shale has a strike length of 5 kilometres. Towards the margins, a facies change by interlayering to whitish dolomitic shale occurs.

Thickness can only be estimated, because of the susceptibility to weathering of the dolomitic rocks, and may thin from 450 metres at Jillawarra Bore to virtually zero at Coobarra Dome.

The lower contact against the West Creek Formation is well defined where coarse beach deposits of the WC₄-unit are present, but is somewhat arbitrary when such rocks are absent.

The ferruginous shale consists of thin layers of micaceous, fine-grained siltstone and thin layers of particularly Fe-rich shale. Within the siltstone layers, subangular potash feldspar is present. Only insignificant amounts of lithic clasts have been observed.

Within some dolomites abundant rounded to subrounded micrite pellets (0.2 - 0.5 cm in diameter) occur in a ferruginous micritic carbonate matrix, the latter containing subordinate fine-grained, well-rounded detrital quartz. According to a pellet/matrix ratio of more than three the rock can be classified as a "pellet dolomite", after Folk (1959).

The facies of the lower Jillawarra Formation (Mjd) does not differ significantly from the WC₃-unit although it probably is more variable. While the pellet dolomite probably formed in an upper intertidal environment the arenites may be tidal channel fillings or beach deposits.

Although a shallow water, intertidal environment also was assumed for the WC₃-unit, the Mjd-unit has less coarse clastic intercalations and no wackestones. This decrease in terrigenous clastics may indicate the commencement of a transgression of a shallow sea which did not greatly increase the water depth.

2.3.3.2. Mjs

The main features of the upper Jillawarra Formation (equivalent to the facies of the Jillawarra Formation of Brakel and Muhling, 1976) have been discussed in chapter 1.2.5.2.

For the interpretation of facies development in the Jillawarra Belt it is, however, noteworthy that west of the Woodlands Fault

fine-grained, moderately sorted, rounded quartz arenites are more abundant than the shale facies. In addition, there is probably a decrease in thickness west of the fault. It is likely that some interfingering of open marine shale facies with barrier bar facies occurred in this area. The barrier bar west of the Woodlands Fault probably was the western barrier of the evolving Jillawarra Basin in which shale deposition took place. Interestingly, the Jillawarra Belt corresponds to the area of maximum thickness of the Jillawarra Formation in the whole Bangemall Basin (cf chapter 1.2.5.3.) according to P.Muhling (pers.communication 1983, Fig. 2.67).

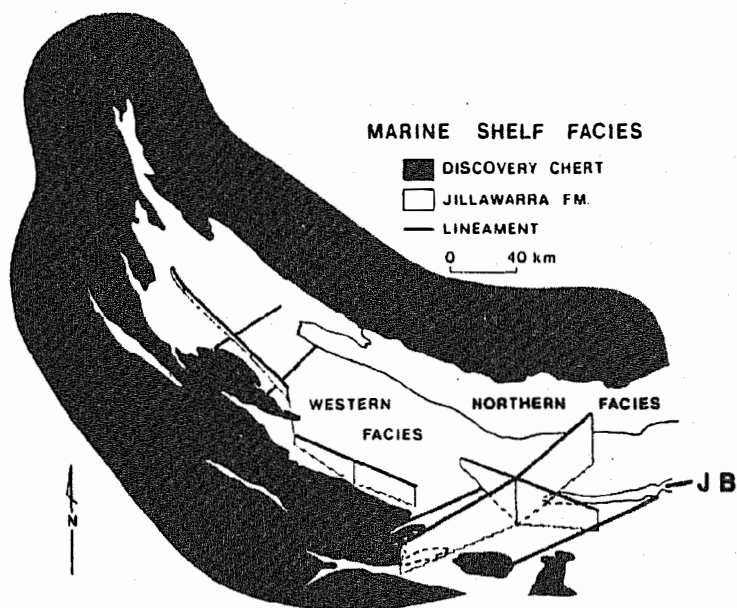


Fig. 2.67: Variations of thickness of the Jillawarra Formation within the western Bangemall Basin; J.B. = Jillawarra Belt.

2.4. Structure of the Jillawarra Belt

The Jillawarra Belt can be subdivided into 2 structural units based on style and intensity of deformation. East of the Abra Fault System gentle deformation and normal faulting prevails in the area of the Coobarra granitic basement dome, the western margin of the stable Bullen Platform (cf chapter 1.2.4.). West of the Abra Fault System the Jillawarra Belt forms part of the Edmund Fold Belt, a zone of both open and tight folds and various types of faults. The intensity of folding decreases west of the Woodlands Fault, where rocks of higher stratigraphic level are exposed.

2.4.1. Folds

Folds in the Jillawarra Belt range from gentle undulations, through tight upright folds with axial-plane cleavage, to thrust over-turned folds with cleavage parallel to bedding planes. For convenience of terminology, folds are referred to as regional (half wavelength more than 2 km), major (0.5 - 2 km) or minor (100's to 10's of metres).

The overall structure of the Jillawarra Belt is a regional E-W striking anticlinorium which comprises the Manganese Range and Jeds Anticlines. Both these anticlines plunge eastwards towards the Abra Fault System (the Coolina Anticline). Towards the west, the axis of the anticlinorium runs parallel the Quartzite Well Fault, and extends beyond the mapped area in a WNW-direction.

Equally important, but restricted to the western half of the Jillawarra Belt is a regional anticline, whose axial trace trends E-W and plunges in both directions, to form the Woodlands Dome.

While both these regional anticlinal structures have a tight style of folding, the major synclines (Woodlands Syncline, West Creek Syncline, the syncline south of Abra) and the major Abra Anticline

are of more open style with moderate to shallow dips.

The occurrence of tight anticlines and open synclines is in contrast to the deformational style generally in the Bangemall Basin where synclines are the tighter structures. Also important is that most tight regional folds (regardless whether syn- or anticline) are present in grabens. Thus this structural feature of the Bangemall Basin is also found in the Jillawarra Belt.

Folding in the Jillawarra Belt comprises four types which will be described in the presumed order of formation.

2.4.1.1. Slump folds

Slump folding and sliding on low-angle slide planes are evident in drill cores from the Gap Well and West Creek Formations within the Jillawarra Belt. Similar structures have been noted by Muhling & Brake1 (1985) in the Kiangi Creek Formation of the Glen Ross Anticline (some 25 km north of the Jillawarra Belt).

These features are interpreted as the result of deformation within a plastic sediment.

2.4.1.2. Drape folds

With progressive burial of the sediments (dewatering, higher confining pressure) complete strata became subject to plastic deformation in the form of drape folding. This ductile style of folding develops in the sedimentary strata ("cover") over the edges of vertically moving basement blocks. Its geometry and strain pattern has been demonstrated in experiments by Friedman et al. (1976) and Weinberg (1979). The resultant folds are box-shaped with relatively steep limbs and a shallow central part (Fig. 2.68).

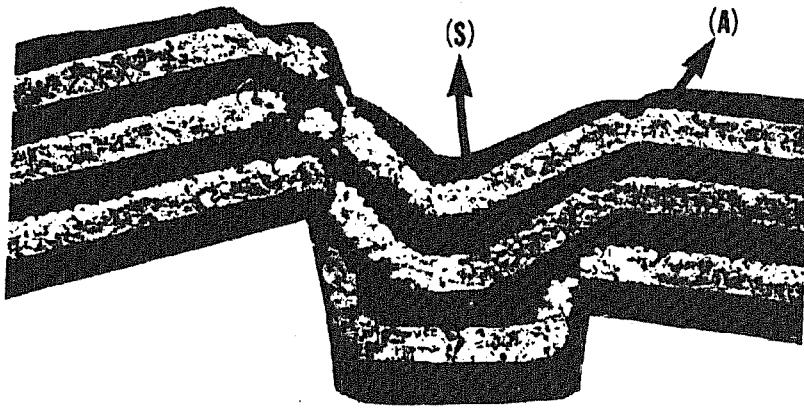


Fig. 2.68: From Weinberg (1979) showing the resulting fold style when basement blocks are faulted.

Many fold structures in the Jillawarra Belt, particularly the anticlines, cannot be described as drape folds as they are of tight style with steeply dipping limbs. However, they probably once have been drape folds and it is likely that this style of folding has been widespread in the Jillawarra Belt.

2.4.1.3. Tight folds

The main tight fold structures are the regional Jeds and Manganese Range Anticlines and the major Woodlands Dome Anticlinorium. However, small scale tight folds have been observed in the limbs of open folds, like in the southern limb of the major West Creek Syncline (Fig. 2.69), in the regional Range Creek Syncline 3 kilometres NW of Quartzite Well and in the southern limb of the major Abra Anticline. Minor tight folds are abundant in the Gap Well Formation between the West Creek Syncline and the Woodlands Syncline.

These subsidiary tight folds probably formed through shortening subsequent to the extensional period and were superimposed onto major open folds.

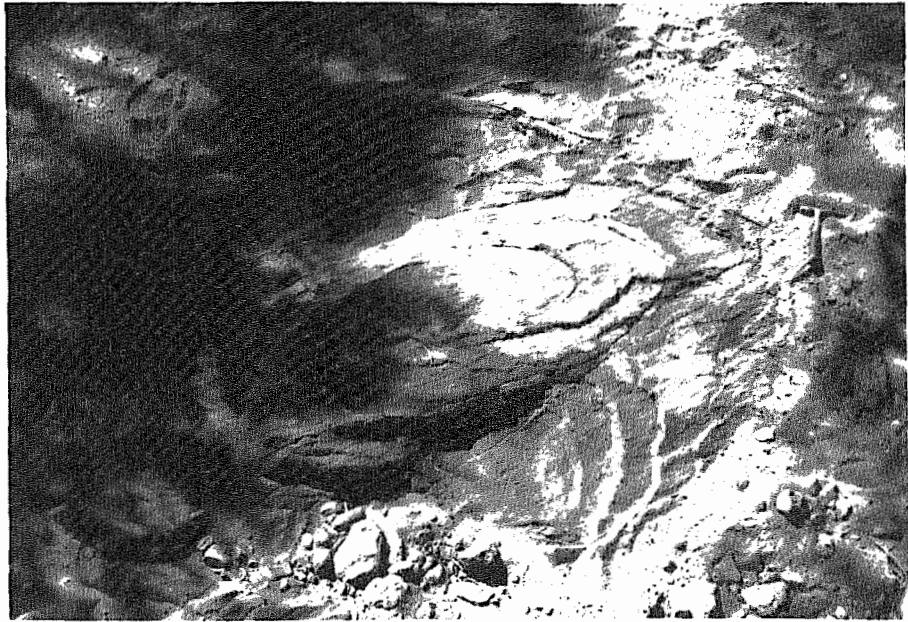


Fig. 2.69: Tight fold in the southern limb of the major open West Creek Syncline.

It is evident from consideration of the Bangemall Basin (see chapter 1.2.4.) and from the Jillawarra Belt (e.g. thrusting along the Quartzite Well Fault) that shortening occurred after the extensional period. Although shortening of basement can generate drape fold (Weinberg, 1979) once compression is applied to the overlying sediments themselves, this would cause tightening of the drape fold structures. This probably was the mechanism of formation of the tight folds in the Jillawarra Belt.

The style of folds is roughly similar (Hobbs et al., 1976); for synclines it is inherent from drape folding resulting in thinned limbs and thickened hinge zones when measured parallel to the axial surface.

The tight anticlinal structures were the sites of upward release of strain created by differential shear related to the development of folds at depth (Ramsey, 1962). They are not ideal similar folds but because of the alternation of competent and incompetent layers, are of class 1c (convergent isogons) and class 3 (divergent isogons, according to Ramsey, 1967).

It is possible that in the western parts of the Jillawarra Belt the area between the Quartzite Well Fault to the north and the West Creek Fault to the south was a regional box-shaped, drape folded syncline (the "Jillawarra Basin") initially related to graben formation. When the shortening strain regime commenced the graben was uplifted and compressional forces were applied to the sedimentary strata. The drape folded margins of the former graben continued to shorten to form two tight anticlines; the Jeds Anticline and Woodlands Dome Anticlinorium.

The principal process of formation of two tight anticlines at the margins of a graben is depicted in Fig. 2.70.

Folds associated with thrusting

Where the increase in lateral shortening could not be compensated by upward movement of the former graben, it caused thrusting of the basement. Section C-D on map 1 shows the presumed style of thrusting of the basement and the respective folding in the cover. The thrusting took place along the Quartzite Well Fault, one of the two major thrust fault systems in the Bangemall Basin.

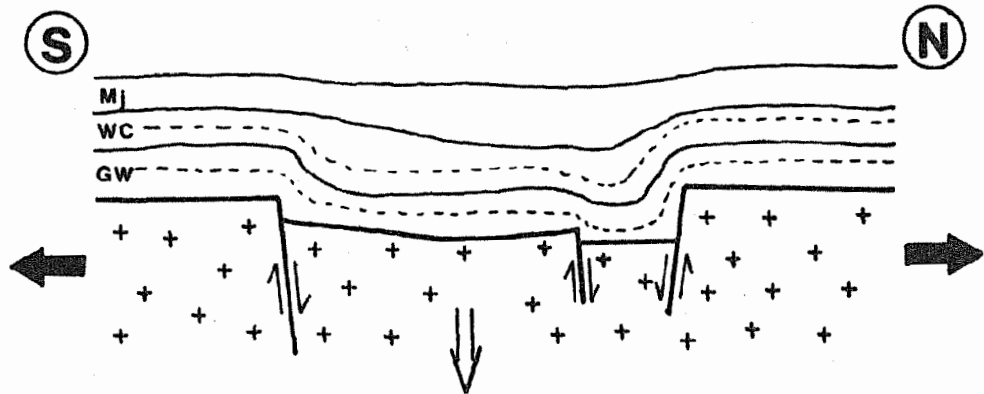
The Manganese Range Anticline - in which thrusting was most intense - has its anticlinal axis truncated by the Quartzite Well Fault in the western part, due to the arcuate nature of the fault. Its southern limb dips steeply south (60° - 70°) and provides no subsidiary folds; thus with respect to the southern limb the fold style is that of the tight folds described above.

The northern limb of the anticline however, is thrust towards the NNE. In this zone tight, subsidiary folding is abundant with tight minor folds, locally overturned towards the main thrust zone in the north. In some folds the north-dipping limb is suppressed or absent due to break-thrusting.

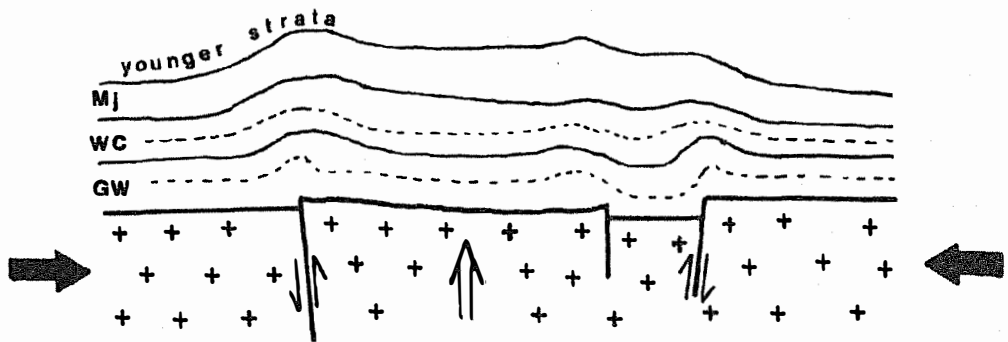
Fig.2.70: Schematic structural cross section through the western part of the Jillawarra Belt (near section A-B, map 1) showing the development of tight folds at the margins of an upfaulted graben.

➡ applied forces ⇨ principal movement

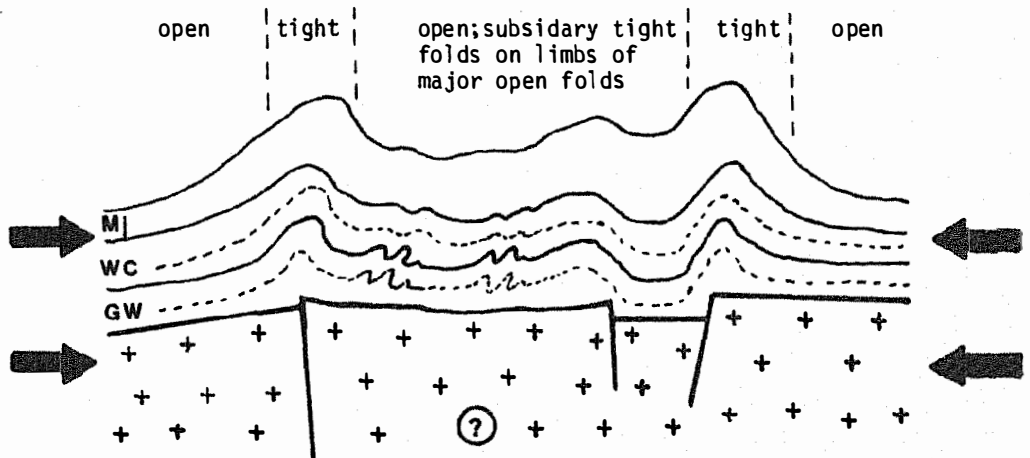
a) middle Bangemall Group



b) onset of compressional tectonics, post Bangemall Group



c) compressional tectonics affecting sedimentary cover

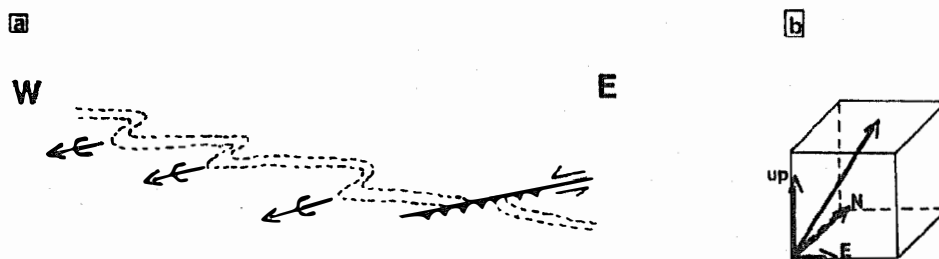


That tight folding is related to the thrusting is evident from two observations:

- I) The vergence - in the sense of Stille (1930), the facing of a geological structure - of all minor folds in the northern limb of the Manganese Range Anticlinorium (see section C-D on map 1), is into a northward direction. Thus the minor tight folds are asymmetrical in profile with very steeply dipping north-limb and shallow south limbs.

- II) The trend of the tight minor fold axes parallels the strike of the main (northernmost) thrust of the Quartzite Well Fault. This fact alone indicates a relation between thrusting and folding. Furthermore the folds are asymmetrical in plan view as shown schematically in Fig. 2.71a.

Fig. 2.71 a: Schematic plan view showing asymmetry of fold traces and break thrusting; b: vectoral forces inferred from the resultant northnortheastward-upward movement.



Sometimes small scale break thrusting along the axial plane surfaces occurs. Remarkably, the plunge of these minor folds often is into a WSW-direction while the overall plunge of the Manganese Range Anticlinorium is eastwards here.

The mechanism of formation of these fold structures becomes evident when the tectonic forces are regarded as the resultant of three principal vectoral forces as displayed in Fig. 2.71b; while the initial tight folding can be ascribed to the N-component and break thrusting to the up-component, the asymmetry in plan view of the fold traces probably is due to an E-component. Thus the tight, asymmetrical minor folds in the northern part (limb) of the Manganese Range Anticlinorium may be drag folds formed by the thrusting along the Quartzite Well Fault.

2.4.1.4. Variations in fold style

Lateral variation - The regional E-W trending anticlinorium determining the overall structure of the Jillawarra Belt ("The Gap" - Jeds Anticline - Manganese Range Anticlinorium - and its closure east of Copper Chert Prospect) is characterized by different styles of folding along strike.

- I) East of Copper Chert where the closure of the regional anticlinorium is marked by the Y-shaped ridges of the West Creek Formation (WC₂) the dips of arenite ridges are steep, even though the fold style approaches that of open folds. Open-style folding is best in the anticline of "The Gap", in the NW-edge of area mapped.
- II) In the western parts of the Jillawarra Belt, north of the Woodlands Syncline (cf Section A-B on map 1) folding is tight and symmetrical with steep dips on both limbs.
- III) Finally, in the Manganese Range Anticlinorium the last stage of folding is related to thrusting, resulting in tight, north-vergent, asymmetrical folding.

There appears to be a relation between faulting and the style of folding; where faults are absent the resultant fold style is open (case I). These folds are interpreted to have formed on rigid basement blocks. Tight folds (case II) occur in the vicinity of faults

e.g. the Quartzite Well Fault which probably mark the boundaries between basement blocks. Where the basement blocks are thrust case III applies.

Therefore it is concluded that the basement has control on the deformation in the cover, in that the locus and degree of block faulting in the basement determine the location and degree of deformation in the sedimentary cover.

Vertical variation - Locally there is a marked difference in degree of deformation between the Gap Well Formation including the WC₁-unit, and the WC₂ to WC₄-units of the West Creek Formation and overlying formations which is expressed in abundant small-scale subsidiary (parasitic) folding of the lower parts and possibly in a disconformity between the WC₁ and WC₂-unit in the area SE of the Copper Chert Prospect.

These variations in deformation may be interpreted in the following manner:

- I) Difference in competency between the Gap Well Formation (dolomitic shale which deforms plastically) and the West Creek Formation (arenite) which is far more competent, probably is the main reason.
- II) However, the WC₁-unit - even with its coarse arenite portions - behaves similar to the incompetent Gap Well Formation.

This unit has been interpreted as the sedimentary filling of localized, rapidly subsiding basins and it is likely for such coarse clastic deposits that a single sediment complex would be wedge-shaped and horizontally inclined. When subsidence took place on a more regional scale it could further have inclined the surface of the WC₁-unit with respect to the sedimentary base of the WC₂-unit which subsequently was deposited

with a disconformity on the WC₁-unit. However, this disconformity does not necessarily indicate a significant time break.

III) When drape folding over moving basement blocks commenced strain was greatest in the lowermost strata, and decreased upwards as differential shear transferred from below was progressively compensated by the deformation of these strata (Weinberg, 1979). Although this process may be important on a large scale with respect to the Bangemall Group as a whole it probably has had little significance for the deformational difference between the Gap Well and West Creek Formation.

2.4.2. Cleavage and lineation

Within the central zone of the Jillawarra Belt where open folds predominate cleavage is poorly developed. Newly grown muscovite usually lies parallel to bedding and is presumably due to compaction during burial.

However, in the hinge zones of subsidiary tight folds, which are common in the Gap Well Formation within the central zone of open folds (see Fig. 2.70c), axial plane cleavage is common. Fig. 2.72 shows sparitic carbonate growth parallel to the cleavage at approximately 30° to bedding.

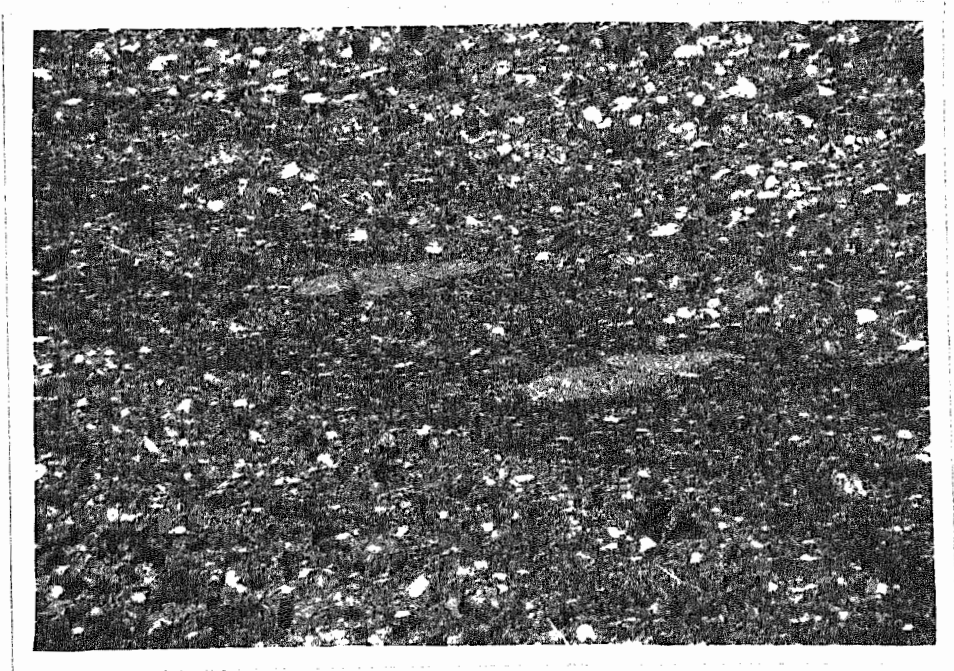


Fig. 2.72: Growth of sparitic carbonate in cleavage direction, about 30° to bedding. Base of picture = 3.6 mm (+).

Cleavage expressed by chlorite growth occurs in the Manganese Range. However, as the latest folding was related to thrusting the cleavage strikes parallel to Quartzite Well Fault in the northern limb of the Manganese Range Anticline and has a deviation from the strike of the regional axial plane of about 20° . Thus the cleavage - at least in vicinity to the Quartzite Well Fault - developed through differential shear associated with the thrusting; movement along cleavage planes probably was executed into an upward - northward - eastward direction.

Shear cleavage also is in good agreement with the frequent parallelism of bedding and cleavage, particularly in the northern limb of the Manganese Range Anticline.

The dominant cleavage direction in the whole Jillawarra Belt is 110° . Dips are mainly vertical. It maintains its strike of 110° irrespective of the local trends of minor and major folds. With a mean strike of 110° it is orientated normal to the regional NNE-SSW compressional forces inferred from thrusting along the Quartzite Well Fault. However, this cleavage is not related to the thrusting itself as the 110° strike is still abundant, where no thrust faults have been observed.

Lineations are abundant in the Manganese Range Anticline. They occur in the vicinity of the Quartzite Well Fault where it trends about 80° (eastnortheast). The lineations are visible on bedding surfaces and plunge with 35° - 45° towards the southwest while strike of the respective bedding is about 80° - 85° .

2.4.3. Faults

Within the Jillawarra Belt there are three main trends of faults - northeastward, subordinate southeastward and eastward. The latter fault trend may have an arcuate fold trace, like the Quartzite Well Fault and the West Creek Fault. Most faults are normal except the east-trending Quartzite Well Fault which is thrust.

2.4.3.1. Normal Faults

Although very few fault planes are exposed it is assumed that the normal faults have steeply dipping fault planes.

- I) The NE-trending faults are the most abundant group of normal faults. They confine the depository system of the Jillawarra Basin in the West (Woodlands Fault) and in the East (Abra Fault System).

Commonly they affect lower stratigraphic levels; while the offset is obvious in the Gap Well Formation and lower levels of the West Creek Formation, faulting has minor influence on strata of the Jillawarra Formation and higher levels. For example, in the southern parts of the Woodlands Faults the arenite ridge of the WC₂-unit is displaced about 300 metres by the fault while in the outcrop of Jillawarra Formation (Mjs) the horizontal offset by faulting is less than 100 metres (see map 1).

The NE-trending faults have been active since early times of sedimentation of the Bangemall Group; the Manganese Range Fault acted as a boundary between reef carbonate and sandy carbonate sedimentation in the upper Gap Well Formation (cf chapter 2.3.1.6.), the Woodlands Faults marks the transition from beach deposits to shallow water slope turbidites on the western margin of the Jillawarra Basin, in the WC₂-unit of the West Creek Formation.

Faulting along the NE-trending faults is older than folding; this is also shown by a folded fault in the eastward extension of the anticline south of "The Gap" (in the northwestern part of map 1).

Except for the Manganese Range Fault, the sense of the last horizontal movement of the NE-trending normal faults - which may have been executed after Bangemall Group deposition - has been dextral, i.e. the rocks east of the fault have relatively moved to the SW.

The Abra Fault system is a component of the regional NE-trending Tangadee Lineament, 100 kilometres due west another NE-trending regional lineament occurs (Flint Hill lineament) leaving the area of the Jillawarra Belt (plus some 15 km to the west) as a structural domain limited by two regional lineaments. It is likely that the NE-trending normal faults of the Jillawarra Belt are related to these lineaments, and that they are the products of the same regime of crustal strain, and extend over the same time range (i.e. from the upper Gap Well Formation beyond the end of the Bangemall Group), as the regional lineaments (cf chapter 1.2.4.).

- II) SE-trending faults are present in the eastern part of the Jillawarra Belt and affect the West Creek Formation (e.g. east of Abra) as well as higher stratigraphic levels (e.g. displacing the Discovery Chert NW of Copper Chert). Variations in displacement with respect to the stratigraphic level could not be quantified.

Although little is known about the SE-trending faults, their existence and relative abundance in the eastern part of the Jillawarra Belt (i.e. at the eastern margin of the Edmund Fold Belt) indicate the occurrence of an additional structural trend in the eastern part of the Jillawarra Belt.

III) The east-trending arcuate West Creek Fault is a normal fault dipping about 60° north. Other, east-trending, normal faults occur north of West Creek Well, as well as in the closure of the regional Coolina Anticline south and southeast of Copper Chert Prospect, and also in the southern limb of the Abra Anticline.

The occurrence of east-trending faults in the hinge zone of anticlinal structures north of West Creek Well and southeast of Copper Chert, suggests that they formed during folding. This style of faulting is characteristic of a higher strain rate. Only minor displacement is associated with this late stage faulting.

The West Creek Fault - which in fact is a fault system - formed early in the Bangemall Group, and has influence on the West Creek Formation (WC_2). This fault system has also been active in the late stage deformation of the Jillawarra Belt; faulting of lithified rocks is evident from brecciation and silification of the fault zone. Late stage faulting has resulted in considerable (2 - 3 km) ENE-movements.

The east-trending fault in the southern limb of the Abra Anticline has formed in the lowermost West Creek Formation. It parallels the inferred margin of the Jillawarra Basin and defines the northern limit of the Abra sub-basin; this fault zone probably had major control on ore forming processes of the Abra mineralization (cf chapter 4.2.). Late stage movement along this fault resulted in upfaulting of the former sub-basin.

Of the normal faults described above, the West Creek Fault and the east trending fault in the southern limb of the Abra Anticline probably had originally been normal faults; the last

movement, however, was executed in the opposite (reverse) sense, due to the late stage upfaulting of the former graben.

2.4.3.2. Reverse faults and thrust faults

Faults associated with the arcuate, east trending Quartzite Well Fault System are either reverse or thrust faults.

The Quartzite Well Fault - probably a major basement fault - defined the northern margin of the Jillawarra Basin. During shortening the graben was upfaulted and reverse faults developed, like north of the Woodlands Syncline and north of the Abra Prospect (as shown in section A-B and E-F, respectively, on map 1). Where lateral shortening was highest thrusts formed.

Both fault types belong to the late-stage tectonism of the Jillawarra Belt; faulting has affected fully lithified rocks as evident from brecciation and silification of the fault zones. The truncation of the NE-trending faults by the Quartzite Well Fault System further corroborates that movement along the fault system was a late-stage event.

Stratigraphic displacement (upward movement) along the Quartzite Well Fault Zone has been about 3 kilometres in the vicinity of Quartzite Well; there also has been a sinistral displacement where the fault zone bends to the northeast.

Westwards from the Jillawarra Camp the fault trace gradually becomes northwestward trending and the NNE movement direction is oblique to the fault. Therefore a number of E- and ENE-trending subsidiary faults have formed to compensate the deviation from the direction normal to the compressional forces.

Near Copper Chert Prospect the displacement along the Quartzite Well Fault decreases rapidly and the fault splays towards the east. The apparent sense of horizontal movement along the southern splay fault turns into dextral.

It can be summarized that the amount and rate of lateral shortening, both within the basement and the sedimentary cover, determines whether reverse or thrust faults form, and the amount of thrusting. However, these factors alone cannot account for the considerable thrusting at Quartzite Well as opposed to the splay fault north of Copper Chert.

There seems to be a relation between the nature of the basement and the amount of thrusting; either the location and strike of the early margin faults (i.e. the shape) of the Jillawarra Basin was governing the later deformation, or the degree of subsidence (i.e. extension of the basement) in the central part of the Jillawarra Belt was highest, resulting in most pronounced uplift and thrusting in the period of compressional tectonics. Possibly both factors - shape of the basin and degree of subsidence together were active in determining the eventual amount and degree of deformation.

2.4.4. Summary

The Jillawarra Basin - bounded by NE-trending and E-trending normal faults - formed due to a tensional crustal regime at an early stage of sedimentation. During times of infilling of the sedimentary basin, drape folding, initiated by normal block faulting in the basement, resulted in stronger deformation in lower stratigraphic levels. Probably after termination of sedimentation compressional forces were applied to the basement which in areas of high shortening transmitted strain to the sedimentary cover. These forces caused an upfaulting of the former basin along the E-trending margin faults; the upward movement was most intense in the area of Quartzite Well and eventually resulted in thrusting into a NNE-direction. The shear associated with the upfaulting caused the development of a regional cleavage direction striking 110° .

Through the whole deformational history the fold style remained open where no major basement faults occurred; however, in the zones of basement faults the former open style drape folds were converted to tight folds, or to north-vergent tight folds related to thrusting.

The general structure of the Jillawarra Belt today is determined by a northern, regional E-trending anticlinorium (Coolina Anticline), which is asymmetric in the area of Quartzite Well probably due to shortening in the basement. In the western half of the Jillawarra Belt a southern, major E-trending anticlinorium plunges eastward and disappears at about $118^{\circ}23'$. Both, the northern and eastern anticlinorium, probably mark the margins of the former Jillawarra Basin.

2.5. Igneous Rocks of the Jillawarra Belt

Most igneous rocks in the Jillawarra Belt are dolerite intrusions (mainly sills and some dykes) into the Jillawarra Formation and higher stratigraphic levels. They have been described in chapter 1.2.6. as they are not characteristic of the Jillawarra Belt.

No igneous rocks have been found in the Jillawarra Basin - between the Woodlands Fault and the Abra Faults System -. In an unpublished report (AMOCO, 1977) the occurrence of volcanoclastic rocks within the GW_{W4} and GW₃-units of the Manganese Range Anticline has been suggested. However, no evidence for a volcanoclastic component in the respective rocks could be found despite examination of some 15 thin sections.

2.5.1. Mafic intrusions

East of the Jillawarra Basin (i.e. east of the Abra Fault System) minor dolerite was encountered in two percussion drill holes south of Coobarra Hill. It intruded the upper Gap Well or lower West Creek Formation. The emplacement probably was controlled by the main NE-trending fault (see map 2) or its splay fault, separating the granitic, stable basement of the Coobarra Dome from the Jillawarra Belt with more mobile basement.

As this NE-trending fault belongs to the regional Tangadee Lineament, and dolerite dyke emplacement related to the regional Flint Hill Lineament and another lineament further west has been reported by Muhling et al. (1978), it is likely that intrusion of the Coobarra Hill-dolerite was controlled by the NE-trending fault.

Although on map 2 the dolerite is shown as a sill, evidence for such a shape is equivocal, as the dolerite was only found in two drill holes separated by some 20 metres. Thus the occurrence of a doleritic dyke instead of a sill is equally possible.

2.5.2. Felsic volcanic activity of the Coobarra Dome

In Fig. 2.73 the occurrence of felsites of the Coobarra Dome are shown.

2.5.2.1. Rhyolite

At 23⁰37'S, 118⁰47'E approximately 60 metres above the basal unconformity of the Bangemall Group there occurs a line of six small rhyolite bodies ("Tangadee Rhyolite") within the lower WC₂-unit. The rhyolite shows vari-coloured flow banding of uncertain origin. In thin section it consists mainly of euhedral quartz and feldspar phenocrysts, in a cryptocrystalline groundmass of quartz and minor microcline, with accessory biotite, chlorite, zircon and opaques.

The quartz phenocrysts are hexagonal or rhomboidal in section, preserving the bipyramidal shape of β -quartz. Most phenocrysts are embayed, indicating resorption or corrosion by the groundmass, and many have become well rounded.

The feldspar phenocrysts now consist of granular intergrowth of quartz and microcline, and are considered by Gee et al. (1976) to have been sanidine phenocrysts.

These authors also report rare, irregular or distinctly spherical-shaped lithophysae of pyrite, ilmenorutile, chlorite and carbonate encased by quartz and microcline, which are wrapped by the flow banding and therefore were in existence as solid objects while the volcanic material was still flowing.

Chemical analyses of four samples of the rhyolite are given in Tab. 2.02. It is obvious from comparison with average chemical composition of rhyolites (Nockolds et al., 1978) that this rock is highly altered, as emphasized by extremely high K₂O, extremely low Na₂O and slight increase in SiO₂. The enrichment of potassium at the expense of sodium is a common type of alteration and has

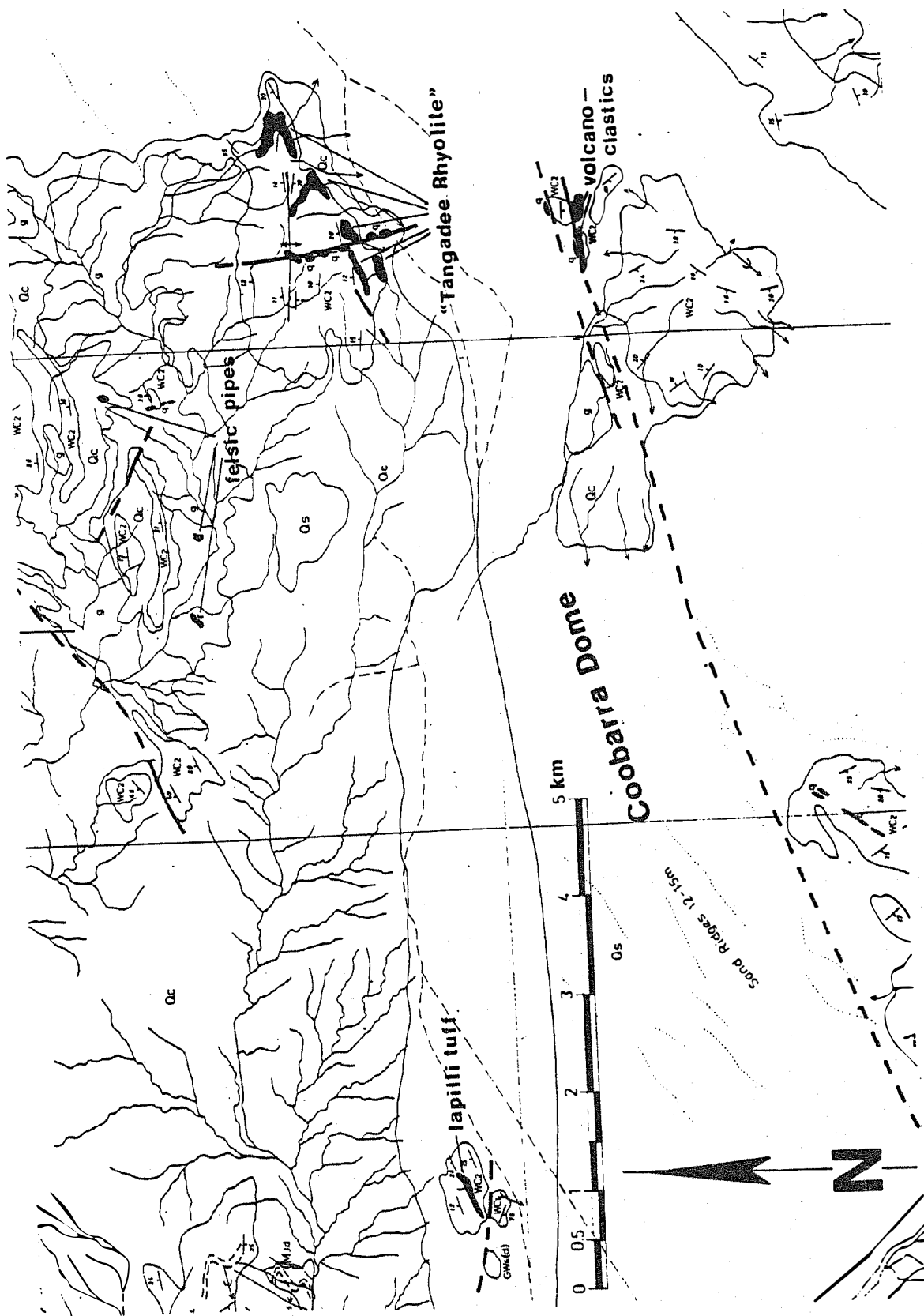


Fig. 2.73: Section of map 1; showing locations of felsites of the Cobbarra Dome

Table 2.02 Chemical analyses of siliceous volcanogenic rocks of the Coobarra Dome

Oxides in weight percent, elements in ppm

	1	2	3	4	5	6	7
SiO ₂	78.0	76.1	74.9	83.4	79.7	85.23	76.45
Al ₂ O ₃	11.1	12.3	12.3	10.24	9.97	9.02	10.62
Fe ₂ O ₃	0.66	0.62	1.06	0.43	2.93	1.97	5.18
MgO	0.02	0.02	0.23	0.17	0.71	1.03	1.92
CaO	0.10	0.06	0.04	0.18	0.11	0.07	0.08
Na ₂ O	0.15	0.15	0.20	0.55	0.27	0.10	0.23
K ₂ O	9.06	9.21	10.45	9.66	3.59	1.99	0.04
MnO ₂	< 0.01	< 0.01	< 0.01	< 0.01	0.02	0.01	0.03
TiO ₂	< 0.01	< 0.01	< 0.01	0.04	0.11	0.13	0.34
P ₂ O ₅	< 0.01	< 0.01	< 0.01	0.01	0.03	0.03	0.04
SO ₃	0.04	0.03	0.03	-	-	0.03	0.03
Mo	< 10	< 10	< 10	2	1	-	-
W	5	< 5	< 5	< 10	< 10	-	-
Zn	17	16	15	7	46	< 1	24
Pb	110	110	65	6	46	-	-
Bi	-	-	-	< 2	< 2	-	-
Cd	-	-	-	< 0,5	< 0,5	-	-
Co	-	-	-	< 1	2	< 1	3
Ni	-	-	-	4	5	3	16
Ba	-	-	-	460	2950	3356	85
Cr ⁺⁺	2189	1779	274	325	85	26	16
V	< 56	< 56	< 56	< 1	14	28	12
Be	-	-	-	< 0,5	3	-	-
Cu	45	190	110	5	10	17	24
As	-	-	-	< 0,2	< 0,2	-	-
Sr	20	20	20	18	71	57	83
Rb	150	160	180	-	-	111	< 1
H ₂ O ⁺	0,51	0,80	0,29	-	-	2,95	1,13
TOTAL [%]	99,97	99,57	99,87	104,78	97,74	102,53	96,43

1,2,3: Rhyolite near Tangadee. From Gee et al. (1976)

4: Rhyolite near Tangadee. Analyst: CHEMEX LABS Ltd., Canada,
using ICP and AAS, no H_2O^+ -
determination.

5: Lapilli tuff south of Coobarra Hill. Analyst: see 4

6: Lapilli tuff south of Coobarra Hill. Analyst: Geol.Pal.Institut,
University of Hamburg
West Germany, using
XRF.

7: Black, felsic, pipe-like intrusion in granite, about 2.5 km
NNW of the rhyolite. Exterior, weathered surface has not been
removed. Analyst: see 6

-: not determined

*: Cr-values in excess of 60 ppm probably are analytical arte-
facts.

been reported by Nockolds et al. (1978) and Fischer and Schmincke (1984).

Gee et al. (1976) conclude from the excellence of textural preservation and the occurrence of fresh sulphides that alteration of the Tangadee Rhyolite considerably predates any recent weathering. However, complete chemical reconstitution of the rock does not allow the determination of timing and mechanism of the alteration. The Rb/Sr-age of 1098 ± 42 m.y. is believed to date this alteration event.

According to these authors the rhyolite formed by local melting on a movement plane in the granitoid basement of the Coobarra Dome - although experimental data yield no indication of the true initial $^{87}\text{Sr}/^{86}\text{Sr}$ ratio and hence no isotopic evidence of the origin. It has been interpreted as extrusion of glassy viscous lava along fissures with an ENE-trend, hence with a trend parallel to the regional Tangadee Lineament.

2.5.2.2. Lapilli tuff

About 10 km west of the rhyolite, south of Coobarra Hill, a small elongated outcrop of lapilli tuff occurs. It has a thickness of about 1 metre, a strike length of 50 metres into N 70° E direction, and probably is conformably over- and underlain by rocks of the lower WC₂-unit.

The lapilli tuff is composed of layers of lapilli of different grain size (1 - 8 mm) but similar grain size or graded bedding within the individual layers. These layers are separated by bands (1 - 3 centimetres thickness) of lapilli-free tuffaceous material.

The lapilli are ovoid-shaped with their longer axis almost perpendicular to bedding. A similar orientation of the longer axis of quartz crystals perpendicular to the laminations of crystal tuffs has been noted by Pettijohn (1975, p.307) who suggested that this orientation is inherited from the "way they have fallen into it".

In thin section the lapilli resemble accretionary or armored lapilli with coarse vesicular pumice shards in the core and fine-grained tangentially aligned platy shards forming the rim (Fig. 2.74).

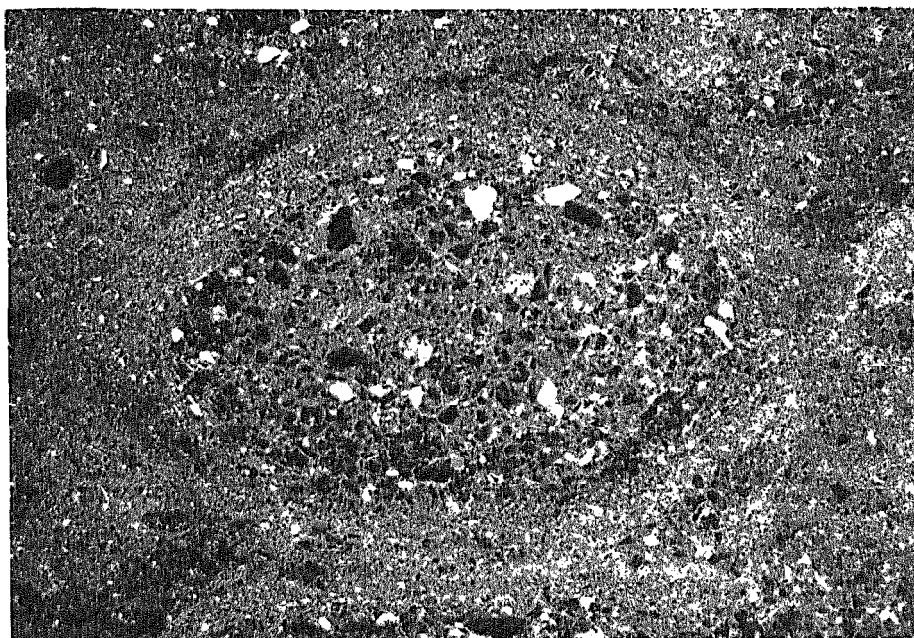


Fig. 2.74: Lapilli with coarse pumice shards in the core and fine-grained platy shards as rims. Base of picture = 5.6 mm (+).

Notably, minor angular, sometimes embayed, quartz grains occur in the coarse parts of the lapilli.

The recognition of the type of lapilli can be helpful in distinguishing between a) pyroclastic eruptions (caused by expansion of gases initially contained with the magma) and b) hydroclastic eruptions (caused by vaporization of external water in contact with hot magma or lava), which are the two general categories of eruption, after Fisher and Schmincke (1984). Accretionary lapilli are often, and armored lapilli are reported exclusively, from hydroclastic eruptions. As the lapilli are probably intermediate between accretionary (pumice and ash aggregates) and armored (crystalline

aggregates i.e. the quartz grains mentioned above) it is likely that they formed during hydroclastic eruptions.

The type of magma can be inferred from the nature of the glass shards. Although there are many variables affecting the shape of glass shards, Izett (1981, in Fisher & Schmincke, 1984) presents evidence to show that pumice shards tend to develop from relatively high viscosity magmas with temperatures below 850⁰ C. The whole rock chemistry (Tabl 2.02) shows that the K-alteration reported of the rhyolite did not affect the lapilli tuff.

By comparison with chemical analyses of 7 tephras of rhyolitic fallout and flow deposits presented by Fisher and Schmincke (1984) it becomes evident that the lapilli tuff is impoverished in both potassium and sodium, and enriched in silica. This chemical trend can best be explained by leaching of the Na⁺ and K⁺ ions with concomitant relative enrichment of SiO₂. However, the timing of this leaching remains unclear; it could have occurred when the presumably subaerially deposited lapillis were first covered by water in the WC₂-unit, or through recent weathering processes.

The existence of some recent weathering is indicated by the occurrence of liesegang rings which also may cause increase in iron values (Tab.2.02).

Barium is enriched within the lapilli tuff when compared to the results of the above authors. As the immobility of barium during weathering has been shown (e.g. Mann, 1982; Taylor, 1983) it can be inferred that the introduction of barium has been an early event.

Two possible processes for barium introduction are envisaged:

- I) The barium-rich hydrothermal system, which probably was most active during deposition of the lapilli tuff, was linked to the sites of rhyolitic magma generation within the basement.

The water added to the magma through faulting and fracturing of the basement in the lower WC₂-unit was enriched in barium, and during vaporization of the water barium was added to the vapor phase, prior to eruption.

II) After deposition and initial burial of the lapilli tuff, the diagenetic formation waters were rich in barium - as they seem to have been in the Abra hanging wall which now has about 3000 ppm Ba in rocks some 30 - 40 metres above the top of the mineralization - and precipitated their solutants as barite or as replacement of sodium and potassium. In this case barium was added after eruption.

2.5.2.3. Other volcanoclastic rocks.

About two kilometres south of the Tangadee Rhyolite, on the down-faulted southern side of a ENE-trending fault, two elongated bodies of poorly preserved, silica-rich volcanoclastic rocks occur. To the north the outcrops are limited by the fault, to the south the rocks seem to be overlain by the WC₂-unit.

Mesoscopically, the rock consists of large, occasionally rounded quartz grains (up to 1 cm) in a fine-grained siliceous matrix. It is poorly sorted and no bedding or lamination is visible.

In thin section, rounded quartz grains with enhanced undulatory extinction probably represent a detrital sedimentary component. The volcanogenic quartz grains comprise euhedral quartz (Fig. 2.75), embayed grains, angular and fractured grains, and curved laths of quartz (Fig. 2.76).

These grains (0.01 - 1 centimetre in diameter) are irregularly distributed in a fine-grained siliceous matrix which probably has formed through devitrification of pumice or glass shards.

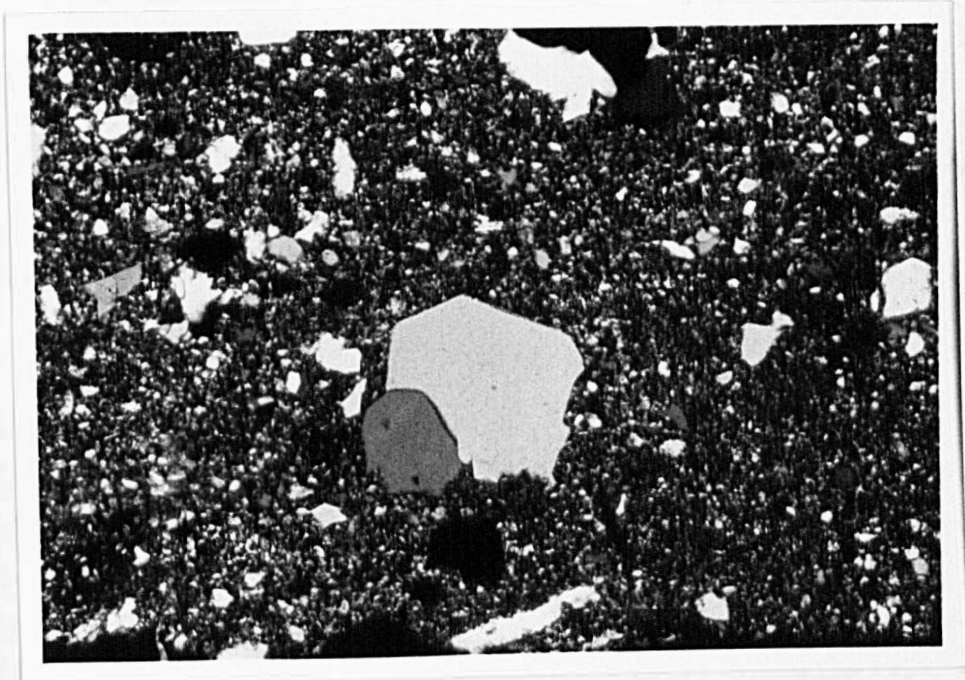


Fig. 2.75: Euhedral quartz grain in siliceous matrix. Base of picture = 3.6 mm (+).

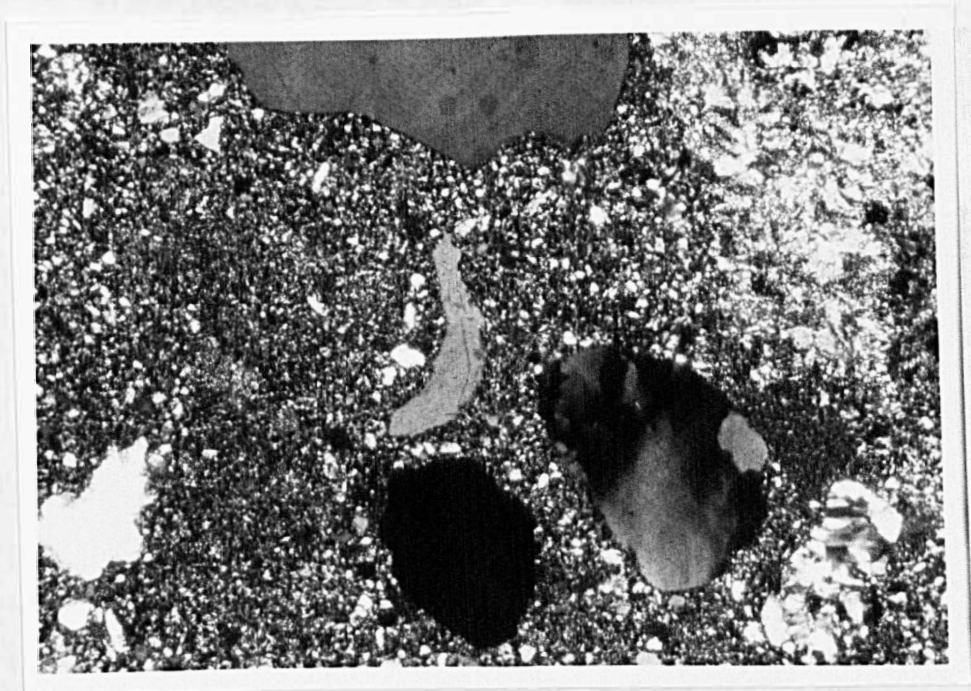


Fig. 2.76: Curved lath of quartz in siliceous matrix. Base of picture = 3.6 mm (+).

It is tentatively concluded that it formed by a subaqueous pyroclastic ash flow which on its path incorporated sedimentary, rounded quartz grains from the probably unconsolidated coarse arenites of the WC₂-unit.

2.5.2.4. Felsic pipes

Some three kilometres northwest of the Tangadee Rhyolite the granitoid basement is intruded by three pipe-like bodies (20 - 40 metres in diameter) of a black siliceous rock. Chemical analysis is shown in Tab. 2.02. It has low sodium and potassium which possibly were removed during weathering. High iron and magnesium content is due to abundant chlorite (causing the black colour), and minor pyrite.

In thin section the rock is poorly sorted, with subangular to subrounded quartz grains of various size (0.01 - 0.5 centimetres), plus large (more than 1 centimetre) irregular shaped and vermiform quartz aggregates, in a very fine-grained chloritic matrix. Some chlorite needles are enriched at the contact of the quartz aggregates to the chloritic matrix (Fig. 2.77).

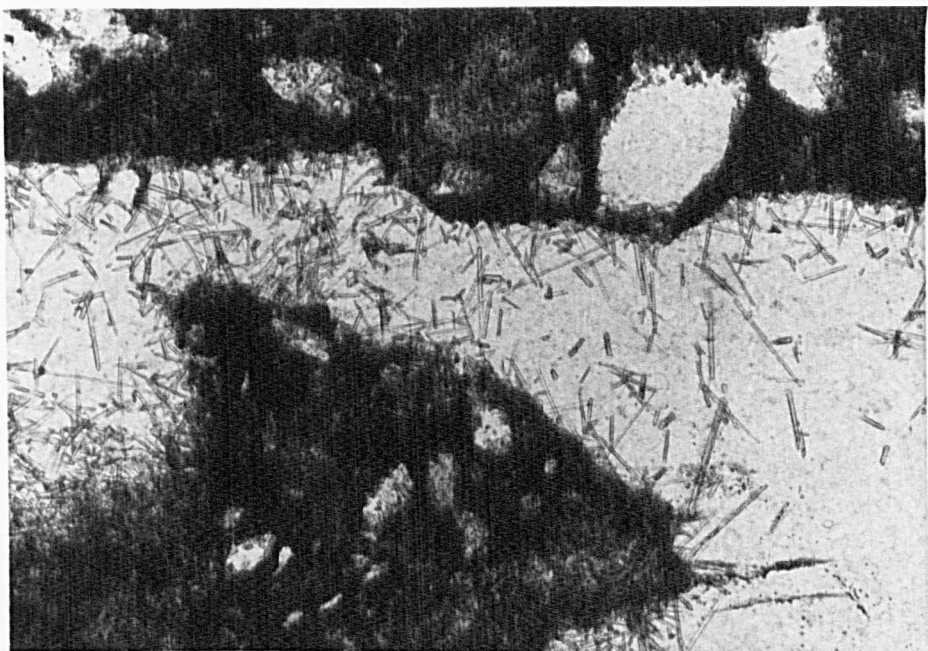


Fig. 2.77: Chlorite needles enriched at the contact between chlorite matrix and a vermiform quartz aggregate. Base of picture = 0.9 mm (-).

There are no textural or mineralogical clues for the origin of this rock, however, the chemistry points to an altered, siliceous volcanogenic rock, and the field occurrence can be interpreted as a volcanic vent. In which case the filling of this vent (i.e. the black felsic pipes) may be a pyroclastic breccia and/or talus from the crater rims.

Despite the chemical differences (Tab. 2.02) with respect to iron, magnesium content and the K_2O/Na_2O -ratio it is suggested that this vent has formed in relation to the Tangadee Rhyolite.

2.5.2.5. Summary

With the exception of the felsic pipes all rocks described in chapter 2.5.2. were emplaced within the lower WC_2 -unit and it can reasonably be assumed that they form one suite. The felsic pipes possibly represent the vents of the eruptive system.

The lapilli tuff shows that the volcanic eruption was hydroclastic, i.e. the addition of water to a rhyolitic magma led to an increase in viscosity which in turn resulted in an explosive eruption. The addition of water probably was enhanced through the onset of faulting and fracturing of the basement (subsidence) in the lowermost WC_2 -unit. Thus, the extrusion is related to the incipient rifting.

Extrusion of the rhyolite as a glassy, viscous lava (Gee et al., 1976) seems unlikely in view of a hydroclastic eruption. The rhyolite could alternatively be interpreted as a welded ash flow tuff which also can show flow banding.

Irrespective of how barium came to be enriched in the lapilli tuff, i.e. prior or after eruption; introduction of barium is related to the hydrothermal system. If the lapilli tuff is related to the rhyolite (dated 1098 ± 42 m.y.) this puts further constraints on the age of the mineralization.

2.6. Development of the Jillawarra Basin

In this chapter the main features of the sedimentological (chapter 2.3.) and structural (chapter 2.4.) history are considered with respect to the development of the Jillawarra Basin during early Bangemall Basin sedimentation.

The limits of the Jillawarra Basin (cf Fig. 2.61) are defined by the Woodlands Fault in the west, the Quartzite Well Fault System in the north, the Abra Fault System in the east and - at least in the western portion of the basin - by the West Creek Fault in the south (map 3). The Jillawarra Basin has an E-W extension of about 55 kilometres and a N-S extension of 5-6 kilometres.

The oldest sediment on the granitic basement in the west (Woodlands Dome) is a quartz-muscovite-potash feldspar clastic rock, which formed as a talus slope breccia on the granite in times of continental condition, intermediate between the granite emplacement and beginning of aqueous sedimentation of the Bangemall Group. In the east (Coobarra Dome) a thick arkose unit underlying the marine sediments of the Gap Well Formation is inferred.

2.6.1. Transgression

Commencement of marine sedimentation was a transgression from the SW along a NE-trending elongated graben, probably due to moderate subsidence of this graben along the regional Flint Hill and Tangadee Lineaments.

Increase in water depth during the GW₂-interval, is indicated by the abundance of reef dolomites along with the intertidal siltstones and beach arenites. At this time synsedimentary faulting became evident. The Manganese Range Fault apparently acted as a facies divide between a western carbonate facies and an eastern fine-grained clastic intertidal facies.

During the GW_3 -interval intertidal flat sedimentation covered many parts of the Jillawarra Basin. The dolomitic fine-grained siltstones though, are intercalated by numerous arenite beds, indicating significant clastic contribution. The GW_{W4} -unit (up to 250 metres coarse clastites) interfingers with, and is partially time-equivalent to, the GW_3 intertidal siltstone. The former unit may represent a barrier island system to the GW_3 intertidal flats.

To this point the sedimentary history is a transgression of a shallow epicontinental sea which led to near-shore depositional systems in the Jillawarra Basin. The local abundance of clastites suggests contribution of continental debris in the Jillawarra Basin which behaved as a shallow sink. The hinterland from which the clastics are derived was composed of granitic rocks.

2.6.2. Regression (Doming)

Within the lower GW₅-interval a sedimentary regression commenced.

The barrier island system of GW_{W4} is overlain by dolomitic siltstone (GW₅) deposited in a water depth of 10's of centimetres. Intercalated lime sand shoals formed from reworking of clastics in an intertidal environment. The GW₅-unit terminates with laminated dolostones and columnar stromatolites, and resembles a shallowing-upward carbonate sequence described by James (1979).

During the GW₆-interval the amount of clastic input decreases. Abundant cryptalgae laminations, stromatolites and pellets point to an upper intertidal, low-energy environment. Intermittent supratidal, hypersaline conditions are indicated by gypsum casts, authigenic potash feldspars and thin laminae of red iron-hydroxides i.e. hematite facies of sabkhas (Kendall, 1979).

Throughout, the Manganese Range Fault had control on the adjacent facies and it is likely that the Woodlands Fault in the west as well as the Abra Fault System in the east also were active.

As syndimentary faulting is evident in the upper Gap Well Formation (e.g. no massive biostromal dolomites occur east of the Manganese Range Fault) it can be assumed that the regression was also tectonically controlled. In comparison with the Irregully Formation (partially equivalent to the Gap Well Formation) elsewhere in the Bangemall Basin the regressional development in the Jillawarra Basin has been enhanced (locally supratidal, hypersaline conditions). Therefore, some active emergence (uplift) may have taken place in the area of the Jillawarra Basin.

2.6.3. Transgression (Rifting)

After the upper Gap Well Formation regression, the onset of the West Creek Formation marks another transgression. On a regional view it is indicated by the re-establishment of an inter- to sub-tidal environment with low-energy carbonate deposition of the WC₁-unit.

Within these intertidal flats however, there formed 3 rapidly subsiding, fault-controlled sub-basins defined by up to 40 metres coarse clastic facies (i.e. at TP-Prospect, Copper Chert Prospect and Abra Prospect). In addition to NE-trending faults, which already have been active during the Gap Well Formation, movement along E-trending faults also became significant.

The apparent relationship between these sub-basins and areas of significant mineralization bears similarities to the middle-Proterozoic Sullivan Pb-Zn-Ag deposit, B.C., Canada. Here the zones of high-grade mineralization are defined by the lateral occurrence of the underlying, thick "Footwall Conglomerate" (Ethier et al., 1976).

This shallow water transgression of the WC₁-unit, with isolated areas of pronounced subsidence, is followed by a marked transgression which affected many parts of the Bangemall Basin (i.e. the onset of the Kiangi Creek Formation).

Within the Jillawarra Basin the WC₂-unit comprises more than 400 metres of shallow water turbidites the occurrence of which apparently are confined to the basin; outside the basin margins beach or fluvial facies prevail (cf Fig. 2.61).

Thus, subsidence was strongest in the Jillawarra Basin which at this stage developed into an intracratonic, fault-bounded rift valley. Robbins (1983) noted that coarse-grained turbidites are common in such rift valleys and she suggested that the turbidites are induced by earthquakes generated by rifting.

2.6.4. Further basin development

The upward passage of the WC₂-unit into dominantly intertidal dolomitic siltstone of the WC₃-unit, and then coarse beach arenites of the WC₄-unit, marks the filling of the basin. Further slow and minor subsidence is indicated by the re-establishment of intertidal/barrier bar conditions of the lower Jillawarra Formation (Mjd) which is overlain by a shelf facies of the upper Jillawarra Formation (Mjs).

2.6.5. Summary

The regression in the upper Gap Well Formation and transgression in the lower West Creek Formation match the first events of the "rift valley stage" of cratonic rift basins which De Rito et al. (1983) described as doming, central rifting, graben formation and intrusion of basic magmas into the central rift (the intrusion-event probably corresponds to the intrusion of dolerites higher up the sequence; see chapter 1.2.6.2.).

Because lateral crustal extension continued after the incipient rifting (WC₂) further pulses of subsidence occurred. After a period of tectonic quiescence and basin infill the shelf facies of the middle to upper Jillawarra Basin marks a further, though minor, event of subsidence.

According to the classification of Large (1980) who listed parameters indicative of potential mineralization, the Jillawarra Basin can be characterized as a Second-Order-Basin within a First-Order-Basin:

Parameters (Large, 1980)

Jillawarra Basin

I) First-Order Basin

a) Epicratonic and intracratonic basins (100's km dimensions)

The Bangemall Basin

b) Fault-bounded at margins

Jeeaila-Mount Vernon-Lofty Range Fault System in the N

Steep faults on Robinson Range, Stanley, Nabberu Sheets in the S

c) Thick sequences of clastic sediments, shallow marine carbonates, delta sandstones, turbidites

Clastic sediments - Tringadee Formation

Shallow marine carbonates; Tringadee F. Delta sandstones, turbidites; Kiangi Creek Formation

II) Second-Order Basin

a) Becken and Schwellen (10's km dimensions)

Jillawarra Basin, Becken-facies

b) Abrupt changes in sedimentary facies and thickness at basin margins

e.g. within the WC₂-unit the basin margin faults acted as facies divides (cf Fig. 2.61)

III) Contemporaneous Igneous Activity

a) Tuffs, tuffites, ashfalls (< 1 m thick, fine-grained)

rhyolite, lapilli tuff etc. (cf chapter 2.5.2.)

b) Bimodal volcanic activity in First-Order Basin

despite minor felsics only dolerites (continental tholeiites)

c) Minor intrusions

none

IV) Regional Tectonic Activity and Lineaments

a) Active hinge zones at margins of basins

Tight and overturned folds along the Mount Vernon Fault on the northern margin of the Bangemall Basin. Tight folds at N and S margins of the Jillawarra Basin (cf Fig. 2.70)

- b) Regional change in sedimentary environment e.g. facies change across the Tangadee lineament (cf Fig. 1.07) or see point II)b)
 - c) Intersection of lineaments and hinge zones Jeeaila-Mount Vernon- Lofty Range Fault System intersects Tangadee lineament; or on the scale of the Jillawarra Basin: Quartzite Well Fault System intersect Woodlands Fault in the W and Abra Fault System in the E.
- V) Third-Order Basin
- a) Local depressions (100 m - 10 km dimensions) The Abra Sub-Basin, discussed in section 3.

Section 3 The Abra sub-basin

3.1. Introduction

In the following three chapters the Abra sub-basin will be described, a basin the accurate limits of which are unknown. No surface outcrop of the respective rocks occurs; investigations and reconstruction of the basin are based on eight diamond drill holes.

Fig. 3.02 shows the local geology of the Abra area, the main Geoneko grid lines, position of the eight drill holes, and the surface trace of the faults probably limiting the basin; except towards the south where no limiting fault could be identified.

Additional evidence for the extension of the Abra sub-basin stems from the occurrence of the coarse clastic WC₁-facies (Fig. 3.01).

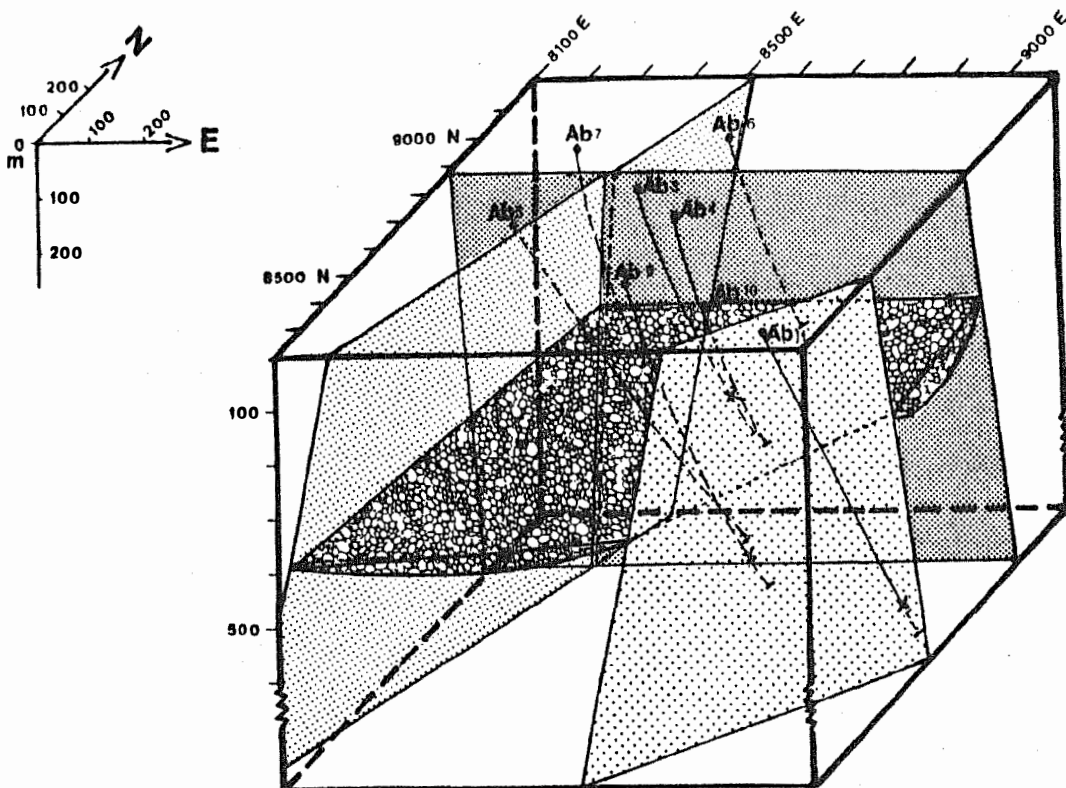


Fig. 3.01: The occurrence of the coarse clastic WC₁-unit is limited by three faults, which define the Abra sub-basin. Surface position and downward extension of the eight diamond drill holes are shown; x marks the intersection of fault.

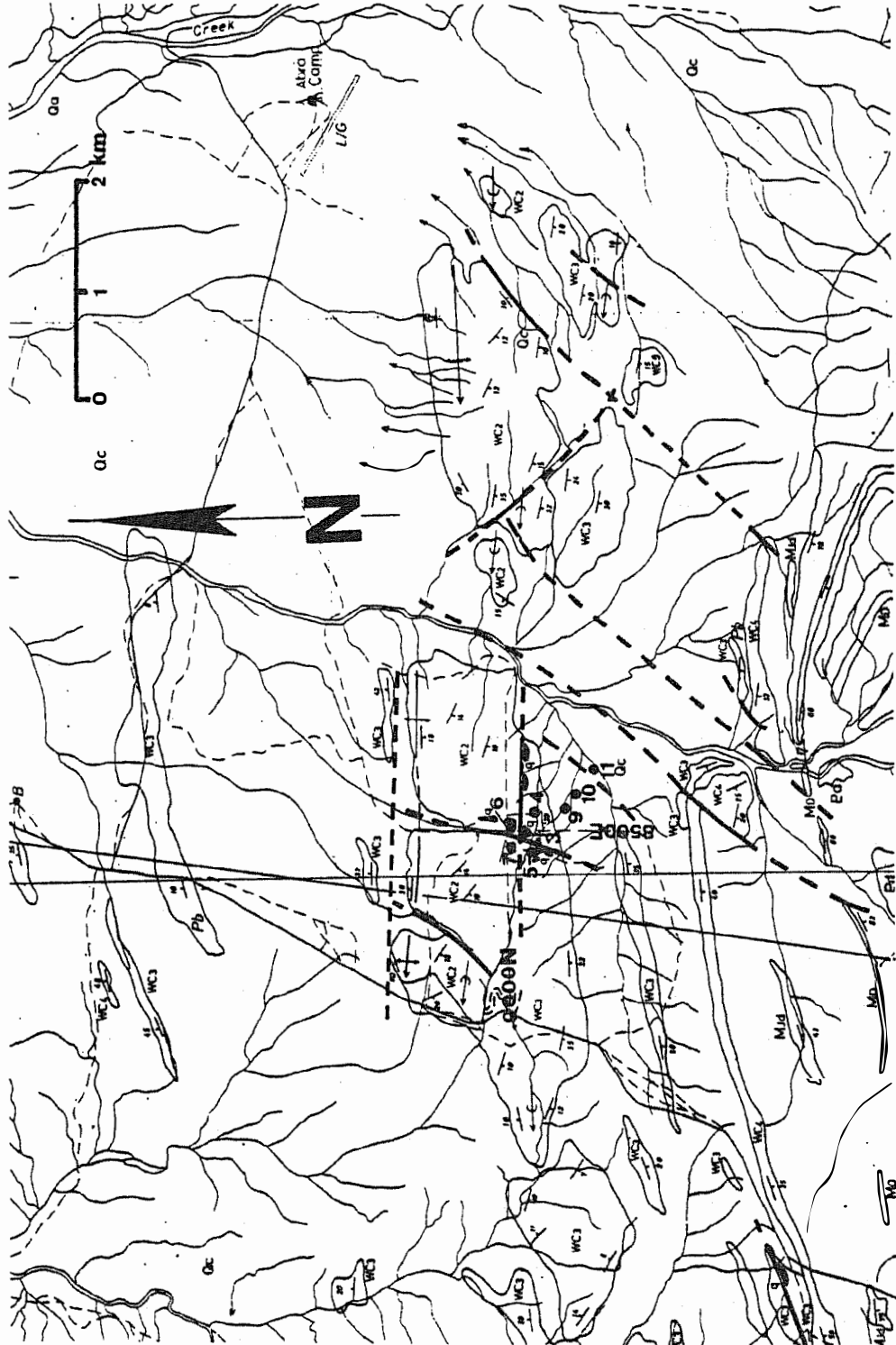


Fig. 3.02: Section of map 1, showing locations of eight diamond drill holes and main Geopeko grid lines at the Abra Prospect

3.2. Stratigraphy of the Abra succession

Fig. 3.03 diagrammatically displays the stratigraphy of the Abra area projected onto a N-S section at 8500 m East (Geopeko grid). The stratigraphic divisions - as compared to the stratigraphy of the Jillawarra Belt - encountered in the diamond drill holes comprise the upper Gap Well Formation (GW₅ - GW₆) and the lower to middle West Creek Formation (WC₁ - WC₂ - WC₃) as it is shown in Fig. 2.05. In this chapter sedimentological analogies between the Abra area and the Jillawarra Belt are occasionally demonstrated in order to evaluate the facies of the Abra succession.

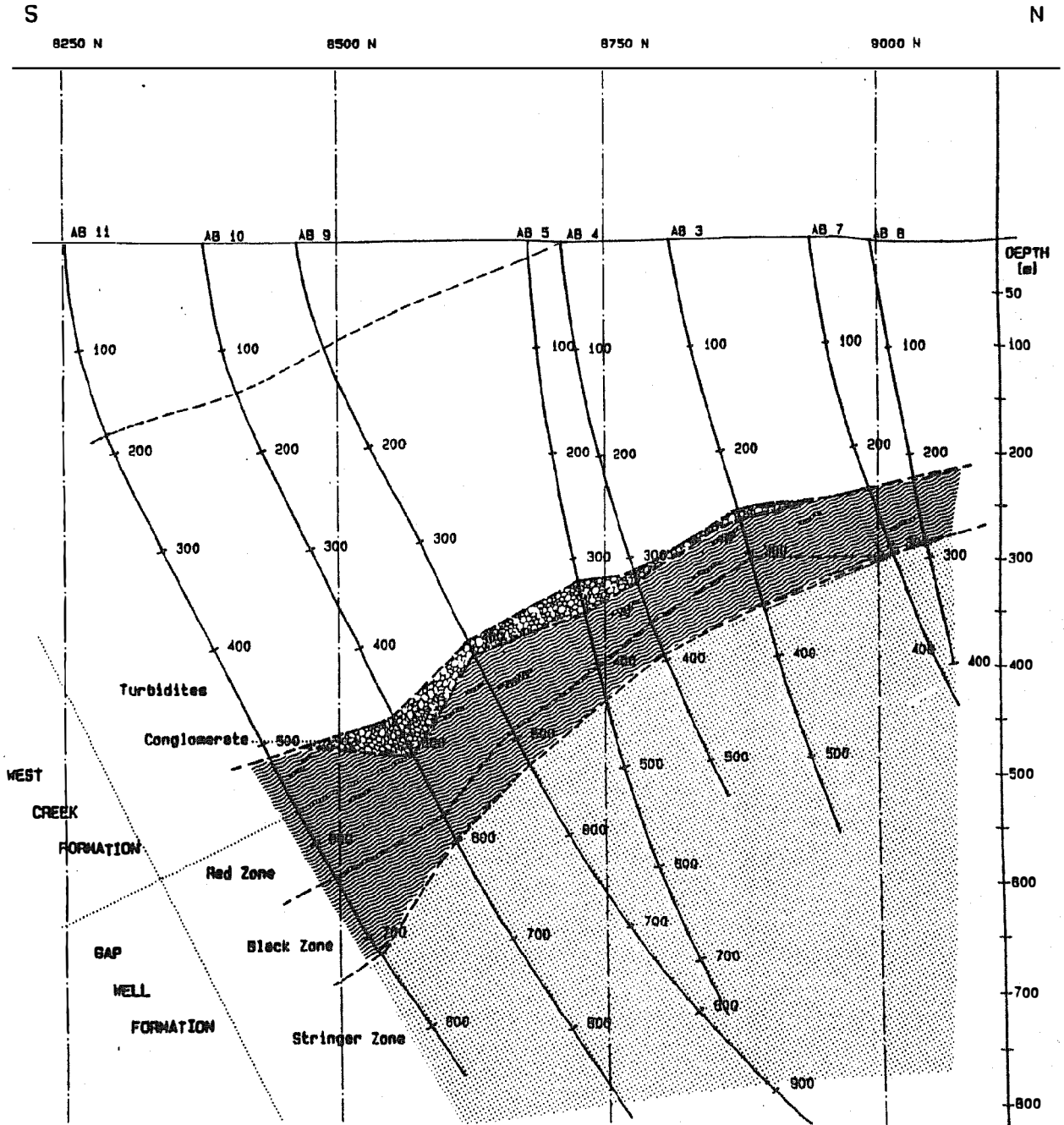
3.2.1. The Gap Well Formation

For the Gap Well Formation the correlation with GW₅ - GW₆ of the Jillawarra Belt is valid only with respect to the thickness of the units. Alteration (silification-chloritization, brecciation) commonly obliterates the original features of the rocks in the Abra succession. It therefore seems inappropriate to attempt subdivision into the GW₅- and GW₆-units.

Although the thickness of the strata of the Gap Well Formation intersected implies that both units are present the intensity of alteration rather favours a description of the Abra-succession as 3 local lithostratigraphic units according to different mineral composition and textures. Nevertheless, a facies interpretation of these local units is warranted; the boundaries of which though do not correlate with those evaluated for the Gap Well Formation of the Jillawarra Belt succession in chapter 2.3.1.

The Gap Well Formation in the Abra succession comprises the ore bearing unit and is subdivided into a footwall "stringer zone", overlain by a "black zone" and a "red zone". These names are macroscopically descriptive terms designed for core logging purposes by Geopeko geologists and are dealt with in the following chapter as lithostratigraphic units.

Fig. 3.03: Stratigraphy of the Abra area projected onto a N - S section at 8500m East (Geopeko grid)



3.2.1.1. Stringer zone

In Ab 9 hole the longest intersection of the stringer zone (416.3 core-metres, corresponding to a true depth of 310 metres) terminated within this zone.

Although the veining gradually decreases in the bottom part this lithostratigraphic unit probably extends further down hole.

Mineralization in the stringer zone is limited to veins and veinlets of various composition (see chapter 4.1.).

The dominant rock types are chloritic siltstone and shale with intercalation of very fine-grained arenite (Fig. 3.04). These sediments are interbedded irregularly with subordinate thin lithic and/or feldspathic fine- to coarse-grained arenites which often are poorly sorted.

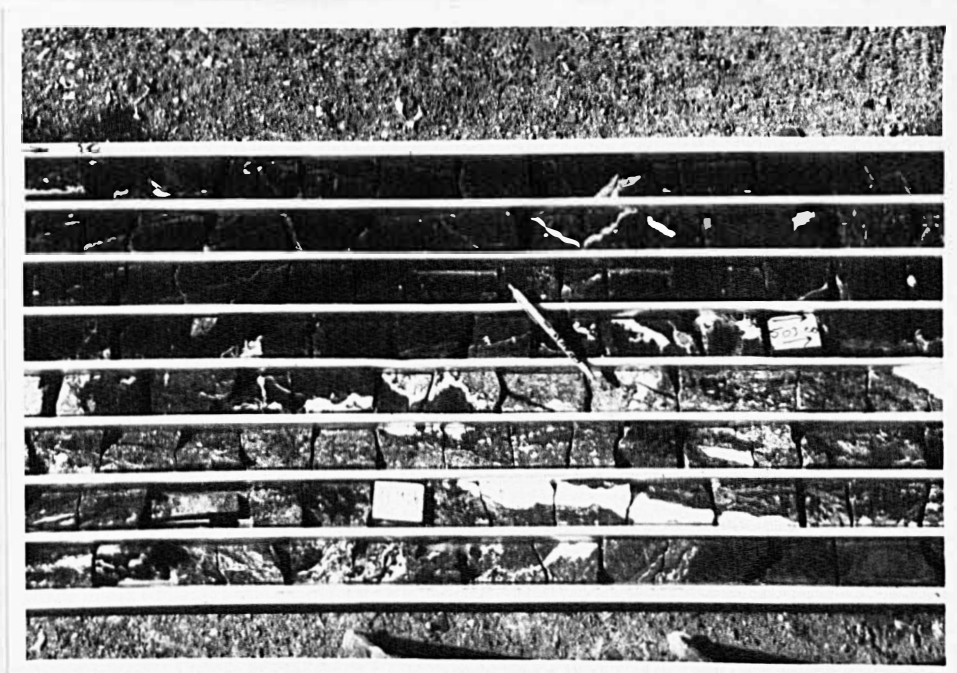


Fig. 3.04: Drill core from the stringer zone (Ab 3, 499-507 m) showing chalcopyrite, carbonate and quartz veining in chloritic siltstone.

Lithic arenites are more abundant in holes Ab4 and Ab 6; in the latter the arenites comprise the upper 30 metres of the stringer zone whereas in Ab 4 they are dominant throughout the hole.

Mesoscopically (scale of the drill core) a number of sedimentary features have been observed in the Abra succession which point towards an intertidal sedimentary environment like that postulated for the GW₆-unit of the Jillawarra Belt; these include:

- flaser bedding; this type of ripple cross-lamination where muddy parts occur in the troughs of the ripples often forms in intertidal sediments (Reineck and Singh, 1973);
- intraclastic brecciation; although not diagnostic of intertidal sediments this feature has also been observed in the GW₆-unit near the Copper Chert prospect, and may indicate an analogous mode of origin;
- thinly interbedded shale (muddy) and fine-grained arenite (sandy); this is the dominant type of sediment in intertidal zones.
- subordinate thin lithic and/or feldspathic, poorly sorted, fine- to coarse-grained arenites; these rocks probably are the equivalents to the calcareous wackes of the GW₆ in the Jillawarra Belt. The lack of a significant carbonate component can be attributed to the intense silification which affected all rocks in the Abra succession. Abundant tiny inclusions witness the former existence of carbonate (cf chapter 2.3.1.);
- scattered sand grains in muddy layers; up to about 10 % scattered quartz grains in the fine-grained sediments frequently occur in all drill cores. According to Reineck and Singh (1973, p.359) this is a common feature of intertidal sediments where individual sand grains are attached to algal filaments or other organic

matter, and kept in suspension prior to deposition with mud aggregates (Wunderlich, 1969, in Reineck and Singh);

- conformable lensoidal pyrite layers; such layers commonly form diagenetically at the boundary between oxidizing and reducing conditions within the sedimentary column in intertidal sediments (Vogt, 1981) and are also present in the Gap Well Formation of the Jillawarra Belt.

These sedimentary features confirm the assumption that the sediments of the stringer zone formed in a similar (inter-subtidal) environment as the GW₆-unit of the Jillawarra Belt some 10 kilometres to the west.

Further sediment structures such as clastic dykes, scour channels, sole marking and graded bedding have been reported in Geopeko drill logs but are not indicative of any particular environment.

Intense brecciation is associated with the veining (mineralization) of the stringer zone (Fig. 3.05); it may be difficult though to distinguish between a clastic dyke in which the matrix has been mineralized preferentially, and a true vein-type brecciation.

Microscopically recognition of the original petrology of the sediments is rendered difficult by the intense alteration. In the bottom of Ab 11 (852 metres), the southeasternmost drill hole, the alteration is insignificant. These rocks probably resemble the original sediments of the stringer zone.

The rocks can best be described as micaceous calcareous siltstone with faint laminations. Very few micas have been chloritized, most seem to be detrital. The carbonate dominantly is micritic and occurs in patches of which some possibly are diagenetic pellets (Fig. 3.06).



Fig. 3.05: Brecciation of chloritic siltstone in the stringer zone. The fine-grained matrix is mineralized (chalcopyrite).

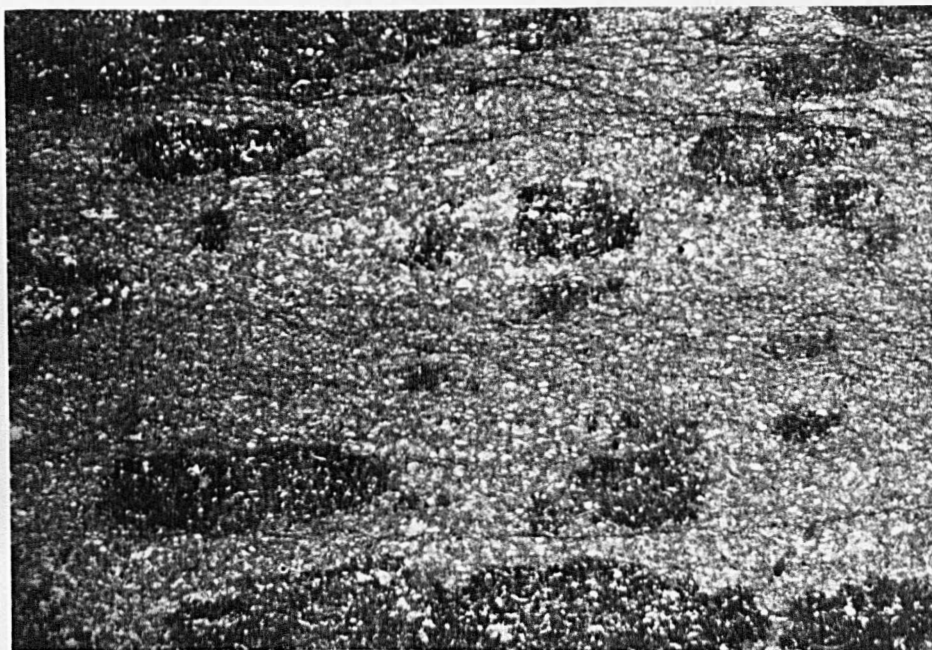


Fig. 3.06: Calcareous siltstone with ferruginous pellets. Base of picture = 5.6 mm (-).

All carbonates are very dark through a significant iron and manganese content (cf chapter 4.1.).

Detrital quartz grains are angular to subrounded and are of silt-size. The existence, however, of patches and streaks of secondary quartz with abundant small carbonate inclusions shows that silification has taken place.

The nature of the silification is comparable to that of the Jilla-warra Belt where secondary quartz with abundant carbonate inclusions occurs throughout the Gap Well and West Creek Formations. As a seemingly unaltered rock is affected by silification, whereas chloritization is negligible, it can be inferred that silification is a widespread (more "distal") phenomenon while chloritization is more "proximal" with respect to the hydrothermal system.

A sample from Ab 5, 759.0 metres is in a more "proximal" position in spite of the absence of significant mineralization. This rock is texturally very similar to the one above - a micaceous, laminated siltstone - but the matrix is completely chloritized.

Two generations of chlorite are present in this rock:

- a) One phase formed in association with a 3 millimetres wide quartz - minor carbonate veining. It occurs as aggregates of fibrous radiating clusters within the vein and probably grew from the vein material without any precursor phase. It has a blue birefringence colour (Fig. 3.07).

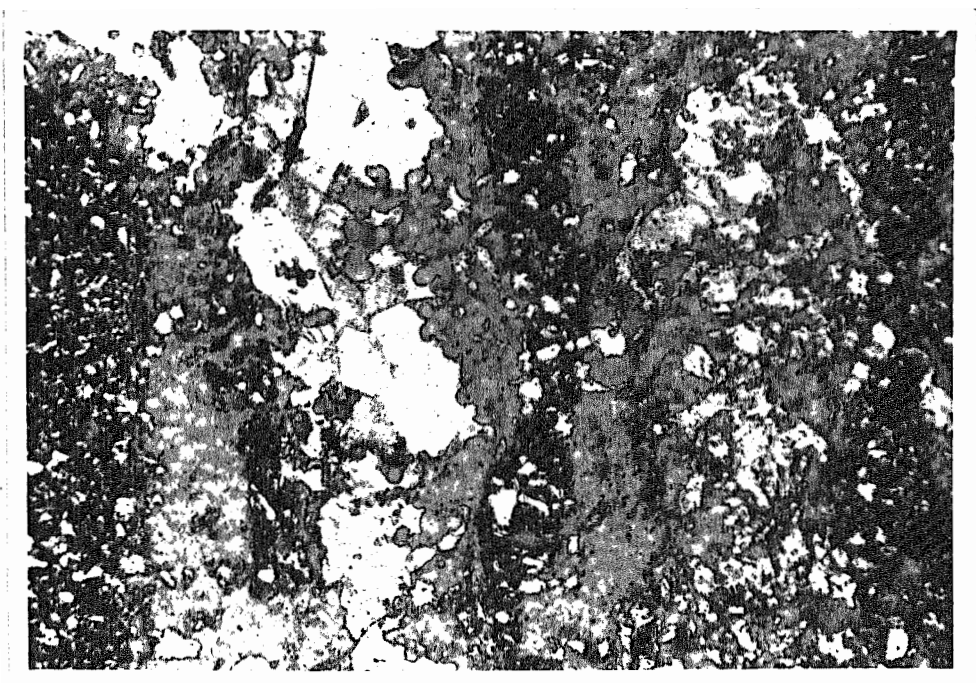


Fig. 3.07: Chlorite formation within vein. Base of picture = 3.6 mm (-).

- b) The second generation constitutes the matrix of the laminated siltstone. It is of a "micritic" nature i.e. the chlorite is very finely dispersed throughout the rock with few larger aggregates (Fig. 3.08).

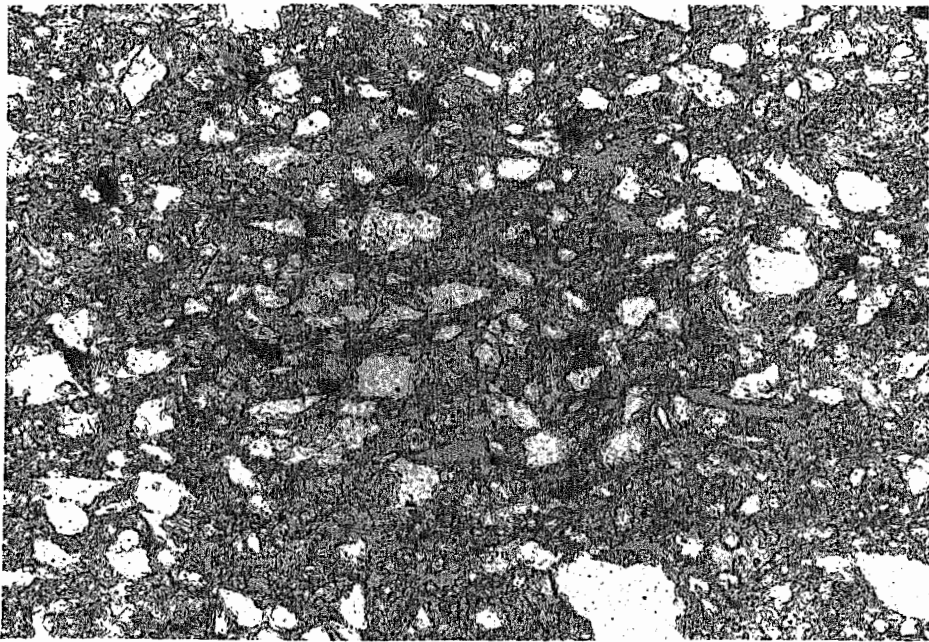


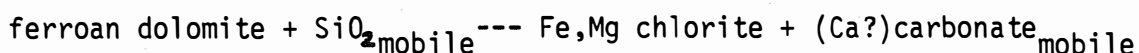
Fig.3.08: Chlorite distributed throughout the wall rock (matrix chlorite). Base of picture = 0.9 mm (-).

Notably most of the white micas are preserved, except a subordinate number showing incipient or complete chloritization. It thus appears that, in addition to micas, another group of precursor minerals has been chloritized. Control of the nature of the precursor minerals on the chloritization is corroborated by different birefringence colours of the chlorites; while the "micritic" chlorite is very dark brown, the few larger aggregates have blue to blue-purple colours and chloritized micas have grey-purple (+/-brown) colours.

For a number of reasons it can be inferred that the chloritized matrix has been carbonate, these include:

- the micritic nature of the chlorite
- the apparent control of the precursor mineral on the chloritization
- the textural similarity to the unchloritized but calcareous sample of Ab 11
- general textural analogy to the GW_6 -unit of the Jillawarra Belt.

A possible reaction pathway (simplified) to explain this type of chloritization is:



Further indication of chloritization of carbonates is given by the existence of authigenic albite (only marginally altered) in the chloritic siltstone; authigenic albite preferentially formed in calcareous sediments in the Jillawarra Belt. There are also some rounded chlorite aggregates which may have been calcareous pellets (Fig. 3.09).

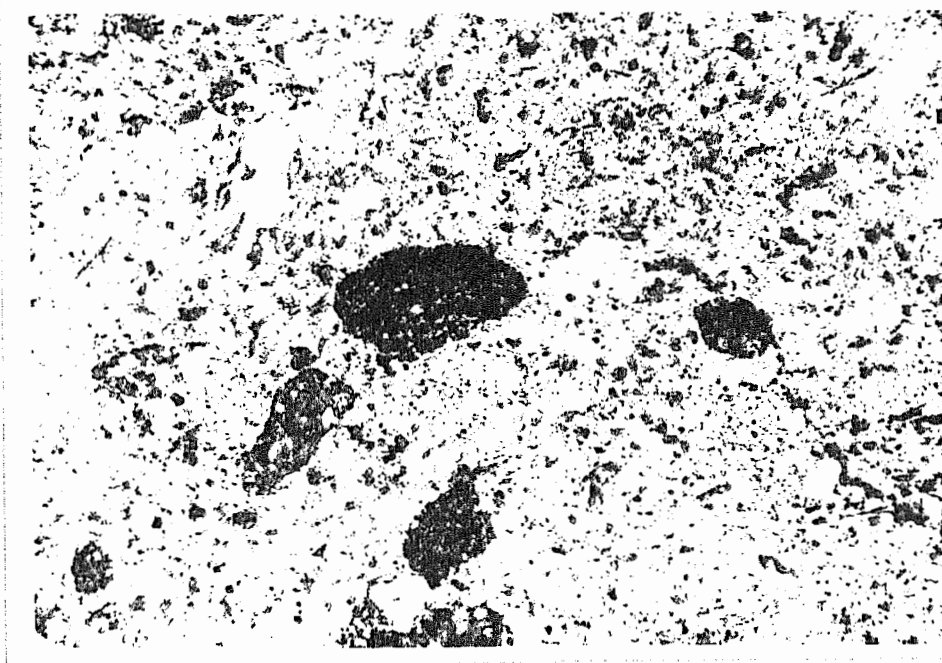


Fig. 3.09: Rounded chlorite aggregates, possibly after pellets. Base of picture = 3.6 mm (-).

A second, dominant rock type in the stringer zone is a lithic arenite. These rocks are particularly abundant in Ab 4 and Ab 6.

With feldspar content frequently in excess of 30 % the rock is a medium- to coarse-grained, poorly sorted, subangular to sub-rounded feldspathic arenite. The cement consists of very fine-grained ("cherty") quartz; few secondary muscovites are scattered irregular through the rock. Locally, the interstitial volume ("matrix") is occupied by galena-sphalerite-barite plus large subhedral carbonate and authigenic albite, both the latter are clearly associated with the ore minerals. Here it is not certain whether an original carbonate component has been present. The chloritization selectively affected muscovite and altered potash-feldspars (Fig. 3.10).

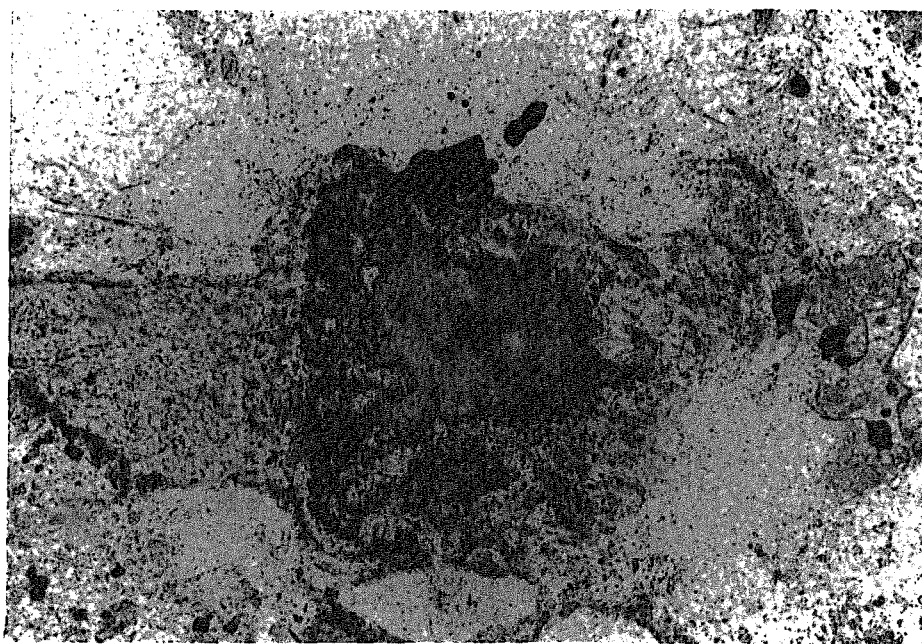


Fig. 3.10: Partially chloritized potash feldspar.
Base of picture = 0.9 mm (-).

The potash feldspars show authigenic seams which usually have been altered more intensely than the detrital grains (Fig. 3.11).

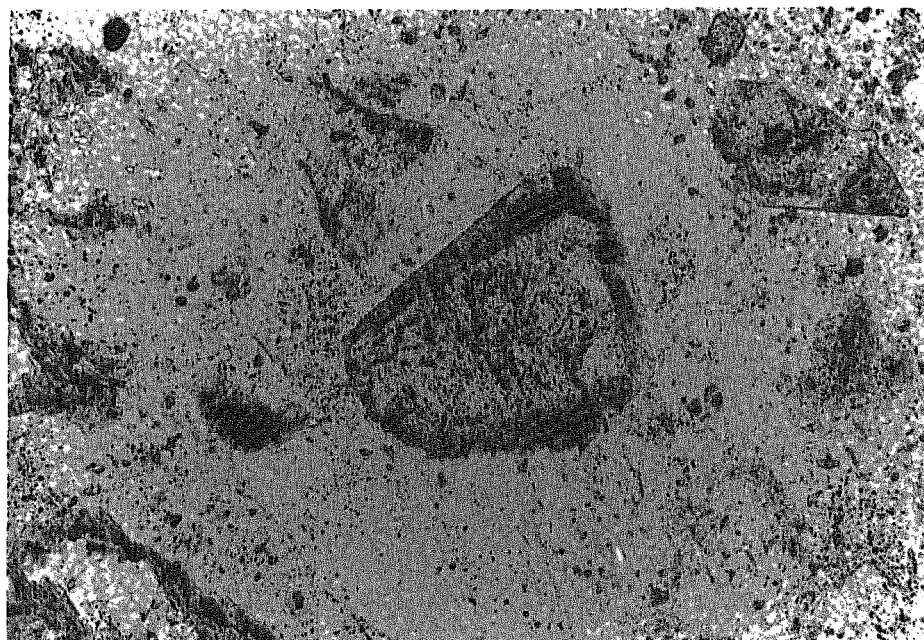


Fig. 3.11: Altered authigenic seams to potash feldspar.
Base of picture = 0.9 mm (-).

Similar seams occur in eastern parts (Copper Chert) of the Jillawarra Belt and probably have formed by formation waters with elevated salinity, according to a process proposed by Tröger (1969).

In summary there have originally been two major rock types; most abundant is a \pm calcareous, micaceous siltstone which represents the common intertidal deposits comparable to the GW₆-unit of the Jillawarra Belt.

Intercalated is a medium- to coarse-grained lithic arenite which may be interpreted as tidal channel fillings or storm deposits. In Ab 4 and the upper parts of Ab 6 the thickness of these arenites increases considerably; indicating alluvial fan deposits rather than tidal channels.

Although the lithological evidence for tidal deposits is not unequivocal, the sediment structures described before, and the above microscopic features, provide further support for the facies interpretation of the stringer zone as inter- to subtidal deposits.

3.2.1.2. Black zone

The black zone consists of laminated, often distinctively banded hematite/magnetite-quartz-jaspilite-carbonate-barite-galena-pyrite-chalcopyrite rocks (Fig. 3.12). Locally intense veining and brecciation is well developed.

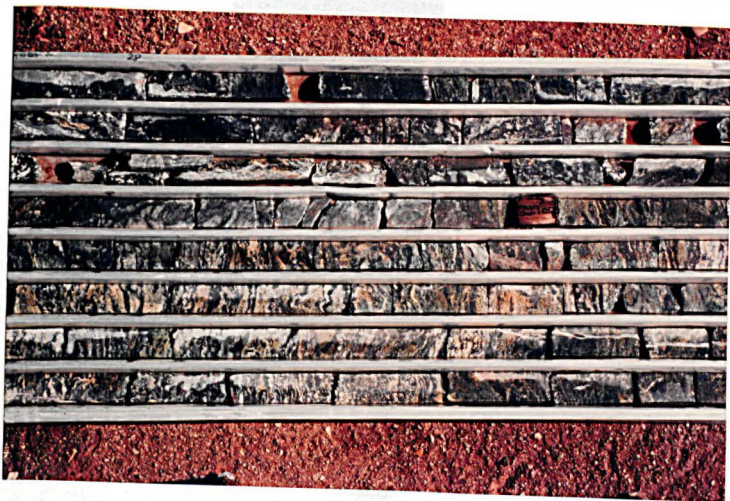


Fig. 3.12: Drill core from the black zone (Ab 3, 325-333 m) showing magnetite/Fe-carbonate laminites. Note veining and brecciation in upper part of photograph.

The average thickness is about 35 metres; however in Ab 6 and Ab 7 the black zone is absent while in Ab 11 (southeasternmost drill hole) the thickness increases to over 70 metres.

The fine banding - often less than one millimetre for an individual layer - usually is crenulated or colloform, contorted or disrupted by blister-like structures (Fig. 3.13) pointing into both directions; up and down the drill hole. Sometimes the layers are contracted to form nodular aggregates now filled with quartz or carbonate.

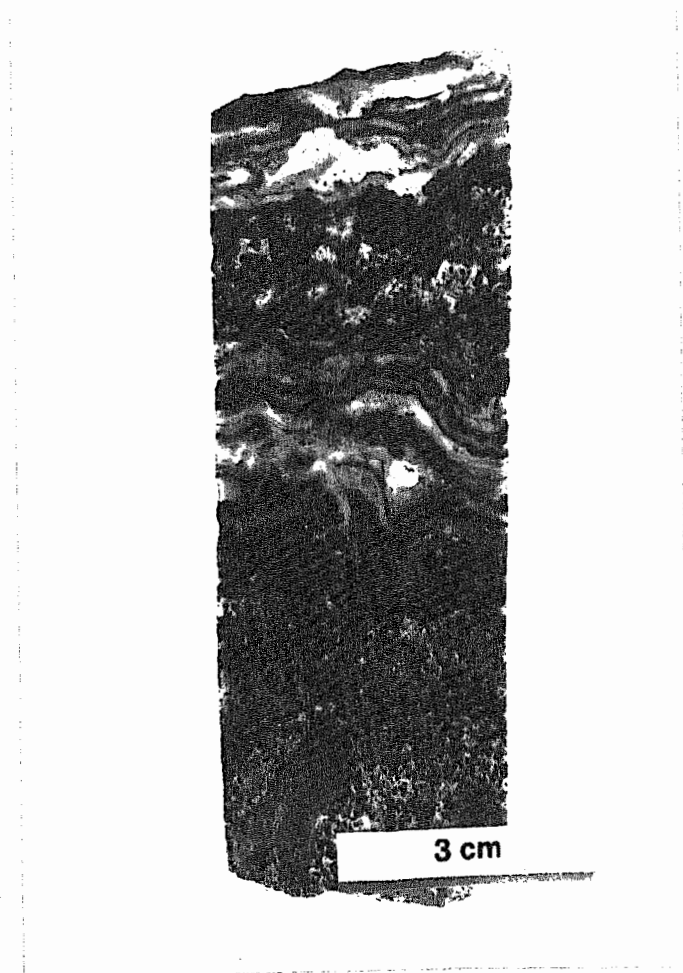


Fig. 3.13: Core specimen from the black zone with crenulated quartz-carbonate-magnetite layering.

Individual layers are composed of:

- I) hematite-magnetite (usually intergrown) and/or subordinate jaspilite (Fig. 3.14)
- II) quartz, massive, non detrital (Fig. 3.14)
- III) carbonate, usually with yellow-brown colours, i.e. iron- and manganese-bearing (Fig. 3.14)
- IV) pyrite (Fig. 3.14)
- V) barite (Fig. 3.22).

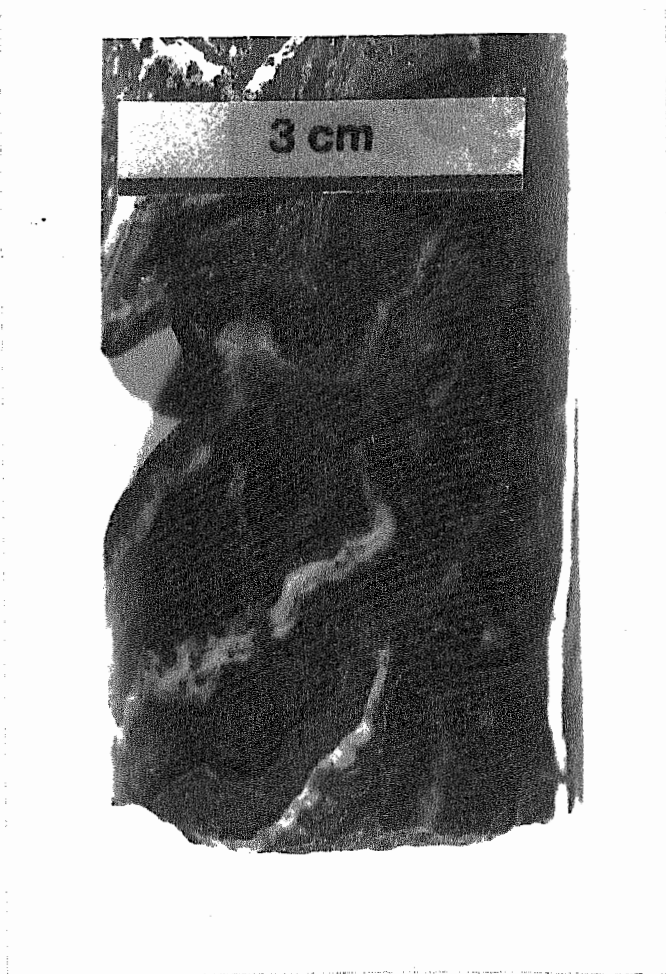


Fig. 3.14: Core specimen from the black zone with magnetite-carbonate layering (upper left) and quartz (white) - pyrite (light grey) - jaspilite, magnetite (black) layering. Note small, vertical quartz-chalcopyrite vein.

No regularity or cyclicity in the sequence of layering could be found. Hematite/magnetite and quartz and carbonate layers are most abundant while the others are subordinate and barite layers are rare.

I) Hematite/magnetite

In thin section the hematite/magnetite layers consist of recrystallized bands of hematite with irregularly dispersed sub-euhedral magnetite grains. Magnetite is ubiquitous and always intergrown with hematite. While magnetite occurs as aggregates composed of varying numbers of small ($< 10\mu$) cubes hematite has the form of acicular crystals or clusters of crystals.

Locally layers of iron hydroxydes (goethite or lepidocrocite) are associated with hematite layers (magnetite is rare then) or occur separately in quartz, imparting a jaspilitic appearance.

The banding often is colloform or completely destroyed and hematite/magnetite are recrystallized to irregular masses.

Penetration of a hematite/magnetite layer by an elongated scheelite-quartz-barite aggregate suggests that these layers formed very early (i.e. syngenetic) as the barite crystallization probably occurred diagenetically (Fig. 3.15). The presence of scheelite, although not in economic quantities, is considered particularly relevant in view of the possible metal sources, and, as a further indication of hydrothermal activity. A similar situation is given in Fig. 3.16 where a large barite crystal (about 1.3 centimetres) grew through a hematite/magnetite-pyrite layer without changing its crystallographic orientation.

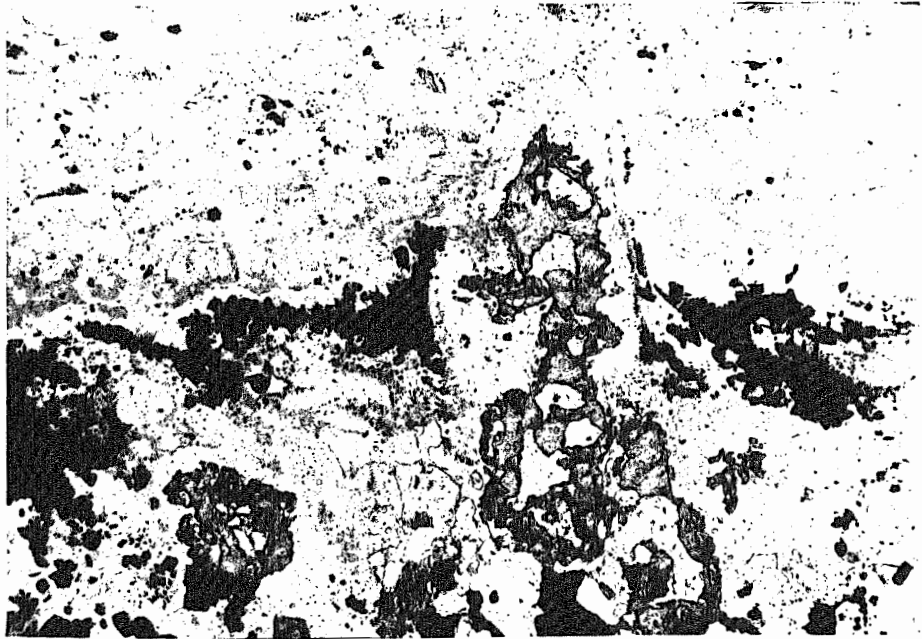


Fig. 3.15: Protrusion of scheelite crystal into hematite/
magnetite layer. Base of picture = 3.6 mm (-).

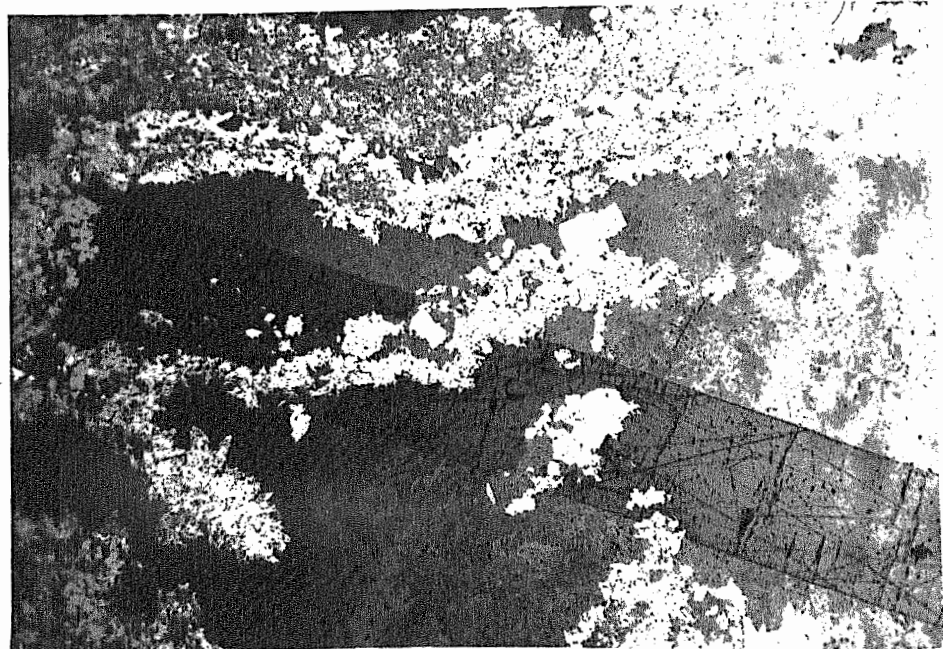


Fig. 3.16: Diagenetic growth of barite through hematite/
magnetite-pyrite layer. Base of picture = 5.6 mm,
polished section (-).

II) Quartz

Quartz occurs in various forms mainly due to differences in crystallinity. Most of it has been emplaced either as chemical sediments or as replacement of pre-existing minerals. No detrital quartz grains have been found within the layered black zone.

The predominant forms are:

- large crystals (up to 2 centimetres) which probably have re-crystallized from another form of silica as indicated by frequent 120° triple junctions of three grain boundaries. The habitus of single grains varies from anhedral to euhedral.
- fine crystalline "cherty" quartz, either as irregularly distributed masses or very often in bands parallel to hematite/magnetite layers.
- flamboyant quartz, usually along the margins of larger quartz grains or nodular quartz aggregates (Fig. 3.17).

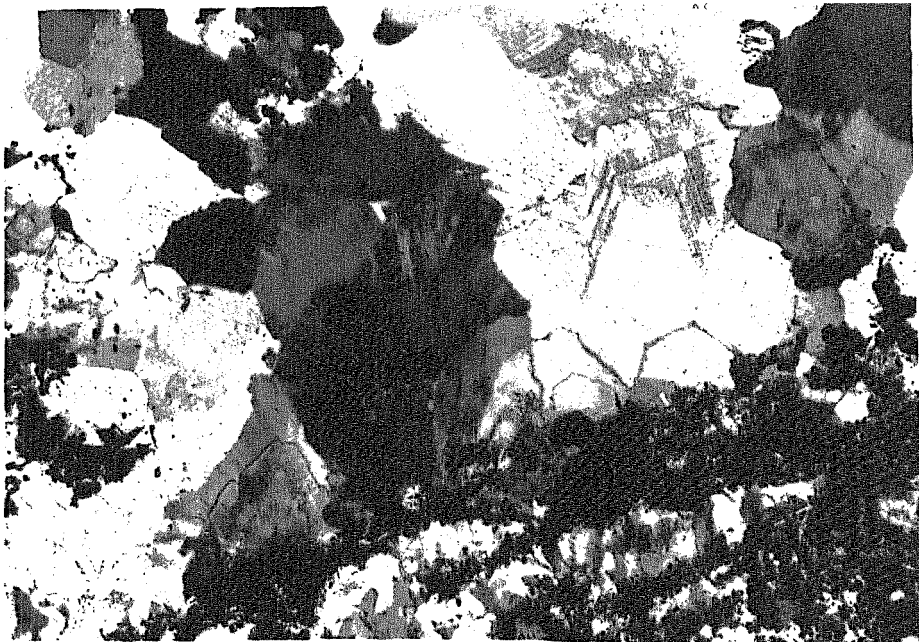


Fig. 3.17: Flamboyant quartz along the margins of angular quartz grains. Base of picture = 3.6 mm (+).

The abundance of inclusions mainly in the form of blebs (about 5 μ in diameter) of carbonate, iron-oxides (hydroxides) or as fluid inclusions is characteristic of all quartz types.

Fig. 3.17 shows inclusions outlining euhedral crystal shapes. In other places dispersion of fluid and iron-hydroxide inclusions is causing jaspilitization which locally occurs in patches of 0.5 to 3 centimetres. When iron-hydroxide inclusions form thin bands (in the recrystallized quartz) which are parallel the main hematite/magnetite banding they probably represent poorly developed jaspilite layers as described in the previous paragraph.

While fluid and iron-(hydr-)oxide inclusions may be inherited from the aqueous solution or gel out of which quartz crystallized this is not true for carbonate. It has been shown that pre-existing carbonate was subject to silification as witnessed by numerous small carbonate inclusions.

Carbonate inclusions are even more abundant in the black zone; where they outline crystal shapes or are dispersed within quartz, the respective crystals or areas probably have been carbonate originally.

In the black zone silica seems to replace entire carbonate layers; this is particularly obvious in the vicinity of hematite/magnetite or pyrite layers. In Fig. 3.18 almost all "dusting" visible in the quartz between the opaque layers consists of carbonate inclusions, and Fig. 3.19 shows some relicts of carbonate layers.

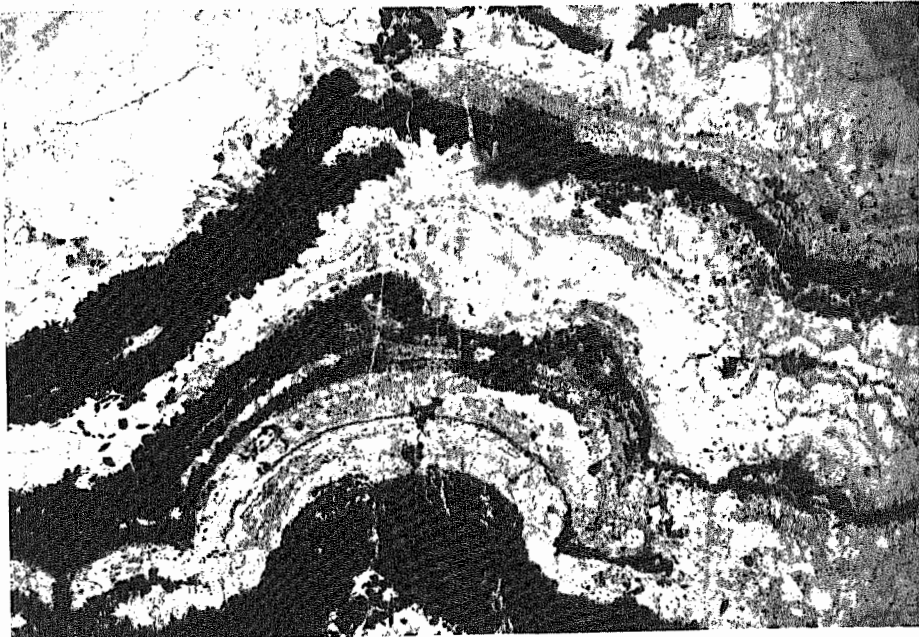


Fig. 3.18: Numerous carbonate inclusions in quartz.
Base of picture = 5.6 mm (-).

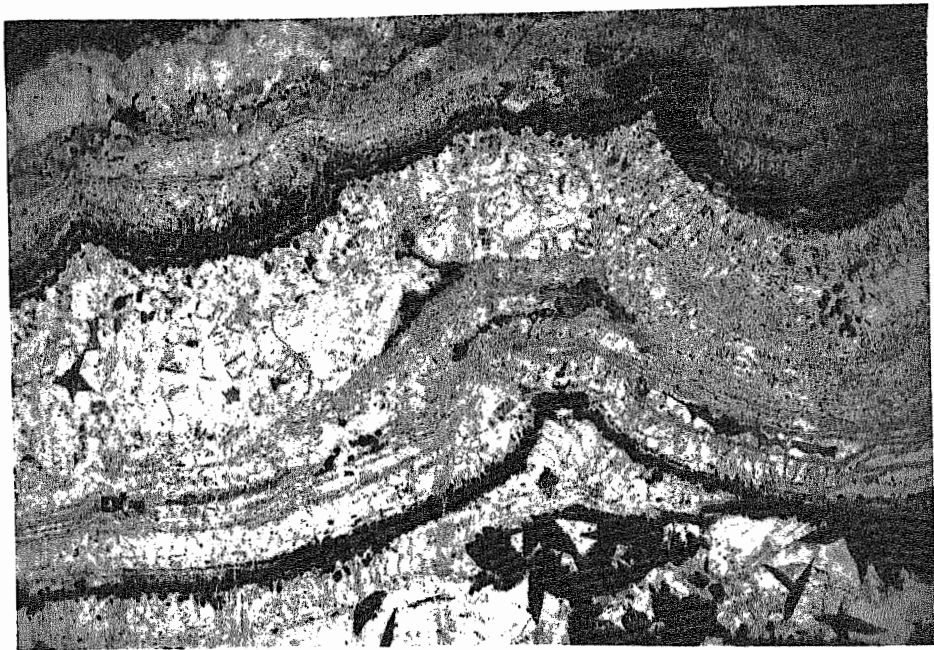


Fig. 3.19: Relict carbonate layers and carbonate inclusions
in quartz. Base of picture = 5.6 mm (-).

In summary there were two sources of silica:

- a) Chemical sedimentation in association with the hematite/magnetite as indicated by iron-oxide (-hydroxide) inclusions in some quartz. Interestingly, cherts from South African banded iron formation have red colours under reflected light in polished sections (Klemm, 1984) also suggesting some iron-hydroxide content.
- b) Replacing solutions which preferentially affected carbonate. This type of quartz can be free of iron-hydroxide inclusions and it presumably stems from the Abra hydrothermal system. Although somewhat speculative, it appears conceivable that the replacement of carbonate took place while it still was a water-rich carbonate mud. In that case access of the silica solutions would be facilitated and the silica would occupy the "position of the water" while the finely dispersed carbonate could nucleate without destroying the delicate banding.

III) Carbonate

Although now subordinate to quartz in abundance widespread silification of carbonate suggests that the original sediment commonly has had a carbonate component.

Carbonate occurs as:

- small inclusions or relict carbonate as described above
- euhedral crystals in clear (secondary) quartz; probably formed together with the secondary quartz
- dark and "dusty" layers or zones of partially sparitic carbonate containing significant amounts of Fe-Mg-Mn with a pronounced Ca-deficiency. As the distribution of Mg/Ca ratios of 57 whole rock analyses in the Abra area cuts across lithological boundaries, the composition of the carbonates is obviously governed by post-depositional processes (either common dolomitization or hydrothermal alteration).

The dark and "dusty" appearance of the latter group is due to finely dispersed iron-manganese compounds. Although affected by post-depositional processes this type of carbonate was deposited with the sediments. A high iron and manganese content is to be expected in this particular environment (i.e. the hematite/magnetite deposition).

There are indications that carbonate has replaced sulphates (barite or gypsum); while the carbonate usually recrystallized to sub- or euhedral rhombs locally it has the form of acicular or lenticular crystals. Pseudomorphs of calcite after gypsum occur, for example, in the Aquitaine Basin, Southwest France (Bouroulllec, 1980). In one sample replacement of a nodule apparently took place: acicular carbonate crystals occur perpendicular to a micritic core (Fig. 3.20) not unlike silicified gypsum/anhydrite nodules described by Milliken (1979).

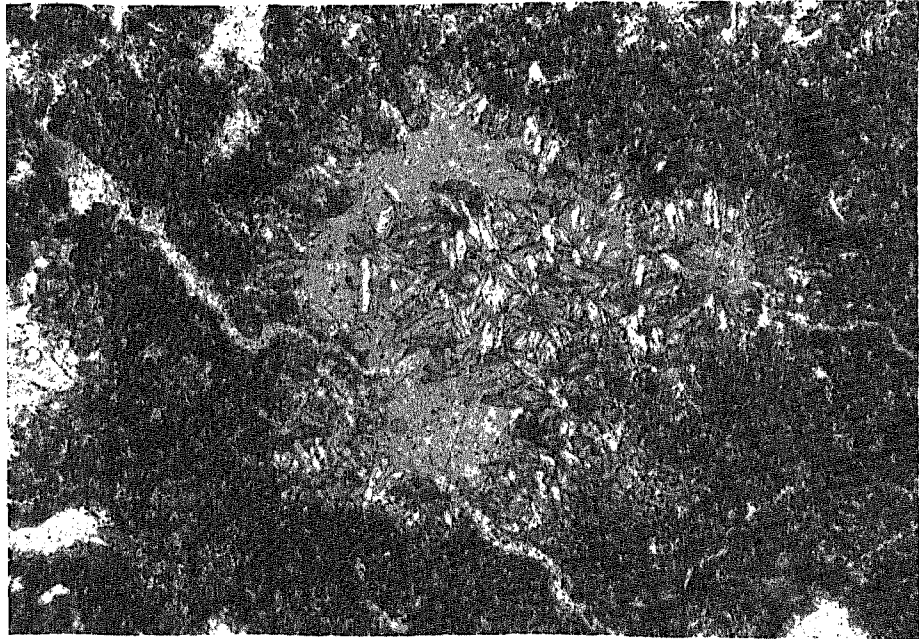


Fig. 3.20: Acicular carbonate crystals along the margins of a micrite nodule. Base of picture = 3.6 mm (-).

IV) Pyrite

Pyrite occurs a fine layers within, or clearly parallel to the hematite/magnetite layers. The vein-type pyrite (coarse, euhedral) is discussed in chapter 4.1.1.

Despite their massive appearance the layers are composed of small individual pyrite cubes (Fig. 3.21) which are recrystallized to give the massive appearance.

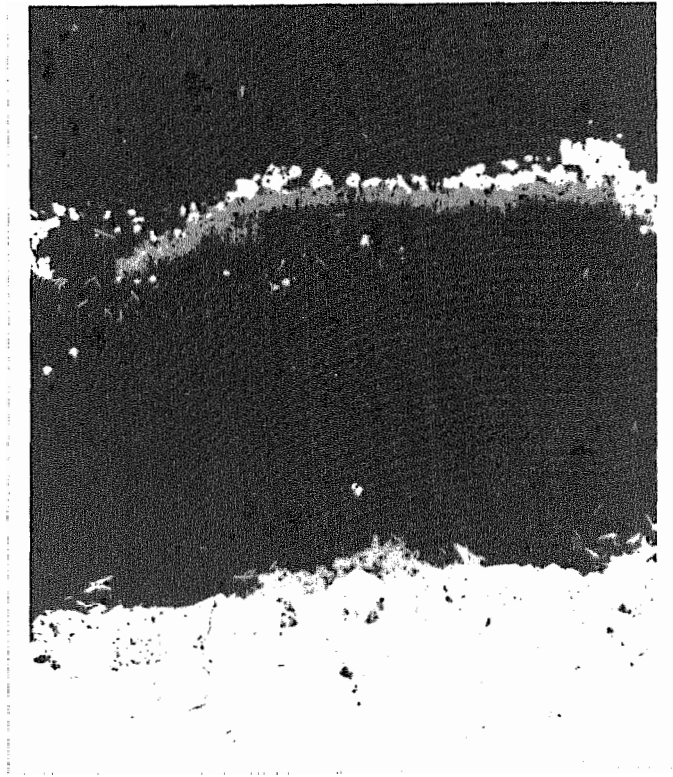


Fig. 3.21: Pyrite layer adjacent to hematite/magnetite layer.
Base of picture = 1.15 mm, reflected light (-).

The layering and the fine-grained nature support the view that pyrite is "syngenetic", as in McArthur (Williams, 1978) or Mt. Isa (Finlow-Bates, 1978), and thus is an integral part of the sediments of the black zone.

It is not so certain, however, whether pyrite is an indicator for euxinic conditions in the water column. The ubiquitous occurrence of iron oxides rather suggests oxidizing conditions and it is more likely that pyrite formed in localized ("micro"-) environments within the sediment. The hydrogen sulphide required may have been generated by the interaction of sulphate reducing bacteria (SO_4^{--} has been available in excess) and decomposition of intermittently occurring microbial mats (e.g. Renfro, 1974) as the process of bacterial sulphate reduction also is dependent upon, and often controlled by, the supply of organic matter (Trudinger, 1981).

A better term for the pyrite of the black zone therefore is "syndiagenetic".

V) Barite

Barite is common in the black zone, however, it is usually associated with veining or alteration processes (cf chapter 4.1. and 3.2.1.4.).

Little barite occurs as massive bands or layers of acicular crystals arranged +/- perpendicular to bedding with the crystals pointing uphole from a common base (Fig. 3.22).

Only this type of barite can be termed sedimentary or early diagenetic, i.e. having formed in the sedimentary environment of the black zone. It is discussed in chapter 3.2.1.4. however, that the primary sulphate has been gypsum or anhydrite and, subsequently, has been replaced by barite. The barite in the layer of Fig. 3.22, therefore, could be a diagenetic replacement of gypsum.



Fig. 3.22: Layer of acicular crystals composed of barite and quartz in magnetite-carbonate-quartz laminae of the black zone.

Facies of the black zone

With respect to iron content the black zone can be termed an iron formation which formed in a (at times) hypersaline basin. The abundance of carbonate and absence of volcanics place it into the Superior Type although a pre-1800 m.y. age is characteristic for that type (Eichler, 1976). The origin of the iron and the iron formation is disputable (e.g. Dimroth, 1979; Klemm, 1984, pers. comm.), but here it possibly stems from the continental red beds which developed on the inferred arkose underlying the Gap Well Formation (see chapter 4.7.).

Iron formation can form in tidal-flat environments; this has been demonstrated by Dimroth (1979) who discovered stromatolitic iron formations amongst other very shallow water features in the Sokoman Formation, Canada.

Furthermore, the occurrence of hematite layers in hypersaline environments has been reported e.g. by Dellwig (1955) from the Salina Basin, Michigan.

Although it is not clear whether barite is primary or has replaced gypsum the presence of early diagenetic sulphates indicates hypersaline or evaporitic conditions.

The usual (Mg-Fe-Mn dominated) carbonate chemistry also points towards an evaporitic environment; Kendall (1979) proposed to term such carbonates evaporites, too, as they form by the same processes as the more saline minerals.

All these features permit the interpretation of the black zone as a shallow-water, subaqueous evaporitic iron formation which formed in an oxidizing restricted basin (pyrite generation within the sediments).

3.2.1.3. Red zone

A banded, veined and locally brecciated rock with variable portions of jaspilite, hematite, barite, dolomite, calcite, quartz, pyrite, galena, chalcopyrite, sphalerite, chlorite (Figs.3.23 and 3.24).



Fig. 3.23: Drill core from the red zone with layers of hematite, jaspilite, quartz, carbonate and magnetite.

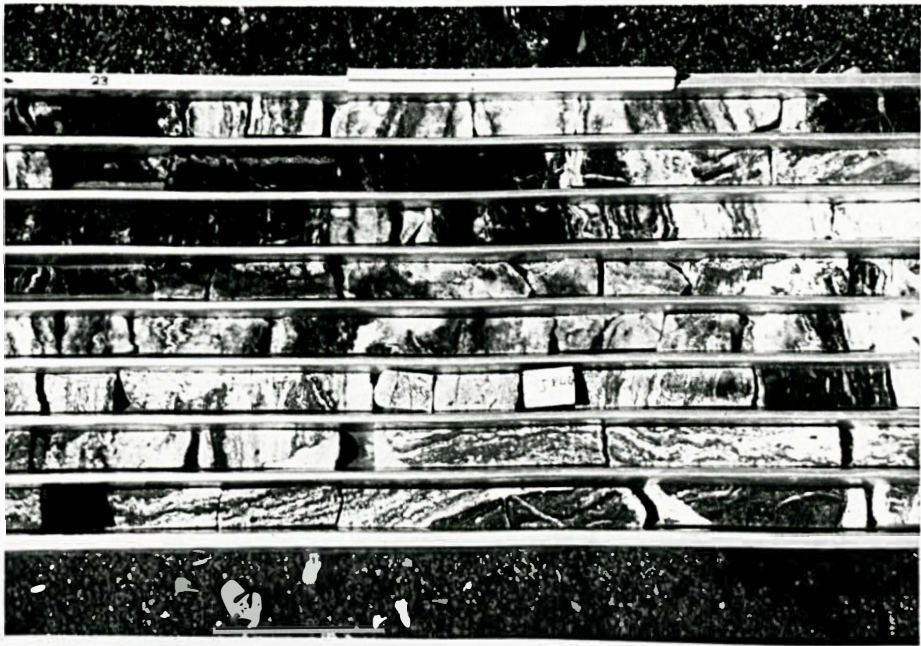


Fig. 3.24: Laminated red zone, with layered hematite/magnetite-carbonate vein (bottom).

Distinctive interbeds of lithic arenite, polymict conglomerate and silicified lutite-siltstone are characteristic. Some clastic dykes are reported in Geopeko drill-logs (1983, unpublished).

The thickness ranges from 40 metres to 120 metres with an increase towards the south-southeast. The red zone was encountered in all drill holes of the Abra prospect.

The nature of the laminations is similar to the black zone; however, jaspilite-hematite-chert-pyrite-barite are dominant and cause the overall reddish colouring (Fig. 3.25).

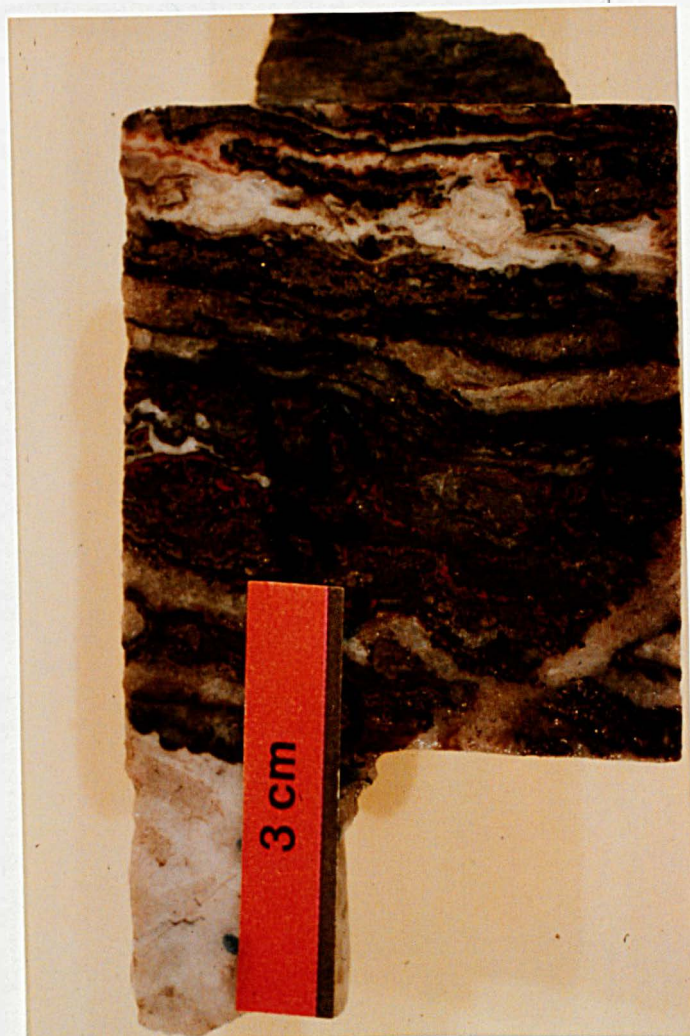


Fig. 3.25: Core specimen from the red zone showing layers of quartz, barite, pyrite and jaspilite.

Barite

Barite is a major constituent, particularly in the upper part of the red zone (up to 49 % Ba over 2 core metres in Ab 3), where it occurs as massive zones without any sedimentary structures and it is not certain whether massive barite zones represent recrystallized layers or massive veins.

In this chapter massive barite is excluded and only barite without a recognizable affinity to veining is discussed.

The diagenetic growth of barite crystals up to several centimetres in length is a common feature.

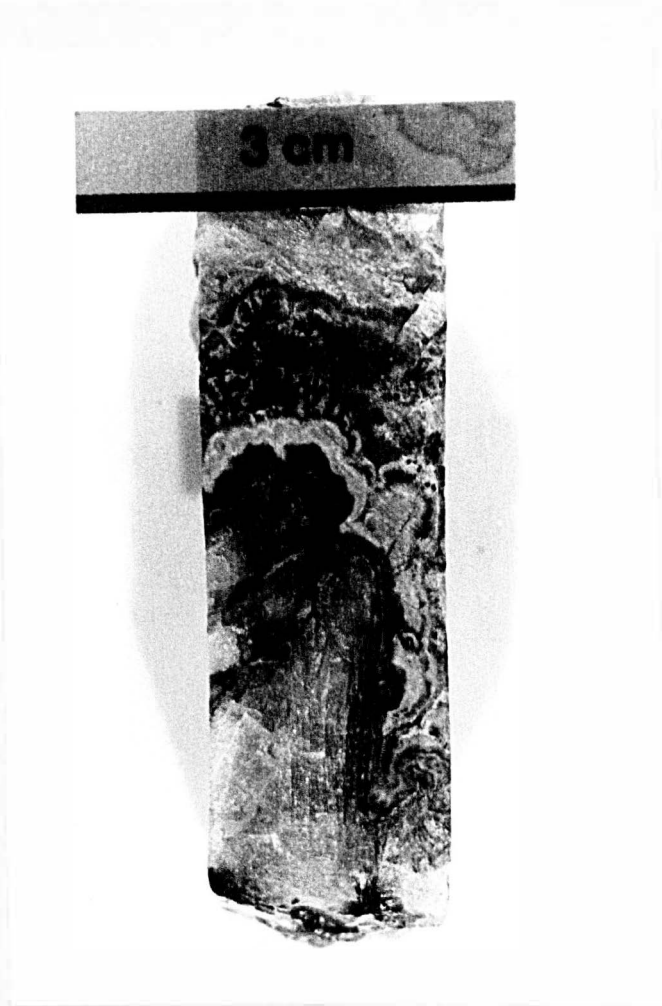


Fig. 3.26: Diagenetic barite crystals surrounded by colloform jaspilite-chert.

Fig. 3.26 shows that the surrounding jaspilite-chert layering has always grown perpendicular to crystal faces or edges. This can be interpreted only as the result of post-crystallization growth of jaspilite-chert layers, and as early-diagenetic crystallization of barite.

Fig. 3.27 shows part of a layer of lath-shaped crystals (now quartz with relict barite) surrounded by jaspilitic chert and carbonate, and overlain by a layer of anhedral barite.

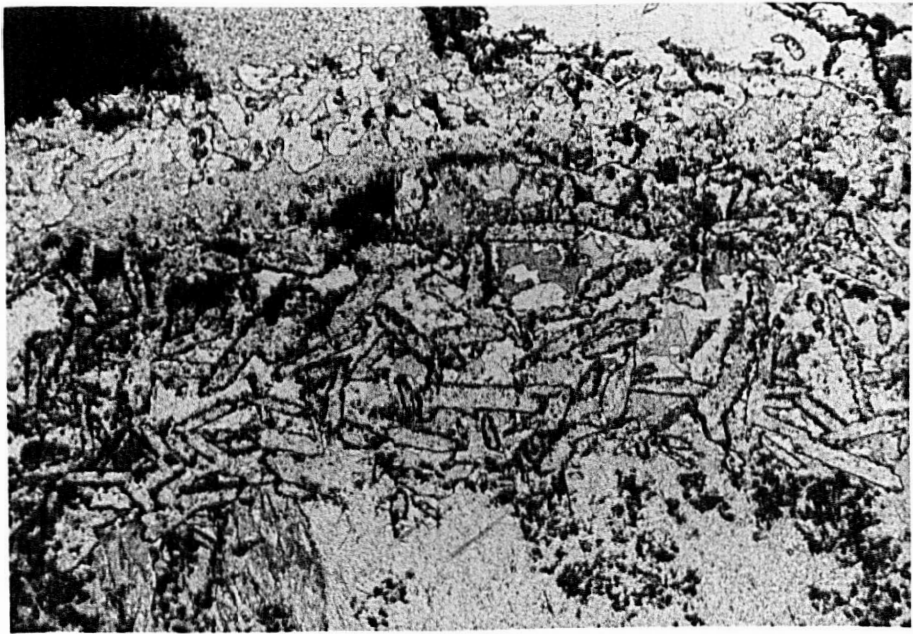


Fig. 3.27: Band of lath-shaped crystals (quartz and barite) surrounded by jaspilite and carbonate, overlain by barite layer. Base of picture = 3.6 mm (-).

While the above figures show a pre-(or syn-) jaspilite formation of barite - the jaspilite seems to surround, or grow on fully crystallized barite - there are other barite crystals clearly displacing jaspilite (hematite), suggesting a post-jaspilite (hematite) growth of barite. There are two interpretations for this: two or more generations of barite or two generations of jaspilite formation.

There appears to be an affinity of these crystals (now barite) to jaspilitic-chert sediments which may indicate that more oxidizing environments favoured the growth of the crystals. The mode of occurrence resembles that of gypsum, but there is no evidence so far whether or not gypsum was primary and later replaced by barite.

Carbonate

The nature of carbonates in the red zone is similar to the black zone. The dark colour and electron microprobe analyses suggest that they are dominantly Mg-Fe-Mn carbonates.

In contrast to the black zone there is frequent "spherulitic extinction" in zones of apparently micritic carbonate, and a tendency to form nodules.

Fig. 3.28 shows a nodule within colloform micritic carbonate. The centre of the nodule is filled with some chlorite and a diffuse, cherty and streaky variety of quartz, a texture very similar to finely crystalline and streaky gypsum. Towards the margin the nodule is occupied by fibrous, sparitic carbonate.



Fig. 3.28: Nodule in micrite. Acicular carbonate crystal along the margins and diffuse, cherty quartz in the centre. Base of picture = 3.6 mm (+).

Fibrous carbonate is also very abundant in the nodule shown in Fig. 3.29 which now is silicified; all dusting (dark inclusions) seen there consists of carbonate.

Nodular pseudomorphs of gypsum by calcite in a dolomicrite are described by Bouroulllec (1980) from the Aquitaine Basin, France; and the fibrous nature of the carbonate in the nodules from the zone suggests that substitution of lath-shaped sulphates (barite or gypsum) by carbonates took place.

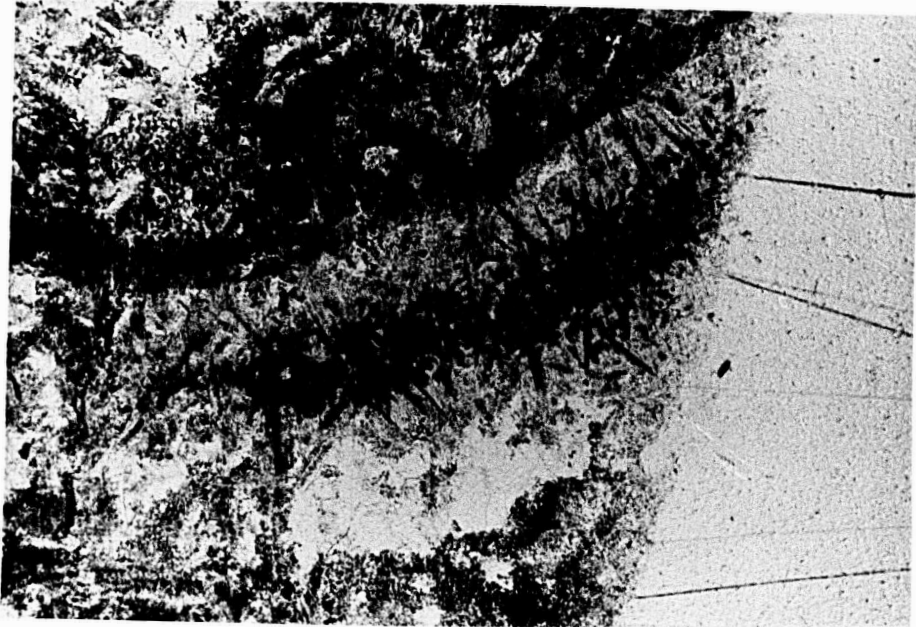


Fig. 3.29: Silicified carbonate nodule. Fibrous texture preserved by carbonate inclusions. Base of picture = 3.6 mm (-).

Hematite/magnetite-jaspilite-pyrite

As mentioned before magnetite is subordinate in abundance (in contrast to the black zone) to hematite and jaspilite. This indicates a shift to a more oxidizing environment of sedimentation which is compatible with a change to sabkha conditions.

Abundant layers of pyrite probably were generated by decomposition of abundant microbial mats within the sediment; this is further indication of sabkha conditions where large numbers of microbial mats are common (e.g. Renfro, 1974).

Co-existence of hematite and pyrite is not contradictory but indicates oxidizing conditions at the sediment - water/air interface and, locally, reducing conditions within the sediment (in the vicinity of decaying microbial mats, cf chapter 3.2.1.2.).

In contrast to hematite which often is layered, jaspilite and iron-hydroxides usually are colloform. Colloform iron-hydroxides also occur in carbonate. Although deposition of an iron-rich gel (creating colloform structures during dewatering) cannot be excluded for jaspilite-layers there are irregular zones of jaspilitisation as well as jaspilitic veins (in the stringer zone). Thus, some jaspilite probably is related to secondary (alteration) processes.

Clastites

The banded hematite-jaspilite-pyrite-chert-etc. rocks are often interspersed by clastites comprising wackes, polymict conglomerates, and minor siltstones and arenites.

Coarse-grained rocks predominate; they are usually poorly sorted with subangular to poorly rounded grains of quartz, potash feldspar (often sericitized and/or chloritized:), lithic clasts of shale, chert and jaspilitic rocks, and minor tourmaline plus titanomagnetite and scheelite.

The matrix consists of cherty quartz, sometimes barite, and commonly is jaspilitized.

The low degree of maturity of the clastites in the sedimentary context suggest that they were deposited as channel fillings within the sabkha environment, and some possibly as storm deposits. The non-correlation of the clastites between the drill holes provides further supporting evidence for this mode of deposition.

The mineralogy of most of the epiclastic grains (potash feldspar, tourmaline, scheelite) suggests a granitic source; others (chert, jaspilitic clast) certainly are derived from contemporaneous sediments without being transported over long distance.

Further consideration

In Ab 3, 292.2 metres an important texture occurs (Fig. 3.30). A typical banded red zone-rock is veined by barite-galena. The banded portion consists of chert-carbonate with various portions of jaspilite.



Fig. 3.30: Sabkha textures in jaspilite-chert of the red zone.

The manner in which the laminae are deformed very closely resembles features of evaporitic deposits. The hummocky type of bedding just below the red jaspilite layer is identical to mammillated anhydrite structures from the Oligocene Valence Basin, Southeast France described by Guillemin (1980) as one of the common features of anhydrite (Fig. 3.31).



Fig. 3.31: Mammillated anhydrite structures from the Valence Basin. Photograph from Guillevin (1980).

The zone immediately below, characterized by reddish contorted structures, is very similar to enterolithic structures which frequently occur in sabkha sediments. Shearman (1980) presented several examples (Fig. 3.32) and concluded that they are primary growth structures (i.e. not only surficial hydration of anhydrite causing contortion of former layers through up to 63 % volume increase). Enterolithic structures develop where anhydrite nodules have coalesced to form layers and continued growth of the nodules created a demand for space. The lateral pressures which result cause the layers to become contorted. Production of enterolithic structures is no doubt facilitated by the high natural moisture content of the nodules, and the platy habit of the tiny anhydrite crystals which allows easy slip between them (Shearman op.cit.).

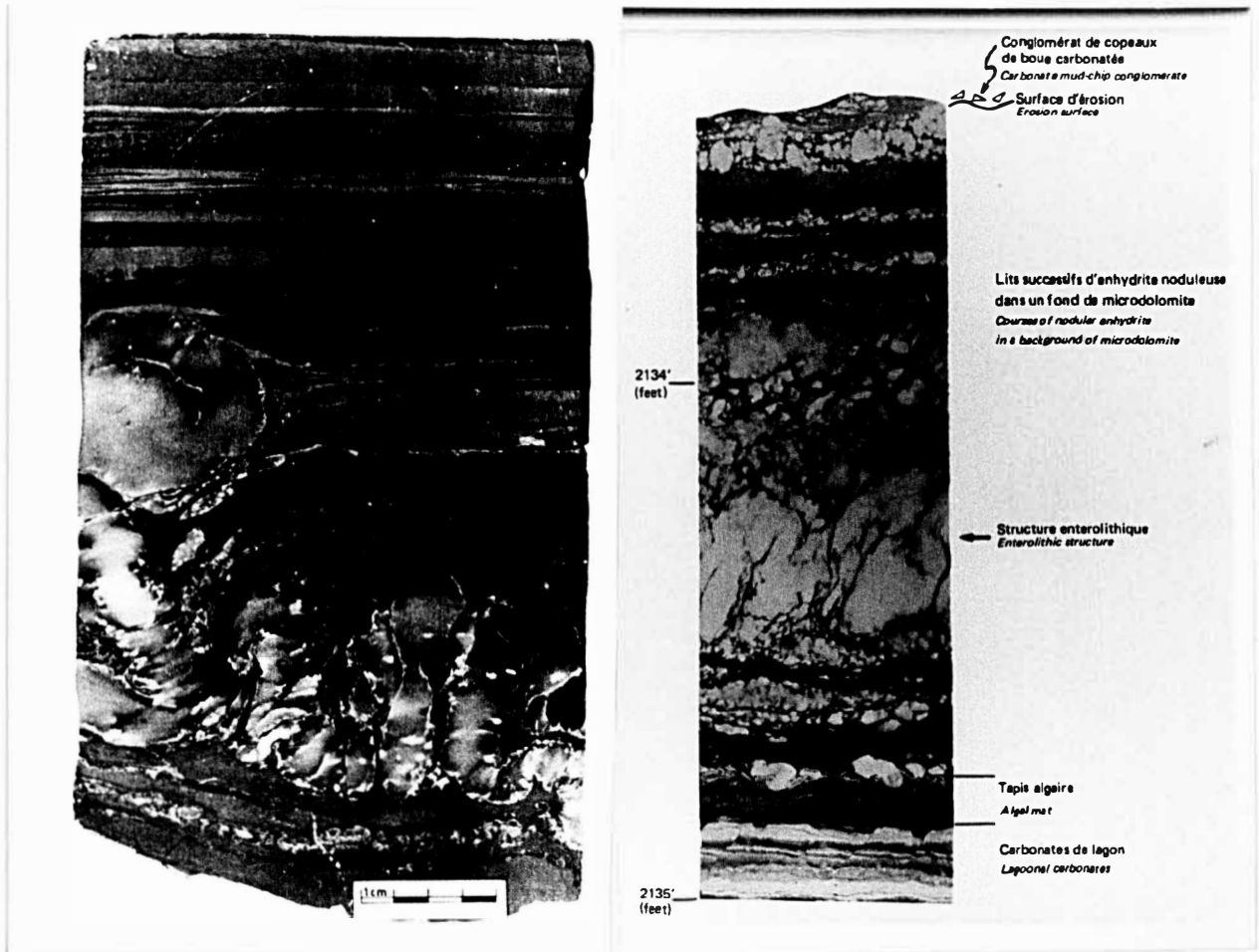


Fig. 3.32a and b: Enterolithic structures in sabkha deposits. Photographs from Shearman (1980).

It is likely that the silicified enterolithic structures of Fig. 3.30 originally have been anhydrite rather than barite. Barite may not have the crystallographic properties to permit the development of such structures; although both anhydrite and barite are orthorhombic the structure of the former is very different from that of the barite group of sulphates (Deer et al., 1972), and only anhydrite displays the tendency to become hydrated.

Thus, the structures in Fig. 3.30 provide the best available textural evidence that a) sabkha conditions did exist in the red zone

b) anhydrite, i.e. calcium-sulphates were present

c) the mineral constituting diagnostic textures have been replaced (silicified, carbonated, jaspilitized)

Although no halite has been found in the Abra succession there are some indications that it has been present or that the interstitial waters have had elevated Na-contents:

Fig. 3.33 shows several cubes within a cherty, micaceous groundmass. The cubes consist of Fe-Mg chlorite with scattered quartz and micas. The textural similarity between the interior of the cubes and the surrounding groundmass suggests that they formed within the sediments. The fine-grained micas resemble hydromuscovite; a characteristic mineral of evaporitic series (Haditsch, pers.comm., 1984).

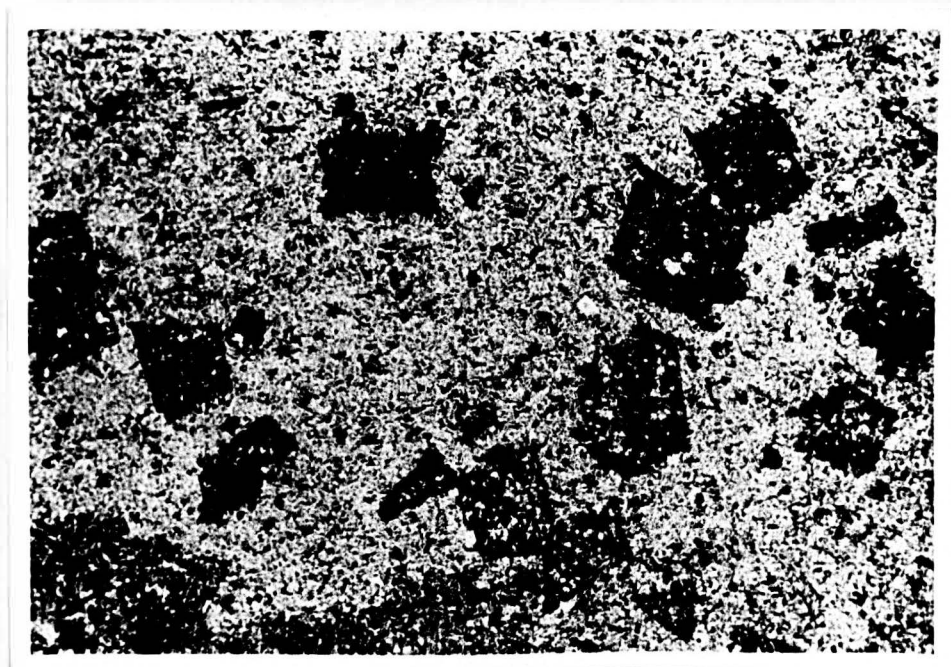


Fig. 3.33: Chloritic cubes within cherty, micaceous groundmass. Base of picture = 3.6 mm (-).

These cubes possibly have originated as chloride salts (NaCl ?) which have grown in the sediment, through significant increase in salinity of the formation waters, and incorporated sediment.

Subsequent chloritization is compatible with this interpretation as any chlorides would readily be dissolved by a decrease in salinity of the formation water, and the late (?) diagenetic chemical regime apparently favoured chloritization (chloritized carbonate, micas, potash feldspars).

Top of the red zone

The nature of the contact between the red zone and the overlying West Creek Formation (either WC₁ or WC₂) is variable between the individual drill holes.

Whether the red zone is overlain by the WC₁ or WC₂-unit has no implications for its sedimentary development and will be discussed in the following chapter on the West Creek Formation.

The variable appearances of the contact can be summarized into two different groups:

I) The first group is represented by the "southern" drill holes Ab 3, Ab 4, Ab 5, Ab 9, Ab 10, Ab 11. Here the typical jaspilite-hematite-pyrite-etc. laminae in the uppermost red zone are intercalated with conglomeratic portions with jaspilitic matrix.

Towards the top, jaspilitic conglomerates become dominant and are then overlain by "clean" (no jaspilitic but carbonate-quartz-barite matrix) clastites of the West Creek Formation. This is a conformable, normal geological contact and the abundance of coarse clastites in the top of the red zone may even suggest that it is gradational.

II) The contact is different in Ab 6 and Ab 7 (the "northern") holes. In Ab 6 the uppermost banded jaspilite-hematite-pyrite rock, overlain by a fine- to medium-grained lithic quartz arenite with sharp

basal contact, shows abundant growth of large barite crystals and oxidation of jaspilite-hematite to goethite in the uppermost millimetres (Fig. 3.34).



Fig. 3.34: Top of red zone with abundant barite crystals overlain by quartz arenite (upper left).

In thin section it becomes evident that there is hardly any textural difference between the uppermost millimetres of the red zone (goethite cemented clastites) and the overlying West Creek Formation (carbonate cemented clastites).

In Ab 7 hole the uppermost red zone is characterized by some well developed, small (about 1 centimetre wide) digitate stromatolites, over laminated jaspilite-hematite rock with thin veins of oxidized and partially oxidized pyrite resulting in local formation

of limonite-goethite (Fig. 3.35). Some minerals have been dissolved leaving irregularly distributed casts in the rock.

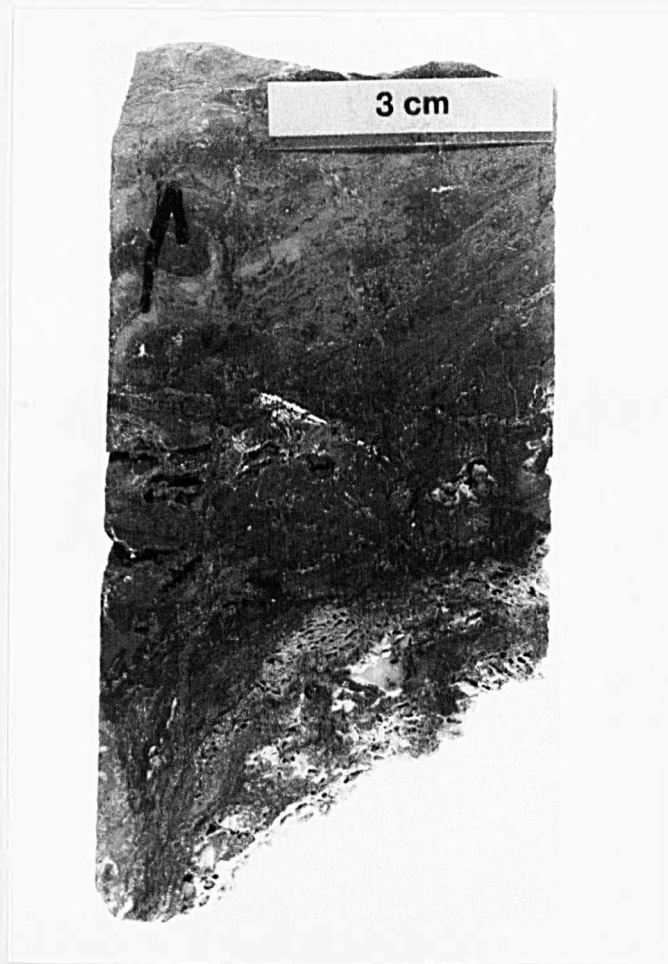


Fig. 3.35: Proterozoic chemical erosion of the top of the red zone (in Ab 7 hole) resulted in leaching (voids) and oxidation.

Thus, in both the northern drill holes Proterozoic chemical erosion and oxidation have probably taken place. However, this does not necessarily imply a significant time break between the red zone and the overlying West Creek Formation. In a sabkha environment, prolonged subaerial exposure and rapid lithification are common

(Kendall, 1979). As the red zone probably represents coastal sabkha deposits, the pronounced oxidation and erosion in the northern drill holes suggests that the contemporaneous continental area has been due north (and east, as will be shown later) with respect to the Abra area.

Facies of the red zone

Textural features presented on the previous pages, abundance of jaspilite-hematite and the occurrence of isolated coarse, immature clastic units constitute sufficient sedimentological evidence for a coastal sabkha depositional environment of the red zone. Along the section of drill holes the seaward or basinward direction is due south.

The original sediments of the coastal sabkha probably consisted of hematite-chert/jaspilite-carbonate layers and bands of pyrite which formed diagenetically through the decay of microbial mats. The emplacement of barite and base metal sulphides was not related to sedimentary processes but occurred diagenetically when the hydrothermal system was coupled with diagenetic formation waters.

Contemporaneous sea water was concentrated (through evaporation) until precipitation of sulphate took place; locally - within the sediment - the salinity may have reached chloride (NaCl?) saturation.

The absence of primary evaporitic minerals is compatible with a sabkha environment as the solubility in water (under normal conditions) of these minerals facilitates removal and transformations of the components even when changes of physico-chemical parameters of diagenetic formation waters are only slight. According to Kendall (1979) many fine-grained dolomitic red bed sequences (e.g. the Keuper of Europe) represent evaporitic deposits but occurred in non-evaporite-preserving environments.

3.2.1.4. The sulphate problem

On the previous pages it frequently has been discussed whether anhydrite or gypsum was the primary sulphate mineral which later has been replaced by barite, carbonate or silica. This question bears important genetic implications with regard to the commencement of hydrothermal activity at Abra.

Complete replacement in this case (Ba for Ca) presumably would not leave chemical traces of the replaced mineral and can be deduced from textural features only. Unfortunately, little is known of any diagnostic textural habits of barite that may distinguish it from Ca-sulphates.

Nevertheless, there are a number of textural observations and chemical constraints, listed in the following, which suggest a non-sedimentary, replacement origin of barite:

a) Carbonate pseudomorphs after sulphates

Carbonate commonly occurs as acicular or lenticular crystals in the red and black zones, suggesting replacement of sulphate minerals, because this habit is unusual for carbonates. Only aragonite would display such forms, but analysis of carbonates clearly shows that no aragonite occurs. Furthermore aragonite is readily converted to other carbonates during early history of the sediments (Blatt et al., 1980). The newly formed carbonates are iron- and manganese-bearing dolomites, which usually recrystallize to sub- or euhedral rhombs.

The lath-shaped body in Fig. 3.36 consisting of carbonate and minor quartz resembles a section of a tabular, former gypsum crystal.



Fig. 3.36: Ca-carbonate plus quartz pseudomorph after gypsum, within ferroan dolomite and quartz. Base of picture = 0.9 mm (-).

Remarkably, the carbonate filling of this body consists of (almost pure) calcite, while the surrounding carbonates are Fe, Mn-dolomites. Replacement of a lath-shaped crystal by Ca-carbonate (which is extremely rare in Abra rocks) indicates that the original mineral also has been calcium bearing. This is strong evidence that the original sulphate mineral has been Ca-sulphate.

Replacement of sulphates by carbonate thus has taken place. Presumably, only Ca-sulphates were susceptible to replacement by carbonate because replacement processes are considered to have occurred diagenetically at temperatures below 200⁰ C, conditions at which barite is hardly soluble (e.g. Deer et al., 1972). Therefore, it is inferred that Ca-sulphates have been present in the early Abra sediments.

b) Barite layers

Only one barite layer has been found in the black zone (Fig. 3.22) whereas these layers are common in the red zone (Fig. 3.27). The individual crystal casts are usually filled by a barite-quartz phase.

Paar (1974) described barite layers from the Breithorn Ba-Pb deposit in Eastern Greenland that are similar (but more abundant, and the crystals only consisting of barite) to the layer in Fig. 3.22. He termed this mode of appearance "palisade fabric" and concluded that it has formed syndiagenetically from Ba-containing solutions which were exhaled onto the seafloor and penetrated into the early diagenetically dolomitized sediments.

Gypsum layers and nodules occur in the vicinity of the deposit at the same stratigraphic level (analogous to the Abra situation where gypsum casts occur in the upper Gap Well Formation, see Fig. 2.36). Furthermore, the bird's eye structures and palisade fabrics reported by Paar (1974) closely resemble features of Ca-sulphate evaporitic series; Reading (1978) mentions bird's eye structures of gypsum in sabkhas, and Langbein's (1979) classification of anhydrite micro-fabrics contains a group ("normal to bedding") similar to the palisade fabric. Angerer et al. (1980) described such gypsum fabrics in the Montafon gypsum deposits, Austria.

Hence, diagenetic replacement of former gypsum (or anhydrite) layers by barite is possible for both Abra and the Breithorn deposit. Paar (1974) has shown that most of the Ba-bearing solutions ascended after deposition of the host sediments; this mechanism may, thus, be invoked in particular for the Breithorn deposit.

c) Sabkha textures

Some conspicuous textures (Fig. 3.30) in the red zone have been compared with typical sabkha deposits in chapter 3.2.1.3., and it has been shown that they resemble enterolithic structures and mammillated structures diagnostic of sabkhas. These structures consist of chert-jaspilite-carbonate now, but originally they may only have been produced by anhydrite, because of its crystallographic properties and its ability to become hydrated (cf chapter 3.2.1.3.).

d) Strontium content of barites

All barites (21) analysed by electron microprobe have a remarkably uniform strontium content, varying between 0.26 % and 0.86 % Sr (see chapter 4.1.). The barites analysed comprise vein-type barite from the stringer zone, lath-shaped crystals from the red and black zones, and veins and layers from prospects 60-80 km west of Abra in the Jillawarra Belt.

This suggests a single and common event of barite formation, i.e. all barite formed in the major phases of the hydrothermal activity and were emplaced after deposition of the host sediments. Any barite which would have formed as primary sulphate in the sabkha environment should reflect higher strontium values than vein-type barite, because sabkha sediments are usually enriched in strontium (Moine et al., 1981, Morrow et al., 1978, p.1403). Increasing closed system conditions of precipitation are reflected in increasing Sr-content of barite (Morrow, op.cit.). However, elevated Sr-values of whole rock analysis of samples from the red and black zone (130-510 ppm Sr compared with 20-60 ppm of other rocks, cf chapter 4.3.) - suggesting Sr-enrichment in the evaporitic sediments - do not correlate with elevated Sr-content of barites from the respective zones.

Whereas barium can be replaced by strontium in a continuous solid solution series and therefore would incorporate the Sr available (up to 14.7 % Sr in barite is reported by Deer et al., 1972, p.189), anhydrite and gypsum have only traces of Sr (Deer et al., op.cit.).

This indicates that barite formation was not related to sedimentary or early diagenetic conditions, but was replacing anhydrite or gypsum later in the diagenetic history, and thereby incorporating the minute quantities of Sr in anhydrite (gypsum), that

are not sufficient to distinguish these replacement barites from vein-type barite.

Summary

There is sufficient cumulative evidence from consideration of the above paragraphs (a-d) together, that Ca-sulphates were the primary sulphates formed in the sedimentary and early diagenetic phases of the evaporitic series of the black and red zones. Subsequently, with the onset of major hydrothermal activity, Ca in the sulphates was quantitatively replaced by Ba to form barite.

Very low solubility of barite (in contrast to anhydrite/gypsum) and the water-saturated nature of diagenetic evaporitic sediments facilitated quantitative replacement.

Almost complete replacement of carbonate by quartz without destroying the delicate banding has been demonstrated in chapter 3.2.1.2. and, therefore, replacement of gypsum/anhydrite by barite presumably could proceed with the same ease.

3.2.1.5. Correlation with the Gap Well Formation of the Jillawarra Belt

While the stringer zone - with respect to thickness and facies - corresponds to the upper GW_5 and lower \pm middle GW_6 -unit, the black and red zones correlate with the upper GW_6 -unit of the Jillawarra Belt (see Fig. 2.05).

However, the sedimentation rate of sabkha sediments is slower than that of the (slightly clastic) dololutes (Kendall, 1979) of the Jillawarra Belt; this renders correlation by thickness impossible.

The GW_6 -unit of the Jillawarra Belt is characterized by a regressional development with inter-supratidal deposits. The Abra succession

also displays a distinct regression; from inter-subtidal sediments of the stringer zone over shallow-water subaqueous evaporitic iron formation (black zone) to coastal sabkha deposits of the red zone. Although the differences to the depositional parameters of the GW₆-unit of the Jillawarra Belt are minor (slightly shallower water, restricted basin), the resultant sediments are very different. Obviously the regressional development in the Abra area was more pronounced than in the Jillawarra Belt further west.

3.2.2. The West Creek Formation

This formation is encountered in all Abra-drill holes with intersections ranging from 220 metres (Ab 6) to over 500 metres (Ab 11) in the southeast.

Mineralogical and sedimentological characteristics are widely similar to the Jillawarra Belt and render a detailed discussion unnecessary.

Therefore, in the following only a short description of some features unique in the Abra succession will be given; for comprehensive description and facies interpretation see chapter 2.3.2.

3.2.2.1. WC₁

This coarse clastic unit has a maximum thickness of 40 metres and is absent in Ab 6 and Ab 7 holes in the north and Ab 11 in the southeast (cf Fig. 3.03).

Dominant rock types are a medium- to coarse-grained, moderately sorted, rounded to subangular lithic quartz arenite and polymict granule to pebble conglomerate (see Fig. 2.51). The cement usually consists of carbonate and minor cherty quartz. In the lower part of this unit, locally barite occurs as cement (up to 6.4 % Ba over 2 core metres). The barite probably has been introduced post-depositional to the clastites and may have been mobilized from

the underlying red zone or emplaced through hydrothermal activity.

The epiclastic grains comprise quartz, potash feldspars, chert and shale clasts, and clasts of jaspilitic rock. The shale clasts sometimes are chloritized or entirely consist of chlorite.

Locally the bedding is defined by detrital Ti-bearing iron oxides which have been altered in situ to sphene; a phenomenon also found in the underlying red zone.

While shale, chert and jaspilite clasts are derived from the red zone, the abundance of quartz, potash feldspar and Ti-bearing iron oxides suggests a granitic source. The overall compositions of the clastics is very similar to the clastic intercalations in the red zone pointing towards a common source.

The WC₁-unit was deposited in a near shore position as a coarse clastic carbonate-cemented sediment, possibly in a fluvial-fan-mode of deposition. To allow deposition of up to 40 metres of coarse clastites, rapid subsidence of the depository must be invoked. Because the drill holes without WC₁-unit are separated by faults from the holes with this unit (see Fig. 3.01) the WC₁-clastites conceivably have been deposited in a fault-bounded, subsiding basin. This basin is termed the Abra-sub basin, the limits of which are defined by the occurrence of the WC₁-unit.

3.2.2.2. WC₂

While there is a difference in lithology of the WC₁-unit between the Abra-sub basin and the Jillawarra Belt (the common dolomitic shale and siltstone is absent in the Abra succession), the WC₂-unit of the Abra succession probably is identical to the Jillawarra Belt.

With a thickness of about 330 metres it represents the shallow water turbidite facies described in chapter 2.3.2.2.

After an interval of subsidence of local sub-basins (WC_1) 330 metres of turbidites indicate a prolonged period of subsidence which - in contrast to the WC_1 -unit - was widespread and affected the entire Jillawarra Basin.

3.2.2.3. WC_3

This unit was encountered only in the southernmost drill holes (Ab 9 - Ab 11). It comprises interbedded lutite-siltstone (frequently carbonaceous) and fine-grained quartz arenite with subordinate coarse-grained lithic quartz arenite and rare conglomerate.

The lack of significant carbonate (massive or as dolomitic siltstone) is the main point of difference to the WC_3 -unit of the Jillawarra Belt. A tidal flat environment of deposition is also invoked. The change from shallow-water turbidites (WC_2) to tidal-flat sediments is taken to indicate an attenuation of subsidence.

3.3. Deformation of the Abra sub-basin

The Abra sub-basin occurs close to the eastern margin of the Jillawarra Basin defined by the regional Tangadee Lineament. The latter also marks the boundary between the structural domains of the Edmund Fold Belt and the Bullen Platform.

The Abra sub-basin is located in the southern shallow limb of a broad major anticline (see section E-F on map 1).

3.3.1. Faults

The area of the Abra mineralization is limited by three faults (Fig. 3.03). The two NE-trending faults are probably related to the Abra Fault System in the east while the E-trending faults parallels the regional Quartzite Well Fault.

By comparison with NE-trending faults in the Jillawarra Belt it can be assumed that the corresponding faults in the Abra area are normal, have steeply dipping fault planes, and have been active from the GW₆-unit onwards; i.e. synsedimentary with respect to the Abra succession.

E-trending faults in the Jillawarra Belt originally have been normal faults - in places outlining the margins of the Jillawarra Basin - which subsequently became reverse faults in the compressional tectonic regime. Whereas thrust faults with shallow fault planes occur in the Manganese Range area, steeply dipping fault planes and lower deformational grade can be inferred from regional considerations in the Abra area.

Intersections of faults in Abra drill cores confirm the steep dip of the fault planes:

- Ab 3: 504.0 - 511.5 core metres
silicified and chloritic brecciated and veined interval with significant chalcopyrite mineralization
- Ab 9: (835-) 850 core metres
whole interval intensively veined and brecciated, at 850 metres indications of faulting
- Ab 5: 274.5 - 275.0 core metres
disintergrated breccia
vein quartz, silicified arenite
- Ab 11: 794 - 796 core metres
silicified and brecciated fault zone

Through calculations of azimuth and dip (measured in 30-40 metres interval in each drill hole) the three-dimensional coordinates of the fault zone intersections have been determined. The end-of-hole (EOH) coordinates are shown in Tab. 3.01.

Tab. 3.01 Geometrical data of the Abra drill holes.

	core length	true depth	EOH-coordinates	surface coordinates
Ab-3	575 m	542 m	8991 N 8624.5 E	8800 N 8500 E
Ab-4	536 m	509 m	8868 N 8704 E	8700 N 8620 E
Ab-5	759.5 m	713 m	8930 N 8633 E	8670 N 8340 E
Ab-6	400 m	390 m	9072 N 8674 E	8985 N 8590 E
Ab-7	459 m	431 m	9117 N 8406 E	8955 N 8310 E
Ab-9	945.3 m	803 m	8938 N 8664 E	8460 N 8650 E
Ab-10	899 m	795 m	8794 N 8902 E	8375 N 8850 E
Ab-11	855 m	758 m	8646 N 9080 E	8250 N 9000 E

Surface traces of the faults (allocated to the Geopeko 100-metres exploration grid) and coordinates of the fault zone intersections (calculated for the same grid) have been used to construct the block diagram (Fig. 3.01).

This illustrates the fault-bounded nature of the Abra-sub basin and also the occurrence of WC₁-clastites, restricted to the sub-basin; i.e. therefore, the WC₁-unit is absent in Ab 6, 7, 11 holes.

Synsedimentary tectonic activity is evident from the stringer zone onwards; soft sediment deformation and slump structures are abundant. Clastic dikes, particularly abundant in the stringer zone, are further indication of synsedimentary tectonics as they represent injection of sedimentary material into fractures created by shrinkage (can be excluded in the stringer zone), shock waves, slumping, etc. (Reineck and Singh, 1973).

3.3.2. Cleavage

No penetrative cleavage has been seen in core specimens or thin sections. Open style folding of the Abra anticline and the siliceous, non-micaceous nature of the rocks prevented the development of a pervasive cleavage.

3.3.3. Pseudo-tectonic features

There are deformational fabrics in the red and black zones which are similar to feature of synsedimentary tectonics.

- Crenulation of lamination is common and sometimes of a regular nature, similar to micro-faulting or cleavage (see for example the mamillated structures in Fig. 3.30).
- Distortion of bedding also is common (see enterolithic structures in Fig. 3.30) and often resembles slump structures or other kinds of soft sediment deformation.

However, both these phenomena can be generated in evaporitic sediments without the influence of tectonics. Growth of microbial mats, dissolution and reprecipitation, and hydration of the evaporitic minerals have been shown to account for these structures (Kendall, 1979).

- Much of the brecciation so characteristic in the Abra succession probably is either related to veining (i.e. the hydrothermal activity) or to intraformational brecciation; or even to collapse breccias common in supratidal or evaporitic sediments (James, 1979).

3.4. Development of the Abra sub-basin (3. Order Basin)

It has been shown before that the Abra sub-basin is limited by an E-trending fault to the north and two NE-trending faults to the E and W, respectively.

The sub-basin has an E-W extension of 600 to 1000 metres while it stretches at least 600 metres in N-S direction with an open termination towards the south.

The development of the Abra sub-basin is analogous to the Jillawarra Basin (chapter 2.6.). After a regression in the GW_6 -unit (stringer, black and red zone) at first localized (WC_1 -unit), and subsequently widespread transgression (WC_2 -turbidites) occurred.

While the transgression clearly is related to subsidence of the Abra sub-basin and, later, the whole region, the behaviour of the basement during the regressional period is more complex and will be discussed in detail:

Sediments of the stringer zone formed in the same inter-subtidal environment as the lower to middle GW_6 -unit of the Jillawarra Belt. However, in the upper GW_6 -unit the regressional development of the Abra area is enhanced.

Decreasing water depth eastward - to be expected in a coastal section when the continental areas were in the east and north - probably did not govern the above difference; Proterozoic erosion is shown not in the eastern- or northernmost drill hole but in the westernmost (Ab 7).

Proterozoic erosion indicates emergence in the west (with respect to the Abra sub-basin) and possibly marks a barrier zone forming the western limit of the sub-basin. To explain the subaqueous evaporites of the black zone a barrier is required to prevent

exchange between saline basin waters and the open sea. In view of synsedimentary fault activity it is likely that this barrier formed along the western fault.

To account for the deposition of up to 40 metres of subaqueous evaporites, subsidence of the (fault-bounded) sub-basin must be invoked (Kendall, 1979).

There are apparently two opposite trends of movements in the basement; while an enhanced regressional development and the formation of a barrier indicate uplift in the Abra area the subaqueous evaporites point to subsidence of the Abra sub-basin.

If a fault-bounded basin developed in a "normal" coastal environment it represents a sink into which tidal channels are depositing clastics. The absence of a significant clastic component in the black zone suggests a different situation.

However, when such a basin forms on the slope or summit of an emergent basement complex (dome) - downfaulting of the basin is the result of crustal strain through extension, most effective in the periphery of the dome - the area is sufficiently elevated to divert rivers and tidal channels elsewhere, and a limited amount of clastics only would be transported into the basin. A similar situation is envisaged by Jackson and Seni (1983) to explain the paucity of terrigenous sediments in evaporites and shallow marine carbonates in a marginal rift basin of the Gulf of Mexico.

In view of the above discussion it is likely that doming in the Abra area took place (active emergence is also inferred for the Jillawarra Basin, see chapter 2.6.) accompanied by the development of a fault bounded basin due to crustal extension in the domed area.

The dome shaped elevation of the granitic Coobarra Dome (on COLLIER SHEET, east of Abra) further corroborates domal uplift in this particular region.

Figures 3.37 a to f diagrammatically summarize the development of the Abra sub-basin. It should be noted that the limited number of drill holes and lack of outcrop render evidence for active emergence of the Abra area and location of the barrier equivocal. Therefore, these figures can only be a model of the development of the Abra sub-basin.

Fig. 3.37a: app. middle GW_6 -unit (stringer zone)

The contemporaneous coastline was in the north and east although the basin seems to deepen towards the south-east. Sediments are dominantly calcareous siltstone with some arenaceous fan deposits, and possibly related minor turbidites, intercalated in a more basinward position.

No significant fault activity is evident from this interval; the Abra sub-basin has not yet formed. The whole area probably was gently emerging.

Fig. 3.37b: upper GW_6 -unit (black zone)

While the surrounding areas were progressively uplifted, the Abra sub-basin developed through downfaulting; it is uncertain whether movement occurred along the southeastern fault. Because of the continuing uplift of the surrounding areas a barrier formed and separated the Abra sub-basin from the sea.

Subsidence of the Abra sub-basin caused the deposition of subaqueous evaporitic iron formations (black zone) while in the adjacent areas tidal flats became supra-tidal and turned into a coastal sabkha (lower red zone in Ab 6, 7).

Fig. 3.37c: uppermost GW₆-unit (top of the red zone)

No further subsidence of the Abra sub-basin took place and the whole area was affected by general uplift. The subaqueous evaporites grade into coastal sabkhas with minor clastic sedimentation. The former coastal sabkhas in the north are characterized by abundant clastic intercalations and resemble continental sabkhas. Locally, in the zone of the former barrier, prolonged subaerial exposure led to Proterozoic chemical erosion of the sabkha sediments.

Fig. 3.37d: WC₁-unit (coarse clastites)

Rapid subsidence of the Abra sub-basin occurred along the three faults.

The subsiding basin was filled by up to 40 metres coarse, carbonate cemented shallow water clastites in a fluvial mode of deposition.

The clastics are derived mainly from a granitic source probably in the northeast. Some of the areas adjacent to the Abra sub-basin remain sabkhas; they are rapidly lithified and contribute a minor portion of jaspilitic rocks to the clastites.

Fig. 3.37e: WC₂-unit (turbidites)

Regional subsidence caused deposition of several 100 metres of coarse-grained shallow water turbidites, sometimes with complete Bouma cycles.

The clastics were derived from a landmass in the north-east.

Fig. 3.37f: present

During regional folding of the Bangemall Group a major broad, asymmetrical anticline formed on the southern

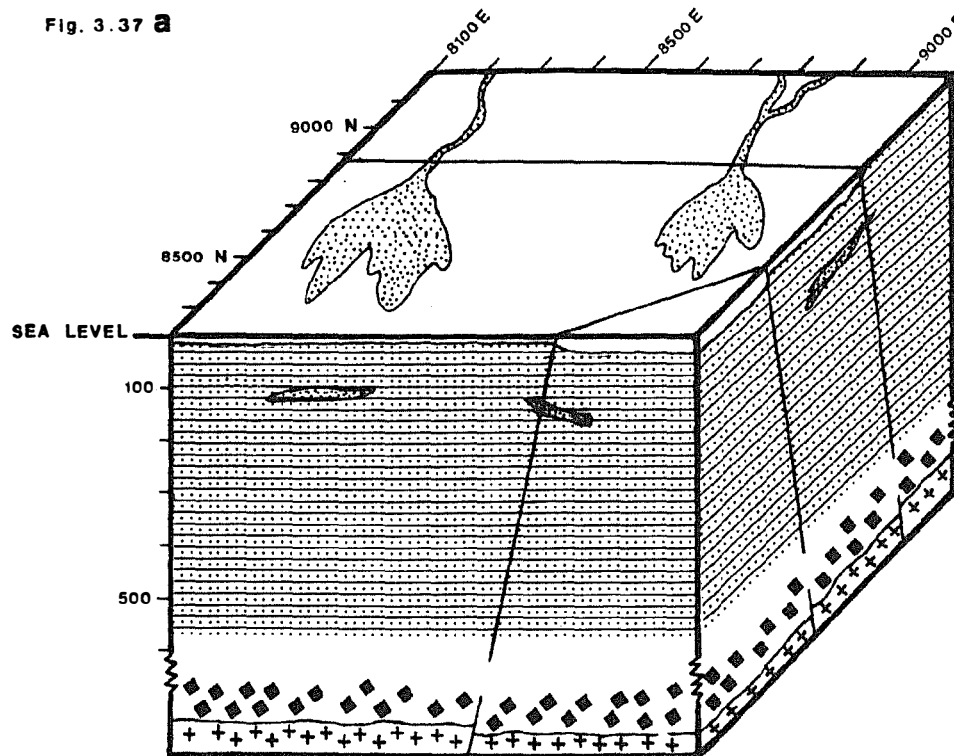
limb of which the Abra sub-basin is located.

The major anticline has a shallow plunge towards the west causing a mean dip of 20° to 30° (into a SSW-direction) in the Abra area.

The arrows indicate the latest sense of relative movement of faulting related to the late stage folding of the Bangemall Goup.

Dips on the N-S section are exaggerated.

Fig. 3.37 a



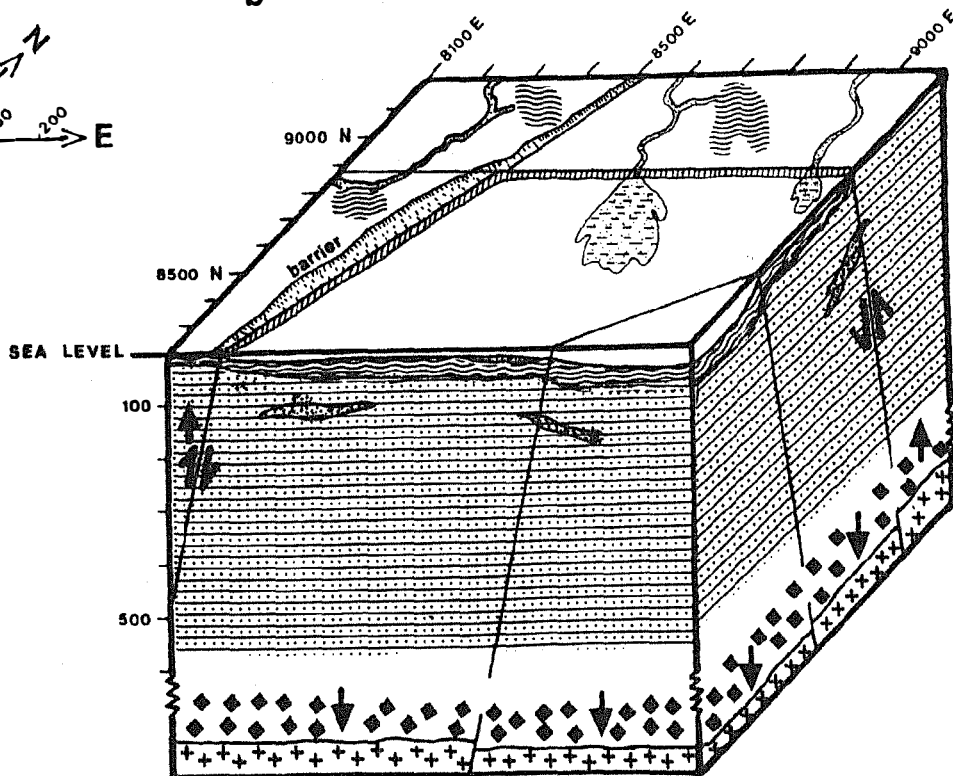
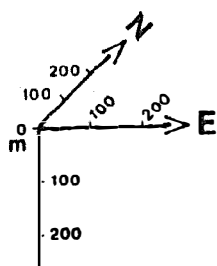
intertidal deposits

medium grained siltstone
dolomitic wackestone

inter-subtidal deposits

medium grained siltstone
dolomitic wackestone
arenaceous fan deposits

b

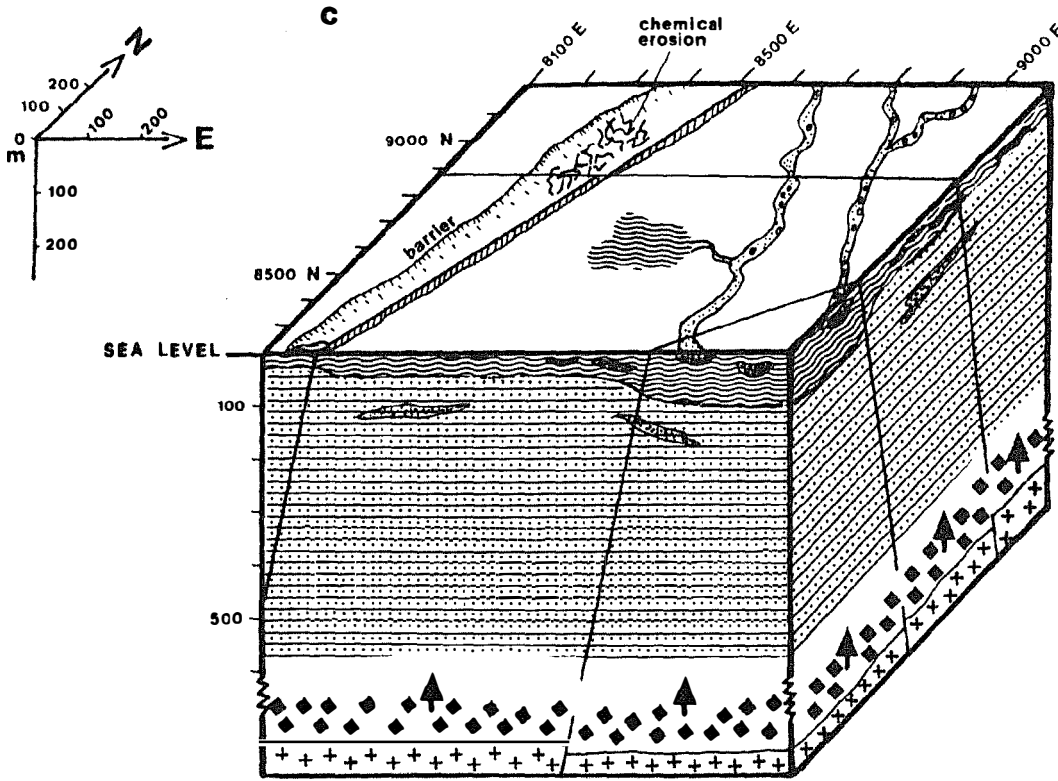


sabkha evaporites

hematite facies
channels and playa lakes
[red zone]

subaqueous evaporites

hematite-magnetite facies
intercalated dololutes
[black zone]

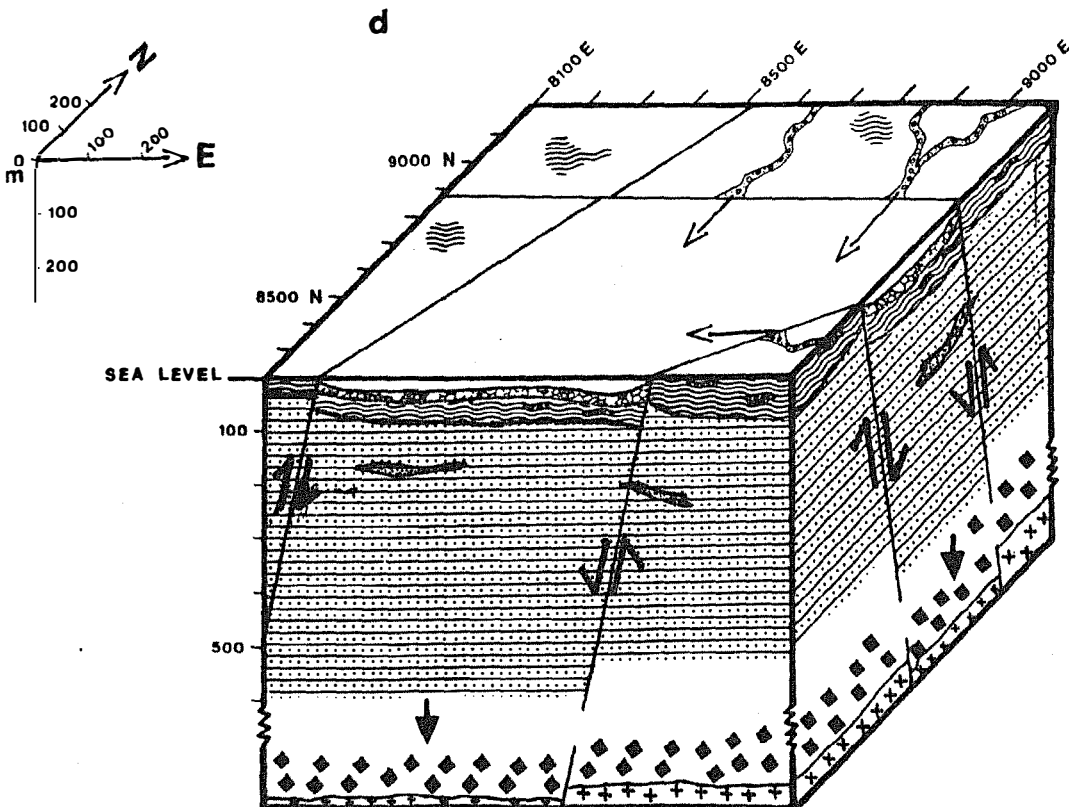


sabkha evaporites

hematite facies
intercalated coarse clastites
[red zone]

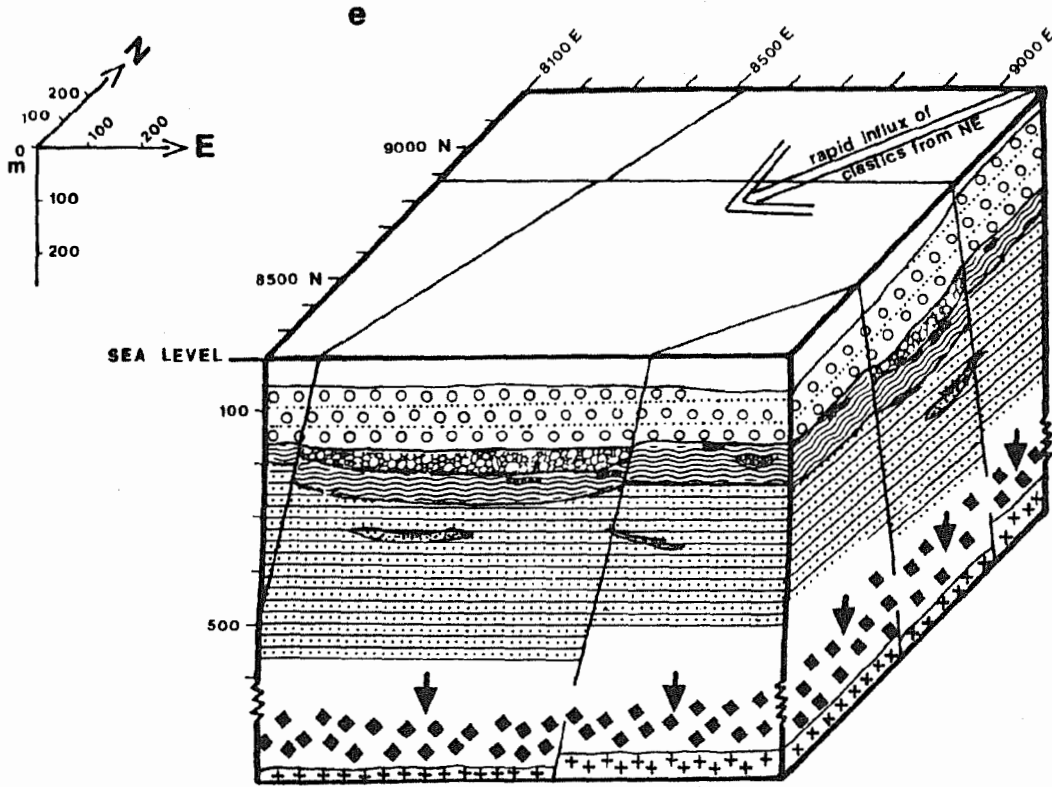
sabkha evaporites

hematite facies
channels and playa lakes
[red zone]



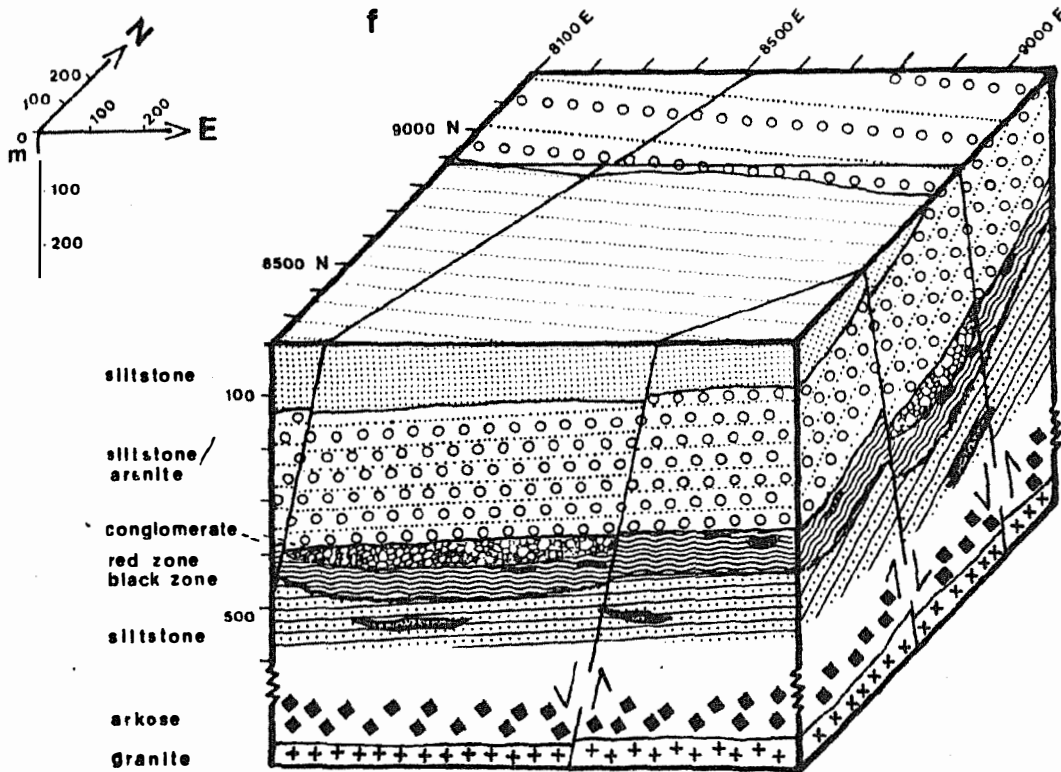
clastic wedges

coarse fluvial facies
plus sabkha detritus
carbonate matrix



turbidites

shallow water facies
dominantly coarse grained
Bouma cycles



Section 4 The Abra mineralization

4.1. Mineralogy of the Abra mineralization

4.1.1. Sulphides

4.1.1.1. Pyrite

Within the Abra mineralization two distinct groups of pyrite occur:

- conformable layers in the black and red zone, and minor conformable lenses in the stringer zone. This type is described in chapter 3.2.1.2.; the layers formed syndiagenetically and are unrelated to the mineralization.
- associated with veining (and minor disseminations) in all zones.

The vein-type pyrite clearly is related to the mineralization. Often pyrite is a minor component of the vein mineralization which mainly consists of galena and chalcopyrite. Pure pyrite veins (veinlets) are subordinate in number and preferably occur in the red zone.

Although pyrite is very abundant in the red (and black) zone as conformable bands the veins and veinlets generally have low pyrite content; veins in the stringer zone are probably most depleted in pyrite. Within the red zone pyrite occasionally is relatively enriched at the vein-wallrock contact.

Vein type pyrite often is corroded with an anhedral, porous appearance. It has abundant inclusions of hematite, minor galena and is intergrown with chalcopyrite and magnetite.

No pyrrhotite has been observed in the Abra mineralization, neither in veins nor in the conformable bands.

25 electron microprobe analyses of pyrite from Abra are shown in Tab. 4.01, representing conformable and vein-type pyrite.

Without considering variations in Fe and S content, the range of the trace elements is:

As	0 - 8000 ppm
Co	0 - ?
Ni	0 - 700 ppm

Arsenic contents of pyrites from Abra are up to one order of magnitude higher than those of pyrite (and pyrrhotite) from drill holes in the Jillawarra Belt further to the west (cf Tab. 1.04). However, some diagenetic pyrites (including "atoll pyrite") from black shales of the Jillawarra Formation generally have arsenic contents of up to 2.86 % (Tab. 1.04) which are distinctly higher than the Abra values.

Considering that diagenetic pyrite has a higher concentration of arsenic than Abra pyrite, and the relatively low overall variation (less than 3 % As) between pyrites from Abra, the Jillawarra Belt and the Jillawarra Formation, the arsenic content of pyrite probably is not diagnostic of the Abra type mineralization.

The Co/Ni ratio in pyrite is regarded as a reliable geochemical indicator for the genesis of sulphide deposits (Bralia et al., 1979). When plotted in a diagram several genetic fields according to the Co/Ni ratio can be distinguished (Fig. 4.01).

Due to the remarkable absence of cobalt (allowance is made for an analytical error of 0.01 % in Fig. 4.01) in all pyrites analysed the Abra data plot within the field of sedimentary and diagenetic pyrite and, to a lesser extent, in the field of Sn and Pb-Zn veins. The latter group probably can be excluded because the vein-type pyrites analysed have higher Ni-values.

Table 4.01: Electron microprobe analyses(wt %) of pyrites from the Abra mineralization

	Ab 7, 274 m red zone recrystall. py-layer	Ab 7, 274 m red zone recrystall. py-layer	Ab 4, 365 m black zone py-layer corase, anhedral	Ab 4, 365 m black zone py-layer finer, anhedral	Ab 9, 910 m stringer zone euhedral py vein type	Ab 4, 394 m black zone recrystall. py-layer	Ab 4, 372 m black zone recrystall. py-layer	Ab 4, 317 m (contact WC ₁ /WC ₂) mineralizing front in py clastites	Ab 3, 276 m red zone vein-type py
Fe	45,305	44,488	46,685	47,446	46,693	45,742	45,991	46,411	46,470
S	52,063	53,041	53,928	55,199	53,607	54,087	53,052	52,246	55,618
As	0,446	0,250	0,001	0,123	0,346	0,359	0,746	0,106	0,236
Co	0,0	0,0	0,0	0,0	0,0	0,0	0,0	0,0	0,0
Ni	0,021	0,0	0,011	0,002	0,035	0,07	0,0	0,021	0,049
total	97,836	97,779	100,625	102,769	100,681	100,258	99,762	98,783	102,273
Fe	46,735	46,617	46,910	45,028	46,310	45,344	45,612	46,527	46,338
S	53,151	53,731	54,685	51,445	53,773	53,483	53,117	52,004	55,316
As	0,345	0,274	0,0	0,037	0,037	0,308	0,798	0,079	0,064
Co	0,0	0,0	0,0	0,0	0,0	0,0	0,0	0,0	0,0
Ni	0,027	0,050	0,042	0,030	0,011	0,047	0,002	0,044	0,022
total	100,257	100,672	101,636	96,539	100,131	99,182	99,529	98,654	101,740
Fe	46,192		46,090		46,807		46,111		46,655
S	53,001		54,835		53,880		53,098		54,359
As	0,289		0,078		0,072		0,385		0,037
Co	0,0		0,0		0,0		0,0		0,0
Ni	0,0		0,008		0,015		0,003		0,062
total	99,482		101,011		100,774		99,597		101,113
Fe					46,955				
S					53,936				
As					0,0				
Co					0,0				
Ni					0,055				
total					100,946				

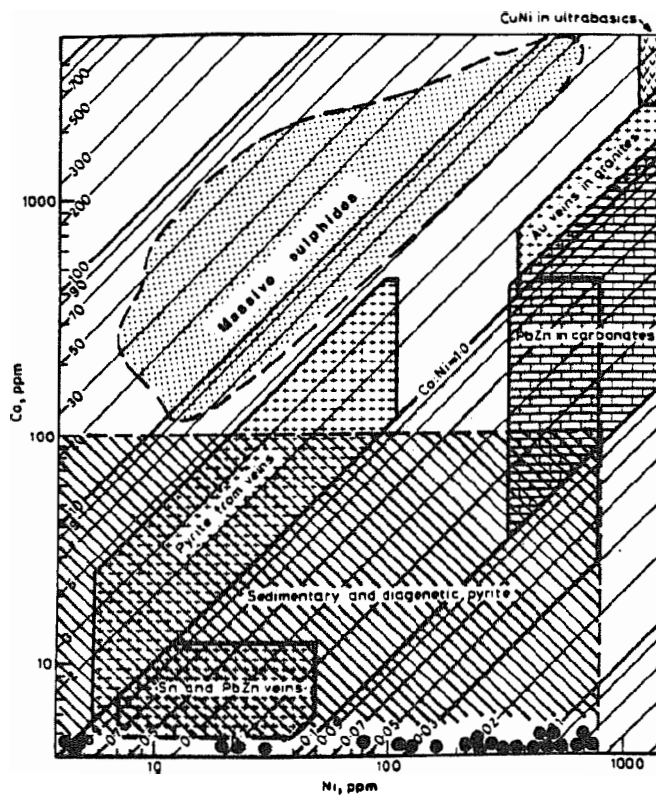


Fig. 4.01:

Average Co versus Ni plot of pyrite from various sulphide deposits, modified from Willan and Hall (1980). Data for massive sulphide deposits (mainly volcanogenic) according to Braila et al. (1979).

● Plot of Abra pyrites.

▨ allowance for an analytical error of 0.01% Co

Most of the Abra data plot into the field of sedimentary and diagenetic pyrite (even with an assumed Co content of 100 ppm). This applies to pyrites from conformable layers ("syndiagenetic pyrite") as well as to vein-type pyrites and suggests a genetic relationship.

In this context it is interesting to note that the sulphur isotopic data indicate that no major isotopic differences occur between vein-type base metal sulphides and conformable pyrite (see chapter 4.5.).

4.1.1.2. Galena

This is the most abundant sulphide mineral at Abra; the best drill core assay was 27 % Pb from 490 to 492 metres in Ab 9, which is equivalent to 31.2 % galena over two core metres.

It commonly occurs as anhedral masses or irregular streaks. The continuous drill core assays (one or two metres intervals were analysed for Pb, Cu, Zn, Ba, Ag, Au, Mn, for Geopeko) indicate a clear correlation of Pb with Ag. Moderate amounts of tetrahedrite have been found within galena crystals, and account for the silver content of whole rock analyses (2-50 ppm, but usually below 20 ppm).

Galena predominantly occurs in veins in the upper stringer zone and the black zone (see Fig. 4.10), but is ubiquitous in smaller amounts in the red zone, except Ab 3 where the maximum galena content is near the top of the red zone. In Ab 6 veinlets of galena-quartz-carbonate ascended up to 16 metres beyond the top of the red zone into the otherwise barren clastites of the WC₂-unit (Ab 6, 2.73 % Pb from 206 to 208 core metres).

Within the individual veinlets galena is variably associated with quartz, carbonate, barite, chlorite and pyrite. In places it is intergrown with albite, particularly where it occurs as disseminated grains in calcareous or clastic wall rock (Fig. 4.02).

Galena emplacement and albitization probably are contemporaneous; in places, areas of more than three square centimetres consist entirely of irregularly intergrown galena and albite.

In some of the low-grade mineralizations in the Jillawarra Belt (e.g. 46 - 40 prospect) galena occurs as thin layers, parallel to 001 within biotite, or is intimately intergrown with biotite. No biotite is present in Abra; this type of intergrowth has not been found with chlorite.



Fig. 4.02: Galena associated with albite and hyalophane.
Base of picture = 3.6 mm (+).

In the stringer zone galena is invariably associated with veining. In the black and red zones, in addition to veins, it is also common in the layered hematite/magnetite-quartz-carbonate-pyrite sediments without a recognizable affinity to veining. This may indicate a strataform (i.e. syndimentary) portion of galena mineralization and was examined in detail.

The non-vein-associated variety of galena in the black and red zones has two dominant modes of occurrence:

- 1) It is intimately intergrown with syndiagenetic pyrite layers (Fig. 4.03). The pyrite itself is recrystallized to larger grains. Galena fills interstices, or fissures within pyrite. Emplacement of galena probably is related to the recrystallization of pyrite as pyrite layers without galena usually consist of finely crystalline pyrite (cf Fig. 3.21). Minor chalcopyrite also occurs.

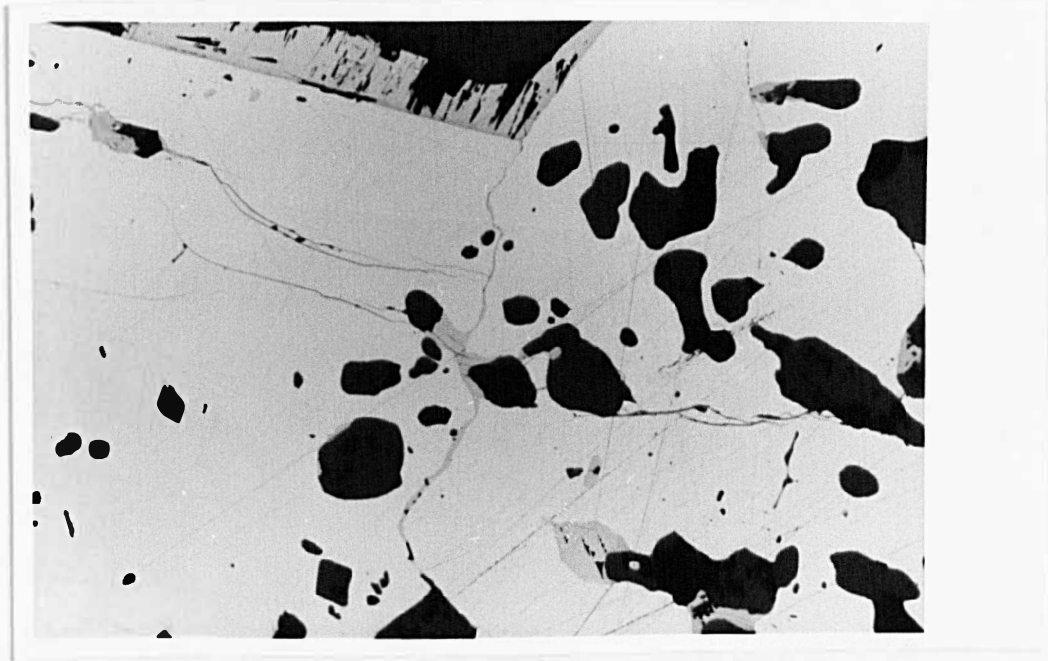


Fig. 4.03: Galena on fissures in recrystallized pyrite.
Base of picture = 2.3 mm, reflected light (-).

Replacement of pyrite by galena has been observed in some cases and is evident from Fig. 4.04. Textural evidence for replacement of sulphides often is equivocal, but here it is obvious that galena is a later phase surrounding pyrite, while pyrite itself has been corroded. This mechanism is plausible in this case, despite Ramdohr's (1975) conclusion that mainly pyrite is the replacing mineral, due to its high crystallization power.

Complete replacement of pyrite by galena may substitute all sulphur bound to iron and result in a magnetite-galena layer as shown in Fig. 4.05.

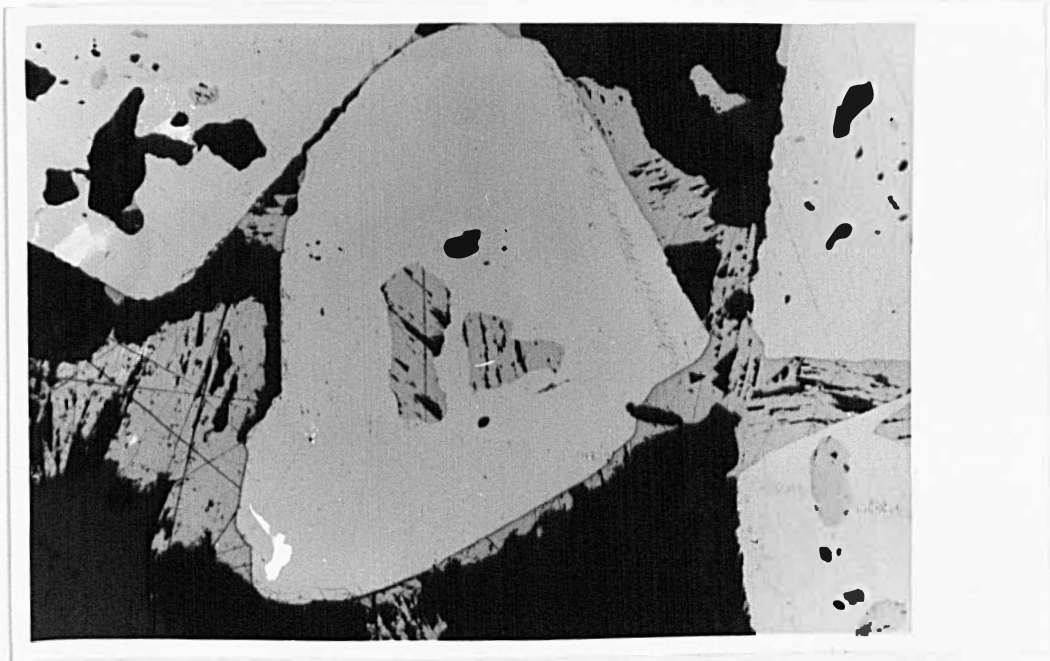


Fig. 4.04: Galena in, and as rims around, pyrite.
Base of picture = 2.3 mm, reflected light (-).

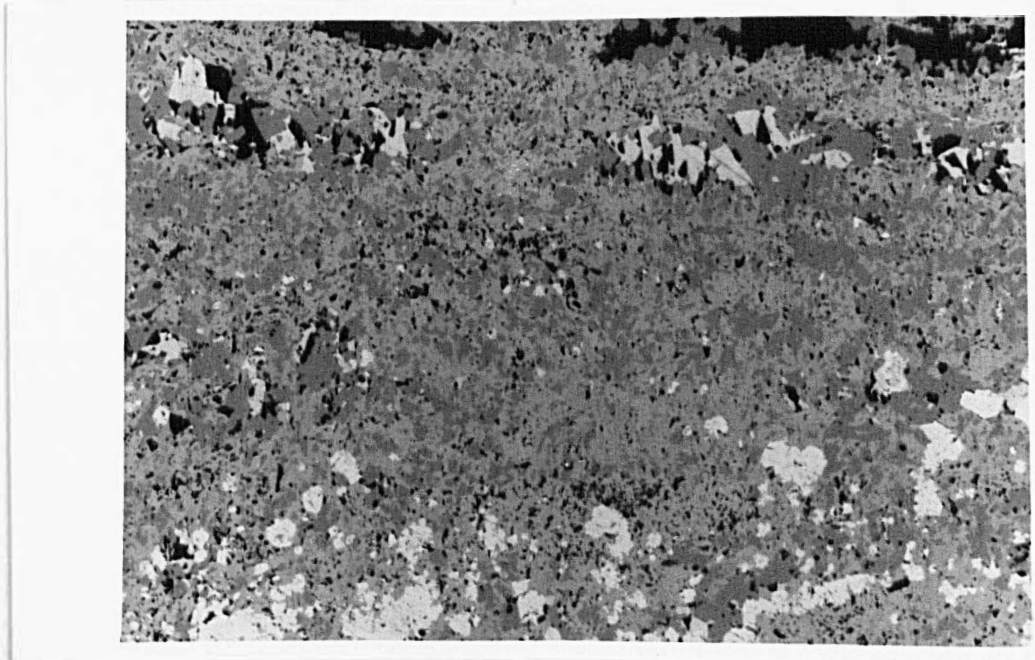


Fig. 4.05: Band of galena-magnetite intergrowth in a hematite-
magnetite-pyrite layer. Base of picture = 2.3 mm,
reflected light (-).

II) Galena occurs as anhedral masses or streaks within jaspilitic quartz bands between magnetite/hematite-pyrite layers. In places it is intergrown with hematite (Fig. 4.06). The association with hematite, jaspilite or with magnetite rules out sedimentary conditions where galena could precipitate. The environment has been oxidizing and any HS^- or H_2S would have been oxidized to sulphate.

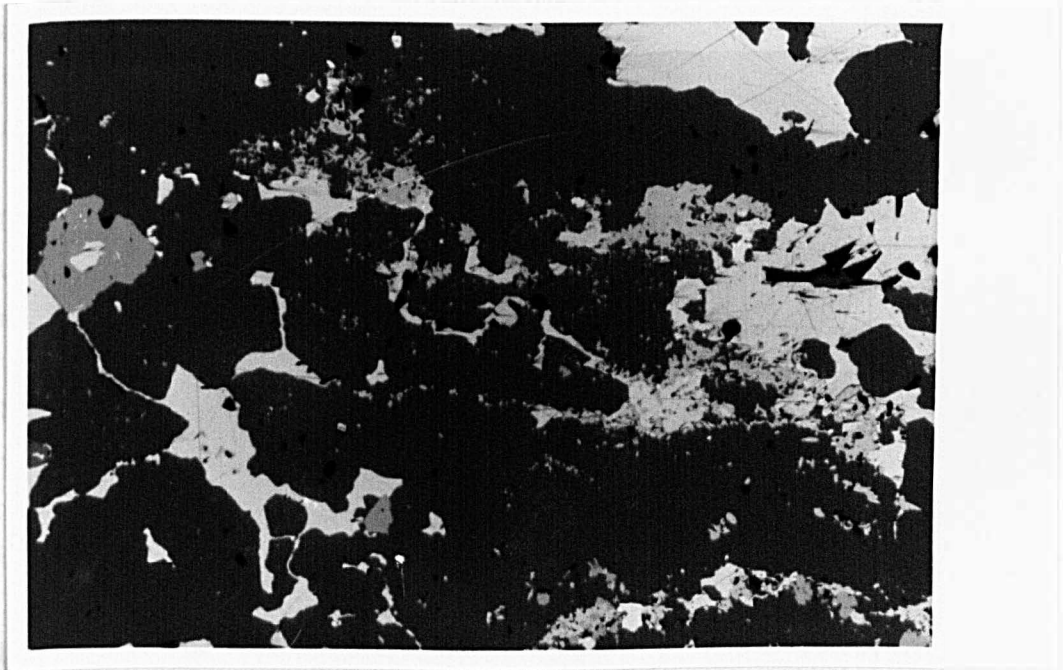


Fig. 4.06: Galena intergrowth with hematite (right) and magnetite (left) in quartz between magnetite-hematite layers. Base of picture = 2.3 mm, reflected light (-).

The strataform galena (subordinate to the amount of vein-related galena) was emplaced after deposition of the host sediments by replacement of pyrite and by scavenging of free sulphide from bacterial sulphate reduction, which was trapped in the sediment.

4.1.1.3. Chalcopyrite

This is the only copper-sulphide (except one bournonite occurrence, see chapter 4.1.1.5.) and it is dominantly present in the lower stringer zone, but ubiquitous in trace amounts within the entire mineralized body. The abundance of copper is roughly 1/5 that of lead, and in drill cores chalcopyrite content rarely exceeds 4 % (extreme values are above 15 % chalcopyrite).

Copper correlates with gold in the continuous drill core assays but no free gold has been found during examination of chalcopyrite in polished sections from the interval of highest gold mineralization (Ab 3, 506-512 metres, averaging 6.9 ppm Au).

Chalcopyrite invariably occurs as anhedral grains or masses in veins or mineralized breccias. Fig. 4.07 shows a typical chalcopyrite vein from the stringer zone.

It is usually associated with carbonate, quartz and magnetite/hematite in the stringer zone whereas in the uppermost stringer zone and black zone it may be concurrent with barite and pyrite, in addition to carbonate, quartz, magnetite/hematite.

In the stringer zone, chalcopyrite commonly is intergrown with magnetite, has inclusions of magnetite, or occurs as inclusions in magnetite (Fig. 4.08).

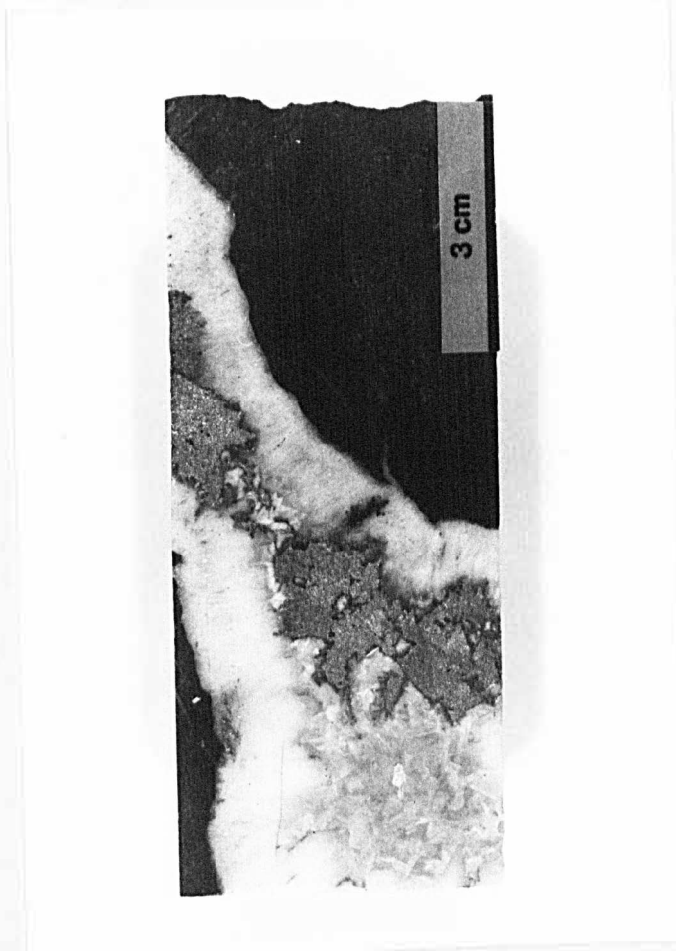


Fig. 4.07: Core specimen from the stringer zone with chalcopryrite - carbonate - quartz vein.

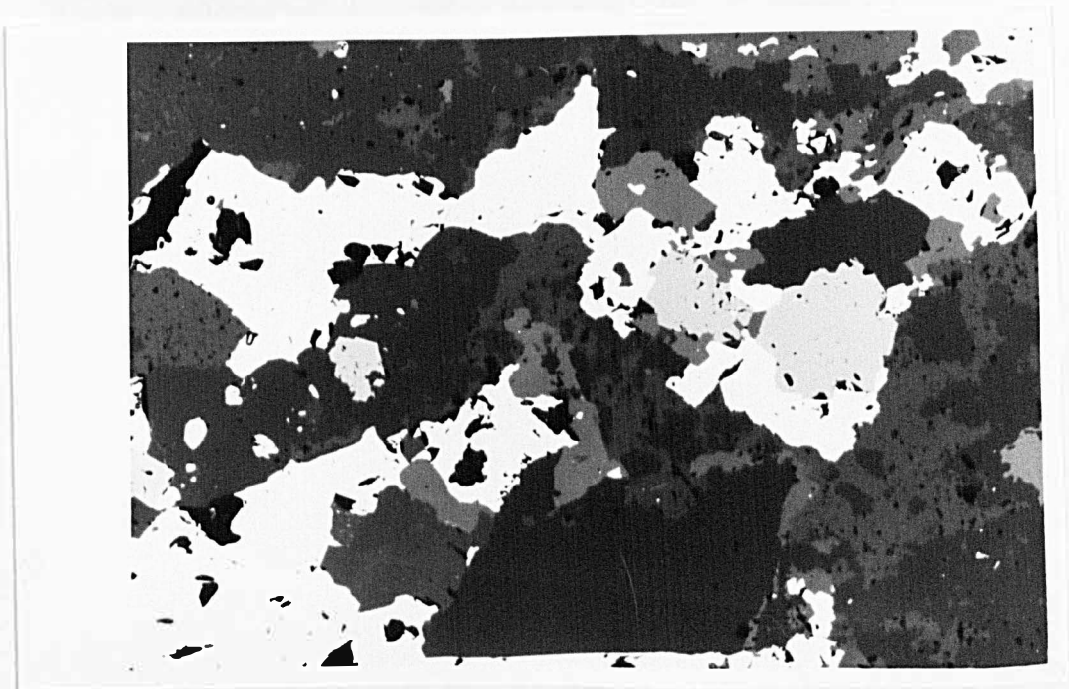


Fig. 4.08: Chalcopryrite-magnetite intergrowth in quartz and carbonate. Base of picture = 2.3 mm, reflected light (-).

Hematite usually is present at the margins of chalcopyrite veins. Coexistence of chalcopyrite and iron-oxides places constraints on the temperature of sulphide formation, and on f_{S_2} , because iron-oxides formed instead of iron-sulphides. This is discussed in chapter 4.4.

In the layered portions of the black and red zones chalcopyrite is a minor constituent and is closely associated with galena. It may also be a replacement of pyrite as shown for galena in Fig. 4.04. The close spatial association of galena and chalcopyrite in the "strataform" mineralization suggests that both have presumably been emplaced by one ore forming event. In a syngenetic exhalative type of mineralization it is unlikely however, that galena and chalcopyrite would co-precipitate (Barnes, 1975; Solomon and Walshe, 1979). Therefore, the coexistence of galena and chalcopyrite can be considered as further evidence against exhalative ore formation and instead, indicates precipitation from metal bearing solutions containing both copper and galena, which percolated the diagenetic sediments and crystallized as sulphides where they encountered free H_2S , or where they replaced pyrite. It thus appears that, within the black and red zones (i.e. on a comparatively small scale), metal sulphide precipitation was rather governed by H_2S -availability than by physico-chemical gradients (e.g. temperature, salinity, pH etc.).

4.1.1.4. Sphalerite

This is a minor sulphide mineral, usually present in trace amounts ($\leq 1\%$) throughout most of the mineralized body. In the upper stringer zone slightly higher concentrations are encountered (up to 3.4 % Zn from 434 to 438 m in Ab 4), but this is exceptional.

Sphalerite occurs as anhedral grains commonly associated with carbonate, quartz and galena. It is of bright yellow-brown colours.

Fourteen sphalerite grains have been analysed by electron microprobe (Tab. 4.02).

Iron content of sphalerite, ranging from 0.25 % to 1.18 % Fe (0.39 % to 1.86 % FeS, respectively) is very low when compared with Mt. Isa (4 - 8 % Fe; Finlow-Bates, 1978), Gamsberg, S.A. (2 - 10 % Fe; Stumpfl, 1979) or a zinc-lead mineralization in Scotland (mean of 8.8 % Fe; Willan and Hall, 1980). Manganese contents below 0.5 % also are very low in contrast to up to 8 % Mn in sphalerites from Gamsberg (Stumpfl, *op.cit.*).

Geothermometry or geobarometry using the Fe-content of sphalerite was not attempted as Stumpfl (*op.cit.*) has demonstrated that no relationship between sphalerite compositions and metamorphic temperatures or pressures does exist.

Table 4.02. Electron microprobe analyses (wt.%) of sphalerites from the Abra mineralization

	Abra 4, 393.5 m black zone	Abra 4, 317.4 m top red z.	Abra 3, 509.6 m stringer z.	Abra 3, 360.4 m stringer z.	Abra 3, 275.9 m red zone
Fe	0.329	0.750	1.070	0.500	0.252
Cu	0.000	0.030	0.657	1.065	0.052
S	34.913	33.600	31.541	33.136	34.540
Zn	66.674	66.416	65.450	67.862	65.940
Cd	0.000	0.094	0.000	0.106	0.340
Mn	0.000	0.000	0.048	0.000	0.011
In	0.000	0.007	0.299	0.081	0.132
Total	101.916	100.898	99.064	102.750	101.267
Fe	0.335	0.703	1.178	1.134	0.261
Cu	0.092	0.075	0.670	0.954	0.085
S	34.178	33.910	32.153	33.244	34.910
Zn	66.570	66.661	65.351	67.058	65.765
Cd	0.000	0.000	0.000	0.120	0.000
Mn	0.000	0.000	0.000	0.026	0.000
In	0.306	0.000	0.270	0.315	0.063
Total	101.481	101.348	99.622	102.851	101.084
Fe	0.373	0.752			
Cu	0.058	0.000			
S	33.519	32.948			
Zn	66.531	66.960			
Cd	0.253	0.132			
Mn	0.000	0.000			
In	0.000	0.000			
Total	100.733	100.792			
Fe	0.412	1.014			
Cu	0.038	0.000			
S	33.931	33.714			
Zn	66.669	66.782			
Cd	0.065	0.171			
Mn	0.000	0.000			
In	0.000	0.000			
Total	100.116	101.681			

4.1.1.5. Sulphosalts

Only minor amounts of tetrahedrite and bournonite have been found in the Abra mineralization. Bournonite occurs exclusively, and tetrahedrite is most abundant, at the contact between the WC₁- and WC₂-units in hole Ab 4 (317.4 m). Within the uppermost coarse-grained siliceous arenite (Fig. 4.09) of the WC₁-unit two bands of sulphides occur, overlain by micaceous shale of the WC₂-unit. The upper sulphide band is composed of pyrite whereas the lower band consists of galena-tetrahedrite-bournonite-chalcocopyrite intergrowth.

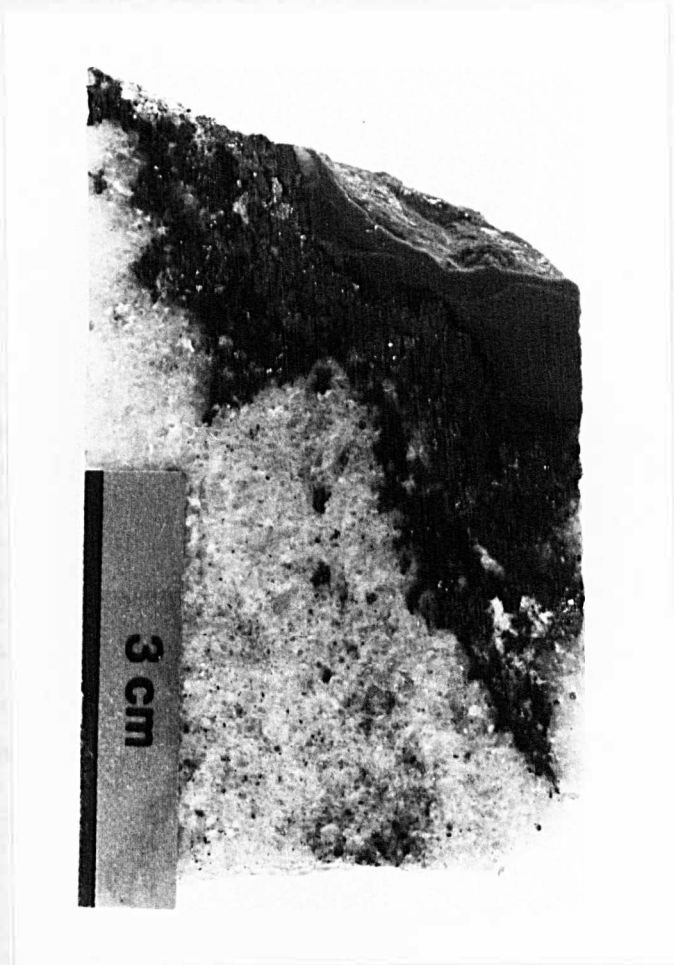


Fig. 4.09: A band of pyrite underlain by a black zone of sulphosalts, galena and chalcocopyrite at the contact between coarse-grained arenite (WC₁) and micaceous shale (WC₂).

The formula of bournonite as determined by electron microprobe is $Sb_{1.01}Pb_{1.02}Cu_{0.83}S_3$ with traces of Bi, Ag and As.

Chalcopyrite from this section contains 0.84 % Ag and 0.667 % Pb by weight, and traces of Sb, contrasting to pure chalcopyrite elsewhere in Abra. These impurities of chalcopyrite in the vicinity of bournonite suggest a genetic relationship.

Tetrahedrite occurs within, or as rims surrounding galena (this is the common association in the entire Abra mineralization). Table 4.03 shows the results of electron microprobe analyses of tetrahedrite from the sample of Figure 4.09 and other samples of stratigraphically lower levels in Abra.

Table 4.03. Selected electron microprobe analyses of Abra tetrahedrite. Values in weight %.

sample description	Cu	Ag	Fe	Zn	Sb	As	Pb	Bi	S	total	formula
Ab 4, 317.4 m contact WC ₁ /WC ₂ see Figure	34.74	8.69	1.61	2.57	25.54	0.40	0.21	-	23.85	97.67	$Cu_{9.57}Ag_{1.41}Fe_{0.50}Zn_{0.69}Sb_{3.67}As_{0.09}S_{13}$
	34.40	7.63	1.65	2.27	27.59	0.27	0.48	0.32	23.85	98.47	$Cu_{9.46}Ag_{1.24}Fe_{0.52}Zn_{0.61}Sb_{3.96}As_{0.06}S_{13}$
	29.47	11.66	1.49	3.20	27.15	0.44	-	-	23.16	96.53	$Cu_{8.33}Ag_{1.94}Fe_{0.48}Zn_{0.88}Sb_{4.01}As_{0.11}S_{13}$
Ab 7, 274 m lower red zone, with galena and chalcopyrite on fractures in recrystallized pyrite	41.75	1.06	5.79	0.79	22.49	1.60	0.17	-	26.10	99.76	$Cu_{10.50}Ag_{0.16}Fe_{1.66}Zn_{0.19}Sb_{2.95}As_{0.34}S_{13}$
	41.53	1.38	5.86	0.72	23.07	1.89	0.17	0.07	26.33	101.02	$Cu_{10.35}Ag_{0.20}Fe_{1.66}Zn_{0.17}Sb_{3.39}As_{0.40}S_{13}$
	41.40	1.02	6.24	0.73	24.50	1.65	0.24	-	25.30	101.08	$Cu_{10.73}Ag_{0.16}Fe_{1.84}Zn_{0.18}Sb_{3.72}As_{0.36}S_{13}$
Ab 6, 328 m stringer zone, galena-barite- chalcopyrite vein	41.28	1.58	1.14	2.72	28.35	0.85	0.15	-	24.78	100.85	$Cu_{10.93}Ag_{0.25}Fe_{0.34}Zn_{0.70}Sb_{3.92}As_{0.19}S_{13}$

The tetrahedrites from lower levels have significantly lower Ag but higher Cu contents than those from the WC₁/WC₂ contact. Riley (1974) reported that tetrahedrites from a chalcopyrite-quartz vein in the Cu-orebody of Mt. Isa have lower Ag/higher Cu values than those from the stratiform mineralization. This relationship may indicate higher Ag contents in more distal mineralizations, if the copper mineralization at Mt. Isa is accepted as the proximal mineralization to the contemporaneous distal lead-zinc mineralization (Finlow-Bates and Stumpfl, 1979).

Tetrahedrite in the sample shown in Fig. 4.09 certainly represents distal mineralization in Abra and has high Ag content, and thereby suggests a principally analogous situation as in Mt. Isa.

The mode of emplacement of the distal sulphosalts in Abra, however, was different. The impermeable shale band overlying the sulphosalts and sulphides, and the coexistence of complex sulphosalts and sulphides (tetrahedrite, bournonite, galena, chalcopyrite, pyrite) which occur separately elsewhere, implies ascent of metal bearing fluids up to the shale barrier. Here some H₂S may have been trapped and the metals precipitated rapidly. Non-equilibrium precipitation is indicated by the impurities of chalcopyrite and the Cu-deficiency of bournonite (see formula).

4.1.2. Sulphates

The only sulphate in Abra is barite occurring a) in veins in the upper stringer zone and the black and red zones, b) as large (more than 4 centimetres length) euhedral crystals in the red zone, c) as layers or clusters of crystals, d) as anhedral masses throughout the black and red zones and e) in massive form (in places over several core metres) in the red zone.

Barite is most abundant in the upper red zone (see chapter 4.2.) where it constitutes a "barium body" of 25 mt at 20 % Ba.

Textural features and the mode of occurrence are described in chapters 3.2.1.2. and 3.2.1.3. while the possible quantitative replacement of Ca-sulphates by barite (in particular in the sabkha sediments of the red zone) is discussed in chapter 3.2.1.4.

Here, the chemistry of the barites is discussed briefly. 21 barites from the Abra mineralization and the low-grade mineralizations in the Jillawarra Belt have been analysed for Sr by electron microprobe.

The Sr content is remarkably uniform throughout, varying between 0.029 and 0.72 % (by weight) strontium in barite. There is no trend linking Sr content with stratigraphy or mode of occurrence; Sr contents in barites from the red and black zones in Abra vary in the same range as in different vein-type barites within or outside Abra. This invariable range of Sr content in barites suggests a common source, and common mode of emplacement of all barites.

If, for example, barite was a primary sulphate mineral in the sabkha deposits of the red zone in Abra it should display higher Sr values than vein-type barite, because Sr is enriched in evaporitic sequences (Morrow et al., 1978), and, barite forms a continuous solid solution with celestine (Dear et al., 1972);

a more detailed discussion is given in chapter 3.2.1.4.

Puchelt (1967) has noted that there is a distinctive geochemical difference between submarine exhalative barite and so-called magmatic-hydrothermal (epigenetic vein-type) barite. The former is characterized by a low Sr content (0.3 - 1.5 %), whereas the latter usually contains more Sr (greater than 1 % and often exceeding 1.5 %). However, the vein-type barites in Abra have Sr values clearly below the range given by Puchelt. Furthermore, marine barites without any relation to hydrothermal activity exhibit a range of 0.3 - 1.9 % Sr (Church, 1979), suggesting that the Sr content in barite is not diagnostic of the kind of hydrothermal activity.

4.1.3. Oxides

4.1.3.1. Fe-oxides

Hematite and magnetite are the main Fe-oxides in the Abra mineralization and in the sediments of the upper Gap Well Formation, with the exception of insignificant amounts of detrital ilmenite and chromite. Due to the omnipresence of magnetite in the Abra mineralization geo-magnetics have proved a reliable tool in the search for Abra-type mineralization. The Abra mineralization itself has originally been detected by magnetics.

Syndiagenetic (sedimentary) iron-oxide layers occur in siltstones of the GW₅-unit (Fig. 4.26) and the GW₆-unit (Fig. 2.36) in the Jillawarra Belt. but are most abundant in the black and red zones in Abra. Magnetite and hematite are commonly intergrown and form delicate layers of 0.1 - 3 mm thickness. Hematite is more abundant in the red zone, suggesting fully oxidizing depositional conditions. In the black zone hematite is ubiquitous, but subordinate to, or equally abundant with, magnetite. A discussion of the iron oxides layers of the black and red zone is given in chapter 3.2.1.2. and 3.2.1.3. They are interpreted as evaporitic iron formations.

Vein-type iron-oxides are present in almost all veins of the Abra mineralization and of mineralizations in the Jillawarra Belt. Magnetite usually is intergrown with hematite, but in places hematite is concentrated along the vein margins. In the lower part of the stringer zone hematite is rare, locally it stems from martitization of magnetite.

Further occurrences of iron-oxides are a) jaspilite (particularly in the red zone) associated with veining, or as layers, thus being present in two modes like the hematite/magnetite described above, b) very few detrital ilmenite grains along the foresets of cross-bedding in the WC₁-unit (Ab 10, 489,5 m). The detrital grains are

unrelated to the Abra mineralization and may indicate the provenance of the clastites.

25 electron microprobe analyses (TiO_2 , MnO , FeO) have been performed on magnetites, hematites and jaspilites of sedimentary and vein-type association. No significant difference in the proportions of Ti and Mn between magnetite, hematite and jaspilite occurs, and in the following discussion these three minerals are summarized as Fe-oxides.

TiO_2 content in Fe-oxides varies between ≤ 0.005 and 0.52 wt. %, and that of MnO between ≤ 0.005 and 0.27 wt. %. There is no trend in the MnO or TiO_2 content towards sedimentary or vein-type Fe-oxides. Within both groups the entire spread of TiO_2 or MnO values is realized, i.e. the sedimentary and vein-type Fe-oxides are identical with respect to these elements.

Eichler (1976) found insignificant amounts of major elements only in comparative chemical analyses of iron formations from different sedimentary facies (e.g. oxide facies, carbonate facies, etc.). The manganese content of whole rock analyses is below 1 wt. % in most cases, as well as that of Ti and Mg (4.2 % in silicate facies).

In particular, the oxide facies of many iron formations examined (the Abra black zone represents oxide facies) is characterized by trace amounts only of elements others than Fe and Si. Therefore, Eichler (1976) concluded that the chemistry of oxide facies iron formations (especially hematitic) is governed by a general chemical (or biochemical) precipitation process and cannot be explained by local environmental conditions only.

The question, whether the black (and red) zone iron formation represents the sedimentary-exhalative facies to the stringer zone hydrothermal system, cannot be resolved by Fe-oxide chemistry.

The work of Eichler (1976) suggests that the chemistry of Fe-oxides does not allow a distinction between exhalative iron formations and those which precipitated from weathering solutions. However, the onset of hydrothermal ("exhalative") activity in Abra has been post-deposition of the black and red zones; this is concluded from the development of the Abra sub-basin (chapter 3.4.) and the replacement-barite (chapter 3.2.1.4.). Therefore, it is likely that not exhalation of iron-bearing solution accounted for the black (and red) zone sediments but precipitation from weathering solution in a restricted, littoral basin. Furthermore, exhalation of ferruginous hydrothermal solution resulting in banded iron formation with a lateral persistence of more than 0.7 km² seems unlikely in the sabkha environment of the red zone where no permanent water cover was present. Vein-type iron-oxides in the stringer zone are probably derived from the same source (because iron-bearing solutions have also been transported into the Jillawarra Basin during times of deposition of these sediments) and were concentrated into veins when hydrothermal activity commenced.

4.1.3.2. Scheelite

Scheelite has been found in minor amounts in the Abra mineralization. Preferentially, it occurs in veins and disseminated in the upper stringer zone, but minor disseminated grains are present in the black zone and the red zone. In the black zone it is intergrown with barite to form a scheelite-barite-quartz aggregate (Fig. 3.15). Whole rock analyses of intervals of one core metre yield maximum tungsten values in the range of 500 ppm (in Ab 6) in the upper stringer zone, in clearly sub-economic concentrations.

The common association of scheelite with veining and its concentration in the stringer zone indicate a post-sedimentary emplacement of scheelite, related to the hydrothermal system.

4.1.4. Carbonates

Carbonates are ubiquitous throughout the Abra mineralization. The textures of carbonate in the various zones in Abra are described in chapter 3.2.1., and its common replacement by silica in chapters 3.2.1., 2.3.1. and 2.3.2.3.

In addition to the carbonate of sedimentary association, vein-type carbonate is also common. It occurs as large anhedral crystals (up to 5 mm) within the veins and variably is associated or intergrown with all sulphide minerals, barite, chlorite, iron oxides and quartz.

35 electron microprobe analyses (Fe, Mn, Mg, Ca, Ba, Sr) of carbonates of various settings revealed that all are ferruginous. However, only one true siderite has been found in a vein at the Copper Chert prospect (i.e. outside Abra) and will not be considered. Ba and Sr values are below 0.05 wt.%, and only Fe, Mn, Mg and Ca are discussed here.

The carbonates in Abra comprise two groups with respect to chemistry (Tab. 4.04):

- Carbonate of sedimentary association, occurring as conformable bands between iron-oxide layers without a recognizable affinity to veining. This group is rich in iron and low in calcium, and can be micritic.
- Vein-type carbonates, plus recrystallized or mobilized carbonate which is sparitic, in places occurring as euhedral rhombs within quartz. There is no significant textural difference between recrystallized and vein-type carbonate. This group can be termed ferroan dolomite.

In view of the ferruginous nature of all carbonates, in Tab. 4.04 the weight ratios of Mn, Mg and Ca are calculated with respect to Fe.

Table 4.04: Weight ratios of Mn, Mg and Ca with respect to Fe of representative carbonates from the Abra mineralization.

	Fe	Mn	Mg	Ca
a) Sedimentary carbonate				
Ab 5, 409 metres	1	0.30	0.31	0.00
micritic	1	0.20	0.29	0.00
Ab 4, 394 metres	1	0.14	0.38	0.00
micritic and sparitic	1	0.14	0.28	0.00
b) Vein-type carbonate				
Ab 4, 433 metres	1	0.21	1.58	2.69
large, anhedral	1	0.45	2.80	4.50
Ab 6, 304 metres	1	0.66	2.03	3.60
large, anhedral	1	0.47	1.70	3.01
recrystallized				
Ab 5, 409 metres	1	0.40	1.41	2.56
sparitic, acicular	1	0.40	1.82	3.06
mobilized				
Ab 4, 394 metres	1	0.69	1.96	3.12
sparitic, euhedral	1	0.29	1.49	2.43

It is evident from the ratios in Table 4.04 that sedimentary carbonate in the black zone is extremely rich in iron, which is compatible with sedimentation in connection with iron formation.

Vein-type and recrystallized/mobilized carbonate have similar compositions (which, however, is unique), suggesting that vein-type carbonate is derived from the same sedimentary pile as the recrystallized/mobilized carbonate; i.e. vein-type carbonate may represent carbonate that is recrystallized and mobilized over longer distances.

The difference between sedimentary and recrystallized carbonate is mainly due to the Ca-content (sedimentary carbonate may also be richer in Mn), and the ratios in Tab. 4.04 delude an additional difference with respect to the Mg content. But the absolute values of Mg in both sedimentary and recrystallized carbonate vary only between 13 and 16 wt. % MgO. In places (e.g. Ab 5, 409 m, see Tab. 4.04) recrystallized carbonate occurs adjacent to micritic sedimentary carbonate, and it is likely that the sparite crystallized from the micrite. Possibly, the Ca which is incorporated during recrystallization may stem from replacement of Ca-sulphates by barite (cf chapter 3.2.1.4.), releasing some two million tons of calcium in the black and red zones. However, the mechanism proposed could be valid in these zones only, and does not explain the composition of vein-type carbonate in the stringer zone unless a huge convective system is invoked.

4.1.5. Silicates

4.1.5.1. Chlorite

Chlorite is the dominant phyllosilicate, in addition to muscovite, in the Abra mineralization whereas outside the Abra area biotite has been found in the GW₅ and GW₆-units, i.e. at a comparable stratigraphic level.

Chlorite is ubiquitous in the Abra mineralization; it occurs as finely-crystalline aggregates (up to 2 mm across) in the black and red zones or dispersed in the clastites of the stringer zone. It usually shows grass-green colours, and purple to brownish birefringence colours.

Several textural settings of chlorite have been recognized:

- Vein-chlorite; occurring within, or marginal to, veins; commonly associated with quartz, carbonate or sulphides
- Wallrock chlorite; no affinity to veining, dispersed in the stringer zone and as larger aggregates in the black and red zones; commonly associated with carbonate and quartz
- Replacement chlorite; chloritization of muscovite and potash feldspars within clastic wallrock. Chloritization of detrital potash feldspar is inferred from the occurrence of sub-rounded to sub-angular chloritic "clasts" in a quartz sandstone. Some 0.5 metres below this rock (in Ab 4, 398 m) a texturally similar arkose occurs.
- Replacement chlorite; chloritization of calcareous pellets in the upper red zone. There are partly chloritized calcareous pellets in the same thin section.

Tab. 4.05: Representative electron microprobe analyses of chlorite (wt %) at Abra.

	vein chlorite	wall rock chlorite	replacement chlorite(of potash feldspar)	replacement chlorite(of carbonate pellet)
Si	28.273	26.927	26.440	25.525
Ti	0.000	0.121	0.069	0.048
Al	16.740	19.412	18.182	20.591
Fe	32.569	29.397	30.111	35.023
Mg	13.701	15.421	14.814	12.159
Ca	0.000	0.008	0.027	0.069
Na	0.089	0.048	0.072	0.077
K	0.036	0.000	0.000	0.000
Mn	0.035	0.230	0.166	0.362
Total	91.444	91.564	89.882	93.854
<u>Fe</u>	0.570	0.520	0.530	0.620
Fe+Mg				

In Table 4.05 four representative electron microprobe analyses (from a total number of 25 analyses) of these distinct textural types of chlorite are presented. There is little difference between these groups indicating a common process of chlorite formation. This process was governed by the hydrothermal system at Abra because vein chlorite, which clearly is a product of the hydrothermal system, has only minor deviation from the chemistry of the wall rock chlorites (including potash feldspar - and muscovite-replacing chlorite).

The chemical differences between vein chlorite and wall rock chlorite are mainly due to higher Al and Mg contents of the latter. The change

in Mg content may indicate a reaction of the hydrothermal, iron-rich fluids (vein chlorite is rich in iron) with (ferroan) dolomite in the wall rock resulting in chlorite with higher Mg content.

Replacement chlorite of carbonate pellets has a higher Fe-content than other chlorite, which is compatible with the assumption of very iron-rich sedimentary carbonate in the black and red zones (see previous chapter); and it emphasises the control of wall rock-chemistry on the composition of chlorites.

It is inferred from the above discussion that chlorite generation was governed by the hydrothermal fluids, and that there is no indication of chlorite growth in relation to regional metamorphism. Chlorite has formed syn-hydrothermal and only small amounts of chlorite may have grown later (e.g. a thin seam of chlorite around a subhedral galena grain).

4.1.5.2. Feldspar

Three authigenic feldspar varieties have been found in Abra, in addition to the detrital potash feldspar, and are listed in decreasing order of abundance:

- 1) Albite; some 20 electron microprobe analyses confirmed that it is pure albite ($< \text{An}_2$). Albite is widespread, and commonly intergrown with sulphide minerals (Fig. 4.02) or barite suggesting that albitization is linked to the mineralization. Albite is present in all zones in Abra, but dominantly in the wall rock; i.e. it does not occur in spatial relation to veining. Albitization in relation to hydrothermal processes is not uncommon, and has been reported from the Sullivan, B.C., lead-zinc deposit (Ethier et al., 1976).
- 2) Barium feldspar; mainly hyalophane which can be considered as a mixture of celsian ($\text{BaAl}_2\text{Si}_2\text{O}_8$) and potassium feldspar (Deer et al., 1972). Hyalophane is a minor mineral (present in all zones in Abra), commonly in intimate contact with sulphide

minerals, in places actually surrounding sulphides. No hyalophane has been found in veins. It usually occurs adjacent to disseminated sulphide mineralization in clastic wall rock but it is also present in small amounts within micritic, sedimentary carbonate of the black zone, where it is not associated with sulphides. The formation of barium-bearing feldspar is obviously related to hydrothermal processes, considering the abundance of barium in the Abra hydrothermal system. It can be assumed that the formation of hyalophane and albite was governed by a common process involving percolation of hydrothermal fluids through the wall rock and crystallization of albite or hyalophane as a function of the chemistry of the hydrothermal fluid in relation to that of the formation water, at the site of crystallization (notably, both feldspar varieties only occur in the wall rock).

According to Deer et al. (1972) barium feldspars have a very restricted paragenesis and most of them occur in association with manganese deposits. Interestingly, hyalophane and other barium-bearing feldspars have been described from lenses and streaks in acid gneiss at Broken Hill, N.S.W. (Segnit, 1946).

- 3) Potassium feldspar; this has only been found as seams to detrital potash feldspar (see Fig. 3.11). In the GW_6 -unit of the Jillawarra Belt complete authigenic, euhedral potash feldspar occur in calcareous rocks, and this has been interpreted as in situ formation of K-feldspar due to hypersaline formation waters (see chapter 2.3.1.6.) according to a process suggesting by Tröger (1969). Possibly, the authigenic seams of K-feldspar in Abra (around detrital feldspars in the uppermost stringer zone) have formed by hypersaline diagenetic solution which stem from the overlying evaporitic interval and have penetrated the underlying clastites. Evaporitic solutions have a high density.

Of the three feldspars described above, albite and hyalophane formation was closely linked to hydrothermal processes affecting the wall rock. These processes mainly involved percolation of hydrothermal fluids but may also, thereby, have increased the temperature (convective) to enable crystallization of these feldspars.

The growth of authigenic potassium feldspar probably was unrelated to hydrothermal processes but was due to hypersaline formation waters during diagenesis.

4.1.5.3. Quartz

This is the most common, most widespread and most abundant mineral of the Abra mineralization. It occurs as vein filling, cement, layers in the black and red zones, and as replacement of sulphates, carbonates and of the matrix of clastites.

Silification, probably related to the Abra mineralization, is still recognizable in the WC₄-unit (see Fig. 2.66), some 1000 metres stratigraphically above. Numerous examples of silification are given in the text throughout this study.

The bulk of SiO₂ certainly has been derived from the hydrothermal system, but for some jaspilite layers in the red zone a sedimentary origin cannot be refuted. Recent investigations of a sodium lake in Tanzania (Behr et al., 1984) showed that layers of pure SiO₂-sediments are intercalated with carbonates.

4.1.6. Summary

The Abra mineralization is characterized by two groups of minerals, those of sedimentary association which may have been mobilized in the course of subsequent developments and those which have formed in connection with hydrothermal processes.

The sedimentary association comprises carbonate, iron-oxides, (Ca-)sulphates and pyrite of the black and red zones, and carbonate plus clastics (quartz, feldspars, micas) of the stringer zone. These minerals - mainly carbonates, sulphates and iron-oxides - have been mobilized and recrystallized, and also occur in veins. There is no chemical difference between sedimentary- and vein-types.

The post-sedimentary, "hydrothermal" minerals comprise all sulphides (except syndiagenetic pyrite), scheelite, possibly some Fe-oxides, quartz, barite, chlorite, albite and hyalophane.

The mode of emplacement of these minerals is different with respect to the stratigraphy; in the stringer zone veining, silification, chloritization prevails whereas in the black and red zones replacement of carbonate (by quartz), of sulphates (by barite, quartz, carbonate), of pyrite (by other sulphides) and albitization is added to the aforementioned processes.

In the lower stringer zone veins of chalcopyrite, quartz, magnetite, chlorite, carbonate and pyrite prevail. In the upper stringer zone and lower black zone, galena, pyrite, magnetite/hematite, quartz, carbonate, chlorite and barite veining is abundant, while in the red zone veins predominantly consist of barite, pyrite, hematite, quartz and carbonate. Veining is accompanied by brecciation in places, and, in particular in the stringer zone, the fine-grained breccia "matrix" preferentially is mineralized by sulphides.

Replacement of pyrite by other sulphides in the black and red zone is preceded by syndiagenetic growth of pyrite within the upper layers of sediment ("syngenetic pyrite") in connection with bacterial sulphate reduction. With the onset of hydrothermal activity metal-bearing fluids percolated through the sedimentary pile and replaced pyrite. Further precipitation of sulphides was governed by the availability of H_2S from bacterial sulphate reduction which was trapped in the sediments. Recrystallization of fine-grained syndiagenetic pyrite continued throughout the mineralizing phase and facilitates replacement by other sulphides and the intergrowth with galena, chalcopyrite and tetrahedrite. Tetrahedrite in recrystallized pyrite is rich in Fe and As suggesting that its growth was related to the recrystallization of pyrite.

The abundance of replacement (sulphate, carbonate, pyrite) and the occurrence of veins in the uppermost stringer zone (and locally up to 16 metres into the overlying clastites) indicates commencement of hydrothermal (i.e. mineralizing) activity after deposition of the host sediments and rules out significant syn-sedimentary exhalative processes.

The onset of hydrothermal activity is linked to the generation of deep-seated faults during incipient rifting which led to deposition of coarse clastic WC₁-unit, overlying the host rock sequence. The host rocks still were in the state of diagenesis, and the abundance of diagenetic formation waters and of pore space enabled widespread replacement of Ca-sulphates, carbonates and pyrite. With respect to the host rock sequence, the mineralization best is described as syndiagenetic.

The mineralogy of the Abra mineralization has features in common with major sediment-hosted base metal deposits listed by Large (1980). These include barite, silification, chloritization and albitization. Abra is unique with respect to this list, however, due to its remarkable paucity of zinc mineralization.

4.2. Metal zonation in the Abra mineralization

There is a distinct vertical metal zonation within the Abra mineralization, expressed by the distribution of sulphides and barite in drill cores. Drill cores were assayed in intervals of one or two metres for Cu, Pb, Zn, Ag, Au, Ba, Mn by order of Geopeko; the results are presented in Fig. 4.10. This plot of the 10 m-averages of the assay results for each drill hole clearly displays the nature of the zonation and provides analytical support for the zonation which is macroscopically visible from sulphide distribution.

At Abra there is a vertical Cu-Pb-Ba zonation. Zinc assay results, rarely exceeding 1 wt.% Zn, do not show a distinct interval of Zn-abundance; Zn loosely correlates with Pb. Detailed plots (1 metre intervals) of the assay results of Ab 3 and Ab 4 holes indicate maximum abundance of Zn slightly below (20 - 40 metres) the zone of highest Pb-assays. Considering the Zn distribution, the metal distribution in Abra can be characterized as a vertical Cu-Zn-Pb-Ba zonation sequence.

Barnes (1975, p.296) stated that "the least soluble mineral in a particular solution will be deposited first nearer the source of the metal-carrying solution, and followed by others in order of decreasing solubility". Element and mineral zonation is observed in all types of mineral deposits, including both volcanic and sediment hosted massive sulphide deposits.

By definition, any zonation pattern must be related to a point (the centre of zonation) around which the variables (metal concentration) vary according to their distance from this point. It is presumed (Large, 1980) that the centre of zonation is that point in the path of the metal-bearing solution where the least soluble metal sulphides were precipitated.

Fig. 4.10:

10 m - average assays of the Abra diamond drill holes with respect to the lithostratigraphic units projected onto a N - S section at 8500 E

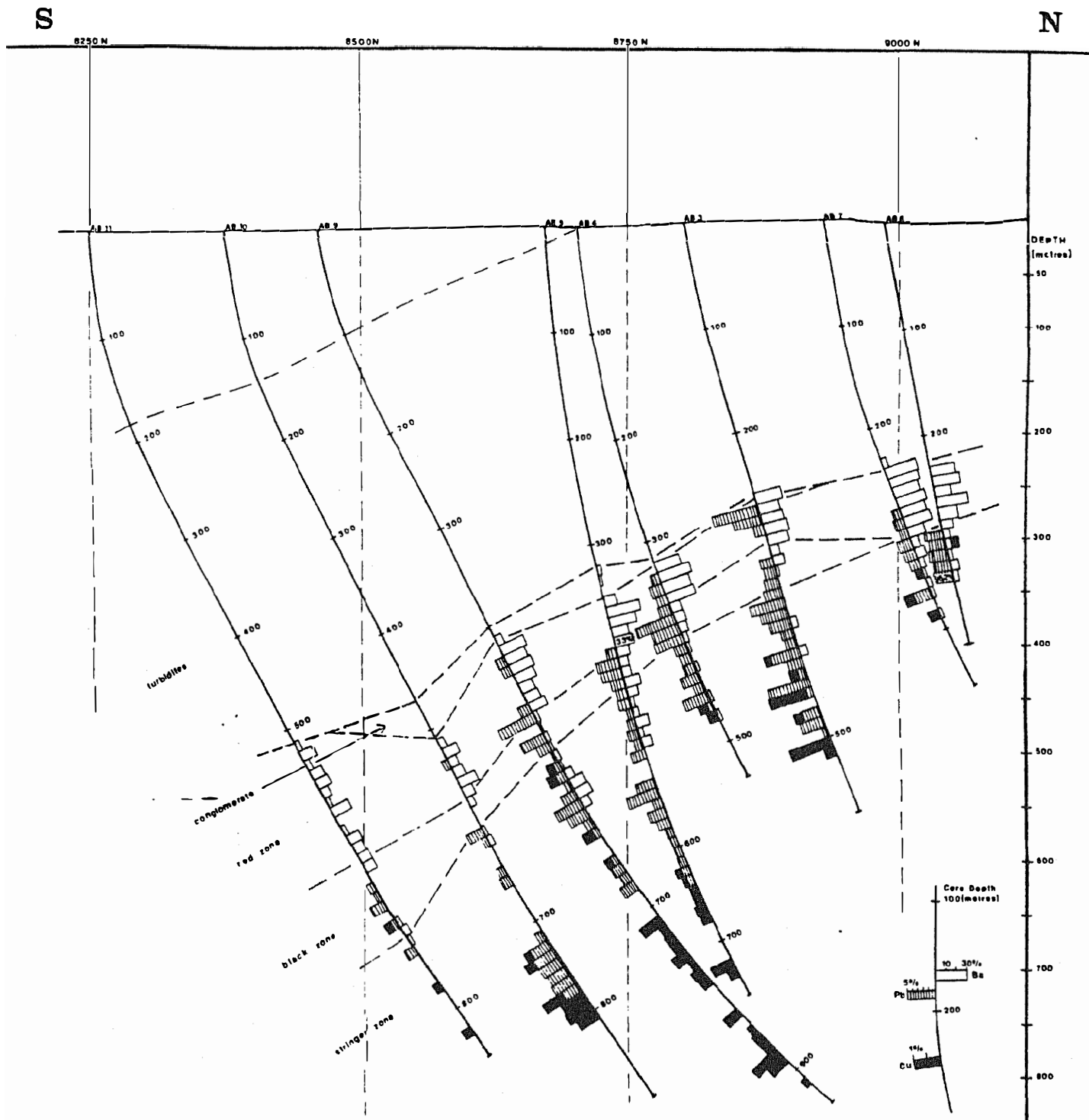


Table 4.06 gives some examples of metal zonation in sediment hosted Pb-Zn deposits (after Large, 1981). The sequence of zonation generally is Cu-Pb-Zn-Ba in laterally zoned deposits and Cu-Zn-Pb-Ba in vertically zoned deposits. Fe is sometimes enriched at the centre of zonation (e.g. Rammelsberg and Sullivan), or there may be a Fe-halo around the base metal sulphides, e.g. the hematite-chert formation that is laterally equivalent to the sulphide facies at Tynagh, Ireland.

The zonation sequence of Abra fits into this general classification and is comparable to Rammelsberg where there also is a lower cross-cutting Cu-rich zone, barite with sulphides in the median zone, and a barite dominated body at the top (Hannak, 1981).

Table 4.06 and references from Large (1981)

Examples of metal zonation in the stratiform mineralisation of selected sediment-hosted, submarine exhalative Pb-Zn deposits

Deposit	Metal Zonation in the stratiform mineralisation
Rammelsberg Meggen	Vertical zonation Cu → Zn → Pb → Ba upwards through the stratiform ore. Mn-halo in the ore horizon sediments around the ore body. Barite ore body laterally equivalent to the stratiform sulphides.
Silvermines	In the stratiform Upper G zone the Pb/Zn ratio decreases towards the periphery of the zone away from the Silvermines fault.
Tynagh	Mn-halo in the stratiform iron-oxide facies and laterally equivalent sediments. Lateral increase of Zn towards the cross-cutting mineralisation.
Mount Isa	Lateral zonation Pb → Zn within the stratiform ore, away from the contact with the "silica-dolomite".
McArthur River	Lateral zonation within the stratiform mineralisation of Pb → Zn → Fe, away from the cross-cutting vein-type mineralisation.
Sullivan	Within the stratiform mineralisation there is a decreasing Pb/Zn ratio towards the periphery of the deposit. Central core zone is Fe-rich.
Tom	Within the stratiform mineralisation the Pb/Zn ratio decreases laterally away from the massive ore and the underlying cross-cutting mineralisation.

References: Rammelsberg (Gunzert, 1969), Meggen (Krebs, 1981), Silvermines (Taylor and Andrew, 1978), Tynagh (Russel, 1975), Mount Isa (Mathias and Clarke, 1975), McArthur River (Williams, 1978a, b), Sullivan (Ethier et al., 1976), Tom (Carne, 1976).

It is evident from Fig. 4.10 that the metal zonation in Abra is independent of the host rock lithology, i.e. the zonation is transgressive. Whereas in holes Ab 3 and Ab 4 the Pb-maxima are located within the black and red zones, in Ab 6, 7, 5, 9, 10 their position is within the black zone. Only the distribution of Ba is controlled by the occurrence of a sedimentary unit (the red zone), i.e. strataform.

This spatial separation of Ba and Cu-Pb(Zn) within the zonation sequence implies two different processes of emplacement of these elements:

- Cu and Pb(Zn) form two approximately concentric zones, transgressing sedimentary strata, which are centred around an elongated area. In comparison with Fig. 3.01, where the three-dimensional position of the faults limiting the Abra sub-basin is shown, it is likely that the Cu-Pb(Zn) zonation is centred around the E-trending, northern margin fault of the Abra sub-basin. This fault zone probably has been the major feeder channel along which hydrothermal fluids ascended. Sulphide minerals were emplaced in the wall rock percolated by the fluids, and the order of precipitation of the sulphides was controlled by their relative solubilities.
- Barium, which was transported in solution by the same fluids, could only precipitate as barite depending on the amount of sulphate (SO_4^{--}) available. The SO_4^{--} content of the hydrothermal fluids and, probably more significant in volume, of the formation waters was consumed by barite precipitation. This explains the ubiquitous but low-grade barite mineralization in the stringer and black zones, and is comparable, in principle, to the precipitation of the sulphides. The bulk of barite, however, formed in the Ca-sulphate rich sabkha sediments of the red zone as replacement of Ca in the sulphates by Ba; i.e. the barium-bearing hydrothermal fluids ascended through the sediments until they encountered copious sulphate and quantitatively replaced Ca by Ba because of the extremely low solubility of barium. The apparent relation of Ba distribution to a certain

sedimentary horizon, therefore, does not indicate synsedimentary exhalative deposition of barite but a post-depositional control on the mineralization by the chemical composition of this horizon which is susceptible to replacement. This process took place prior to lithification; it thus differs fundamentally from replacement of lithified rocks.

In summary, the zonation pattern in the Abra mineralization is compatible with a post-depositional, fault-controlled, transgressive emplacement of the metals. This is evident for Cu and Pb(Zn) dominantly occurring as sulphides in veins, and distributed discordant to the stratigraphy. The strataform barite distribution originates from the replacement of a sedimentary horizon rich in sulphate, and therefore, also was related to post-depositional but pre-lithification, transgressive hydrothermal processes.

4.4. Physical and chemical controls on ore formation in the Abra mineralization

In this chapter it is attempted to assess pH, sulphur (fS_2) and oxygen (fO_2) fugacities on the sites of metal sulphide formation (i.e. within veins occurring in all zones, and within the strata-form mineralization in the black and red zones), in order to understand the chemical environment and temperature of ore formation.

4.4.1. Vein mineralization

The following are constraints on the environment of ore formation in veins:

- 1) Iron has been available in excess; this is obvious from the large proportion and omnipresence of either pyrite/magnetite in the lower stringer zone, or magnetite/hematite/pyrite in veins of the upper stringer zone and in the red/black zones. The absence of any Cu-sulphides others than chalcopyrite also suggests abundant iron.
- 2) Isothermal conditions are assumed for the individual sites of sulphide precipitation. On the scale of the entire mineralization however, a vertical temperature gradient (upward decreasing) is likely.
- 3) Hematite, magnetite and pyrite are invariably associated throughout the upper stringer zone and the red/black zones, while there is a predominance of magnetite/pyrite in the lower stringer zone, suggesting effective buffering of fO_2 and fS_2 during the majority of ore forming processes in the upper parts and no buffering in the lower stringer zone.
- 4) The hematite-magnetite-pyrite assemblage can be considered as a buffer (see 3), but also as an indicator of chemical conditions

(Barton, 1970). The triple point of the three coexisting iron species is strongly pH-dependent (Large, 1977) and therefore of use in determining the pH during ore formation. In Fig. 4.13 the stability fields of iron species are calculated for 250^o C and an H₂O pressure of 40 bars (both these parameters are considered to approximate conditions in the upper parts of Abra). A pH of about 6.5 results from the position of the triple point in Fig. 4.13, which makes the solution slightly alkalic (at 250^o C). The omnipresence of carbonate in the Abra mineralization is compatible with a non-acidic solution and suggests that a pH of 6.5 represents a realistic approximation for the hydrothermal fluids.

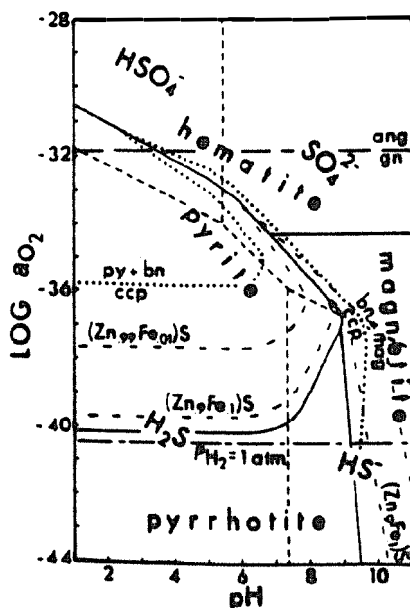


Fig. 4.13: from Barton and Skinner (1979). Stability fields of various iron species in a log aO₂ versus pH diagram calculated for 250^o C and H₂O pressure of 40 bars.

Abbreviations: py=pyrite; gn=galena; ang=anglesite; ccp=chalcopyrite; bn=bornite; mag=magnetite.

- 5) Coexisting hematite, magnetite and pyrite are excellent indicators of the fS_2 and fO_2 for a given temperature, when the pH is fixed. Fig. 4.14 is calculated for $250^{\circ}C$ and H_2O pressure of 40 bars. This gives fS_2 of about 10^{-11} and fO_2 of about 10^{-34} for the hematite-magnetite-pyrite triple point. For lower temperatures the resultant fS_2 and fO_2 would be shifted to correspondingly lower values.

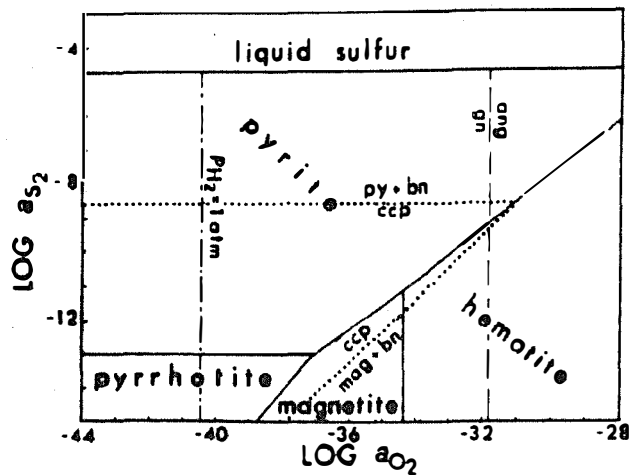


Fig. 4.14: modified after Barton and Skinner (1979). Stability fields of various iron species in a $\log a_{O_2}$ versus $\log a_{S_2}$ diagram calculated for $250^{\circ}C$ and H_2O pressure of 40 bars. Abbreviations as in Fig. 4.13

Note: $fS_2 = a_{S_2}$ for certain conditions given by Scott (1976, p. 5 - 27)

A fS_2 of 10^{-11} plots well into the centre of the "main line" ore-forming environment presented by Barton (1970, p.195) and probably was maintained in general throughout the Abra mineralization.

Regarding fO_2 , the situation is more complex. In the lowermost 200 - 300 metres of the stringer the iron species dominantly are magnetite/pyrite indicating conditions deviating from the hematite-magnetite-pyrite triple point to either higher temperatures or lower fO_2 . In the upper red zone, the dominant species in veins are hematite/pyrite, and suggest a shift to either lower temperature or higher fO_2 . Thus, there is a change in the relative abundance of the iron species vertically through the Abra mineralization which is either due to an upward decrease of temperature or an upward increase in fO_2 . An upward decrease of temperature is a feature common in many hydrothermal sulphide deposits and also a realistic assumption for the situation at Abra, where hydrothermal fluids from a deep-seated source (the E-trending fault zone) penetrated the wall rock. The ascent of the fluids is characterized by cooling rather than by increasing fO_2 , and therefore, decreasing temperature is considered as the main control of the changes in the relative abundances in iron species.

- 6) Fluid inclusions studies (Roedder, 1967) on moderate to high temperature hydrothermal deposits indicate solution strengths at 1-2 molar NaCl. Presumably, in Abra the hydrothermal system was partially fed by a convective system which added comparatively saline solutions (from the evaporitic red zone) to the hydrothermal fluids, and thereby increased the molarity of the fluids.

The strength of the hydrothermal solutions in Abra is estimated at 4 molar NaCl, as an arbitrary fixation, only devised for thermodynamic calculations. This is permissible because salinity mainly affects the metal solubilities (which are not discussed here) and has little influence on e.g. the position of the hematite-magnetite-pyrite triple point.

From consideration of points 4, 5, 6 the general conditions of ore formation in veins of the Abra mineralization are recognized to include neutral to slightly alkalic solutions (pH6), with a salinity of 4 molar NaCl equivalents (arbitrary), an fO_2 of 10^{-34} and an fS_2 of 10^{-11} . The values of fS_2 and fO_2 mark the triple point of the stability fields of magnetite-hematite-pyrite for 250° C. The values are temperature dependent but it will be shown in the following that the temperatures were around 250° C, and therefore, the fO_2 values are a realistic approximation.

The distribution of barite coexisting with iron species is used for determination of the temperature of ore formation. Three groups of associations of barite and iron species are observed:

- | | |
|--|--|
| upper red zone | - hematite/pyrite and abundant barite |
| red/black zone and upper stringer zone | - hematite/magnetite/pyrite and barite |
| lower stringer zone | - magnetite/pyrite and no barite |

Thus, the first significant barite occurrence is associated with three iron species marking a triple point in a fS_2 or fO_2 versus $1/K$ diagram. The position of the triple point is dependent on both fS_2 and fO_2 (among further variables) whereas the transition $Ba^{++}/BaSO_4$ probably is mainly dependent on fS_2 (and pH) according to Finlow-Bates (1980, Fig. 13). In a ΣS versus temperature diagram the transition $Ba^{++}/BaSO_4$ should be independent of changes in the fO_2 . The total sulphur concentration is preferred to fS_2 , to exclude changes in fugacity by different activity coefficients of the various sulphur species during redox reactions. Fig. 4.15 represents a ΣS versus temperature diagram where the hematite/magnetite/pyrite triple point has been calculated for $fO_2 = 10^{-38}$ (data from Helgeson, 1970) and for $fO_2 = 10^{-34}$ (data from Barton and Skinner, 1979). The $Ba^{++}/BaSO_4$ transition has been calculated from data of Finlow-Bates (1980) and it is marked by a

horizontal line because it is largely independent of temperature. As this transition is not a redox reaction a change of f_{O_2} would not be influential in the position of this line.

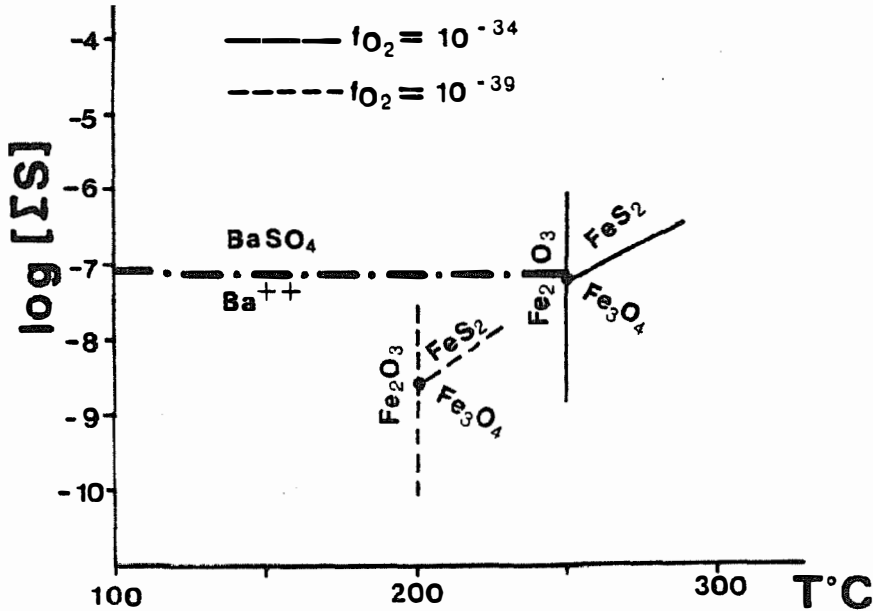


Fig. 4.15:

Change of the triple point hematite-magnetite-pyrite with increase in f_{O_2} , calculated for pH 6 and a solution strength of 4 molar NaCl equivalents. The transition of $Ba^{++}/BaSO_4$ remains unchanged during f_{O_2} -rise (according to data of Finlow-Bates, 1980). Coexistence of hematite, magnetite, pyrite with barite allows estimates of temperature and f_{O_2} at above $250^\circ C$ and 10^{-34} for the upper stringer and black/red zones. Data of stability fields of iron species are from Helgeson (1970) and Barton and Skinner (1979).

It is evident in Fig. 4.15 that the position of the triple point hematite/magnetite/pyrite for $200^\circ C$, determined by an f_{O_2} of 10^{-38} , is below the stability field of barite whereas by an increase in temperature (corresponding to increase in f_{O_2}) to about $250^\circ C$ conditions for the coexistence of barite and the

three iron species are met for the first time. This suggests temperatures above 250⁰ C during ore formation in the upper stringer zone and the black/red zones, where the above phases coexist.

These estimates of temperature are only valid for a single mineralization event and equilibrium reactions without any interference of kinetics. As kinetic effects probably were influential on the formation of sulphides in a temperature regime of 250⁰ C, this can only be an approximation of the real temperatures.

Assuming that there was no significant change in the f_{O_2} during ore formation in veins, the history of cooling in the Abra mineralization can be explained by considering the various iron species coexisting, or not coexisting with barite. In Fig. 4.16 the triple points of magnetite/hematite/pyrite for 200⁰ C and 250⁰ C are marked on the linear hematite-magnetite transition. The triple point for 250⁰ C has the same position than the $Ba^{++}/BaSO_4$ transition at pH 6 (see Fig. 4.15) which in this diagram also is a point. Interestingly, the boundary "sulphide dominant/sulphate dominant" from Barton (1984, Fig. 8.3.) occurs at a f_{O_2} of about 10^{-35} , i.e. almost coinciding with the $Ba^{++}/BaSO_4$ transition at pH 6.

In Fig.4.16 a hypothetical path of the thermal evolution of the Abra mineralization is shown, taking into account the various associations of iron species and barite. This model is only valid for minor changes in f_{O_2} .

Three phases are discernible during thermal evolution. Phase one is represented by the magnetite-pyrite-no barite association, and is characterized by cooling of the system without buffering.

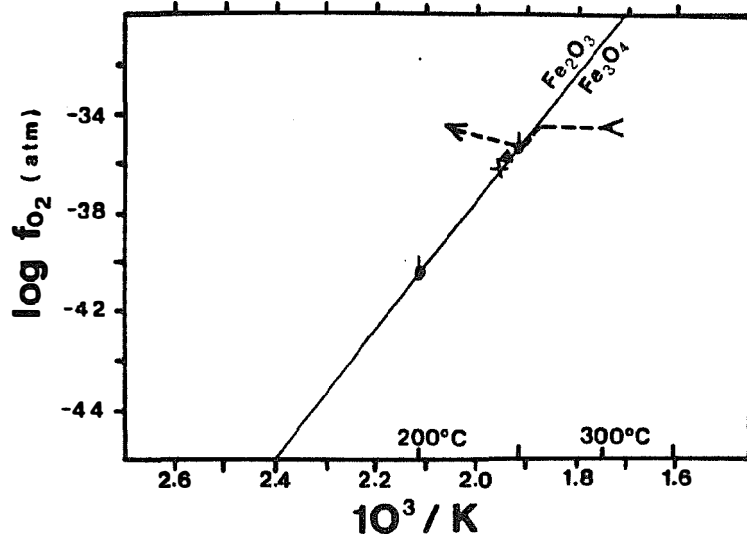


Fig. 4.16: Log f_{O_2} - $1/t$ diagram showing hypothetical thermal evolution in the Abra mineralization. The triple points hematite-magnetite-pyrite for 200° and 250°C, and the $Ba^{++}/BaSO_4$ transition, are marked on the linear hematite-magnetite transition.

- hematite-magnetite-pyrite triple points at 200° and 250°C
- X $Ba^{++}/BaSO_4$ transition, calculated for pH 6, from data of Finlow-Bates (1980)
- ▲ "sulphide dominant/sulphate dominant" boundary from Barton (1984)

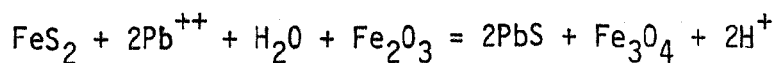
Phase two commenced when the hematite/magnetite line was reached during cooling; it is represented by coexisting hematite-magnetite-pyrite with barite. It is possible that barite formation was inhibited at first (through kinetic effects, or by the comparatively good solubility of Ba at higher temperatures), and only hematite, magnetite, pyrite formed until cooling along the line of buffering allowed precipitation of barite. Finally, in the upper red zone, some admixture of oxidizing formation water led to an increase in f_{O_2} and phase three commenced. The addition of oxygenated water prevented further cooling along the buffer line because the hematite-magnetite-pyrite equilibrium was disturbed. From then on, the f_{O_2} was not buffered during further cooling and probably increased upwards.

4.4.2. Conformable mineralization in the black and red zones

Whereas closed system conditions were assumed as an approximation for the ore formation in veins (i.e. a high hydrothermal fluid/formation water ratio), this does not apply to the conformable mineralization. The ratio of hydrothermal fluid to formation water was low and variable (variable water content of the sedimentary layers, impermeable horizons etc.), and caused variations of salinity, pH, fO_2 and fS_2 . In particular, the fS_2 was governed by the activity of sulphate reducing bacteria, or the presence of syndiagenetic pyrite layers, and thereby was subject to drastic changes between individual sedimentary horizons.

No sulphide minerals could precipitate from the hydrothermal fluid-formation water mixture when it percolated the hematite/magnetite-sulphate-carbonate sedimentary layers. The dominant sulphur species was SO_4^{--} leading to precipitation of large amounts of barite (from the solutions and as replacement of Ca-sulphates). However, in micro-environments dominated by reduced sulphur species, there was some free biogenic H_2S trapped under impermeable, non-reactive layers (e.g. quartz or magnetite), and there were syndiagenetic pyrite layers ($fS_2 = 1$) which could be replaced by metals transported in the hydrothermal fluids.

Pyrite commonly is intimately intergrown with galena and in places there are indications of pyrite replacement by galena (Fig. 4.04). Replacement of a pyrite layer by galena within more massive hematite/magnetite bands would cause oxidation of the sulphur, balanced by reduction of adjacent hematite to magnetite. This mechanism is summarized in the formula



and Fig. 4.05, where a galena layer is surrounded by magnetite, within a more massive hematite/magnetite band, probably is an

example of complete replacement of pyrite by galena according to this formula Thermodynamic calculations (A.Fluch, pers.comm., 1984) of the above reaction for 200^o C, pH 6 and the presence of lead ions, proved that the equilibrium is shifted to the right.

4.5. Sulphur isotopes

A reconnaissance study of sulphur isotopic compositions in the Abra mineralization was carried out on 2 sulphates and 5 sulphides. Despite the small number of analyses the data shown in Fig. 4.17 clearly reveal a sulphate and sulphide group with rather uniform values, respectively. From the distinct grouping it can reasonably be argued that further analyses would not yield significant deviations from the two trends; for the purpose of discussion the data are considered representative of the Abra deposit.

The $\delta^{34}\text{S}$ -values in Fig. 4.17 express the per mil deviation of the $^{34}\text{S}/^{32}\text{S}$ ratio of the compound relative to that of the troilite phase of the Canon Diablo meteorite (CDT):

$$\delta^{34}\text{S sample} = \left[\frac{(^{34}\text{S}/^{32}\text{S})_{\text{sample}}}{(^{34}\text{S}/^{32}\text{S})_{\text{standard}}} - 1 \right] \times 1000$$

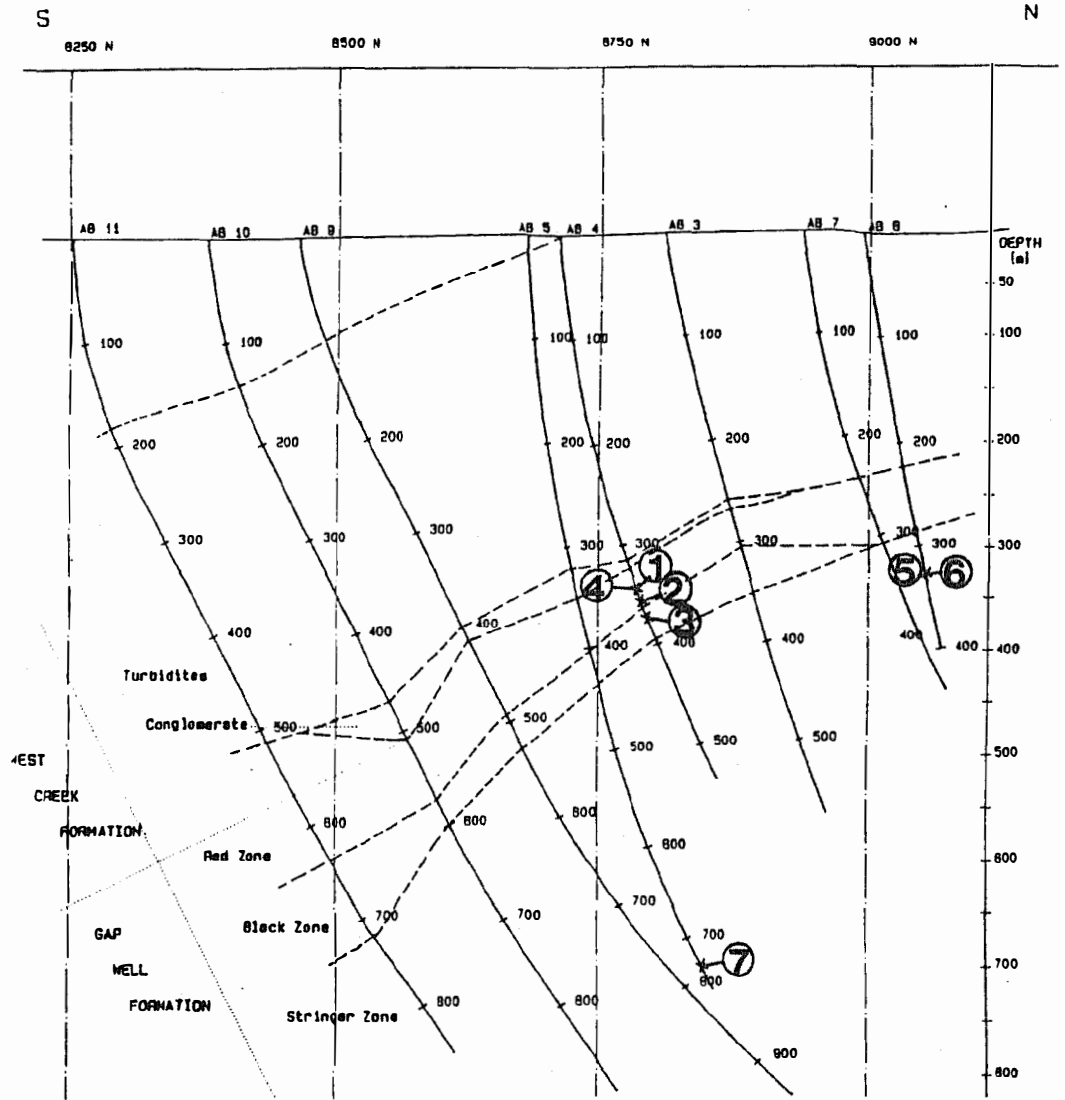
Standard deviation is in the range of $\pm 0.2\%$.

Sulphates

The two barite analyses yielded very high $\delta^{34}\text{S}$ values when compared with the compilation of sulphur isotope patterns for several major sediment hosted base metal deposits by Gustafson and Williams (1981). In fact, values of +40.8 and +38.4 for the Abra mineralization are among the highest ever reported from Proterozoic deposits and are comparable only to the Lady Loretta barites ($\delta^{34}\text{S}$: +37.4% to +39.7%, Carr and Smith, 1977), and to some extreme values of the "grey ore"-barite from the Phanerozoic Rammelsberg deposit ($\delta^{34}\text{S}$: +27.4% to +36.8%, Angerer et al., 1966).

Recently von Gehlen et al. (1983) presented two $\delta^{34}\text{S}$ analyses of barite from the middle (?) Proterozoic Gamsberg Zn-deposit with similar values ($\delta^{34}\text{S}$: $35.4 \pm 0.2\%$).

Fig. 4.17: Location and type of the sulphate/sulphide analysed



$\delta^{34}\text{S}$ (o/ooCDT)

①	barite, possibly strataform	(AB 4, 345m)	+ 40.8
②	barite, massive vein-type	(AB 4, 356m)	+ 38.4
③	pyrite, strataform	(AB 4, 372m)	+ 21.1
④	galena, possibly strataform	(AB 4, 345m)	+ 20.2
⑤	galena, common vein-type	(AB 6, 328m)	+ 22.3
⑥	chalcopyrite, vein-type	(AB 6, 328m)	+ 24.6
⑦	chalcopyrite, vein-type	(AB 5, 730m)	+ 21.0

+ 0.2 standard deviation

Tab. 4.08 summarizes the data of barite and concurrent sulphides of these deposits:

Table 4.08:

Range of $\delta^{34}\text{S}$ -values (in per mil) of some selected base metal deposits (references see text)

Deposit	barite	galena/sphalerite/ chalcopyrite	pyrite/pyrrhotite
Abra	+38.4 - +40.8	+20.2 - +24.6	+21.1
Lady Loretta	+37.4 - +39.7	+ 9.9 - +17.8	+ 3.9 - +17.8
Gamsberg	+35.4 (± 0.2)	+27.5 - +31.0	+26.0 - +31.0
Rammelsberg	+27.4 - +36.8	+ 7.0 - +20.0	-15.0 - +25.0

While sedimentological evidence for evaporitic condition during formation of barite is equivocal at Lady Loretta and Rammelsberg, or can only be assumed at Gamsberg (Stumpfl, pers.comm., 1984), there is sufficient evidence for a hypersaline, restricted basin in the Abra area.

In view of this the strongly, positive $\delta^{34}\text{S}$ values of barite from Abra obviously are the result of precipitation of sulphates from waters enriched in ^{34}S through evaporation.

In the sabkha environment of the red zone (hosting most of the barite) however, there was probably no permanent water cover. Accordingly the sulphates precipitated within the sediment during evaporation of ascending formation waters.

If the sulphates originally had been anhydrite/gypsum, to be replaced subsequently by barite, as suggested in chapter 3.2.1.4., the isotopic ratio most likely would remain unchanged.

Sulphides

All sulphides, including stratiform pyrite, define a relatively narrow range of $\delta^{34}\text{S}$ values (Tab. 4.08). The limited number of data and the lack of analyses of coexisting sulphide pairs does not allow the determination of fractionation trends, or the discussion of equilibria between sulphides.

When compared with other deposits of Tab. 4.08 $\delta^{34}\text{S}$ of sulphides of the Gamsberg deposit display a similar (although higher) narrow range of values while there is a considerably wider spread of data at Rammelsberg and Lady Loretta.

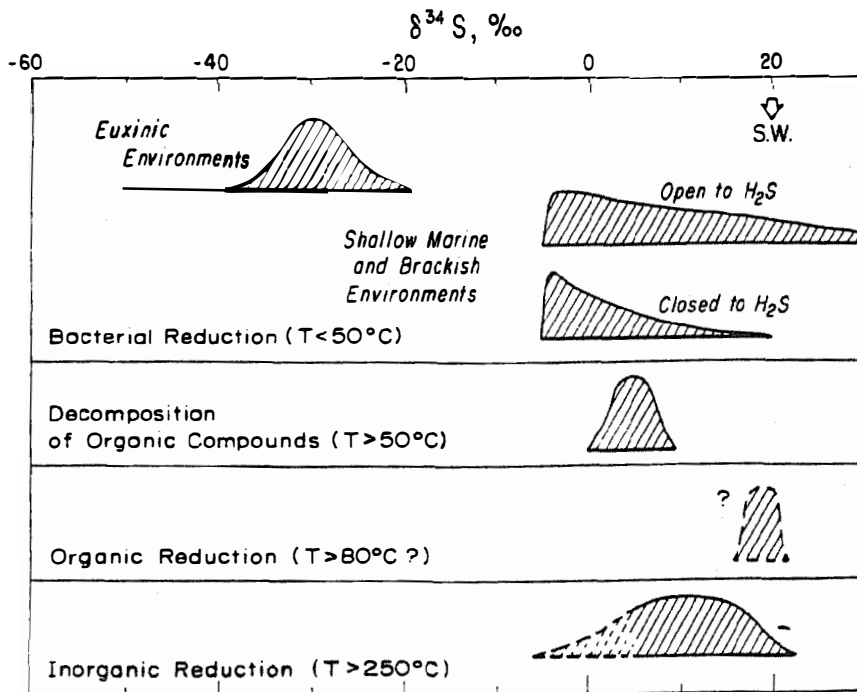
The approach of Sangster (1976b) to determine the source of sulphur in sulphide deposits is not applicable for the Abra mineralization. No comparison can be made between $\delta^{34}\text{S}$ values of stratabound sulphide deposits and coeval sea water - $\delta^{34}\text{S}$ because the sea water sulphate $\delta^{34}\text{S}$ - curve for the Proterozoic is unknown (Gustafson and Williams, 1981).

The two major mechanisms of sulphate reduction (i.e. isotopic fractionation of sulphur) though, are both known at least from the early Proterozoic:

- a) inorganic reduction: because it is mainly temperature dependent; SO_4^{--} will be reduced to form H_2S above 250°C (Ohmoto and Rye, 1979);
- b) bacterial reduction: its significance for sulphur isotope fractionation had increased considerably by about 2300 m.y. (Cameron 1982, 1983)

Fig. 4.18 (from Ohmoto and Rye, 1979) shows the distribution pattern for $\delta^{34}\text{S}$ values of H_2S and sulphide minerals caused by the fractio-

nation effect when sulphate of $\delta^{34}\text{S} = +20\%$ is reduced by various mechanisms.



Distribution pattern for $\delta^{34}\text{S}$ values of H_2S and sulfide minerals when sulfate of $\delta^{34}\text{S} = +20\text{‰}$ is reduced by various mechanisms. SW is sea water.

Fig. 4.18: From Ohmoto and Rye (1979)

Comparing the mean fractionation effect for inorganic reduction in Fig. 4.18 of about -10% with respect to the coeval sea water, with the Abra fractionation of about -18% , inorganic sulphate reduction is not compatible with the Abra distribution pattern.

Organic reduction of sulphate can also be excluded (again with the above assumption of very heavy coeval sea water) because the sulphide formed by such reactions has $\delta^{34}\text{S}$ values essentially identical to the source sulphate (Ohmoto and Rye, 1979).

The optimum temperatures for bacterial reduction of sulphate are between 30° and 45° C; the rate of reduction decreases at higher temperatures.

However, the two mechanisms of bacterial reduction and decomposition of organic compounds (cf Fig. 4.18) cannot be viewed separately.

This is because growth of sulphate reducing bacteria occurs in the temperature range 0° C to 100° C (Zo Bell, 1963). Decomposition of organic compounds is intimately related to sulphate reducing bacterial activity as some organic compounds from the decay are utilized as nutrients by the bacteria (Trudinger et al., 1972; Trudinger, 1981).

Until recently sulphides with variable $\delta^{34}\text{S}$ values (variations above 20 %) were interpreted as biogenic (e.g. Burnie et al., 1972). It has since been realized that data on sulphur isotopic composition alone are usually insufficient to define the genesis of a deposit, and that a number of geological and geochemical factors influence the isotopic ratios of sulphide minerals (Ohmoto and Rye, 1979; Gustafson and Williams, 1981).

Due to the absence of a permanent water cover and to very oxidizing conditions during formation of the red zone, bacterial sulphate reduction only can be expected to have taken place within the sediments.

Bacterial sulphate reduction is particularly effective in the upper millimetres of very shallow water sediments; e.g. in Solar Lake, Sinai (a small salt pond) 90 % of the entire sulphate reduction occurred within the uppermost 0.1 - 3 centimetres (Monty, 1976; quoted in Jørgensen, 1982).

Sedimentological evidence and the above characteristics of sulphate reducing bacteria suggest that sulphides in the red zone were generated by reduction of sulphate from contemporaneous saline formation waters through sulphate reducing bacteria, using decomposing microbial mats as a substrate. $\delta^{34}\text{S}$ fractionation of -15 % to -20 % between barite and sulphides is compatible with the proposed mechanism.

Considering the five sulphide values in Fig. 4.17 no isotopic fractionation between stratiform pyrite and the other sulphides appears to have occurred; there is for example a greater fractionation between two vein-type chalcopyrites (+ 21 % and + 24.6 %) than between pyrite and galena.

In addition, there is no significant fractionation between strataform sulphides (strataform pyrite, possibly strataform galena) in the layered black/red zone and vein-type sulphides in the underlying clastic stringer zone.

This uniformity of the $\delta^{34}\text{S}$ values of sulphides suggests a single sulphur source of the sulphides (i.e. the sulphate of coeval evaporitic formation waters). However, it does not imply that strataform pyrite and base metal sulphides precipitated contemporaneously.

Textural features indicate a post-strataform-pyrite emplacement of base metal sulphides (e.g. while pyrite forms distinct layers base metal sulphides are irregular and often discordant; when of

concordant nature base metal sulphides are intimately intergrown with pyrite suggesting replacement).

The sulphide $\delta^{34}\text{S}$ values of Abra though, are equivocal and can give no clue to the question whether or not contemporaneous emplacement of pyrite and base metal sulphides took place.

Summary

The sulphur isotope data obtained from the Abra mineralization point to a single sulphur source - bacterial sulphate reduction.

High $\delta^{34}\text{S}$ values of barite indicate precipitation of sulphates from evaporitic brines. In view of the sabkha milieu in which most sulphates formed the brines were formation waters rather than evaporitic standing water bodies.

Most of the sulphides probably formed within the sediment through bacterial reduction of the sulphate in these formation waters. Although post-strataform-pyrite emplacement of the base metal sulphides would be compatible with the sulphide $\delta^{34}\text{S}$ values the data are not unequivocal.

Metamorphic exchange is thought to have had minor effects on the sulphide isotopic ratios as the regional metamorphic grade in the Abra area is below greenschist facies.

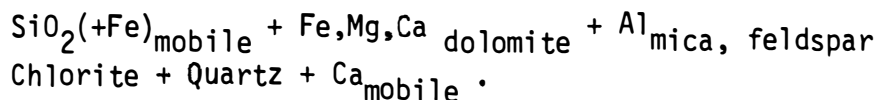
4.6. Alteration and metamorphism in the Abra mineralization and in the Jillawarra Belt

4.6.1. Alteration

Hydrothermal processes leading to Abra-type mineralizations are accompanied by formation of certain alteration assemblages, i.e. silification, albitization and chloritization.

Silification is most significant and widespread, and can be recognized in all strata of the Jillawarra Belt. It is strongest in the Abra area and at the TP- and Copper Chert prospects, with decreasing intensity away from these mineralizations. Silification, therefore, can be regarded a large-scale proximity indicator of mineralizations. When silification affects calcareous sediments it replaces carbonate to various extents, and small relicts, as carbonate inclusions in quartz, witness the former calcareous nature of the sediment (see e.g. chapters 2.3.1.5., 2.3.1.6 and 3.2.1.2.). Silification of arenites leads to exclusively quartz-cemented quartz arenites and thereby produces massive rocks with quartzite-appearance, in particular in the WC₁ and WC₄-units (see chapters 2.3.2.1. and 2.3.2.4.).

Silification may be involved in the chloritization of calcareous rocks as expressed by the general relationship



For the occurrence of rutile (or pseudobrookite) needles, which certainly are of non-sedimentary origin, Ramdohr (1975) provides an explanation. He suggests that rutile forms in wall rocks to hydrothermal systems where SiO₂-alkali-sulphide (?) bearing solutions alter Ti-bearing minerals (mainly Fe-Ti oxides); iron combines with the sulphide to form pyrite whereas the freed Ti yields rutile. The validity of Ramdohrs' interpretation gets some support by the existence of a trigonal relict-network of rutile needles within secondary quartz (Fig. 4.19).

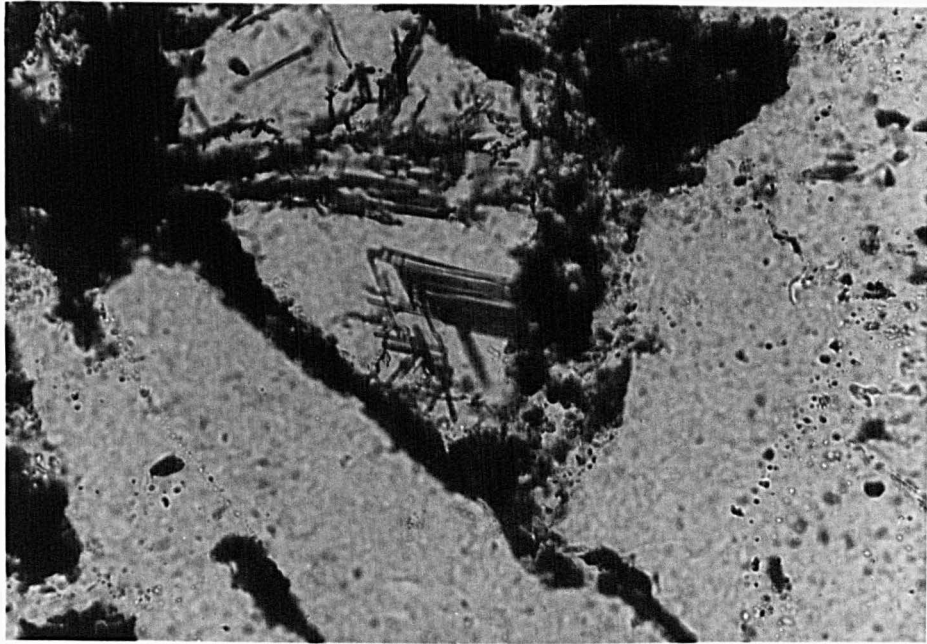


Fig. 4.19: Trigonal network of rutile in secondary quartz.
Base of picture = 0.36 mm (-).

Titanite which is less abundant than rutile, is interpreted by Ramdohr (1975) as an alteration product of ilmenite through introduction of SiO_2 and CaO .

Albitization is less abundant than silification, but it is also recognized throughout the Jilawarra Belt. Albite (< 2 % An) dominantly is associated with galena at the contact of wall rock and veins, or within the wall rock (see chapters 4.1.1.2. and 4.1.5.2.). In calcareous pelites in the GW_5 and GW_6 units of the Jilawarra Belt authigenic albite may have no galena inclusions but probably also formed by hydrothermal solutions, which in this case were more distal and devoid of metals. In Fig. 4.20 a detrital quartz grain in siltstone is enveloped by albite-galena intergrowth, illustrating the genetic relationship between both minerals.



Fig. 4.20: Albite-galena paragenesis in siltstone, surrounding a detrital quartz grain. Base of picture = 5.6 mm (+).

In the Sullivan deposit, B.C. (Ethier et al., 1976) albite-chlorite alteration occurs as a pervasively altered zone in the hanging wall up to 100 metres above the sulphide horizon. This zone is spatially restricted to the immediate vicinity of the massive sulphide mineralization.

In Abra the albitization is more widespread; it occurs in distal and proximal positions to the mineralization. It possibly is related to the hydrothermal silification (also widespread) supplying SiO_2 (and Al?), which reacted with Na in formation waters to form albite. The affinity of albitization to detrital quartz, in the case of Fig.4.20, suggests that additional SiO_2 was required for the growth of albite.

Chloritization is most common in the vicinity of the Abra mineralization. It is related to hydrothermal processes, as discussed in chapter 4.1.5.1. Chloritization affected a) carbonates (see Fig. 2.60), b) micas and clay minerals, and c) potassium feldspars (Fig. 4.21). Chloritization of potassium feldspars took place by

chloritization of sericite, which in turn had formed during the decomposition of potash feldspar. Decay of potash feldspar into sericite and quartz is a common process in the diagenesis of sandstones and may occur above temperature of ca. 100° C (Blatt et al., 1980), which certainly were realized during hydrothermal activity in Abra (see chapter 4.4.).

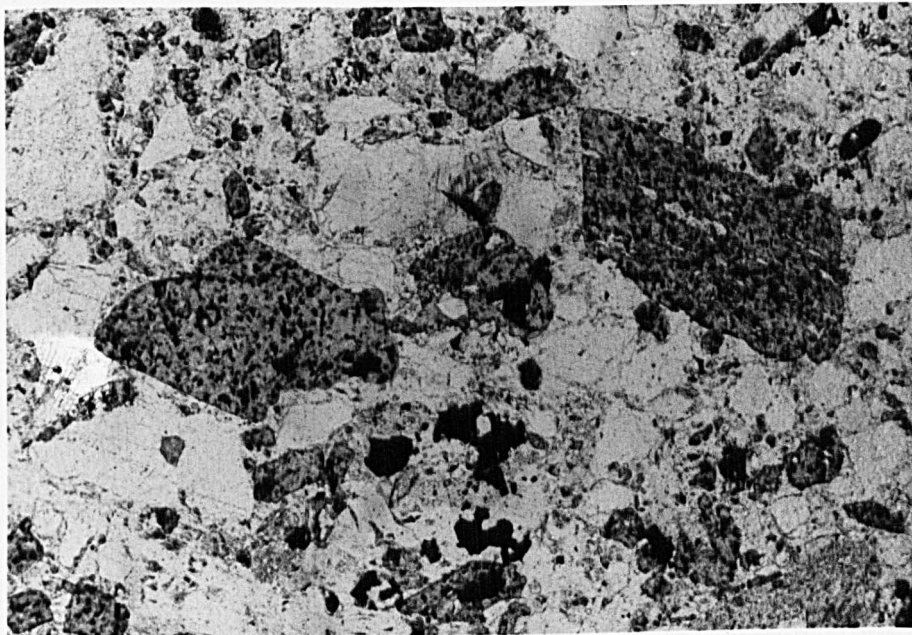


Fig. 4.21: Chloritized potash feldspar in arkose.
Base of picture = 3.6 mm (-).

Chloritization of principally the same nature, but less intense is ubiquitous in the Jillawarra Belt. However, there is chlorite in the Manganese Range Anticline defining foliation in a quartz-chlorite-magnetite schist. This is rather tecto-metamorphic chlorite (thrusting of the rocks towards the NNE after termination of hydrothermal activity) than alteration-chlorite.

In addition to chlorite, biotite is widespread in the Jillawarra Belt (notably, no biotite is present in the Abra area in spite of

the same stratigraphic level). Whereas the relation to hydrothermal alteration is obvious for most chlorites, for biotite and some chlorite in calcareous pelites it is equivocal. Both minerals have lower Fe/Mg ratios than other biotites and chlorites, respectively (see Tab. 4.09). However, silification is present in these rocks and witnesses that they also have been subject to alteration, which was less pronounced due to rather low permeability of the pelites. It is likely that these biotites and chlorites also formed syn-hydrothermal, through wall rock alteration, and that more Mg was incorporated during growth because of abundant Mg from the dolomite. Syn-hydrothermal formation of biotite is equally indicated by the occurrence of galena parallel to 001 planes within biotites in arenite. And, by biotite rimming a quartz-pyrrhotite-chlorite vein in pelites (Fig. 2.42).

Table 4.09: Representative electron microprobe analyses (weight %) of phyllosilicates

	ABRA		JILLAWARRA BELT					
	chlorite	chlorite	low K-phyllosilicates			biotite		chlorite
	in vein	in vein	in vein	associated with galena	in clastites	in dolomitic siltstone	in dolomitic siltstone	
Si	26.58	25.84	45.35	47.21	47.63	36.03	40.28	28.32
Ti	0.00	0.00	0.00	0.00	0.02	0.51	1.34	0.05
Al	17.30	21.30	6.46	6.00	4.80	15.44	14.99	21.56
Fe	32.03	30.45	33.29	24.91	23.48	23.84	15.32	20.60
Mg	14.52	13.32	2.83	10.81	11.62	11.16	15.55	21.02
Ca	0.00	0.00	0.32	0.00	0.00	0.00	0.00	0.09
Na	0.13	0.16	0.19	0.10	0.11	0.09	0.09	0.05
K	0.00	0.07	7.06	5.74	2.87	9.16	9.21	0.01
Mn	0.12	0.30	0.13	1.25	1.83	0.34	0.05	0.06
Total	90.68	91.44	95.63	96.03	92.36	96.57	96.83	91.77

In general, the occurrence of chlorite and biotite seem to characterize two extreme environments during the alteration phase (= late diagenesis?) of the Jillawarra Belt, including Abra. Chlorite clearly represents the proximal ore environment while biotite occurs in the distal, non-ore environment. In intermediate position (with respect to proximal/distal) there occurs a low-K phyllosilicate in the Abra-type (stringer zone, black zone, but no red zone), but low-grade mineralization at the 46-40 prospect (see map 3).

This is a high-Si, Mn (Fe), low-K phyllosilicate (with respect to biotite, see Tab.4.09), with fibrous appearance and brown colour similar to stilpnomelane, but clearly not having the optical and chemical properties of stilpnomelane. The occurrence in veins indicates a relation to hydrothermal fluids, in this case however, being rich in SiO₂ and Mn but depleted in Mg (compared to proximal vein-chlorite).

In summary, there appears to be a genetic relationship between the type of phyllosilicate formed during alteration, and the proximity to hydrothermal systems (provided the phyllosilicates formed contemporaneously). The various phyllosilicates possibly represent differences in the chemistry of hydrothermal fluids, but may also have formed in response to different temperatures:

- proximal - chlorite, high-grade or -temperature hydrothermal activity
- intermediate - low-K phyllosilicate, low-grade or -temperature hydrothermal activity
- distal - biotite, low-temperature alteration.

A similar relationship has been observed in the Bushveld Complex, S.A. (Ballhaus, pers.comm., 1984), where there is a progressive change from biotite over low-K phyllosilicate, to chlorite towards the rocks affected by volatile/fluid activity (these rocks cannot be termed proximal ore environment because they contain graphite as a major constituent).

The composition of chlorites as proximity indicators has been demonstrated by Reimann and Stumpf (in press), and Kalogeropoulos (1983). A relationship of the mineralogy of phyllosilicates to the proximity of ore environments has not been observed hitherto, and it may be worthwhile to further investigate the mineralogy and chemistry of phyllosilicates, in order to examine their use as an instrument in exploration.

4.6.2. Metamorphism in the Jillawarra Belt

Some biotite and chlorite formed during metamorphism of Jillawarra Belt, in addition to syn-hydrothermal phyllosilicates described above. This is evident from chlorite in quartz-chlorite-magnetite schists in the Manganese Range Anticline, and from biotite in the pressure shadow of magnetite (Fig. 2.25) almost perpendicular to bedding.

Biotite and chlorite defining a weak foliation (which is only developed in places) have formed during tectonism and may simply be a recrystallization of pre-existing biotite and chlorite in response to strain. Therefore, they are no reliable indicators of the grade of regional metamorphism.

In arenites of the GW₅-unit (at 585 m in a drill core from the TP-prospect) biotite containing galena along the 001-planes (and therefore regarded as syn-hydrothermal), is partially chloritized. Chloritization of biotite suggests retrograde metamorphism; i.e. temperatures of regional metamorphism within this rock have been lower than the syn-hydrothermal temperatures of biotite formation. In view of this relationship, chlorite is the only phyllosilicate formed during regional metamorphism. An unrealistic higher metamorphic grade suggested by the alteration mineral assemblage of phyllosilicate, has also been observed in Mt. Isa (Finlow-Bates, 1978).

On the contrary, alteration may have inhibited the generation of epidote which is a metamorphic facies mineral of the grade assumed for the Jillawarra Belt (lower greenschist facies). Alteration in

the vicinity of volcanogenic massive sulphide deposits usually leads to the decomposition of feldspars and Ca-bearing minerals, resulting in rocks depleted in Na and Ca (Froese, 1981). In the Jillawarra Belt, sodium has not been removed (albitization) but all carbonates are ferroan dolomites, depleted in Ca. Whole rock chemistry of the Abra mineralization is characterized by a proximal Ca-deficient zone, and a distal zone with higher Ca/Mg ratios. Absolute Ca-values are usually below 1 % CaO (maximum value: 2.5 % CaO) despite the calcareous nature of the rocks. It is inferred that the Ca-deficiency, as a result of hydrothermal alteration, inhibited the formation of epidote.

The mechanism of phyllosilicate generation and non-formation of epidote implies that hydrothermal alteration of a sedimentary sequence produced a unique mineral assemblage which, during metamorphism, produced an equally unique mineral association, capable of significant deviation from the "normal" assemblage of metamorphic minerals for the corresponding metamorphic grade. This is in good agreement with Stanton's (1979) concept of isochemical metamorphism and various precursor mineralogies.

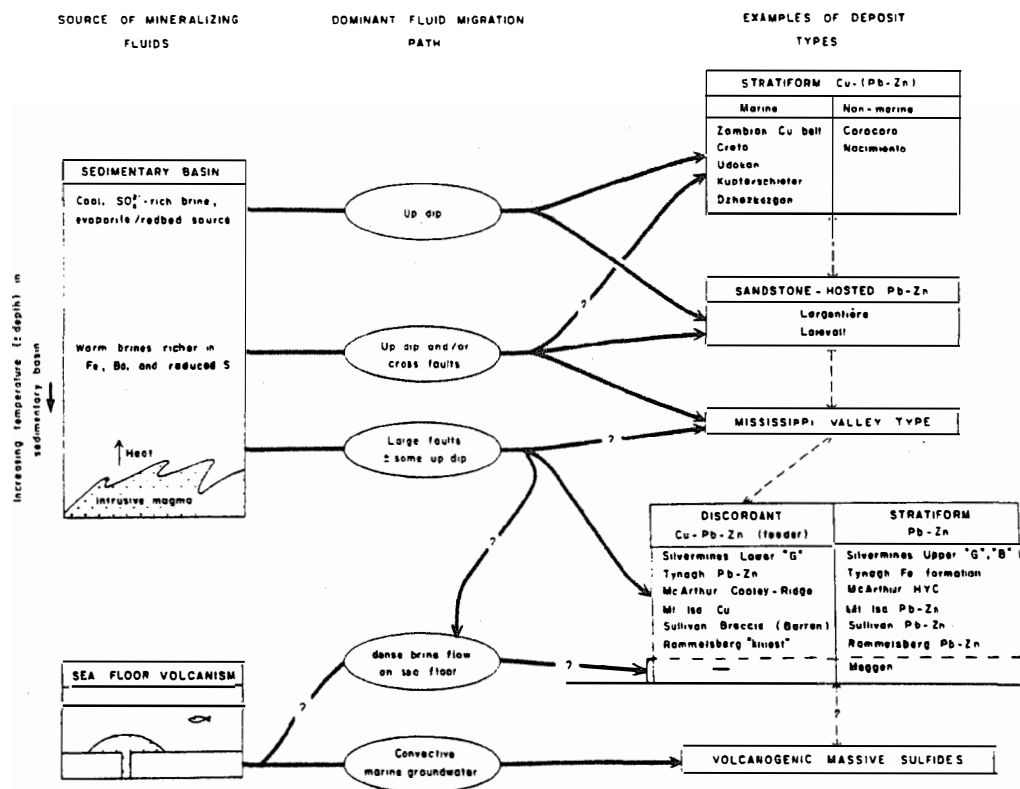
4.7. Source of metals in the Abra mineralization

The absence in the entire Bangemall Basin of any indication of oceanic crust or geosynclinal volcanism/sedimentation, and the tectonic setting (e.g. continental tholeiite intrusions), implies that sea floor volcanism and convection of marine groundwater through basaltic crust can be ruled out as a metal source for the Abra mineralization (cf Fig. 4.22).

The sabkha model of Renfro (1974), invoking lateral transport of metals in contemporaneous terrestrial and/or sea waters, is equally inappropriate because the presence of an extensive stringer zone (i.e. veining) proves vertical, high-temperature movement of hydrothermal fluids.

Source rocks

Formation waters originating from continental rocks (e.g. basement, non-pelagic sediments) provide the remaining potential source of the Abra mineralization and the feasibility of various rock types as a source is discussed in the following. There is a wealth of data published on the sedimentary genesis of hydrothermal fluids (e.g. Hanor, 1979; Skinner, 1979; Dunham, 1970) mainly with respect to Mississippi Valley type deposits (Carpenter et al., 1974) and shale-hosted Pb-Zn deposits (Badham, 1981). The relationship between the source of the fluids and the types of deposits is shown schematically in Fig. 4.22.



Schematic relationships are shown between types of deposits, source of mineralizing fluids, and dominant fluid pathway. Volcanic massive sulfide and Mississippi Valley-type deposits are also shown for comparison.

Fig. 4.22: from Gustafson and Williams (1981).

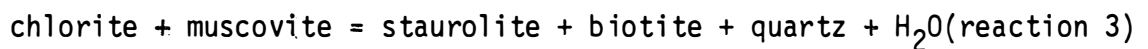
Any consideration of the source rocks and the mechanism of mobilization has to account for the unique metal abundance ratio in Abra, of about 1 : 0.2 : 2.2 for Pb : Cu : Ba, and the lack of Zn. It is convenient first to consider possible host minerals of the "Abra metals" (including zinc) and then discuss potential host rocks of the respective metals.

1) Pb and Ba:

Both elements mainly replace K in silicates. Therefore, potash feldspars and, to a lesser extent, muscovite are the dominant host minerals for Ba and Pb. Diadochy of Pb with Sr, Ba, Ca and Na can occur (Haack et al., 1984), thereby increasing the capacity of Pb-incorporation in feldspars (among other minerals).

2) Zn:

In igneous and metamorphic rocks Zn preferentially replaces Fe^{2+} and Mg in octahedral sites with OH - ligands such as in chlorite, hornblende, biotite and muscovite, but not in OH-free silicates. The highest Zn concentrations - up to several per cent - are found in staurolites; magnetite may also be very rich in Zn (Haack et al., 1984). The incorporation of Zn into staurolite may have significance for the lack of Zn in the Abra mineralization because some 2000 metres below the mineralization (i.e. in a possible source region) the staurolite isograde reaction,



probably was achieved.

3) Cu:

For Cu no clearcut diadochy in silicate minerals is evident. In igneous rocks the bulk of Cu is contained in finely dispersed sulphides (Ramdohr, 1940) and it is not known whether this applies to metamorphic rocks as well. In meta-pelites from the Damaran Orogen Cu does not correlate with sulphur (Haack et al., 1984).

Some potential source rocks are now discussed in the following:

- Basalts, in particular tholeiites, have high Cu and Zn values (Wedepohl, Handbook of Geochemistry). Brines percolating through such rocks should carry both Cu and Zn, and are unlikely to account for the Abra mineralization. Furthermore, there are no basalts in the lower Bangemall Group, and the basement probably consists of granite (see chapter 2.2.).
- Black shales are regarded rather a sink than a source of metalliferous brines (despite abundant metal contents) because of the immobility of metals under reducing conditions (Gustafson and Williams, 1981).
- In sandstones and carbonates subsurface brines are known to be enriched in Ba (among other elements). Brines from carbonates have a molar Sr/Ba ratio of 10^{-2} to 10^2 (Hanor, 1966) which may be too high to account for the generally low Sr content of barites from Abra (see chapter 4.1.2.).
- One potential source of Pb- and Zn-enriched sulphate brines might be carbonates desposited in evaporitic basins (Thiede and Cameron, 1978). But no evaporites are known in the basal Bangemall Group, and the basement consists of granite.
- To form Pb-rich deposits from formation waters, the source strata should comprise large volumes of arkose derived from granites in arid environments inhibiting dispersion by chemical weathering (Gustafson and Williams, 1981).

In view of the predominance of Pb and Ba in the Abra mineralization the source rocks should be rich in potash feldspars and therefore only arkose of the basal Bangemall Group (i.e. equivalent to the Tringadee Formation or the Mount Augustus Sandstone), or the granitic basement are capable of providing sufficient crystallographic sites for Pb and Ba. Carbonates and black shales have been ruled out because the basal Bangemall Group probably did consist of coarse-grained arkose.

However, both arkose and granite are void of Cu, and an additional mechanism must be invoked to explain the Cu content of the Abra mineralization.

Prior to deposition of the Bangemall Group the basement has been subject to erosion for some 200-400 m.y. With the onset of Bangemall Group sedimentation some block faulting led to uplift of basement blocks which were rapidly eroded and provided coarse-grained clastics (arkose) for deposition in adjacent sinks (cf chapter 1.2.5.2). This is the scenario of red-bed copper formation as summarized in Table 4.10. Features of sandstone lead, and carbonate-hosted zinc-lead deposits are also shown for comparison.

Table 4.10 from Bjørlykke and Sangster (1981)

Comparison of the Major Features of Intracratonic Sedimentary Cu, Pb, Zn Deposits			
Deposit type	Red-bed copper	Sandstone lead	Carbonate-hosted zinc-lead
Metal ranking	Cu >> Zn + Pb	Pb > Zn > Cu	Zn > Pb > Cu
Host rock	Arkose, feldspar sandstone, shale	Quartz sandstone	Dolomite
Depositional environment	Continental	Continental-shallow marine	Shallow marine
Tectonic environment	Rifting	Stable	Stable
Climate	Arid to semiarid; warm	Semiarid. warm to cool(?)	Arid to semiarid; warm
Cement	Calcite-dolomite-quartz	Quartz	Dolomite
Ultimate metal source	Basement	Basement	Basement
Immediate metal source	Oxide coating from mafic minerals	Feldspar in arkose or basement	Carbonate, evaporite, shale
Sulfur isotope composition	Light	Light and heavy	Heavy
Transport medium	Ground water	Ground water	?

Note that sandstone lead deposits occur in mature sandstones (Bjørlykke and Sangster, 1981), whereas the basal Bangemall Group consists of immature feldspatic, continental clastites.

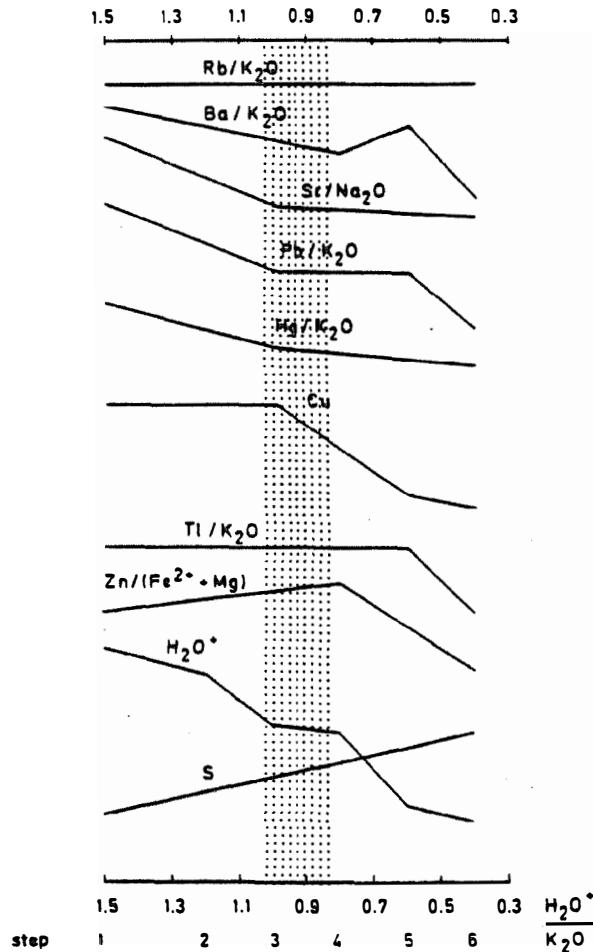
If a red-bed copper mineralization in arkose became subject to metamorphism the resultant fluids would contain Cu derived from the red-beds, as well as Pb and Ba released by the decay of potash feldspars.

Interestingly, Rose (1976) has deduced that copper red-beds have formed from sulphate-rich chloride brines that were slightly alkaline, with Eh values within the hematite field (at those low temperatures). Mobilization of fluids during metamorphism, therefore, could produce solutions of similar composition, and could explain the abundance of sulphate and the comparatively high pH, Eh values (in contrast to sediment hosted base metal deposits) of the Abra hydrothermal system.

Metal release during metamorphism

It has been shown in chapter 4.6.2. that temperatures during mineralization in the wall rocks to the Abra mineralization were sufficient for abundant generation of chlorite, which is equivalent to lower greenschist facies grade, and it can be assumed that in the underlying rocks higher grades were attained. Any zinc in solution or within minerals would be incorporated into staurolite once this isograd reaction (3) occurs (see above). On the contrary, Pb and Ba contained in feldspars and muscovite are released under these metamorphic conditions. Haack et al. (1984) have quantified the loss of metals during regional metamorphism in pelites of the Damara Orogen, Namibia, and their results are summarized in Fig. 4.23. The shaded area marks the envisaged metamorphic range, of the basal Bangemall Group between the representative reactions 3 and 4 (4: staurolite+muscovite+quartz = andalusite+biotite+H₂O).

Fig. 4.23: After Haack et al.(1984), showing the inferred metamorphic range(stippled) of the source rock level. Step numbers represent metamorphic isograd reactions.



Synopsis of element depletion patterns at various degrees of reaction (expressed by the ratio H_2O^*/K_2O). Ordinate: Element ratio or element content as indicated on curves (arbitrary scale)

Fig. 4.23 after Haack et al. (1984). The step numbers represent metamorphic isograd reactions. The possible conditions in the source rocks of the Abra mineralization are marked by the shaded area.

The loss of metals from pelites at this metamorphic interval would be in the range of some 30 % Cu, 30 % Pb and 20 % Ba (Haack et al., 1984). In an arkose, it may be significantly greater because Pb and Ba are dominantly contained in potash feldspars which have completely been destroyed at this metamorphic grade.

For an assumed loss of 75 % Pb from an arkose ($d = 2.5 \text{ g/cm}^3$) with an average Pb content of 30 ppm, the formation of an orebody of about 130 mt at 1.15 % Pb would require leaching of some 25 km³ of arkose. With a possible thickness of 1.6 km it would occupy an area of 4 x 4 km. For generation of the barite mineralization (130 mt at 2.5 % Ba) from arkose (average of 500 ppm Ba, 50 % mobilized) the calculated volume would only be about 4 km³, suggesting that the arkose and an elevated Pb content. No calculation of the volume required to form the Cu mineralization was attempted because not even the order of magnitude of Cu concentration in the red beds is known.

One may argue whether all metals were derived from granite because, in addition to sufficient Pb and Ba, it may contain 30 ppm Cu (Bowen and Gunatilaka, 1977; Wedepohl, Handbook of Geochemistry).

Average values of granite (from Handbook of Geochemistry):

Pb = 15 - 56 ppm

Ba = 1000 - 1300 ppm (Standard Granite, G1)

Cu = 10 - 30 ppm.

However, the Pb/Cu ratio in the Abra mineralization is about 5 (in contrast to 2 in granite), resulting in a theoretical range of Cu in granite of 2 - 10 ppm, and cannot be explained by differential mobilization of Cu and Pb during metamorphism. Furthermore, arkose has a porosity at least four times that of granite, and thereby making it more suitable than granite for the transport of large amounts of fluids in reasonably short time.

Summary

Mobilization of metals from a red-bed arkose of the basal Bangemall Group during thermal (i.e. non-regional) metamorphism is an attractive model and would be the only mechanism that accounts for

the metal abundance ratios in Abra mineralization, the probable metamorphic grade, the tectonic setting of upfaulted basement blocks, the probable source rocks derived from these granites, and the porosity required for rapid lateral and vertical fluid migration.

This model also explains why some low-grade base metal mineralizations in carbonates of the Irregully Formation in the Bangemall Basin are located adjacent to granitic basement highs, and are characterized by Pb and Cu dominance over Zn (see chapter 1.2.7).

Although somewhat speculative, the model of differential metamorphic mobilization of metals (according to Haack et al., 1984) indicates an overall control of the base metal mineralizations in the Bangemall Basin by increasing geothermal gradient: Pb - Cu - Ba mineralizations in the Irregully Formation (including Abra) stem from comparatively low-temperature mobilization of metals which, however, requires above-average heat-flow to reach the staurolite isograd at some 2000-3000 metres depth. During further development of the Bangemall Basin heat flow increases and allows for mobilization of dominantly Cu. These fluids are channelled into major basin faults, like the Mount Vernon Fault, and account for syndiagenetic Cu mineralization in the Glen Ross Shale Member of the Kiangi Creek (see chapter 1.2.7.). In times of the upper Jillawarra Formation heat flow has further progressed, and the decomposition of staurolite and biotite at this metamorphic grade releases significant amounts of Zn, which also were channelled into fault zones and led to syndiagenetic, Zn-dominated mineralizations in the upper Jillawarra Formation at Quartzite Well and Mt. Palgrave (see chapter 1.2.7.).

Finally, mobilization of lead from detrital feldspars derived from granitic basement could give a clue to the lead-lead model

age of 1600 m.y. in the Abra mineralization. Differential mobilization of lead may explain why other, low-grade Pb-Cu mineralizations in the Bangemall Basin have lower lead-lead model ages, because the geothermal gradient was smaller in those area, at that particular time, allowing release of only small amounts of lead, of possibly specific isotopic composition.

4.8. Mineralizations in the Jillawarra Belt (except Abra)

Since explorational activity in the area of the Jillawarra Belt commenced in 1974, several target areas have been defined by magnetic and soil/rock chip geochemical surveys. Geochemical anomalies have been identified, but no significant outcrop of mineralization was discovered so far.

To test the geochemical and geophysical anomalies some 30 diamond drill holes were drilled on nine prospects the locations of which are shown in map 3.

Notably, all prospects are situated within the limits of the Jillawarra Basin and the Gap Well Formation.

Fig. 4.24 displays the stratigraphic interval intersected by the various drill holes in correlation with the Abra stratigraphy, and zones of significant mineralization.

In Tab. 4.11 the grades and characteristics of the mineralization are presented; prospects with negligible grades of mineralization (e.g. "Jeds Prospect", "Manganese Range East Prospect") are excluded from Tab. 4.11 and will not be discussed any further.

According to the nature of the host rock two types of mineralizations can be distinguished. In allusion to Abra these are termed a) black zone type and b) stringer zone type.

a) Black zone type mineralization

The host rock is a 37 metres thick sequence of laminated magnetite-quartz-carbonate rock which frequently is brecciated and veined (Fig. 4.25).

		P r o s p e c t					
		N a m e o f		P r o s p e c t			
Features of mineralization	"46 - 40" representative drill hole: 77 - 28	"Woodlands" representative drill hole: 81 - 5	"IP" representative drill hole: 81 - 8	"TC" representative drill hole: 78 - 35	"Manganese Range" representative drill hole: 77 - 27	"Copper Chert" representative drill hole: 76 - 20	
significant intersections (over core m)							
Pb %	3.10%(110-114), 1.30%(131-134)		3.60%(594-598), 4.70%(623-625)		0.23% (118-130)		
Cu %	0.30%(113-115), 0.25%(135-147)	0.29%(372-410), ~0.40%(442-460)	10.90%(593-598), 9.90%(623-625)	0.31% (519-565) = 46 ml n.d.	0.91% (332-345) n.d.	1 vein with 2.5% (216.8-217.0)	
Ba %	15.00%(132-138) no continuous assays	5.90%(372-410), ~4.00%(422-460)	0.25%(890-891)				
Zn %							
"background" range (enriched in:)							
Pb ppm	50 - 1500 (black zone, footwall)	0 - 325 (-)	50 - 10000 (400 - 960 m)	0 - 70 (-)	0 - 50 (≤ 670 ppm above 86 m)	no assays	
Cu ppm	10 - 500 (lower black zone)	10 - 75 (-)	25 - 375 (594 - 598 m)	5 - 670 (-)	35 - 8500 (313-370 m)	" "	
Ba ppm	n.d.	300 - 1800 (-)	4000 - 60000 (570 - 1200 m)	n.d.	n.d.	" "	
Zn ppm	35 - 100 (upper black zone)	10 - 450 (above mineralized zone)	40 - 350 (-)	15 - 225 (-)	25 - 115 (≤ 410 ppm above 74 m)	" "	
mode of occurrence	cpy in veins (with qz-mag) ga in veins and disseminated, irregular patches of ba	ba, cpy in vein, cpy disseminated with in chloritic fine grained sediment; ba cement and cpy disseminated in Woodlands Arenite	in calcareous vein breccia	disseminated, mag-qty vein; ba-qz-cte veins	cpy-mag-qz veins; patches of cpy	cpy-sph-py veins	
associated minerals	- py, veins and conformable layers - Fe-Mn cte, mag - chl, jaspilite	- abundant mag; - subordinate py, po in hangingwall - Fe-Mn cte - chl, bio, hyalophane	- mag, py - bio, chl	- py, minor po - mag, in layers and disseminated - cte, ba - chl, bio	- mag, layers and disseminated - minor py - ba - chl	- py, po, layers and disseminated - ba - chl	
host rock	brecciated mag-qz-chl-ba-cte rock, laminated (Black Zone-type)	370-410 m: silicified chloritic siltstone/sandstone 422-460 m: silicified coarse grained arenite (Woodlands Arenite)	593-598 m: brecciated dolomitic Arenite 678-788 m: no sulphide mineralization in Woodlands	silicified chloritic magnetite-rich (in layers and disseminated) siltstone / sandstone	chlorite-magnetite-quartz schist, partly brecciated	laminated chloritic and dolomitic siltstone	
stratigraphic position of best interval of mineralization	upper GM6	lower GM5 upper GM4	lower middle GM5	lower GM5	lower GM5 (or upper GM4)	lower GM6	
zoning	not clear; Mn enriched in upper part of black zone and above black zone	more Ba in upper mineralized zone; absence of Pb in Cu-rich zones	extreme "telescoping": highest assays of Pb, Cu, Ba, Ag in 4 m interval (594-598m)	not clear because only Cu mineralization; Mn enriched above Cu-zone(455-500m)	Mn enriched above 250 m		
correlation	Ag (Zn) with Pb	possibly Mn with Ba	- Ba with Pb - Ba with Mn, however, Mn is more widespread - Ag with Pb	Au with Cu (no continuous assay)			
alteration	silification, chloritization brecciation	silification, chloritization	silification, chloritization brecciation	silification, chloritization	silification, chloritization, minor brecciation	silification, chloritization	
remarks	highest Mn-values in lower part of hole, associated with mag-veining, several thin jaspilite interbeds in black zone	Ag, Au ≤ 1 ppm; within mineralized zones Pb, Zn do not exceed 90 ppm; highest Mn values in lower part of hole; no significant mineralization above 360 m.	highest Mn-values associated with mag enrichment, 678-788 m in Woodlands Arenite and 970-1200 m in dolomite/siltstone; mineralization clearly related to veining and brecciation; Au < 0.01 ppm	intense ba-qz veining below about 450 m (no assays); cpy and py generally associated with mag-rich beds. Au < 0.1 ppm (no continuous assay)	ba-veining throughout the hole; mag very abundant throughout the hole	no significant mineralization; probably no ba, mag	

Abbreviations: n.d. - not determined ba - barite cpy - chalcopyrite py - pyrite chl - chlorite
ga - galena sph - sphalerite po - pyrrhotite hem - hematite qz - quartz bio - biotite
mag - magnetite cte - carbonate

Table 4.11



Fig. 4.25: Black zone type magnetite-carbonate laminae in core specimen from the 46 - 40 prospect.

This sequence occurs in hole 77-28 of the "46 - 40 Prospect" only (cf. Fig. 4.24), at a similar stratigraphic level as the black zone of Abra and is similar in thickness. It is, however, not overlain by red zone type sabkha sediments suggesting a less pronounced regressional development.

During sedimentation of this black zone the environment was less oxidizing and probably less saline as opposed to the Abra black zone. Hematite is almost entirely absent and very few pyrite layers indicate growth of only few microbial mats. The occurrence of pyrite layers probably is related to the decomposition of microbial mats through the activity of sulphate reducing bacteria. This points to a permanent cover of only moderately oxidizing water.

The often distinct layering of magnetite-quartz-carbonate (i.e. chemical sediments) suggests very quiet conditions of sedimentation, probably in a restricted basin. However, the absence of conformable sulphate layers (all barite seems vein-related) implies salinities below sulphate saturation within the sediment and basin waters.

The mineralization is dominated by galena and barite with subordinate quantities of chalcopyrite (cf Tab. 4.11). It is of discordant nature (veins and disseminated) and accompanied by silification (replacing carbonate), chloritization and brecciation.

In summary the black zone of the "46-40 Prospect" differs from the black zone of Abra with respect to the following features:

- not overlain by a red zone
- less oxidizing and less saline environment of sedimentation
- low-grade mineralization
- less syndiagenetic pyrite, therefore probably lower fS_2 during times of mineralization

Despite these differences the black zone sediments of the "46-40 Prospect" belong to the same genetic class (subaqueous evaporite iron formation) as the Abra black zone. The mineralization - Pb, Ba, (Cu) dominated and lacking Zn - is almost identical in style (discordant) and mineralogy to the Abra mineralization.

b) Stringer zone type mineralization

This type of mineralization is encountered in all drill holes listed in Tab. 4.11 including the footwall of the "46-40" black zone. The host rock usually is a chloritic, magnetite bearing siltstone and fine-grained sandstone of the GW_5 (and lower GW_6)-unit (Fig. 4.26).

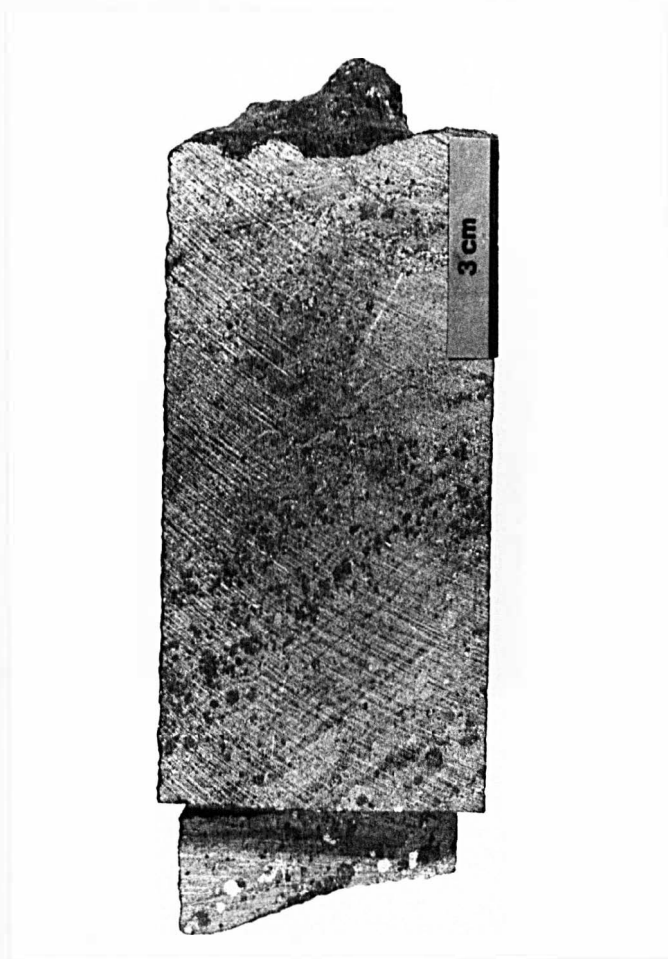


Fig. 4.26: Laminated chloritic siltstone with layers of magnetite, and disseminated blebs of magnetite (subhedral) and pyrite (subhedral).

In the TP-81-8 drill hole the host to the mineralization is a brecciated dolomicrite with chlorite/biotite stringer and secondary (whitish, sparitic) carbonate (Fig. 4.27).

A feature common to all rock types is the frequency of magnetite, either as layers in fine-grained siltstone (up to 60 % magnetite in rocks from the Manganese Range Prospect) or disseminated in arenites (Woodlands Arenite) and dolomites. Hematite and jaspilite are occasionally associated with magnetite but are not abundant.

The mineralization is Cu-Pb-Ba dominated (lacking Zn) with chalcopyrite, galena and barite being the only ore minerals.

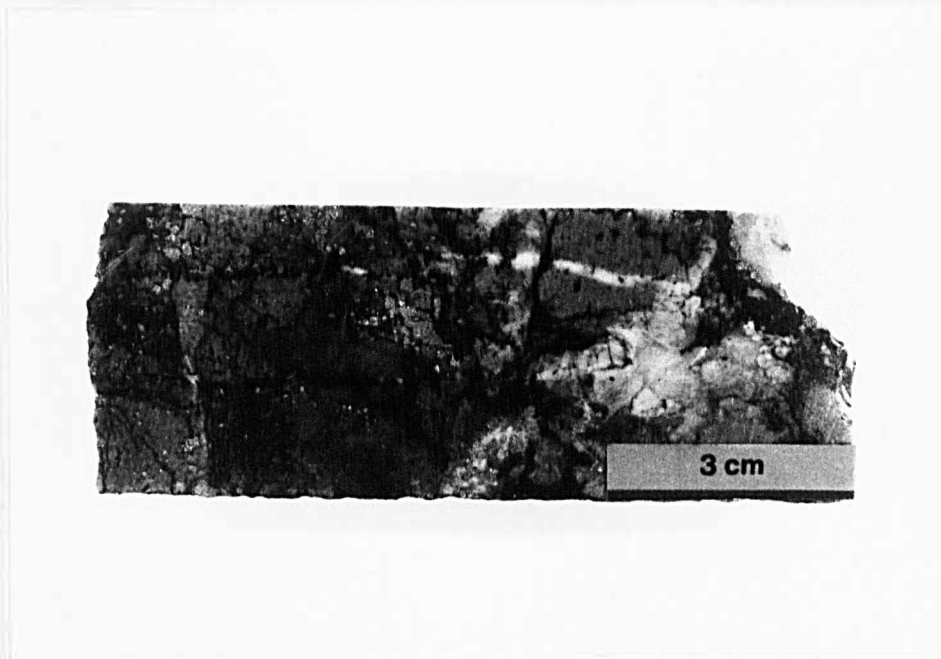


Fig. 4.27: Brecciated dolomicrite with chlorite/biotite stringers and secondary carbonate.

Galena usually occurs together with pyrite, either within or as seam to pyrite (cf Fig. 4.04) which may indicate a post-pyrite emplacement of galena (i.e. pyrite has formed diagenetically and was replaced by galena later during diagenesis).

Abundant inclusions of magnetite/hematite in pyrite suggest diagenetic growth of pyrite within the sediments incorporating pre-existing iron oxides.

Although some chalcopyrite occurs on fractures in pyrite most of the chalcopyrite is associated with magnetite (usually as inclusions, cf Fig. 4.08).

The style of mineralization comprises three types,

- vein
- vein breccia
- disseminated, patchy

All are discordant to bedding and associated with silification and chloritization, and with the emplacement of barite, Fe, Mn-carbonates, magnetite and minor pyrite.

Vein mineralization is by far the dominant type. Fig. 4.28 shows a chalcopyrite-siderite vein in chloritic siltstone which is almost identical to veins from the stringer zone of Abra (cf Fig. 4.07).

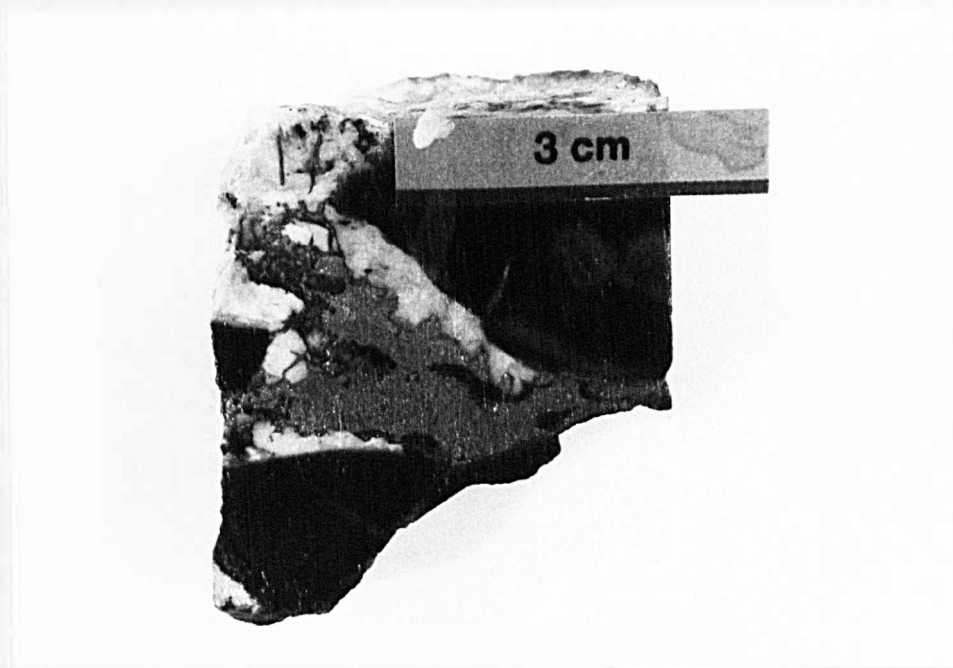


Fig. 4.28: Chalcopyrite-siderite vein in chloritic siltstone (46-40 prospect).

The stratigraphic position of the mineralized intervals is below that reached by Abra drill holes (Fig. 4.24). However, the lithology of the host rocks is comparable to the lower stringer zone of Abra and consists chiefly of chloritic siltstones and fine-grained sandstones, except a brecciated dolomicrite in the TP-81-8 hole.

Significant barium and local copper mineralization occur in the Woodlands Arenite Member (GW_{W4}) underlying the chloritic siltstone/sandstone interval. Higher grades of mineralization though are always found in the hanging wall of the Woodlands Arenite.

Zoning

Vertical metal zonation within a single drill hole is difficult to recognize mainly because only one metal is dominant per drill hole while concentration of the remaining metals usually are in the "background" range and are distributed irregularly throughout the hole.

However, comparison of the stratigraphic position of mineralization between the various drill holes reveals a faint vertical zonation pattern (Fig. 4.24). While all copper mineralizations occur within the GW_{W4} and/or lower GW_5 -unit (except hole 76-20 where the mineralization seems fault-related) lead dominated mineralizations occupy higher stratigraphic levels (81-8; 77-28).

Copper dominated mineralization at lower stratigraphic levels overlain by an interval enriched in lead is compatible with the Abra zonation pattern. However, a barium-rich interval stratigraphically above (as the red zone in Abra) cannot be distinguished; barium is closely associated with the lead and copper mineralizations.

Another important difference to the Abra metal distribution pattern is the occurrence of the mineralizations generally 100-200 metres lower in the stratigraphy.

Thus, the occurrence of barium with lead/copper and the lower stratigraphic level of mineralization suggest lower temperatures

and less volume of the hydrothermal fluids as compared to Abra; lower temperatures prevented ascent of the solution to Abra levels, and less volume resulted in a higher wall rock/hydrothermal fluid ratio which in turn makes the hydrothermal solutions susceptible to wall rock reactions and causes close spatial precipitation of most metals (including barite).

The "46-40 Prospect" is the only exception from the trend described above. Not only is the host rock of black zone type but the mineralization reaches the same stratigraphic level as in Abra suggesting a similar heat regime. A localized high geothermal gradient probably was present in this area because the "46-40" mineralization occurs in the vicinity of the Woodlands Fault which forms the western margin of the Jillawarra Basin (the Abra mineralization is located at the eastern margin fault of the Jillawarra Basin).

Summary

Compared to Abra the mineralizations of the Jillawarra Belt are similar as regards the following major features:

- metals; Cu-Pb-Ba dominated, lack of Zn
- association of ore minerals; while galena preferentially is concurrent with pyrite chalcopyrite has an affinity to magnetite
- association of none-ore minerals; mineralization usually is accompanied by Fe, Mn-carbonates, magnetite, pyrite, chlorite, quartz and minor jaspilite
- alteration; mainly silification, chloritization and minor albitization
- host rock; both stringer zone chloritic siltstone/sandstone and black zone laminated magnetite-quartz-carbonate rock

- mode of emplacement; chiefly veins and disseminations, locally with concomitant brecciation
- zoning; although poorly developed
- fO_2 ; abundant magnetite, slightly less hematite may be due to lower stratigraphic level
- fS_2 ; magnetite dominant over iron sulphide, frequent syndiagenetic pyrrhotite indicates lower fS_2 within the sediments

All mineralizations can be classified as low-grade Abra-type and comprise black zone type ("46-40 Prospect") and lower stringer zone type (all prospects including the lower part of the "46-40 Prospect"). The hydrothermal system(s) probably has been related to the Abra hydrothermal system with respect to timing and metal source.

The differences to Abra described before and the low-grade nature of the mineralizations may be due to a lower geothermal gradient in most parts of the Jillawarra Basin during times of mineralization.

Section 5 Genesis of the Abra mineralization and some impli-
cations for the development of sediment-hosted
metal deposits

5.1. A model for the genesis of the Abra mineralization

Abundant data on the geology, mineralogy and chemistry of the Abra mineralization and the Jillawarra Belt has been presented in this study and permit development of a comprehensive model of the genesis and chronology of ore formation in relation to the geotectonic development.

5.1.1. Geotectonic setting

The intracratonic sedimentary Bangemall Basin is one of the largest intrusive continental tholeiite provinces of the world. Intrusion of dolerite into sediments commenced approximately during deposition of the middle Bangemall Group, and obviously was related to a tensional crustal regime in the sialic basement.

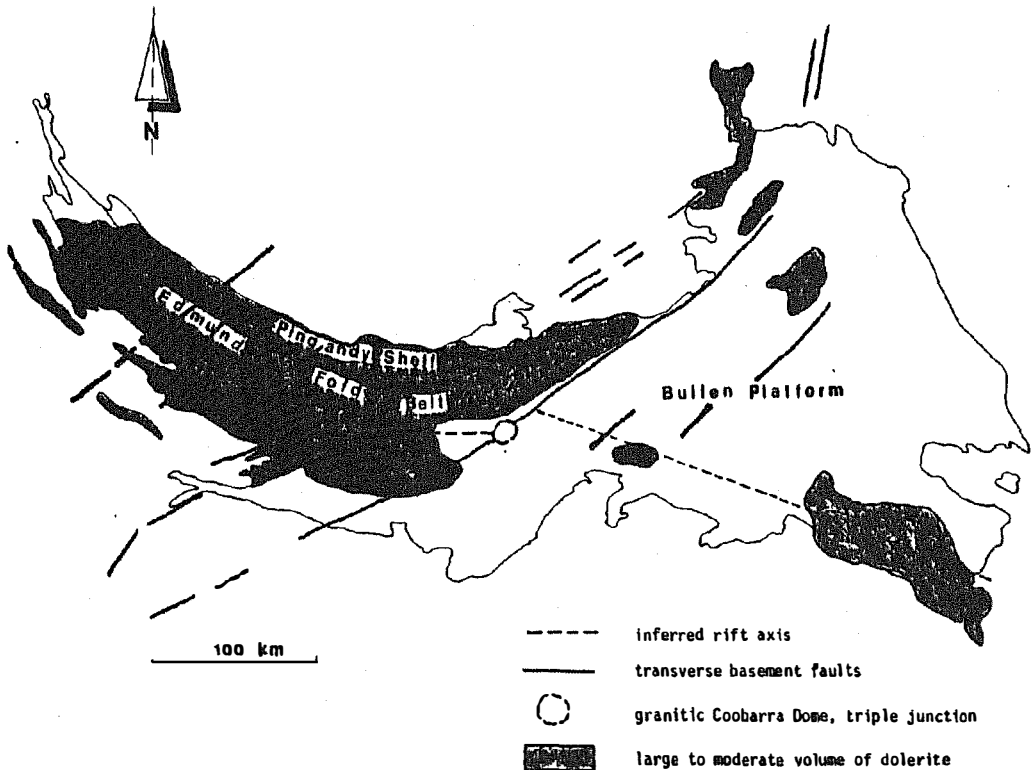
Two sets of folds (NE-trending and E-trending) are dominant, and have been active during and after deposition of the Bangemall Group. These faults are mainly present in the Edmund Fold Belt, one of three structural provinces distinguished, which formed on mobile basement. Folding here produced open-style drape folds which, in the final stage of deformation, have been tightened due to NNE-SSW directed compressional forces.

The sedimentary history of the Bangemall Basin indicates very shallow water conditions in the lower Bangemall Group, followed by a regressional interval and two major transgressions, and subsequently by a regressional interval marking the infill of a sedimentary basin.

Structural and depositional evolution of the Bangemall Basin are in accordance with the development of an intracratonic rift which never reached the state of intercratonic rifts. During times of extension, transgressional sedimentary sequences were deposited, while termination of crustal extension is marked by a regression at the end of the Bangemall Group. Sawkins (1976) presented a list of worldwide examples of continental rifting between 1200 m.y. - 1000 m.y. which have many features in common with the Bangemall Basin.

The irregular quantitative distribution of dolerite (Fig. 5.01) in relation to major basin faults and lineaments implies the former presence of a triple junction (cf chapter 1.2.6.2.), in the area of the granitic Coobarra Dome (Fig. 5.01), east of which the intracratonic rift bifurcates.

Fig. 5.01 Distribution of dolerite in relation to lineaments and structural provinces of the Bangemall Basin



The Jillawarra Belt principally reflects the sedimentological and tectonic development of the Bangemall Basin. However, subsidence within the Jillawarra Basin (cf Fig. 2.61) occurred earlier than elsewhere in the Bangemall Basin; represented by the WC₁-init. Subsidence in WC₂ times was more pronounced (shallow water turbidites) within the Jillawarra Basin than in surrounding areas. This indicates the commencement of rifting of the Bangemall Basin within the Jillawarra Basin, as a central, axial, initial rift valley.

The development of the Abra sub-basin indicates crustal doming in this particular area, characterized by an interval of pronounced regression from subtidal siltstones over subaqueous evaporitic iron formation to coastal sabkha. This sequence was deposited in a fault-bounded restricted basin which formed in the apical zone of the crustal dome, due to greater strain in the periphery.

Doming in the Abra area implies that the adjacent granitic Coobarra Dome also was subject to doming in times of the Upper Gap Well Formation. It is inferred that a thermal plume (hot spot) in the underlying mantle was responsible for doming in the Abra-Coobarra Dome area, analogous to the development of "high spots" over mantle plumes in Africa (Thiessen et al., 1979).

From the hot spot sufficient heat was transferred to high crustal levels to facilitate mobilization and ascent of large amounts of metal-bearing fluids, and the following model is based on this concept.

5.1.2. Source rocks

It has been concluded in chapter 4.7. that the source rock of the Abra metals has been arkose with features of red-bed copper mineralization. The tectonic setting of the depository of the arkose adjacent to a rising granitic dome permits accumulation of great thicknesses (possibly in excess of the 1650 m maximum thickness of the Tringadee Formation), and is in accordance with the typical tectonic setting of red-bed copper deposits (Tab. 4.10). Due to the unusually high heat flow rapid breakdown of potash feldspars occurs releasing Pb and Ba which substitute for K. For an assumed thickness of 1650 metres, and 30 ppm average Pb content, an area of 4 x 4 km would provide sufficient volume to account for some 1.5 mt of lead metal in Abra. Red-bed arkose in the source region also explains the abundance of magnetite/hematite in the stringer zone; hematite, abundant in red-beds, would be reduced to magnetite when the arkose is heated.

Red-bed formation on the basement in the areas surrounding the Jillawarra Belt provides a huge source of iron which was transported into the Abra sub-basin (and the Jillawarra Belt) by weathering solutions, where it was deposited as iron formation of the black and red zone.

5.1.3. Accumulation of metal-bearing fluids

Progressive burial and increasing heat flow induced continuous production of water and metal ions by metamorphic mineral reactions. High porosity of the arkose allowed rapid lateral and vertical migration of the metal-bearing fluids.

The dome structure of the Coobarra Dome led to trapping of the fluids near the top of the permeable strata, analogous to structural traps in petroleum geology. The Tringadee Formation is characterized by an increasing number of siltstone interbeds towards the top (Muhling et al., 1978). Assuming some impermeable horizons in the

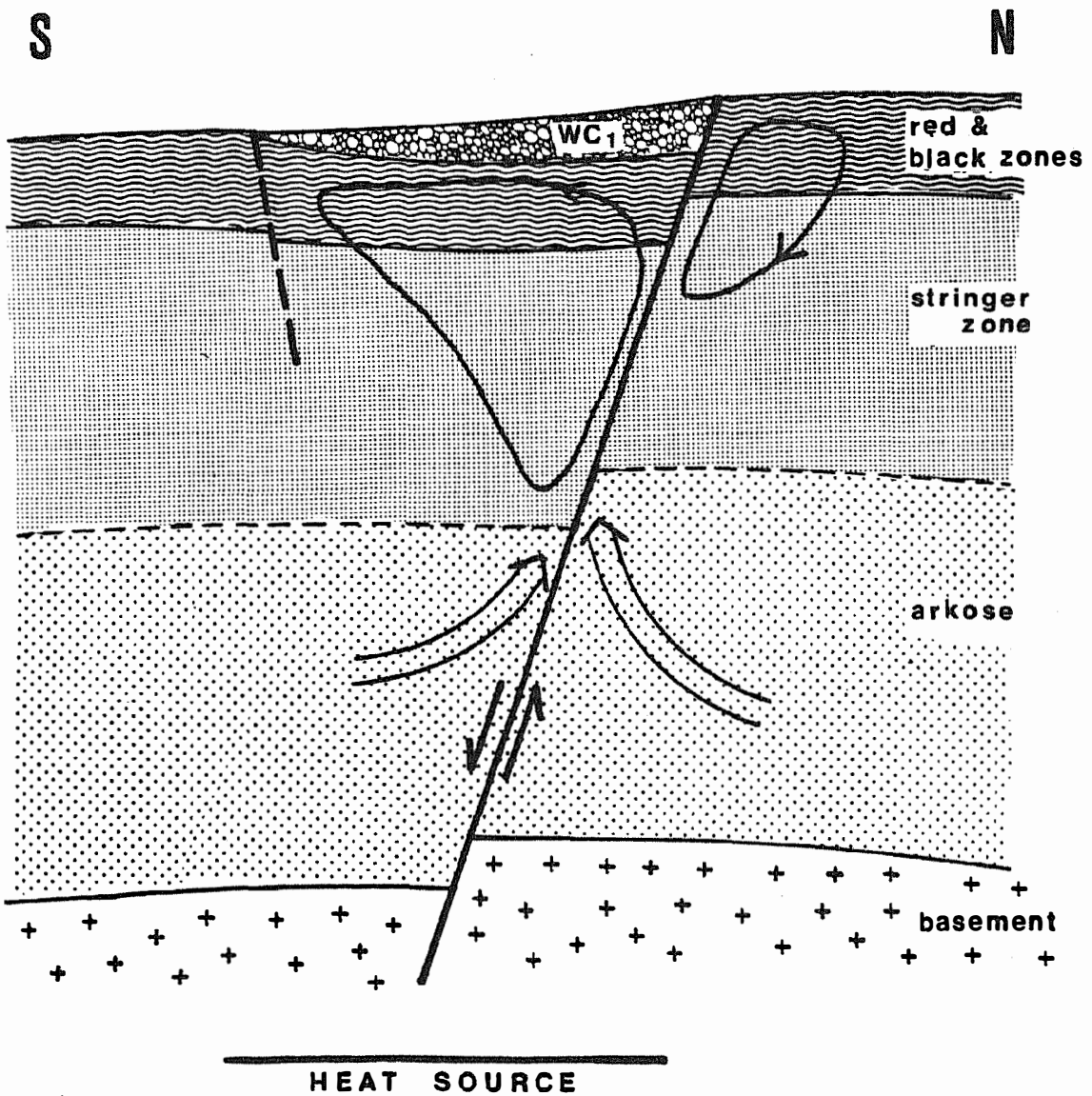
upper arkose large volumes of hot metal-bearing fluids have migrated up-dip and accumulated in a structural trap. No ascent of the fluids to higher stratigraphic levels took place because, at this stage, there were no deep-seated faults which could serve as a conduit.

5.1.4. Ascent of the hydrothermal fluids

Tensional forces in the crust led to incipient rifting which is expressed by the generation of deep-seated normal faults. One of these faults is the northern margin fault of the Abra sub-basin, controlling the distribution of the coarse clastic WC₁ facies. This fault extended into the basement, and cut through the arkose. The hot, metal-bearing solutions in the structural trap within the upper arkose were now channelled into the conduit provided by the fault zone. Because of the comparatively low permeability of the black and red zones a convective system developed. Widespread brecciation seen in the stringer zone indicates that hydraulic fracturing took place facilitating the percolation of hydrothermal fluids. No significant exhalation onto the contemporaneous sea floor occurred. These processes are shown schematically in Fig. 5.02. Surprisingly, of the three margin faults of the Abra sub-basin only the E-trending, northern fault served as a conduit for hydrothermal solutions, possibly because not all faults penetrated the arkose or, because they have also been boundary faults of the arkose depository and therefore did not have access to large amounts of fluids.

The driving force of the hydrothermal system was the heat source at depth, which also controlled the ascent of hydrothermal fluids in response to probably significant vertical temperature gradients. Contemporaneous faulting along the feeder channel suggests that the ascent of hydrothermal fluids was supported by seismic pumping as described by Sibson et al. (1975).

Fig. 5.02: N - S section, not to scale, schematically showing ascent of hydrothermal fluids during times of WC₁-deposition; size of convective system is speculative. Shape of convective cells after Henley and Thornley (1979) and Large (1981).

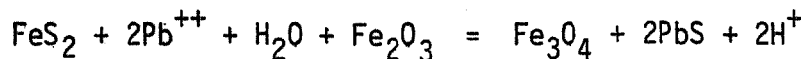


A side-effect of the anomalous high heat flow was felsic volcanism on the Coobarra Dome, characterized by hydroclastic eruptions which were induced by faulting of the basement. Despite their spatial separation, hydrothermal processes and felsic volcanism are thus related in that they are contemporaneous and generated by the same principal mechanism.

5.1.5. Emplacement of the Abra mineralization

The metals were transported in hot (ca. 250^o C, cf chapter 4.4.) solutions in small veinlets radiating from the main feeder channel, which penetrated the sediments of the stringer and black/red zones. These strata were in the state of diagenesis and still contained abundant, partly hypersaline formation waters. The hydrothermal system was coupled to this diagenetic formation water system, which facilitated percolation of the fluids and distribution of metals to distal positions.

Sulphides were emplaced mainly in small veins in the stringer and black zones but also in the red zone. Galena and chalcopyrite precipitated in two elongated, concentric zones - emanating from the main feeder channel and transgressing lithological boundaries - according to their solubility which was largely a function of temperature. In addition to veins, galena (and minor chalcopyrite) also formed as replacement of pre-existing, syndiagenetic pyrite layers within hematite/magnetite bands. This replacement is expressed by the formula



and is thermodynamically favoured at 200^o C in the presence of lead ions. Further galena precipitation occurred where the lead-carrying fluids encountered free H₂S, generated by bacterial sulphate reduction and trapped in the sediment.

Some barite precipitated in veins concurrent with sulphides but the bulk of barite occurs strataform within the red zone. Here,

barite formation is due to quantitative replacement of Ca-sulphates in the sabkha deposits of the red zone. This reaction is favoured because of the very low solubility of barite. The quantitative nature of this replacement was due to high water content, sufficient porosity (intercalated clastites) and non-consolidation, at that stage, of the red zone sediments.

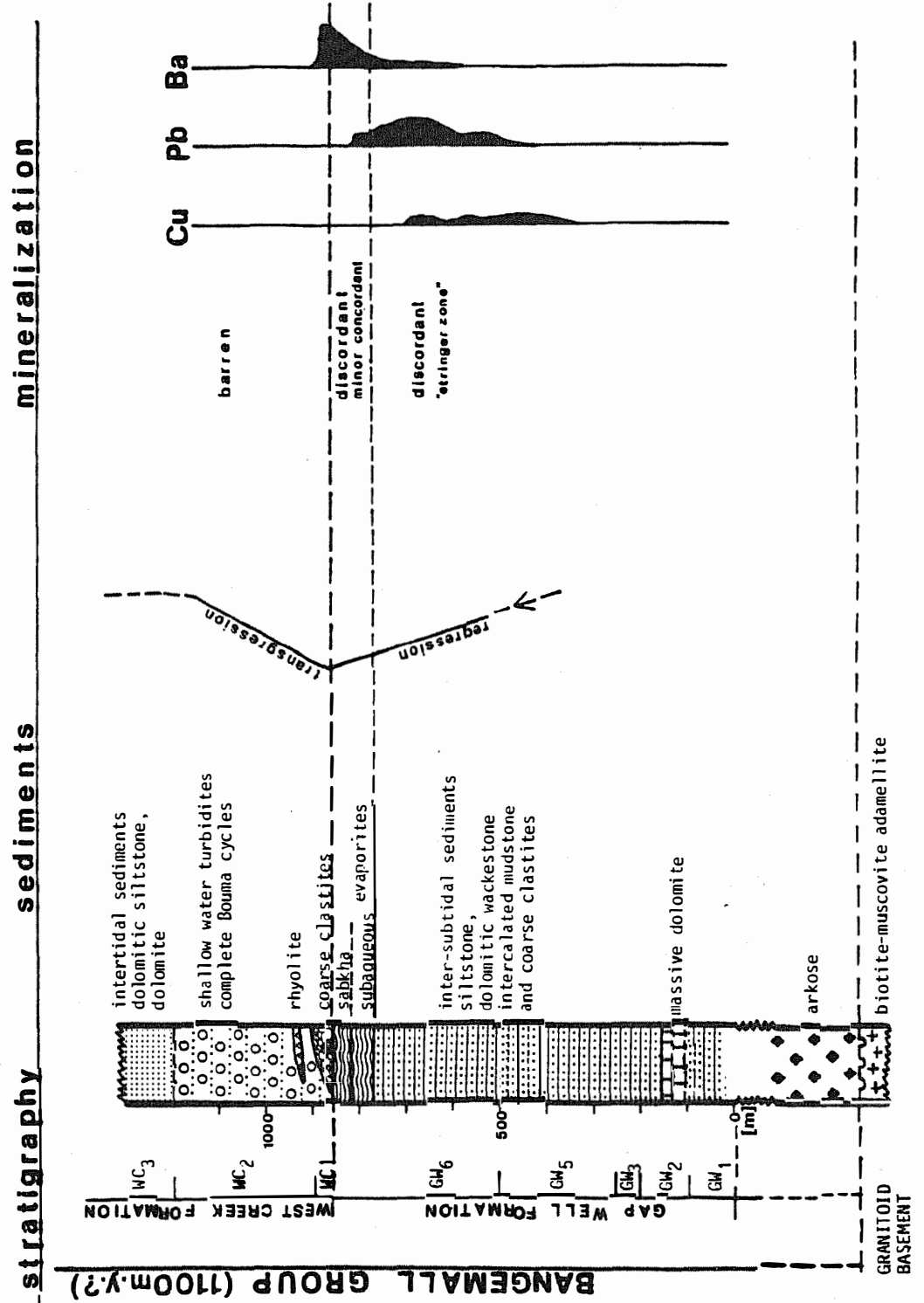
The sulphide-barite mineralization is accompanied by the three iron species hematite-magnetite-pyrite, the proportion of which change vertically through the Abra mineralization, indicating a vertical temperature decrease within the mineralizing system from clearly above 250⁰ C in the lower stringer zone to below 250⁰ C in the upper red zone.

5.1.6. Summary

A continental hot spot below the area of the Coobarra Dome initiated intracratonic rifting of the Bangemall Basin. Prior to rifting, doming occurred which resulted in deposition of a thick sequence of red-bed arkose adjacent to the dome. High heat flow linked the hot spot induced, advanced metamorphic mineral breakdown and mobilization of metal-bearing fluids.

With the onset of rifting faults penetrated into the basement and through the arkose, and channelled the fluids into one fault zone. The hydrothermal fluids ascended along the fault zone and percolated through the sediments of the Upper Gap Well Formation. Sulphides formed mainly in veins and as replacement of pre-existing pyrite. Barium-bearing solutions, however, penetrated the sediments until they encountered abundant sulphate in the red zone. This sulphate was present in the form of gypsum or anhydrite and was quantitatively replaced by barite. Fig. 5.03 summarizes the main features of the metal distribution and the host sediment sequence of the Abra mineralization.

Fig. 5.03: Summary of host rock sequence and main features of the Abra mineralization



5.2. Comparison with sediment-hosted metal deposits.

The Abra mineralization has features in common with sediment-hosted massive sulphide lead-zinc deposits according to Large (1983) and Sangster and Scott (1976), and with the group of Late Proterozoic copper deposits described by Rowlands (1980), Rowlands et al. (1978), Raybould (1978), Sawkins (1984), Lambert et al. (1984) and Fleischer et al. (1976).

5.2.1. Late Proterozoic copper deposits.

There are some similarities between the Abra mineralization and Late Proterozoic copper deposits, as the Zambian Copperbelt (Fleischer et al., 1976), Copper Claim, South Australia (Lambert et al., 1984) and White Pine, Michigan (Ensign et al., 1968). Similarities include the tectonic setting of an intracratonic rift; rifting is inferred by Sawkins (1984, Table 7.1.) for the South Australian province, and was demonstrated by Annels (1984) for the Zambian Copperbelt. Intracratonic rifting is plausible for White Pine (e.g. Gustafson and Williams, 1981), and Burke and Dewey (1973) conclude that in the area of the deposit a late Proterozoic triple junction above a hot spot has formed.

The three examples of Late Proterozoic copper deposits and the Abra mineralization are all hosted by shallow water sediments, and sabkha sediments are common in Mufulira, Zambia (Garlick, 1981), and in the South Australian province (Kapunda, Lambert et al., 1980). Both the Zambian and South Australian deposits are hosted by sediments laid down adjacent to basement highs (Fleischer et al., 1976; Rowlands et al., 1978), analogous to the Coobarra Dome.

While precipitation of Cu-sulphides in anoxic waters is assumed by Garlick (1981) for Mufulira, Zambia, replacement of pre-existing biogenic pyrite by ascending Cu-solutions during diagenesis is inferred for South Australia (Lambert et al., 1984) and White Pine (Wiese, 1973).

Of the Late Proterozoic copper deposits considered here the White Pine deposit most closely resembles features of the Abra Mineralization; it probably formed above a hot spot in the geotectonic setting of a triple junction, of which none of the arms reached the spreading state. The mineralization formed through ascending hydrothermal metal-bearing solutions replacing pre-existing pyrite during diagenesis of shallow water sediments. Interestingly, there is a red-bed sequence underlying the White Pine deposit (Ensign et al., 1968), supporting the assumption of an arkose with red bed features underlying Abra (see chapter 4.7.).

5.2.2. Sediment-hosted massive sulphide lead zinc deposits

Despite the above similarities with the Late Proterozoic copper deposits the Abra mineralization has many features in common with sediment hosted massive sulphide lead-zinc deposits. Large (1980, 1983) has listed parameters that reflect the presence of potentially mineralized geological environments for this group, i.e. first to third order basins, contemporaneous volcanicity, and these parameters apply well to the Jillawarra Basin as second-order, and the Abra sub-basin as third-order basin (cf chapter 2.6.5.).

Large (1980) has also listed parameters that reflect the presence of mineralization of the sediment-hosted massive sulphide lead-zinc type as:

- stratiform barite; this is abundant in the red zone
- stratiform hydrothermal chert; there is some chert and jaspilite in the red zone but it is uncertain whether this is of hydrothermal origin
- element zonation; there is a distinct vertical Cu-Zn-Pb-Ba zonation comparable to the zonation at Rammelsberg (Hannak, 1981)
- alteration; there are several types of alteration in Abra including
 - a) chloritization, like in the footwall of Sullivan, B.C.
 - b) albitization, like in the hanging wall of Sullivan, B.C.
 - c) silification, common in many examples of Large (1980)

- sulphur isotopes; not compatible with an exhalative origin of the Abra mineralization, but the values are comparable with Lady Loretta and Gamsberg (von Gehlen et al., 1983), as discussed in chapter 4.5.

5.2.3. Discussion and conclusions

In summary, the Abra mineralization combines features of the two groups of deposits considered, and a plot of the weight ratios of Cu-Pb-Zn of various deposits (Fig. 5.04) illustrates the uniqueness of Abra. However, this diagram might also indicate the intermediate position of Abra linking two major groups.

The Aggeneys, Namaqualand deposits, S.A., for which Anhaeusser and Button (1976) tentatively proposed a volcanogenic origin, have been classified as sediment-hosted exhalative deposits by Rozendaal and Stumpf (for the related Gamsberg deposit, in press). Weight ratios of Cu-Pb-Zn of the Aggeneys deposits form a trend interceding between Abra and the field of sediment-hosted massive sulphide deposits.

This trend indicates an affinity of Abra to the group of sediment-hosted massive sulphides rather than to the Late Proterozoic copper deposits. Allocation of Abra to the former group also is favoured in view of the large number of features in common with the sediment-hosted massive sulphide lead-zinc group of Large (1980, 1983).

In view of the intermediate position of metal ratios at Abra and Aggeneys between sediment-hosted massive sulphide deposits and Late Proterozoic copper deposits, however, it is suggested that these groups should not be viewed separately but considered as one comprehensive group of deposits which share major features like the tectonic setting and a crustal metal source. The term "sediment-hosted (base) metal deposits" is proposed for this group

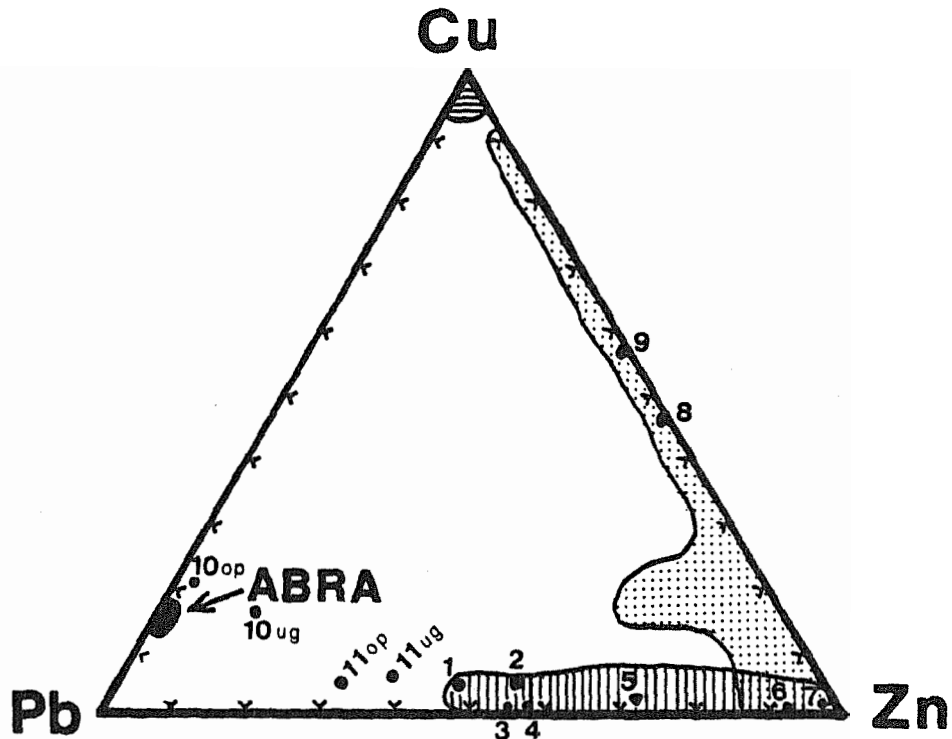


Fig. 5.04: Weight ratios of Cu, Pb, Zn in the Abra mineralization and in:



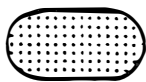
Field of sediment-hosted massive sulphide deposits, after Sangster and Scott(1976); 10,11 after Anhaeusser and Button(1976)

- 1 - Sullivan, Canada
- 2 - Rammelsberg, W-Germany
- 3 - Hilton, Australia
- 4 - Mt Isa, Australia (Pb-Zn body only)
- 5 - McArthur River, Australia
- 6 - Meggen, W-Germany
- 7 - Balmat(N.Y.), USA
- 8 - Sherridon, East Zone(Manitoba), Canada
- 9 - Bob Lake(Manitoba), Canada
- 10- Black Mountain, Aggeneys, S.A.
- 11- Broken Hill, Aggeneys, S.A.

op open pit
ug underground



Field of Late Proterozoic "stratiform" copper deposits; Zambian Copperbelt(Fleischer et al.,1976); Adelaide Geosyncline-Stuart Shelf, South Australia(Rowlands et al.,1978; Lambert et al.,1984); White Pine, Michigan, USA(Ensign et al., 1968)



Field of North American Precambrian massive sulphide deposits in volcanic or volcano-sedimentary host rocks, after Sangster and Scott(1976)

that includes a large number of deposits. Variations between the individual deposits, with respect to discordant-concordant nature of mineralization, exhalation or diagenetic replacement by the mineralizing fluids, relative metal abundance, presence of alteration, ultimately depend on the physical and chemical conditions in the mineralizing fluids and at the site of deposition, and on the composition of the source rocks. These are regarded second-order controls to the overall control of the tectonic setting.

Beales (1975) also followed the line of evaluating a common denominator, in proposing one genetic class of Mississippi Valley and Irish deposits. And Gustafson and Williams (1981), in their comprehensive review, combined stratiform copper, Late Proterozoic copper, sediment-hosted massive sulphide and Irish deposits into one major class, with the descriptive term "sediment-hosted stratiform deposits of Cu-Pb-Zn", although not all examples are in fact stratiform.

5.3. A model for hot spot induced base metal deposits

Mineral deposits

While continental hot spot related magmatic metal deposits (Sawkins, 1976; Mitchell and Garson, 1981) - although rare - are easily identified because of their association with alkaline intrusives, lavas and peraluminous granites, the same is not true for sediment hosted metal deposits. The latter type of deposit of which examples are given in Tab. 5.01, shows limited or unclear connections with magmatic rocks.

However, all deposits share the tectonic setting of an intra-cratonic rift and for some the relation to a triple junction has been proposed. Some deposits occur within or in close association with evaporitic sediments. So far the list of features is comparable with the comprehensive compilation of Gustafson and Williams (1981). But all deposits listed in Tab. 5.01 are associated with shallow water sediments, and more significantly, clearly exhibit a depositional trend which can be a single stage regression/transgression (e.g. Bangemall Basin) or repeated cycles. There is evidence at least from Sullivan, Bangemall Basin, Cobar and McArthur, that the onset of mineralization is related to a sudden deepening of the basin reflected by transgression in the sedimentary sequence.

The model

In pre-rift times the mantle plume caused heating and thermal doming of the overlying continental crust, comparable to the "high spots" of Thiessen et al. (1979), which is reflected in a regressional development in the lower host rock sequence (Bangemall Basin, Footwall Conglomerate in Sullivan, perhaps the lower stromatolitic and evaporitic McArthur Group). Deposition of the host rock sequence commonly with a basal unconformity indicates a significant time gap between lithification/tectonism of the basement and deposition of the younger sediments, e.g.

Table 5.01: Characteristics of selected sediment-hosted base metal deposits

Deposit	Age	Nature of Mineralization	Associated Volcanics	Tectonic Setting	Host Rocks	Associated Shallow Water Sediments	Host Rock Sequence	References
Abra Pb-Cu-Ba	late Prot.	discordant minor, concordant	rhyolites, lapilli tuff	T.J.	footwall clastic, evaporites	sabkha deposits	above unconformity; regressive-transgressive	
Gamsberg Zn-Pb-Ba	mid.Prot.	concordant	h.w. amphibolite= continental tholeiites?	possible I.R.	fine-grained clastics ?	hematite-barite, evaporite facies ?	above unconformity; regressive ?	Stumpfl (1979) Rozendal and Stumpfl (in press)
Mt. Isa Pb-Zn-Cu	mid.Prot.	concordant, Cu discordant	felsic tuffs	T.J.	black shale, dolomite	evaporites, stromatolites Silica Dolomite	above unconformity; transgressive ?	Mathias and Clark(1975) Dunnet (1976)
Lady Loretta/Lady Annie Pb-Zn, Ba/Cu	mid.Prot.	concordant, Cu discordant	K-rich tuffs	close to T.J.	dolomitic siltstone, organic shale, chert	??	above unconformity; small transgressive cycles in h.w., f.w.	Large (1980)
McArthur Pb-Zn	mid.Prot.	concordant, discordant	felsic tuffs in f.w.	I.R.	black shale, dolomite	evaporites, Cooley Dolomite	transgressive in immediate h.w.	Lambert (1976)
Sullivan Pb-Zn	mid.Prot.	concordant, minor discordant	post ore gabbro sills; pegmatites	close to T.J.	laminated shale	"ore"conglomerate f.w. conglomerate	transgressive	Ethier et al. (1976) Sangster and Scott(1976)
Cobar Zn-Pb-Cu	Devonian	originally concordant	K-rich tuffs, felsic volc. E of deposit	asymmetric I.R.	slate, siltstone conglomerate ?	reef carbonate, terrestrial sediments E of deposit	transgressive	Sannster (1979)
Copperbelt Cu	late Prot.	concordant, minor discordant		I.R.	argillites, dolomitic shale, siltstones	f.w. red beds, stromatolitic dolomite and anhydrite adjacent to dep. cycles	above unconformity; major transgressive cycles	Bowen and Gunatillaka (1977) Raybould (1978)
White Pine Cu (Pb-Zn)	late Prot.	discordant	f.w.rhyolites	T.J.	black shale, sandstone	brakish-freshwater, lagoonal basal red-beds	transgressive	Ensign et.al (1968)

Abbreviations: I.J. = triple junction, I.R. = intracratonic rift
f.w. = footwall, h.w. = hanging wall

in the Bangemall Basin subaerial erosion of the pre-Bangemall basement. An intact continental crust (lacking deep-seated faults) would be heated by conduction only, possibly with a steep geothermal gradient in the upper parts.

Incremental doming increases tensional strain within the crust, resulting in the generation of fractures - comparable to the "hogback uplift" of Falvey (1974) where within the central part of a rising dome a fault-bounded basin develops - and eventually in incipient rifting in a triple junction pattern.

This is the critical stage with respect to formation of ore deposits. The generation of deep-seated crustal fractures during incipient rifting allows comparatively rapid release of "stored" crustal heat through discharge of the crustal water reservoir plus crustal melts along the fracture zones. Thus a hydrothermal system is generated the nature of which is dependent on the type and depth of fractures, the amount of hot spot induced thermal anomaly and the composition of the basement. The common association of SHMD⁺ with major faults or lineaments illustrates the situation described above. Whether the final SHMD is concordant or discordant is only partially controlled by the nature of the hydrothermal system but by the environment the metal bearing solutions encounter in their host rock or depositional basin.

Thus, the presence of a hot spot is the first-order control of the development of a hydrothermal system; the generation of fractures and heat, exhalation of hydrothermal fluids and/or replacement processes, and the nature of the associated sediments are dependent on the amount of crustal doming and heating; which are also induced by the hot spot, and which therefore are regarded second-order controls on the variables of a hydrothermal system.

Implications

The model of hot spot induced SHMD in intracratonic rifts provides a number of significant implications and can throw some light on

⁺ sediment-hosted (base) metal deposits

features hitherto not sufficiently explained:

- It has long been known to explorationists that in the area surrounding proven deposits, there is a high probability of discovering further deposits of the same class; this may be called the concept of "ore fields" as in the Mt. Isa (Lady Loretta/Ladie Annie, Hilton), or Aggeneys-Gamsberg areas. If in a hot spot induced incipient rift the rifted crust remains above the hot spot (i.e. the crust moves along the axis of the rift over the hot spot), the probability of inducing a similar type hydrothermal system is high. Difficulties of identifying hot spot influence in areas lacking significant magmatism can be overcome by thorough evaluation of the sedimentary record as shown before. It is suggested that analogous to the Bangemall Basin, minor felsic volcanics which are crustal derived are indicative of hot spot influence. The felsites are related to the metal deposits in so far that they are generated by the same heat source as the hydrothermal system and that their ascent is controlled by faults, too.
- The timing of the mineralization with respect to the stratigraphy of the host rocks can almost certainly be assumed to coincide with the onset of a transgressional period, which in turn signals subsidence through the generation of major faults. The onset of the primary hydrothermal system coincides with the very first rifting stage.
- A genetic relationship between SHMD and evaporites, e.g. in providing sulphur as proposed by Gustafson and Williams (1981) and Muir (1983) may exist but does not apply universally because many deposits are lacking evaporites. However, the author regards the existence of evaporites, and alternatively very shallow water sediments, as significant in being an integral part of the depositional sequence above hot spot induced triple junctions, reflecting the doming stage and generation of doming-related restricted basins (Falvey, 1974).

An intrinsic genetic relationship of sediment hosted base metal deposits with sabkha processes (e.g. Renfro, 1974) is, in consequence, also refuted. Tab. 1 clearly shows that the same type of deposit can form with or without associated evaporites. In addition, timing of the mineralizing events, which can be determined with reasonable accuracy, is not compatible with sabkha processes.

- The discussion whether SHMD are generated through "diagenetic" (Rowlands et al., 1978, Bowen and Gunatilaka, 1977) or "hydrothermal" (Raybould, 1978) processes becomes unnecessary if hot spot-induced heating of crustal formation waters is invoked. All formation waters heated from below and expelled from crustal rocks should be termed hydrothermal regardless of the temperature they eventually have at the site of ore formation (this applies to the Zambian Copperbelt in particular). Any thermal doming would result in pressurized solutions which would ascend; provided they find a conduit. Possibly it was rather the lack of identifiable conduits that led some authors to postulating a "diagenetic" origin.

Source of metals

It is generally accepted that the late Proterozoic was a time of widespread intracontinental rifting (Raybould, 1978; Burke and Dewey, 1973; Sawkins, 1984; Windley, 1977) related to hot spot activity (Sawkins, 1976). It is suggested that previous to this rifting period the continents were exposed subaerially for a considerable time and thus providing conditions favourable for metal concentration. With commencement of doming these weathered rocks would be eroded and deposited, on the flanks of the dome, in fault-bounded basin, allowing for accumulation of a thick sequence of potential source rock. It is suggested that the abundance of copper deposits in late Proterozoic successions is due to widespread rifting after a prolonged period of stable continent conditions and red-bed copper formation. Possibly the crust had

had considerable thickness attenuating hot spot influence and therefore maintaining very low depositional temperatures. The Bangemall Basin deposit, having a "copper interval age" of 1100 m.y. is dominated by Pb and Cu and has a conspicuous lack of Zn. Field evidence suggests a granitic basement to the Bangemall Group, and the basement could have accumulated some red-bed copper concentrations. These copper- and hematite-stained rocks were deposited, together with an arkose derived from the granitic basement, in depressions on the flanks of the dome and reached considerable thickness. Differential mobilization of Cu and Pb, Ba (from feldspars) in the anomalous thermal regime accounts for the unique relative metal abundances in Abra. In the Late Proterozoic copper deposits the source rocks may have been red-bed copper in quartz-sandstone rendering only Cu to be mobilized. In non-Mississippi Valley Type lead-zinc deposits with high-grade metamorphic rocks in the basement, the metals may stem from retrograde metamorphism during the hot spot thermal regime, resulting in mobilization of lead (decay of potash feldspar) and later, zinc (decay of staurolite). When the basement originally was of low metamorphic grade, heat from the hot spot could induce higher-temperature metamorphic reactions, and mobilize lead (progressive decay of feldspars and muscovite) and zinc (progressive decay of staurolite).

Regardless of the nature of enrichment processes in the source rocks it is noteworthy that the Abra mineralization is of Late Proterozoic age and in the same tectonic setting as most of the major copper deposits of that time, but is dominant by lead. This supports the view that the composition of the basement and the amount of heat applied controls the relative metal abundance in the deposit.

It becomes apparent from the above metal source discussion that the metals are crustal derived in the hot spot induced intra-cratonic rift deposits and that the hydrothermal systems merely

fractionate and reconcentrate elements, and are mirroring to some extent preconcentrations of some elements in the source region.

Conclusions

Within the tectonic setting of a hot spot induced triple junction, resulting in intracratonic rifting a large number of sediment-hosted base metal deposits may have principally the same origin; The observed variations are mainly due to:

- 1) the amount of time a lithospheric plate remains stationary with respect to a mantle plume and
- 2) the nature of the lithospheric plate above a hot spot; its composition, thickness and pre-existing zones of weakness which can become fractures. Crustal derived felsic volcanics may indicate ancient locations of hot spots and evaluation of the sedimentary column of the host rocks usually indicates the amount of doming, and the timing with respect to the mineralization.
- 3) Metals concentrated in these deposits may have been derived from eroded continental areas, and/or by leaching from the sedimentary pile. A "mantle contribution" may be found in deposits associated with more advanced rift systems; otherwise there is no need to invoke this possibility.
- 4) Sabkha environments may, in some cases, provide a convenient receptacle for the deposition of metals introduced by hydrothermal systems, because of abundant H_2S produced by bacterial sulphate reduction. Their presence, however, is not essential as H_2S may equally be produced in other sedimentary environments.

Acknowledgements

I owe a sincere debt of gratitude to

- Professor E.F.Stumpfl, who initiated this study and supervised its progress, for his guidance and encouragement.
- Dr. R.D.Gee for introducing me to the geology of Western Australia, and for numerous stimulating and constructive discussions throughout all stages of this study. I thank him and his family for their hospitality while in Australia.
- Dr.A.F.Trendall for making this study possible, and the Geological Survey of Western Australia for its generous financial and logistic supports.
- The Jubiläumsfonds der Österreichischen Nationalbanken for generous financial support.
- Geopeko Inc. and Amoco Minerals Australia Co. for providing access to drill core and internal reports.
- Professor E.T.Degens who encouraged me to enter the field of economic geology.
- C.Ballhaus and O.Thalhammer for many fruitful discussions.
- H.Mühlhans for electron microprobe operation, and Frau M.Lenker and Frau L.Kogler for patiently typing the manuscripts.
- Dr.E.Pak of the Österreichische Akademie der Wissenschaften for sulphur isotope analyses.

References

- Alcoa of Australia Ltd. (1982): Ann.Rept.to West.Austr.Mines Dept.
Temporary Reserve 8657 H.
- Amoco Minerals Australia Co. (1977): Ann.Rept.to West.Austr.Mines
Dept., Temporary Reserve 5936 H.
- Amoco Minerals Australia Co. (1977): Ann.Rept.to West. Austr.Mines
Dept., Temporary Reserve 5945 H.
- Anger, G., Nielsen, H., Puchelt, H. and Ricke, W. (1966): Sulphur
isotopes in the Rammelsberg ore deposit (Germany).
Econ.Geol. 61, 511-536.
- Angerer, H., Haditsch, J.G., Laskovic, F., Leichtfried, W. and
Mostler, H. (1980): Ein Beitrag zur Kenntnis der Gips-
lagerstätten des Montafons (Vorarlberg).
Geol.Paläont.Mitt.Innsbruck, 9, 263-320.
- Anhaeusser, C.R. and Button, A. (1976): A review of southern African
stratiform ore deposits - their position in time and space.
In: Handbook of stratabound and stratiform ore deposits,
K.H. Wolf ed., Vol.5, 257-319.
- Annels, A.E. (1984): The geotectonic environment of Zambian copper-
cobalt mineralization.
J.Geol.Soc.London, 141, 279-289.
- Bachinski, D.J. (1977): Sulfur isotopic composition of ophiolitic
cupriferous iron sulfide deposits, Notre Dame Bay, New-
foundland.
Econ.Geol. 72, 243-257.
- Badham, J.P.N. (1981): Shale-hosted Pb-Zn deposits: products of
exhalation of formation waters?
Trans.Instn Min.Metall. 90, B70-B76.
- Bangemall Bulletin (in press): Geol.Surv.West.Austr.Memoir Ser.
- Barnes, H.L.(1975): Zoning of ore deposits: Types and causes.
Trans.R.S.E. 69, 295-311.
- Barton, P.B.Jr.(1970): Sulfide petrology.
Mineral.Soc.Amer.Spec.Pap. 3, 187-198.

- Barton, P.B. (1984): Redox reactions in hydrothermal fluids;
In: Fluid-Mineral Equilibria in Hydrothermal Systems,
(J.M.Robertson ed.).
Reviews in Economic Geology, Vol. 1, 99-113.
- Barton, P.B. and Skinner, B.J. (1979): Sulfide mineral stabilities.
In: Geochemistry of hydrothermal ore deposits, 2nd edition
(H.L.Barnes ed.), 278-403.
- Beales, F.W. (1975): Precipitation mechanisms for Mississippi Valley-
Type ore deposits.
Econ.Geol. 70, 943-948.
- Behr, H.J., Mushi, J.M. and Schneider, A. (1984): Chemismus und
Genese von Sedimenten des Natron-Sees (Tanzania).
Fortschr.Min. 62, Beiheft 1, 18-19.
- Bjørlykke, A. and Sangster, D.F. (1981): An overview of sandstone
lead deposits and their relation to red-bed copper and
carbonate-hosted lead-zinc deposits.
Econ.Geol. 75th Anniv.Vol., 179-213.
- Blatt, H. Middleton, G. and Murray, R. (1980): Origin of sedimentary
rocks.
Prentice Hall, Inc., 782 pp.
- Blockley, J.G. (1971): The lead, zinc, and silver deposits of
Western Australia.
Geol.Sur.West.Austr.Mineral Resources Bull 9.
- Bouroulllec, J. (1980): Sequential studies of the top of the eva-
poritic series of the Lower Lias in a well in the
Aquitaine basine (Auch 1), south-western France.
In: Evaporite deposits, Editions Technip, Paris, pp.29-31
and 146-159.
- Bowen, R. and Gunatilaka, A. (1977): Copper: its geology and
economics.
Wiley and Sons, New York, 366 pp.
- Brakel, A.T., Elias, M. and Barnett, J.C. (1978): Collier, Western
Australia.
West.Australia Geol.Survey 1 : 250 000 Geol.Series Explan.Notes.

- Brakel, A.T. and Muhling, P.C. (1976): Stratigraphy, sedimentation, and structure in the western and central part of the Bangemall Basin, Western Australia.
Geol.Sur.West.Austr. Ann.Rept., 1975, 70-79.
- Bralia, A., Sabatini, G. and Troja, F. (1979): A revaluation of the Co/Ni ratio in pyrite as geochemical tool in ore genesis problems.
Min.Dep. 14, 353-374.
- Bunting, J.A., Commander, D.P. and Gee, R.D. (1977): Preliminary synthesis of lower Proterozoic stratigraphy and structure adjacent to the northern margin of the Yilgarn Block.
Geol.Sur.West.Austr. Ann.Rept., 1976, 43-48.
- Burke, K. and Dewey, J.F. (1973): Plume-generated triple junctions: Key indicators in applying plate tectonics to old rocks.
J.Geol. 81, 406-433.
- Burnie, S.W., Schwarcz, H.P. and Crocket, J.H. (1972): A sulfur isotopic study of the White Pine Mine, Michigan.
Econ.Geol. 67, 895-914.
- Cameron, E.M. (1982): Sulphate and sulphate reduction in early Precambrian oceans.
Nature, 296, 145-148.
- Cameron, E.M. (1983): Evidence from early Proterozoic anhydrite for sulphur isotopic partitioning in Precambrian oceans.
Nature, 304, 54-56.
- Carmichael, I.S.E., Turner, F.J. and Verhoogen, J. (1974): Igneous Petrology.
McGraw-Hill, Inc. 739 pp.
- Carpenter, A.B., Trout, M.L. and Pickett, E.E. (1974): Preliminary report on the origin and chemical evolution of lead- and zinc-rich oil fields brines in Central Mississippi.
Econ.Geol. 69, 1191-1206.
- Carr, G.R. and Smith, J.W. (1977): A comparative isotopic study of the Lada Loretta zinc-lead-silver deposit.
Min.Dep. 12, 105-110.

- Compston, W. and Arriens, P.A. (1968): The Precambrian geochronology of Australia.
Canad.J.Earth Sci. 5, 561-583.
- Church, T.M. (1979): Marine barite-occurrence and origin.
In: R.G.Burns ed., Marine Minerals. Mineralogical Society of America. Short Course Notes, Vol.6, 175-209.
- Daniels, J.L. (1965): Breccias associated with the Proterozoic Bangemall Group.
Geol.Sur.West.Austr. Ann.Rept., 1964, 34-36.
- Daniels, J.L. (1966): Revised stratigraphy, palaeocurrent system and palaeogeography of the Proterozoic Bangemall Group.
Geol.Sur.West.Austr. Ann.Rept., 1965, 48-56.
- Daniels, J.L. (1969): Edmund, W.A.
Geol.Sur.West.Austr. 1: 250 000 Geol.Series Explan.Notes.
- Daniels, J.L. (1975): Bangemall Basin.
In: Geology of Western Australia. Geol. Sur.West.Austr. Mem.2, 147-159.
- Davy, R. (1975): A geochemical study of a dolomite-bif transition in the lower part of the Hamersley Group.
Geol.Sur.West.Austr. Ann.Rept., 1974, 88-100.
- Davy, R. (1980): A chemical and mineralogical study of low-grade zinc mineralization at three localities in the Proterozoic Bangemall Basin of Western Australia.
Geol.Sur.West.Austr. Report, 10, 1-70.
- Deer, W.A., Howie, R.A. and Zussman, J. (1972): Rock-forming Minerals.
Vol.4, 435 pp., Longman, London; sixth impression (1972).
- Deer, W.A., Howie, R.A. and Zussman, J. (1962): Rock-forming minerals.
Vol.5, 371 pp., Longman, London; sixth impression (1972).
- Degens, E.T., Williams, E.G. and Keith, M.L. (1958): Environmental studies of Carboniferous sediments, Part II; Application of geochemical criteria.
Am.Assoc.Petrol.Geol.Bull, 42, 981-997.

- Dellwig, L.F. (1955): Origin of the Salina Salt of Michigan.
Jour.Sed.Petrol. 25, 83-110.
- DeRito, R.F., Cozzarelli, F.A. and Hodge, D.S. (1983): Mechanism of subsidence of ancient cratonic rift basins.
In: P.Morgan and B.H.Baker, eds., Processes of continental rifting. Tectonophysics 94, 141-168.
- Dimroth, E. (1979): Models of physical sedimentation of iron formations.
In: Facies Models; R.G.Walker, ed.; Geoscience Can.Repr. Ser. 1, 175-182.
- Dunham, K.C. (1970): Mineralization by deep formation waters: a review.
Trans.Inst.Min.Metall. 79, B127-B136.
- Dunham, R.J. (1962): Classification of carbonate rocks according to depositional texture.
In: Classification of carbonate rocks; W.E.Ham ed.; Amer. Assoc.Petrol.Geol. pp. 108-121.
- Dunnet, D. (1976): Some aspects of the Panantartic cratonic margin in Australia.
Phil.Trans.R.Soc.Lond.A, 280, 641-654.
- Eichler, J. (1976): Origin of the Precambrian Banded Iron Formations.
In: Handbook of Strata-Bound and Stratiform Ore Deposits; K.H.Wolf, ed., Vol. 7, 157-200.
- Elias, M. and Williams, S.J. (1977): Robinson Range, Western Australia.
West.Australia Geol.Survey 1 : 250 000 Geol.Series Explan. Notes.
- Ensign, C.O., White, W.S., Wright, J.C., Patrick, J.L., Leone, R.J., Hathaway, D.J., Trammell, J.W., Fritts, J.J. and Wright, T.L. (1968): Copper deposits in the Nonesuch Shale, White Pine, Michigan.
In: Ore deposits of the United States 1933-1967; J.D. Ridge, ed., Vol. 1, 460-488.
- Ethier, V.G., Campbell, F.A., Both, R.A. and Krouse, H.R. (1976): Geological setting of the Sullivan orebody and estimates of temperatures and pressure of metamorphism.
Econ.Geol. 71, 1570-1588.

- Falvey, D.A. (1974): The development of continental margins in plate tectonic theory.
Aust.Petroleum Explor.Ass.J., 10, 95-106.
- Finlow-Bates, T. (1978): Control on the genesis of submarine exhalative ore deposits - with particular reference to Mt. Isa Mines, Queensland, Australia.
Dissertation, Montan-Universität Leoben, Austria, pp.244, unpublished.
- Finlow-Bates, T. (1980): The chemical and physical controls on the genesis of submarine exhalative orebodies and their implications for formulating exploration concepts. A review.
Geol.Jb. D40, 131-168.
- Finlow-Bates, T. and Stumpfl, E.F. (1979): The copper and lead-zinc-silver orebodies of Mt. Isa Mine, Queensland: Products of one hydrothermal system.
Ann.Soc.Geol.Belgique 102, 497-517.
- Fisher, R.V. and Schmincke, H.-V. (1984): Pyroclastic Rocks.
Springer Verlag, Berlin, 472 pp.
- Fleischer, V.D., Garlick, W.G. and Haldane, R. (1976): Geology of the Zambian Copperbelt.
In: Handbook of strata-bound and stratiform ore deposits; K.H. Wolf, ed., Vol. 6, 223-352.
- Friedman, M., Handin, J., Logan, J.M., Min, K.D. and Stearns, D.W. (1976): Experimental folding of rocks under confining pressure: Part III. Faulted drape folds in multilithologic layered specimens.
Geol.Soc.Amer.Bull. 87, 1049-1066.
- Froese, E. (1981): Applications of thermodynamics in the study of mineral deposits.
Geol.Sur.Can.Paper 80-28, 1-38.
- Froude, D.O., Ireland, T.R., Kinny, P.D., Williams, I.S., Compston, W., Williams, I.R. and Myers, J.S. (1983): Ion microprobe identification of 4100-4200 Myr-old terrestrial zircons.
Nature, 304, 616-618.

- Garlick, W.G. (1981): Sabkhas, slumping, and compaction at Mufulira, Zambia.
Econ.Geol. 76, 1817-1847.
- Gee, R.D. (1979): Structure and tectonic style of the Western Australian Shield.
Tectonophysics, 58, 327-369.
- Gee, R.D., Baxter, J.L., Wilde, S.A. and Williams, I.R. (1981): Crustal development in the Archean Yilgarn Block, Western Australia.
Spec.Publ.Geol.Soc.Austr. 7, 43-56.
- Gee, R.D., de Laeter, J.R. and Drake, J.R. (1976): Geology and geochronology of altered rhyolite from the lower part of the Bangemall Group near Tangadee, Western Australia.
Geo.Sur.West.Austr. Ann.Rept., 1975, 112-117.
- Geopeko, Inc. (1980): Ann.Rept. to West.Austr. Mines Dept., Temporary Reserve, 7372 H.
- Glickson, A.Y. and Lambert, I.B. (1973): Relations in space and time between major Precambrian shield units: An interpretation of Western Australian data.
Earth Planet.Sci.Lett. 20, 395-403.
- Guillevin, Y. (1980): Petrographical data of Oligocene evaporites in the Bresse and Valence basins (Eastern France).
In: Evaporite deposits; Editions Technip, Paris, pp.41-48 and 174-213.
- Gustafson, L.B. and Williams, N. (1981): Sediment-hosted stratiform deposits of copper, lead, and zinc.
Econ.Geol. 75th Anniv.Vol., 139-178.
- Haack, V., Heinrichs, H., Boneß, M. and Schneider, A. (1984): Loss of metals from pelites during regional metamorphism.
Contrib.Mineral.Petrol., 85, 116-132.
- Halligan, R. and Daniels, J.L. (1964): Precambrian geology of the Ashburton Valley region, North-West Division.
Geol.Sur.West.Austr. Ann.Rept. 1963, 38-46.
- Hannak, W.W. (1981): Genesis of the Rammelsberg ore deposit near Goslar/Upper Harz, Federal Republic of Germany.
In: Handbook of strata-bound and stratiform ore deposits; K.H. Wolf, ed. Vol. 9, 551-642.

- Hanor, J.S. (1966): The origin of barite.
Ph.D.Thesis, Havard University.
- Hanor, J.S. (1979): The sedimentary genesis of hydrothermal fluids.
In: Geochemistry of hydrothermal ore deposits. H.L.Barnes,
ed., Wiley and Sons, New York, 137-172.
- Henley, R.W. and Thornley, P. (1979): Some geothermal aspects of
polymetallic massive sulfide formation.
Econ.Geol. 74, 1600-1612.
- Helgeson, H.C. (1970): A chemical and thermodynamic model of ore
deposition in hydrothermal systems.
Mineral.Soc.Amer.Spec.Pap, 3, 155-186.
- Hickman, A.H. (1981): Crustal evolution of the Pilbara Block, Western
Australia.
Spec.Publs.Geol.Soc.Austr., 7, 57-69.
- Hobbs, B.E., Means, W.D. and Williams, P.E. (1976): An outline of
structural geology.
John Wiley and Sons, Inc., 571 pp.
- Horwitz, R.C. and Smith, R.E. (1978): Bridging the Yilgarn and Pilbara
Blocks, Western Australia.
Precambrian Res., 6, 293-322.
- Jackson, M.P.A. and Seni, S.J. (1983): Geometry and evolution of salt
structures in a marginal rift basin of the Gulf of Mexico,
east Texas.
Geology II, 131-135.
- James, N.P. (1979): Shallowing-upward sequences in carbonates.
In: Facies Models, R.G.Walker, ed., Geoscience Can.Repr.
Ser. I, 109-119.
- Jørgensen, B.B. (1982): Mineralization of organic matter in the sea
bed - the role of sulphate reduction.
Nature, 296, 643-645.
- Kalogeropoulos, S.I. (1983): Composition and oxidation state dependence
of chlorites from tuffaceous exhalites associated with volcano-
genic massive sulfide ore deposits.
N.Jb.Mineral.Mh., Jg.1983, H.4, 187-192.

- Kendall, A.C. (1979): Continental and supratidal (sabkha) evaporites.
And: Subaqueous evaporites.
In: Facies Models, R.G. Walker, ed., Geoscience Can.Repr.
Ser.I, 145-174.
- Klemm, D.D. (1984): Banded Iron Formations of South Africa.
Seminar on geosciences, May 1984, Montan-Universität Leoben,
Austria.
- Lambert, I.B. (1973): Post-depositional availability of sulphur and
metals and formation of secondary textures and structures
in stratiform sedimentary sulphide deposits.
Journal of the Geological Society of Australia, Vol.20,
205-215.
- Lambert, I.B. (1976): The McArthur zinc-lead-silver deposit: features,
metallogenesis and comparison with some other stratiform
ores.
In: Handbook of strata-bound and stratiform ore deposits,
K.H.Wolf, ed., Vol. 6, 535-585.
- Lambert, I.B., Donnelly, T.H. and Rowlands, N.J. (1980): Genesis of
upper Proterozoic stratabound copper mineralization,
Kapunda, South Australia.
Min.Dep. 15, 1-18.
- Lambert, I.B., Donnelly, T.H., Etminan, H. and Rowlands, N.J. (1984):
Genesis of Late Proterozoic copper mineralization, Copper
Claim, South Australia.
Econ.Geol. 79, 461-475.
- Langbein, R. (1979): Petrologische Aspekte der Anhydritbildung.
Z.geol.Wiss.Berlin, 7, 913-926.
- Large, D.E. (1980): Geological parameters associated with sediment-
hosted, submarine exhalative Pb-Zn deposits: an empirical
model for mineral exploration.
Geol.Jb. D40, 59-129.
- Large, D.E. (1981): Sediment-hosted submarine exhalative lead-zinc
deposits - A review of their geological characteristics
and genesis.
In: Handbook of strata-bound and stratiform ore deposits;
K.H. Wolf, ed., Vol. 9, 469-507.

- Large, D.E. (1983): Sediment-hosted massive sulphide lead-zinc deposits: An empirical model.
In: MAC short course handbook, Volume 8, sediment-hosted stratiform lead-zinc deposits; D.F.Sangster, ed., 1-29.
- Large, R.R. (1977): Chemical evolution and zonation of massive sulfide deposits in volcanic terrains.
Econ.Geol., 72, 549-572.
- Love, L.G. and Zimmermann, D.O. (1961): Bedded pyrite and micro-organism from the Mt. Isa Shale.
Econ.Geol., 56, 873-896.
- Mann, A.W. (1982): Mobilities of metal ions.
In: Geochemical exploration in deeply weathered terrain; R.E.Smith, ed., CSIRO discussion papers, pp.97-115.
- Marshall, A.E. (1968): Geological studies of the Proterozoic Bangemall Group, N.W.Australia.
Ph.D.Thesis (unpublished), Princeton University.
- Marston, R.J. (1980): Copper mineralization in Western Australia; Chapter 12, Bangemall Basin.
Geol.Sur.West.Austr.Mineral.Res. Bull. 13, 101-107.
- Mathias, B.V. and Clark, G.J. (1975): Mount Isa copper and silver-lead-zinc orebodies - Isa and Hilton Mines.
In: Economic geology of Australia and Papua New Guinea-Metals; C.L.Knight, ed., 351-372.
- McElhinney, M.W. and Embleton, B.J.J. (1976): Precambrian and Early Palaeozoic palaeomagnetism in Australia.
Philos.Trans.R.Soc.London, A280, 417-431.
- Milliken, K.L. (1979): The silicified evaporite syndrom - Two aspects of silification history of former evaporite nodules from Southern Kentucky and Northern Tennessee.
Jour.Sed.Petrol. 49, 245-256.
- Mitchell, A.H.G. and Garson, M.S. (1981): Mineral deposits and global tectonic settings.
Academic Press, Inc., London, 405 pp.

- Moine, B., Sauvan, P. and Jarousse, J. (1981): Geochemistry of evaporite-bearing series: A tentative guide for the identification of metaevaporites.
Contrib.Mineral.Petrol. 76, 401-412.
- Morrow, D.W., Krouse, H.R., Ghent, E.D., Taylor, G.C. and Dawson, K.R. (1978): A hypothesis concerning the origin of barite in Devonian carbonate rocks of northeastern British Columbia.
Can.J.Earth Sci. 15, 1391-1406.
- Muhling, P.C., Brakel, A.T. and Davidson, A.W. (1978): Mount Egerton, Western Australia.
West.Australia Geol.Survey 1 : 250 000 Geol.Series Explan. Notes.
- Muir, M.D. (1983): Depositional environments of host rocks to Northern Australian lead-zinc deposits, with special reference to McArthur River.
In: MAC Short Course Handbook, Vol. 8, D.F.Sangster, ed., pp.141-174.
- Nockolds, S.R., Knox, R.W.O'B. and Chinner, G.A. (1978): Petrology for Students.
Cambridge University Press, 435 pp.
- Ohmoto, H. and Rye, R.O. (1979): Isotopes of sulfur and carbon.
In: Geochemistry of hydrothermal ore deposits. H.L.Barnes, ed., pp.509-567.
- Paar, W. (1974): Die Gefüge der synsedimentär-syndiagenetischen Schwerspat-Bleiglanz-Lagerstätte "Breithorn", Ostgrönland.
Archiv Lgstfschg.Ostalpen, Sonderband 2, 215-237.
- Pearce, J.A. and Cann, J.R. (1973): Tectonic Setting of basic volcanic rocks determined using trace element analyses.
Earth Plan.Sci.Let. 19, 290-300.
- Pettijohn, F.J. (1975): Sedimentary Rocks.
Harper and Row, Inc. 628 pp.
- Pettijohn, F.J., Potter, P.E. and Siever, R. (1973): Sand and Sandstone.
Springer Verlag, New York, 618 pp.

- Puchelt, H. (1967): Zur Geochemie des Bariums im exogenen Zyklus.
Sitzungsber.Heidelb.Akad.Wiss., math.-nat.Kl., Jg. 1967,
85-287.
- Ramdohr, P. (1940): Die Erzminerale in gewöhnlichen magmatischen
Gesteinen.
Abh.Preuss.Akad.Wiss.Math.-Naturw.Kl., Nr.2.
- Ramdohr, P. (1975): Die Erzminerale und ihre Verwachsungen.
Akademie-Verlag, Berlin, 1277 pp.
- Ramsay, J.G. (1962): The geometry and mechanics of formation of
"similar" type folds.
J.Geol. 70, 309-327.
- Ramsay, J.G. (1967): Folding and fracturing of rocks.
McGraw-Hill, Inc. 568 pp.
- Raybould, J.G. (1978): Tectonic controls on Proterozoic stratiform
mineralization.
Trans.Instn Min.Metall. 87, B79-B86.
- Reading, H.G. (1978): Sedimentary environments and facies.
H.G.Reading, ed., Blackwell Scientific Publications,
557 pp.
- Reimann, C. and Stumpfl E.F. (in press): Palaeozoic amphibolites,
Kreuzeck Mountains, Austria: Geochemical variations in
the vicinity of mineralization.
Min.Dep., 1985.
- Reineck, H.-E. and Singh, I.B. (1973): Depositional sedimentary en-
vironments.
Springer Verlag, Berlin, 439 pp.
- Reinson, G. E. (1979): Barrier island systems.
In: Facies Models, R.G.Walker, ed., Geoscience Can.Repr.
Ser. I, 57-74.
- Renfro, A.R. (1974): Genesis of evaporite-associated stratiform metal-
liferous deposits - a sabkha process.
Econ.Geol. 69, 33-45.

- Riley, J.F. (1974): The tetrahedrite-freibergite series, with reference to the Mount Isa Pb-Zn-Ag orebody.
Min.Dep., 9, 117-124.
- Robbins, E.I. (1983): Accumulation of fossil fuels and metallic minerals in active and ancient rift lakes.
In: P.Morgan and B.H.Baker, eds., Processes of continental rifting. Tectonophysics, 94, 633-658.
- Roedder, E. (1967): Fluid inclusions as samples of ore fluids.
In: Geochemistry of hydrothermal ore deposits, H.L.Barnes, ed., 515-574.
- Rose, A.W. (1976): The effect of cuprous chloride complexes in the origin of red-bed copper and related deposits.
Econ.Geol. 71, 1036-1048.
- Rowlands, N.J. (1980): Discussion of Raybould (1978).
In: Trans.Inst.Min.Metall. 89, B167-B168.
- Rowlands, N.J., Drummond, A.J., Jarvis, D.M., Warin, O.N., Kitch, R.B. and Chuck, R.G. (1978): Geological aspects of some Adelaidean stratiform copper deposits.
Minerals Sci.Engn.10, 258-277.
- Rozendaal, A. and Stumpf, E.F. (in press): Mineral chemistry and genesis of the Gamsberg zinc deposit, South Africa.
Trans.Instn Min.Metall. (Section B).
- Sangster, D.F. (1976): Carbonate-hosted lead-zinc deposits.
In: Handbook of strata-bound and stratiform ore deposits, K.H. Wolf, ed., Vol. 6, 447-456.
- Sangster, D.F. (1976, b): Sulphur and lead isotopes in strata-bound deposits.
In: Handbook of stratabound and stratiform ore deposits; K.H. Wolf, ed., Vol. 2, 219-266.
- Sangster, D. F. (1979): Evidence of an exhalative origin for deposits of the Cobar district, New South Wales, BMRJ. Australian Geol.and Geophys. 4, 15-24.
- Sangster, D.F. and Scott, S.D. (1976): Precambrian, strata-bound, massive Cu-Zn-Pb sulfide ores of North America.
In: Handbook of strata-bound and stratiform ore deposits, K.H. Wolf, ed., Vol.6, 129-222.

- Sawkins, F.J. (1976): Widespread continental rifting: Some considerations of timing and mechanism.
Geology, 4, 427-430.
- Sawkins, F.J. (1984): Metal deposits in relation to plate tectonics.
Springer-Verlag, Berlin, 325 pp.
- Segnit, E.R. (1946): Barium-feldspars from Broken Hill, New South Wales.
Min.Mag. 27, 166-172.
- Shearman, D.J. (1980): Sebkhah facies evaporites.
In: Evaporite deposits; Editions Technip, Paris, pp. 19 and 96-109.
- Sibson, R.H., Moore, J.McM. and Rakin, A.H. (1975): Seismic pumping - a hydrothermal fluid transport mechanism.
J.Geol.Soc.Lond. 131, 653-659.
- Skinner, B.J. (1979): The many origins of hydrothermal mineral deposits.
In: Geochemistry of hydrothermal ore deposits, H.L.Barnes, ed., Wiley and Sons, New York, 1-21.
- Smith, R.E. and Davy, R. (1980): Exploration geochemistry at the Mount Palgrave and Mount Vernon Cu-Zn localities, Bangemall Basin.
Geol.Sur.West.Austr. Ann.Rept. 1978, 92-100.
- Solomon, M. and Walshe, J.L. (1979): The formation of massive sulphide deposits on the sea floor.
Econ.Geol. 74, 797-813.
- Stanton, R.L. (1979): An alternative to the Barrovian interpretation: evidence from stratiform ores.
Charles F.Davidson Memorial Lecture, University St.Andrews, Nov. 1979, 55 pp.
- Stille, H. (1930): Über Einseitigkeiten in der germanotypen Tektonik Nordspaniens und Deutschlands.
Gesellschaft der Wissenschaften, Göttingen. Mathematisch-Physikalische Klasse, Nachrichten, 1930, 3, 179-219.

- Stuart-Smith, P.G. and Ferguson, J. (1978): The Oenpelli Dolerite - a Precambrian continental suite from the Northern Territory, Australia, BMRJ. Australian Geol.Geophys. 3, 125-133.
- Stumpfl, E.F. (1979): Manganese haloes surrounding metamorphic stratabound base metal deposits. Min.Dep. 14, 207-217.
- Sutton, J. and Watson, J.V. (1974): Tectonic evolution of continents in early Proterozoic times. Nature, 274, 433-435.
- Tanner, W.F. (1971): Numerical estimates of ancient waves, water depth and fetch. Sedimentology, 16, 71-88.
- Taylor, G.F. (1983): Geochemical dispersion. In: Geochemical exploration in deeply weathered terrain, R.E.Smith, ed., CSIRO discussion papers, supplement, pp.45-52.
- Thiede, D.S. and Cameron, E.N. (1978): Concentrations of heavy metals in the Elk Point evaporite sequence, Saskatchewan. Econ.Geol. 73, 405-415.
- Thiessen, R., Burke, K. and Kidd, W.S.F. (1979): African hotspots and their relation to the underlying mantle. Geology, 7, 263-266.
- Tröger, W.E. (1969): Optische Bestimmung der gesteinsbildenden Minerale, Teil 2/Textband. Schweizerbart'sche Verlagsbuchhandlung, Stuttgart.
- Trudinger, P.A. (1981): Origin of sulphide in sediments. BMRJ. Austr.Geol.Geophys. 6, 279-285.
- Trudinger, P.A., Lambert, I.B. and Skyring, G.W. (1972): Biogenic sulfide ores: A feasibility study. Econ.Geol. 67, 1114-1127.
- Vogt, J.H. (1981): Organisch-geochemische Charakterisierung rezenter Wattsedimente. 3. Aminosäuren-Adsorptionsmechanismen und frühdiagenetische Effekte. Diplomarbeit (unpublished), Hamburg University.

- von Gehlen, K., Nielsen, H., Chunnnett, I. and Rozendaal, A. (1983):
Sulphur isotopes in metamorphosed Precambrian Fe-Pb-Zn-
Cu sulphides and baryte at Aggeneys and Gamsberg,
South Africa.
Min.Mag. 47, 481-486.
- Walker, R.G. (1979): Turbidites and associated coarse clastic deposits.
In: Facies Models, R.G.Walker, ed., Geoscience Can.Repr.Ser.I,
91-103.
- Walter, M.R. (1972): Stromatolites and the biostratigraphy of the
Australian Precambrian and Cambrian.
Palaeont.Ass.Lond.Spec.Pap. in Palaeontology no. II.
- Weinberg, D.W. (1979): Experimental folding of rocks under confining
pressure: Part VII. Partially scaled models of drape folds.
Tectonophysics, 54, 1-24.
- Weintritt, D.J. and Cowan, J.C. (1967): Unique characteristics of
barium sulphate scale deposition.
J.Petroleum Tech 1967, 1381-1394.
- Wiese, R.G.Jr. (1973): Mineralogy and geochemistry of the Parting
Shale, White Pine, Michigan.
Econ.Geol. 68, 317-331.
- Willan, R.C.R., and Hall, A.J. (1980): Sphalerite geobarometry and
trace element studies on stratiform sulphide from McPhun's
Cairn, Loch Fyne, Argyll, Scotland.
Trans.Instn Min.Metall.Section B, 89, B31-B40.
- Williams, J.R., Brakel, A.T., Chin, R.J. and Williams, S.J. (1976):
The stratigraphy of the Eastern Bangemall Basin and the
Paterson Province.
Geol.Sur.West.Austr.Ann.Rept. 1975, 79-83.
- Williams, N. (1978): Studies of the base-metal sulfide deposits at
McArthur River, Northern Territory, Australia: II. The sulfide-S
and organic-C relationships of the concordant deposits and
their significance.
Econ.Geol. 73, 1036-1056.

Windley, B.F. (1977): The evolving continents.

John Wiley and Sons Ltd, 385 pp.

ZoBell, C.E. (1963): Organic geochemistry of sulfur.

In: Organic Geochemistry, I.A.Breger, ed., Pergamon,
Oxford, pp.543-578.

GEOLOGICAL MAP OF THE JILLAWARRA BELT

map 1

REF 1:50 000

SHEET 1



LEGEND

BOUNDARIES

[Symbol]	1:50 000
[Symbol]	1:250 000
[Symbol]	1:125 000
[Symbol]	1:62 500
[Symbol]	1:31 250
[Symbol]	1:15 625

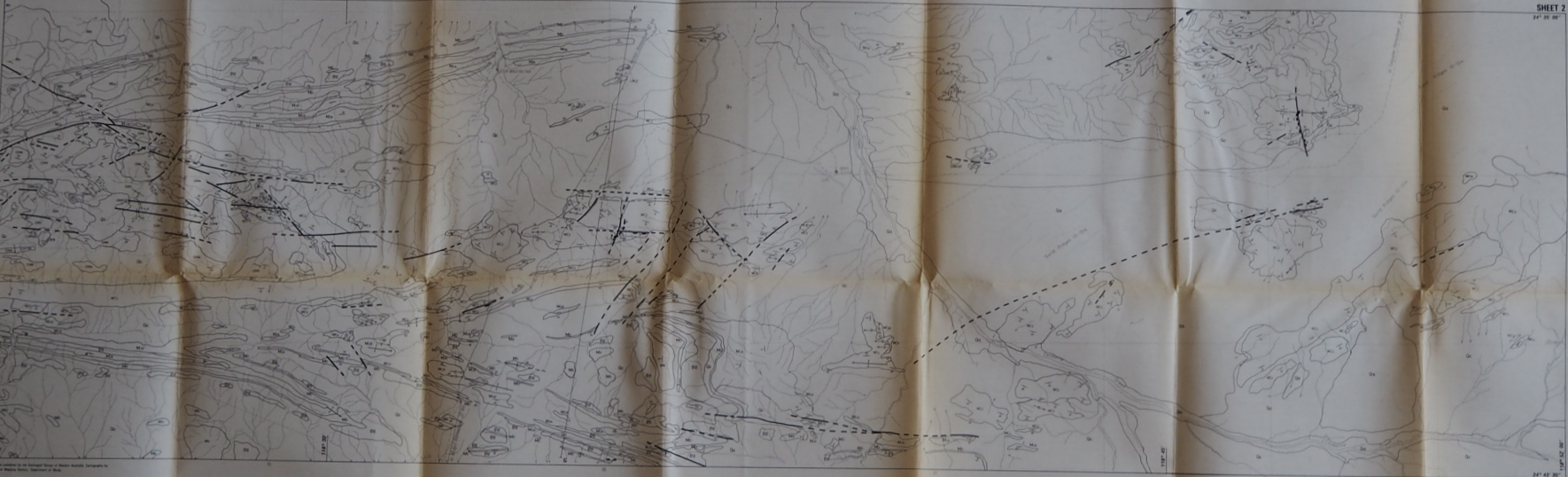
STRUCTURES

[Symbol]	1:50 000
[Symbol]	1:250 000
[Symbol]	1:125 000
[Symbol]	1:62 500
[Symbol]	1:31 250
[Symbol]	1:15 625

SYMBOLS

[Symbol]	1:50 000
[Symbol]	1:250 000
[Symbol]	1:125 000
[Symbol]	1:62 500
[Symbol]	1:31 250
[Symbol]	1:15 625

SHEET 2

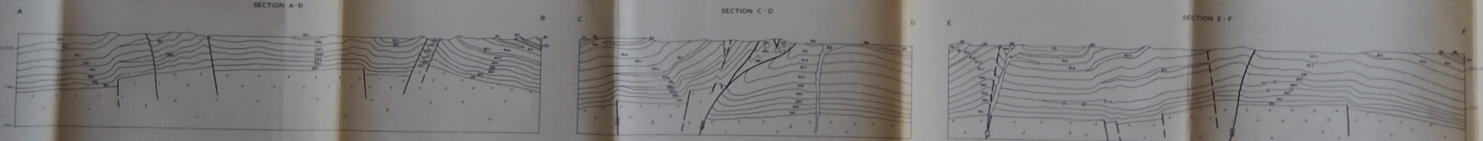


SYMBOLS

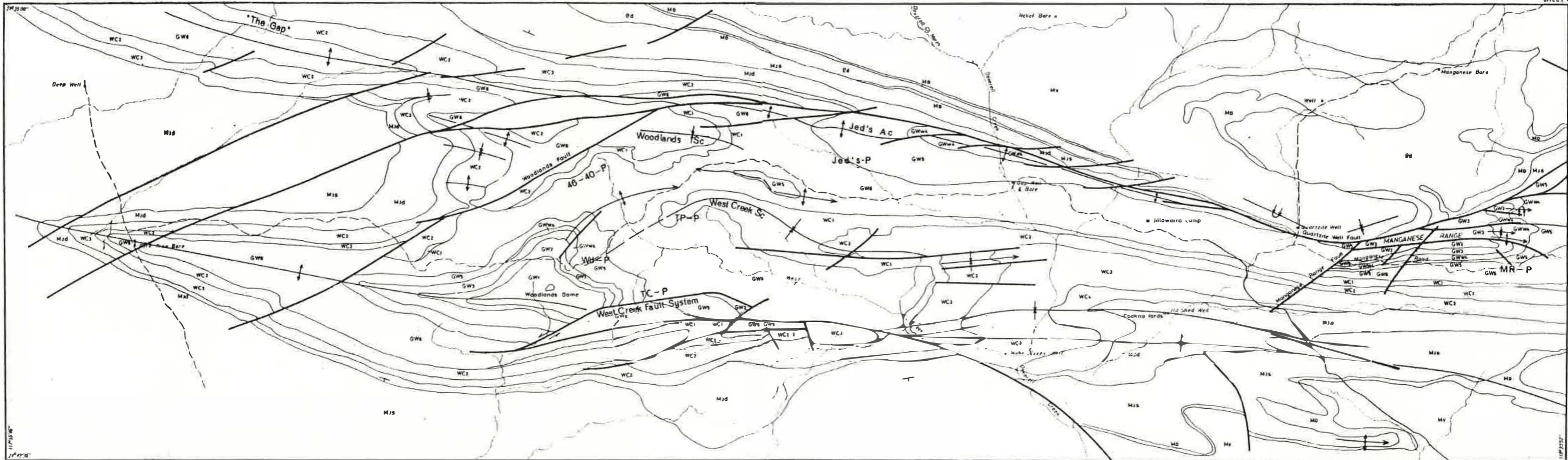
[Symbol]	1:50 000
[Symbol]	1:250 000
[Symbol]	1:125 000
[Symbol]	1:62 500
[Symbol]	1:31 250
[Symbol]	1:15 625



DIAGRAMMATIC SECTIONS



Location Map



Ac - Anticline P - Prospect MR-P - Manganese Range Prospect
 Sc - Syncline CC-P - Copper Chert Prospect MRE-P - Manganese Range East Prospect

